Universitat Ramon Llull



# TESIS DOCTORAL

| | |
|---|---|
| Título | **Diseño, selección y síntesis de nuevos inhibidores de entrada del VIH.** |
| Realizada por | Sofia Henriette Pettersson Salom |
| en el Centro | Escola Tècnica Superior IQS |
| y en el Departamento | Química Orgánica |
| Dirigida por | Dr. Jordi Teixidó i Closa |

*C. Claravall, 1-3*
*08022 Barcelona*
*Tel. 936 022 200*
*Fax 936 022 249*
*E-mail: urlsc@sec.url.es*
*www.url.es*

## 4.6.7. Modelo 10: filtrado mediante comparación del *fingerprint* de MACCS.

4.6.7.1. Introducción.

Los *fingerprints* representan un conjunto de características derivadas de la estructura de una molécula. Las características particulares derivadas de la estructura pueden ser arbitrarias y dependen de la topología del grafo o incluso de la conformación 3D de la molécula. Diferentes *fingerprints* enfatizan diferentes atributos moleculares de acuerdo con el diseño particular de aquel *fingerprint*.

En el presente trabajo se ha utilizado el *fingerprint* de MACCS de 166 bits,[48] donde cada punto del vector indica la presencia (1) o ausencia (0) de cada uno de los 166 fragmentos estructurales o *keys* contenidos en MACCS, y se calcula a partir del grafo molecular. A su vez, cada fragmento estructural describe una pequeña subestructura que contiene de 1 a 10 átomos (sin incluir átomos de hidrógeno). El resultado es un vector de índices donde la presencia de un índice indica la presencia del correspondiente fragmento estructural en la molécula.

La comparación entre moléculas se reduce a comparar grupos de características (vectores de índices) y medir su grado de solapamiento. Dicha comparación se puede realizar con diferentes métricas, la más común, y utilizada en este trabajo, es la métrica de Tanimoto. El valor del coeficientes de Tanimoto, $T_c$, se calcula mediante la Ecuación 4.8, donde *a* indica el número de fragmentos estructurales presentes en el *fingerprint* de la molécula A, *b* indica el número de fragmentos estructurales presentes en la molécula B, y *c* es el número de fragmentos estructurales en común. Por lo tanto, el valor del coeficiente de Tanimoto oscila entre 0 y 1, donde 0 representa máxima disimilitud y 1 representa máxima similitud.[49,50]

$$T_c = \frac{c}{a+b-c} \qquad \textbf{[4.8]}$$

4.6.7.2. Resultados.

Se lleva a cabo el cribado virtual de la base de datos de activos e inactivos compilada con el *fingerprint* de MACCS de 166 bits. Se utiliza como referencia el compuesto más activo de la base de datos (Figura 4.24) y se compara la similitud de cada compuesto de la base de datos frente al compuesto de referencia **105** mediante el coeficiente de Tanimoto.

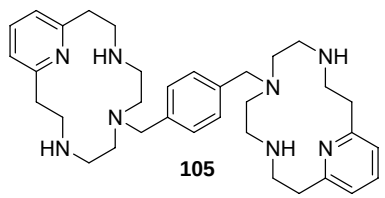


**105**

***Figura 4.24.*** *Estructura de la molécula más activa de la base de datos.*

La curva de enriquecimiento del cribado virtual realizado por comparación del *fingerprint* de MACCS del compuesto más activo de la base de datos **105** frente al resto de moléculas de la base de datos con el índice de Tanimoto se representa en la Figura 4.25. Se observa que la selección de compuestos activos mediante esta técnica es superior a una selección al azar.

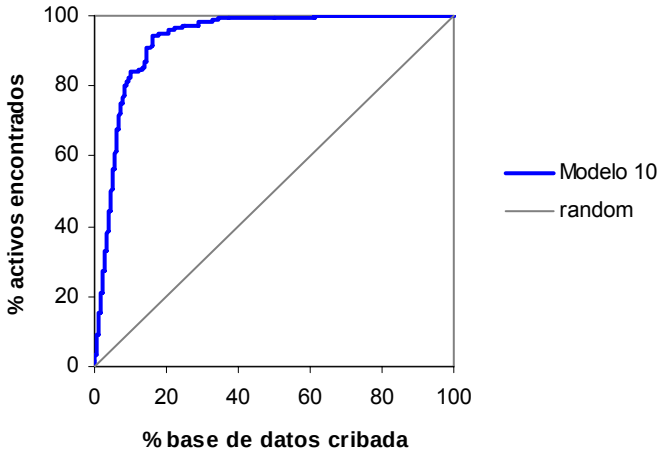


***Figura 4.25.*** *Curva de enriquecimiento obtenida al cribar la base de datos con el modelo 10.*

***Tabla 4.14.*** *Factor de enriquecimiento obtenido distintos porcentajes de base de datos cribada con el modelo 10.*

| % base de de datos cribada | *ef* |
|---|---|
| 1 | 10.68 |
| 2 | 10.68 |
| 5 | 10.56 |
| 10 | 8.23 |

El análisis del factor de enriquecimiento en el 1 y 2% de base de datos cribada presenta el valor máximo, y decae hasta un valor de 8.23 al llegar al 10% (Tabla 4.14).

El análisis de las familias seleccionadas a diferentes porcentajes de base de datos cribada mediante esta técnica muestra que el modelo selecciona preferentemente azamacrociclos seguido de la familia de las poliaminas (Figura 4.26). El primer compuesto del tipo KRH se selecciona en el 9% de base de datos cribada, y el primer compuesto del tipo Dpa en el 12%, aunque esta familia de compuestos en general presenta menor actividad antiviral que los azamacrociclos y los compuestos de tipo KRH. El resultado es el esperado ya que se utiliza como compuesto de referencia un azamacrociclo (**105**), y por lo tanto los compuestos

más similares son los de la misma familia, es decir, los azamacrociclos, seguidos de las moléculas de la familia de las poliaminas.

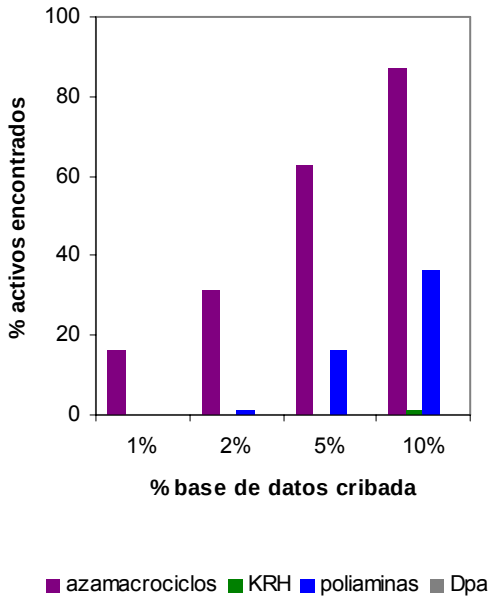


***Figura 4.26.*** *Análisis de diversidad de los* scaffolds *seleccionados al cribar la base de datos con el modelo 10.*

Este modelo selecciona en primer lugar los activos de la base de datos, pero no quedan correctamente ordenados según su actividad anti-VIH. Este resultado no es sorprendente ya que se realiza una comparación estructural de los compuestos de la base de datos de activos e inactivos frente al más activo, un azamacrociclo, y por lo tanto se espera una selección preferente de los compuestos de la misma familia. Sin embargo, dentro de esta familia no se distinguen los compuestos más activos de los menos activos. En el cribado virtual realizado con este modelo sobre la base de datos inactivos reales se observa que no se selecciona ninguno de ellos en el 1 y 2% de base de datos de activos e inactivos cribada. En el 5% de base de datos cribada solamente se seleccionan 3 de los 16 inactivos reales, mientras que la gran mayoría quedan seleccionados por el modelo al cribar un 10% de la base de datos de activos e inactivos. Solamente 2 compuestos de la base de datos de inactivos reales quedan excluidos de la selección al 10% del cribado de la base de datos de activos e inactivos. La principal aplicación de este modelo es en las primeras etapas del cribado virtual de una quimioteca de posibles inhibidores del correceptor CXCR4, pero no en la selección de compuestos más refinada, según su actividad anti-VIH aproximada a la posición en el *hit list* respecto a la base de datos de activos conocidos.

## 4.7. Modelos farmacofóricos: análisis prospectivo.

Se realiza un análisis prospectivo sobre los compuestos no sintetizados de la familia de las poliaminas diseñadas en el Capítulo 1 y de los monociclamos diseñados en el Capítulo 2. Dado que el análisis retrospectivo de los farmacóforos modelados no permite determinar el uso preferente de uno de los modelos, se utilizan los 9 farmacóforos en este análisis. Todos estos compuestos se protonan a pH fisiológico, se les asignan las cargas parciales de Gasteiger, se optimiza su geometría y se calculan 50 conformaciones utilizando el *force field* MMFF94. Esta base de datos multiconformacional se utiliza en el análisis prospectivo. El resultado se expresa como RMSD (*root mean square deviation*) entre las *features* del modelo y la molécula en estudio (Tabla 4.15). Se resaltan en negrita las moléculas que presentan el menor RMSD para cada modelo.

En el análisis prospectivo, se utiliza un consenso de los resultados obtenidos con cada uno de los farmacóforos modelados. Se observa que el compuesto que en general presenta el menor RMSD es **70**{*11*}, seguido de los monociclamos **70**{*8*} y **70**{*9*}. En cuanto a las poliaminas, aquellas que presentan los menores valores de RMSD son **32**{*4,8*}, **32**{*7,8*} y **32**{*7,10*} (Figura 4.27). Cabe destacar la dihidrazona **33**{*1,2*} que se clasifica como inactiva con todos los modelos farmacofóricos.

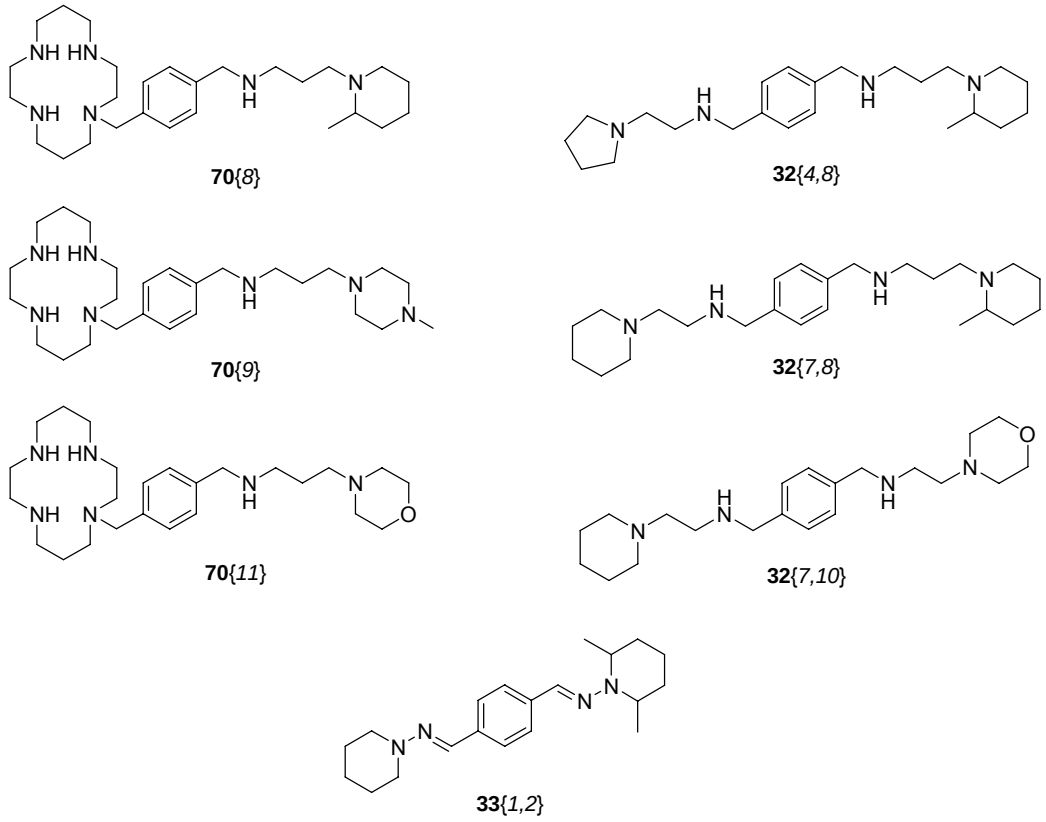


***Figura 4.27.*** *Estructura de los compuestos con menor RMDS en los farmacóforos.*

***Tabla 4.15.*** *Análisis prospectivo con los modelos farmacofóricos. Se indica el RMSD (Å) entre cada compuesto y el farmacóforo. Los guiones indican compuestos clasificados como inactivos por el modelo.*

| Compuesto | Modelo1 | Modelo2 | Modelo3 | Modelo4 | Modelo5 | Modelo6 | Modelo7 | Modelo8 | Modelo9 |
|---|---|---|---|---|---|---|---|---|---|
| **33**{*1,2*} | – | – | – | – | – | – | – | – | – |
| **33**{*1,3*} | – | – | 1.1741 | 0.9086 | 0.9086 | 0.9870 | – | – | 0.9169 |
| **37**{*1,4*} | 0.5712 | 0.9605 | 0.8368 | 0.5261 | 0.5261 | 0.7153 | 1.4686 | 1.4465 | 0.7352 |
| **37**{*1,7*} | 0.6307 | 0.9839 | 0.8310 | 0.5190 | 0.5191 | 0.7327 | – | 1.3353 | – |
| **37**{*1,8*} | 0.6284 | 0.9786 | 0.9101 | 0.4723 | 0.4723 | 0.9790 | – | 1.4332 | 0.6071 |
| **37**{*1,10*} | 0.6307 | 0.8890 | 0.8310 | 0.5110 | 0.5110 | 0.7305 | 1.2161 | 1.0779 | – |
| **33**{*2,3*} | – | – | 1.1755 | 0.9129 | 0.9129 | 0.8400 | – | 1.4695 | 0.7664 |
| **37**{*2,7*} | 0.6338 | 0.9905 | 0.8320 | 0.8506 | 0.8881 | 0.6678 | 1.3628 | 1.1823 | – |
| **37**{*2,8*} | 0.6199 | 0.9909 | 0.9807 | 0.4742 | 0.5346 | 0.6860 | – | 1.2824 | 0.4375 |
| **37**{*2,10*} | 0.6339 | 0.9230 | 0.8323 | 0.7040 | 0.9009 | 0.6660 | 0.8185 | 0.7995 | – |
| **37**{*3,7*} | 0.6306 | **0.8033** | 0.6165 | 0.4368 | 0.4368 | 0.6317 | 0.8388 | 0.8575 | 0.5551 |
| **37**{*3,10*} | 0.6306 | **0.7667** | 0.6165 | 0.4289 | 0.4289 | 0.6291 | 0.8327 | 0.8513 | 0.5551 |
| **32**{*4,7*} | 0.5227 | 1.1105 | 0.8836 | 0.3962 | 0.3962 | 0.4716 | 0.8880 | 0.8962 | 0.7565 |
| **32**{*4,8*} | **0.4166** | 0.8914 | 0.7349 | 0.3923 | 0.3923 | 0.4902 | 0.8354 | 0.8512 | 0.4157 |
| **32**{*4,10*} | 0.5119 | 0.9484 | 0.8688 | **0.3284** | **0.3284** | 0.5366 | 0.7563 | 0.7670 | 0.7308 |
| **32**{*7,8*} | **0.4166** | 0.8914 | 0.7044 | 0.3625 | 0.3625 | 0.5070 | 0.8043 | 0.8118 | 0.4157 |
| **32**{*7,10*} | 0.5119 | 0.9617 | 0.8473 | **0.3284** | **0.3284** | 0.4728 | 0.7508 | 0.7766 | 0.7308 |
| **70**{*1*} | 0.4803 | 0.9030 | 0.8054 | 0.4014 | 0.4014 | 0.5879 | 1.1812 | 1.2167 | 0.4288 |
| **70**{*2*} | 0.4742 | 0.9415 | 0.8831 | 0.3832 | 0.4551 | 0.5254 | 0.8217 | 0.8293 | 0.3235 |
| **70**{*3*} | 0.4805 | **0.7953** | 0.6841 | 0.4012 | 0.4012 | 0.5449 | 0.5568 | 0.5779 | 0.4747 |
| **70**{*4*} | 0.4640 | 0.8499 | 0.7535 | 0.4270 | 0.4270 | 0.4845 | 0.6615 | 0.6580 | 0.3409 |
| **70**{*5*} | 0.4250 | 0.8393 | 0.5836 | **0.3329** | 0.4012 | 0.4800 | 0.7907 | 0.8216 | 0.3671 |
| **70**{*6*} | 0.4250 | 0.9069 | 0.6070 | 0.4079 | 0.4079 | 0.4800 | 1.1394 | 1.1536 | 0.3925 |
| **70**{*7*} | 0.4512 | 0.8064 | 0.7365 | 0.3789 | 0.3954 | 0.3839 | **0.5394** | **0.5433** | **0.2826** |
| **70**{*8*} | **0.4248** | 0.8252 | **0.4611** | 0.4755 | 0.4755 | **0.3568** | **0.5311** | **0.5436** | 0.3321 |
| **70**{*9*} | **0.4248** | 0.8156 | **0.4579** | 0.3462 | **0.3462** | **0.3320** | 0.5408 | 0.5525 | **0.2655** |
| **70**{*10*} | 0.4512 | 0.8064 | 0.7365 | 0.3786 | 0.3954 | 0.3727 | 0.5405 | 0.5446 | **0.2809** |
| **70**{*11*} | 0.4248 | 0.8154 | **0.4604** | **0.2856** | **0.2856** | **0.3483** | **0.5304** | **0.5429** | 0.3755 |

La síntesis de los compuestos seleccionados **32**{*7,8*} (Capítulo 1), **70**{*8*} y **70**{*11*} (Capítulo 2) permite determinar experimentalmente su actividad anti-VIH, cuyos valores son de 0.443, 0.022 y 0.058 μg/mL respectivamente, demostrando así la utilidad de los farmacóforos modelados.

Además, la síntesis (Capítulo 1) posterior de otros compuestos seleccionados mediante técnicas de *docking*[8] incluidos en las predicciones, **33**{*1,3*}, **37**{*1,8*} y **37**{*2,8*} permite comparar el resultado obtenido con el valor experimental de la actividad anti-VIH de estas moléculas (Tabla 4.16). Por una parte, se observa que la dihidrazona **33**{*1,3*}, cuyas conformaciones no se superponen sobre cuatro de los modelos farmacofóricos desarrollados y sobre los que sí se superpone presenta valores del RMSD bastante elevados, ha resultado inactiva en el ensayo de actividad antiviral. Por otra parte, **37**{*1,8*} ha resultado citotóxica a una concentración de 4.1 μg/mL y no ha resultado activa a concentraciones inferiores, por lo tanto no se ha podido determinar el valor del $EC_{50}$, y es detectado como inactivo por el modelo 7. Por último, **37**{*2,8*} ha presentado un valor experimental de $EC_{50}$ de 0.6 μg/mL, aunque el modelo 7 lo clasificaba erróneamente como inactivo.

***Tabla 4.16.*** *Actividad antiviral ($EC_{50}$) y citotoxicidad ($CC_{50}$).*

| Compuesto | | $EC_{50}$ / μg·mL$^{-1}$ | $CC_{50}$ / μg·mL$^{-1}$ |
|---|---|---|---|
| **33**{*1,3*} | 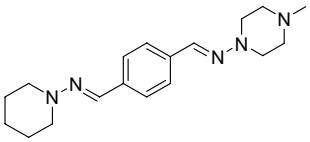 | >25 | >25 |
| **37**{*1,8*} | 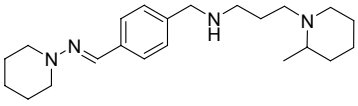 | >4.1 | 4.1 |
| **37**{*2,8*} | 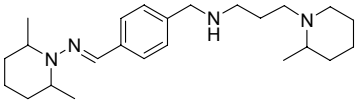 | 0.6 | 14.6 |
| **32**{*7,8*} | 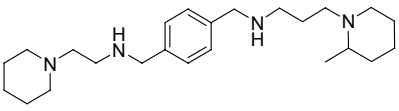 | 0.5 | >25 |
| **70**{*8*} | 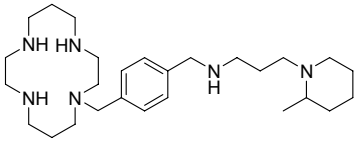 | 0.022 | >25 |

| Compuesto | | $EC_{50}$ / μg·mL$^{-1}$ | $CC_{50}$ / μg·mL$^{-1}$ |
|---|---|---|---|
| **70**{*11*} | 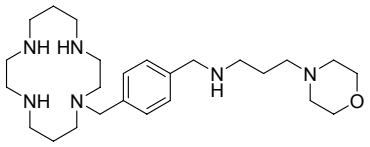 | 0.058 | >25 |

En resumen, la selección de compuestos por cribado virtual mediante un consenso del resultado obtenido a partir de los farmacóforos modelados ha resultado en compuestos con actividad anti-VIH. Este resultado demuestra la utilidad de las técnicas utilizadas, aunque no se haya logrado obtener un compuesto de actividad mayor que la mejor poliamina, **32**{*8,8*}, sin embargo, puede que en la quimioteca diseñada en el Capítulo 1 no haya ningún compuesto con mayor actividad antiviral.

## Bibliografía.


[1] L. A. Mitsher, A. Dutta; Combinatorial chemistry and multiple parallel synthesis. In *Burger's medicinal chemistry and drug discovery*, 6th edition; D. J. Abraham Eds.;, John Wiley & Sons: Hoboken, NJ, **2003**; Vol. 2: Drug development, 1-36.

[2] P. Kuhn, K. Wilson, M. G. Patch, R. C. Stevens; The genesis of high-throughput structure-based drug discovery using protein crystallography. *Curr. Opin. Chem. Biol.* **2002**, *6,* 704-710.

[3] S. Liu, S. Jiang; High throughput screening and characterization of HIV-1 entry inhibitors targeting gp41: theories and techniques. *Curr. Pharm. Des.* **2004**, *10,* 1827-1843.

[4] C. Marchand, N. Neamati, Y. Pommier; *In vitro* human immunodeficiency virus type 1 integrase assays. *Meth. Enzymol.* **2001**, *340,* 624-633.

[5] G. Klebe; Virtual screening: scope and limitations. In *Virtual screening in drug discovery*; J. Alvarez, B. Shoichet Eds.; Taylor & Francis Group: Boca Raton, FL, **2005**; 3-24.

[6] O. Rabal, J. I. Borrell, J. Teixidó; Cribado virtual: aproximaciones y técnicas. *Afinidad* **2007**, *64,* 329-345.

[7] L. Terfloth; Drug design. In *Chemoinformatics*, 1st edition; J. Gasteiger, T. Engel Eds.; Wiley-VCH: Weinheim, Germany, **2003**; 597-622.

[8] V. I. Pérez-Nueno; Herramientas de cribado virtual aplicadas a inhibidores de entrada del VIH. Diseño de nuevos compuestos anti-VIH. Tesis doctoral, IQS (Universitat Ramon Llull), Barcelona, **2009**.

[9] S. Pettersson, V. I. Pérez-Nueno, L. Ros-Blanco, R. Puig de la Bellacasa, O. Rabal, X. Batllori, B. Clotet, I. Clotet-Codina, M. Armand-Ugón, J. Esté, J. I. Borrell, J. Teixidó; Discovery of novel non-cyclam polynitrogenated CXCR4 coreceptor inhibitors. *ChemMedChem* **2008**, *3,* 1549-1557.

[10] P. Ehrlich; Über den jetzigen Stand der Chemotherapie. *Dtsch. Chem. Ges.* **1909**, *42,* 17. Quoted in: E.J. Ariens; *Prog. Drug. Res.* **1966**, *10*, 429.

[11] P. Gund; Three-dimensional pharmacophoric pattern searching. In *Progress in molecular and subcellular biology*; F. E. Hahn Eds.; Springer-Verlag: Berlin, Germany, **1977**; Vol. 5*,* 117-143.

[12] Y. C. Martin, M. G. Bures, E. A. Danaher, J. DeLazzer, I. Lico, P. A. Pavlik; A fast new approach to pharmacophore mapping and its application to dopaminergic and benzodiazepine agonists. *J. Comput. Aided Mol. Des.* **1993**, *7,* 83-102.

[13] D. Barnum, J. Greene, A. Smellie, P. Sprague; Identification of common functional configurations among molecules. *J. Chem. Inf. Comput. Sci.* **1996**, *36,* 563-571.

[14] G. Jones, P. Willett, R. C. Glen; A genetic algorithm for flexible molecular overlay and pharmacophore elucidation. *J. Comput. Aided Mol. Des.* **1995**, *9,* 532-549.

[15] J. H. Van Drie, D. Weininger, Y. C. Martin; ALADDIN: An integrated tool for computer-assisted molecular design and pharmacophore recognition from geometric, steric, and substructure searching of three-dimensional molecular structures. *J. Comput. Aided Mol. Des.* **1989**, *3,* 225-251.

[16] *MOE (Molecular Operating Environment)* 2006.08 Release; Chemical Computing Group, Inc.: Montreal, Canada, **2004**.

[17] O. F. Güner, R. Hoffman, H. Li in *Report by Wndy A. Warr; 217th ASC National Meeting and Exposition, Anaheim, California, March 12-15, 1999*, Wendy Warr & Associates, London, **1999**, 50-53.

[18] O. F. Güner, D. R. Henry; Metric for analyzing hit lists and pharmacophores. In *Pharmacophore, perception, development and use in drug design*; O. F. Güner Eds.; International University Line: La Jolla, CA, **2000**; 195-212.

[19] L. S. Fisher, O. F. Güner; Seeking novel leads through structure-based pharmacophore design. *J. Braz. Chem. Soc.* **2002**, *13,* 777-787.

[20] R. Pascual; Limitationts of current parameters (enrichment, GH) for the evaluation of pharmacophore screening performance. *Teraflop* **2006**, *90,* 5.

[21] G. J. Bridger, S. Padmanabhan, R. T. Skerlj, P. E. Hernandez-Abad, M. P. Sant; Antiviral compounds. US Patent US 5817807 (filing date: 6-6-1996).

[22] G. J. Bridger, R. T. Skerlj, S. Padmanabhan, S. A. Martellucci, G. W. Henson, S. Struyf, M. Witvrouw, D. Schols, E. de Clercq; Synthesis and structure-activity relationships of phenylenebis(methylene)-linked bis-azamacrocycles that inhibit HIV-1 and HIV-2 replication by antagonism of the chemokine receptor CXCR4. *J. Med. Chem.* **1999**, *42,* 3971-3981.

[23] G. J. Bridger, E. M. Boehringer, Z. Wang, D. Schols, R. T. Skerlj, D. E. Bogucki; Antiviral compounds. US Patent US 6506770 (filing date: 8-7-1998).

[24] E. de Clercq; Inhibition of HIV infection by bicyclams, highly potent and specific CXCR4 antagonists. *Mol. Pharmacol.* **2000**, *57,* 833-839.

[25] H. F. Egberink, E. de Clercq, A. L. W. van Vliet, J. Balzarini, G. J. Bridger, G. Henson, M. C. Horzinek, D. Schols; Bicyclams, selective antagonists of the human chemokine receptor CXCR4 potently inhibit feline immunodeficiency virus replication. *J. Virol.* **1999**, *73,* 6346-6352.

[26] J. A. Esté, C. Cabrera, E. de Clercq, S. Struyf, J. Van Damme, G. Bridger, R. T. Skerlj, M. J. Abrams, G. Henson, A. Gutierrez, B. Clotet, D. Schols; Activity of different bicyclam derivatives against human immunodeficiency virus depends on their interaction with the CXCR4 chemokine receptor. *Mol. Pharmacol.* **1999**, *55,* 67-73.

[27] S. Hatse, K. Princen, E. de Clercq, M. M. Rosenkilde, T. W. Schwartz, P. E. Hernandez-Abad, R. T. Skerlj, G. J. Bridger, D. Schols; AMD3465, a monomacrocyclic CXCR4 antagonist and potent HIV entry inhibitor. *Biochem. Pharmacol.* **2005**, *70,* 752-761.

[28] H. C. Joao, K. de Vreese, R. Pauwels, E. de Clercq, G. W. Henson, G. J. Bridger; Quantitative structural activity relationship study of bis-tetraazacyclic compounds. A novel series of HIV-1 and HIV-2 inhibitors. *J. Med. Chem.* **1995**, *38,* 3865-3873.

[29] W. M. Kazmierski, J. P. Peckman, M. Duan, T. P. Kenakin, S. Jenkinson, K. S. Gudmundsson, S. C. Piscitelli, P. L. Feldman; Recent progress in the discovery of new CCR5 and CXCR4 chemokine receptor antagonists as inhibitors of HIV-1 entry. Part 2. *Curr. Med. Chem. -Anti Infect. Agents* **2005**, *4,* 133-152.

[30] K. Princen, S. Hatse, K. Vermeire, S. Aquaro, E. de Clercq, L. O. Gerlach, M. M. Rosenkilde, T. W. Schwartz, R. Skerlj, G. Bridger, D. Schols; Inhibition of human immunodeficiency virus replication by a dual CCR5/CXCR4 antagonist. *J. Virol.* **2004**, *78,* 12996-13006.

[31] K. Ichiyama, S. Yokoyama-Kumakura, Y. Tanaka, R. Tanaka, K. Hirose, K. Bannai, T. Edamatsu, M. Yanaka, Y. Niitani, N. Miyano-Kurosaki, H. Takaku, Y. Koyanagi, N. Yamamoto; A duodenally absorbable CXC chemokine receptor 4 antagonist, KRH-1636, exhibits a potent and selective anti-HIV-1 activity. *Proc. Natl. Acad. Sci. USA* **2003**, *100,* 4185-4190.

[32] T. Muramaki, A. Yoshida, R. Tanaka, S. Mitsuhashi, K. Hirose, M. Yanaka, N. Yamamoto, Y. Tanaka; KRH-2731: an orally bioavailable CXCR4 antagonist is a potent inhibitor of HIV-1 infection, *Proceedings of the 11th CROI, 2004 Antivirals Pipeline Report,* San Francisco, CA, **2004**, Abstract No. 541.

[33] T. Yamazaki, A. Saitou, M. Ono, S. Yokohama, K. Bannai, K. Hirose, M. Yanaka; Novel nitrogenous compound and use thereof. World Patent WO 2003/029218 (filing date: 27-9-2002).

[34] T. Yamazaki, S. Kikumoto, M. Ono, A. Saitou, H. Takahashi, S. Kumakura, K. Hirose, M. Yanaka, Y. Takemura, S. Suzuki, R. Matsui; Amine compounds and use thereof. World Patent WO 2004/024697 (filing date: 5-9-2003).

[35] H. Tamamura, A. Ojida, T. Ogawa, H. Tsutsumi, H. Masuno, H. Nakashima, N. Yamamoto, I. Hamachi, N. Fujii; Identification of a new class of low molecular weight antagonists against the chemokine receptor CXCR4 having the dipicolylamine-zinc(II) complex structure. *J. Med. Chem.* **2006**, *49,* 3412-3415.

[36] M. L. Verdonk, V. Berdini, M. J. Hartshorn, W. T. M. Mooij, C. W. Murray, R. D. Taylor, P. Watson; Virtual screening using protein-ligand docking: avoidin artificial enrichment. *J. Chem. Inf. Comput. Sci.* **2004**, *44,* 793-806.

[37] *Maybridge bringing life to drug discovery* Maybridge Databases Autumn 2005; Fisher Scientific International: England, **2005**.

[38] C. A. Lipinski, F. Lombardo, B. W. Dominy, P. J. Feeney; Experimental and computational approaches to estimate solubility and permeability in drug discovery and development settings. *Adv. Drug Del. Rev.* **1997**, *23,* 3-25.

[39] *Flexible alignment of small molecules.* Chemical Computing Group, Inc.: Montreal, Canada, **2004**.

[40] P. Labute, C. Williams, M. Feher, E. Sourial, J. M. Schmidt; Flexible alignment of small molecules. *J. Med. Chem.* **2001**, *44,* 1483-1490.

[41] L. O. Gerlach, R. Skerlj, G. Bridger, T. W. Schwartz; Molecular interactions of cyclam and bicyclam non-peptide antagonists with the CXCR4 chemokine receptor. *J. Biol. Chem.* **2001**, *276,* 14153-14160.

[42] S. Hatse, K. Princen, L. O. Gerlach, G. Bridger, G. Henson, E. de Clercq, T. W. Schwartz, D. Schols; Mutation of Asp(171) and Asp(262) of the chemokine receptor CXCR4 impairs its coreceptor function for human immunodeficiency virus-1 entry and abrogates the antagonistic activity of AMD3100. *Mol. Pharmacol.* **2001**, *60,* 164-173.

[43] T. M. Hunter, I. W. McNae, X. Liang, J. Bella, S. Parsons, M. D. Walkinshaw, P. J. Sadler; Protein recognition of macrocycles: binding of anti-HIV metallocyclams to lysozyme. *Proc. Natl. Acad. Sci. USA* **2005**, *102,* 2288-2292.

[44] X. Liang, J. A. Parkinson, M. Weishäupl, R. O. Gould, S. J. Paisey, H. Park, T. M. Hunter, C. A. Blindauer, S. Parsons, P. J. Sadler; Structure and dynamics of metallomacrocycles: recognition of zinc xylyl-bicyclam by an HIV coreceptor. *J. Am. Chem. Soc.* **2002**, *124,* 9105-9112.

[45] M. M. Rosenkilde, L. O. Gerlach, J. S. Jakobsen, R. Skerlj, G. J. Bridger, T. W. Schwartz; Molecular mechanism of AMD3100 antagonism in the CXCR4 receptor. *J. Biol. Chem.* **2004**, *279,* 3033-3041.

[46] G. C. Valks, G. McRobbie, E. A. Lewis, T. J. Hubin, T. M. Hunter, P. J. Sadler, C. Pannecouque, E. de Clercq, S. J. Archibald; Configurationally restricted bismacrocyclic CXCR4 receptor antagonists. *J. Med. Chem.* **2006**, *49,* 6162-6165.

[47] V. I. Pérez-Nueno, S. Pettersson, D. W. Ritchie, J. I. Borrell, J. Teixidó; Discovery of novel HIV entry inhibitors for the CXCR4 receptor by prospective virtual screening. *J. Chem. Inf. Model.* **2009**, *49,* 810-823.

[48] MACCS keys, MDL Information Systems: San Leandro, CA.

[49] V. J. Gillet, D. J. Wild, P. Willet, J. Bradshaw; Similarity and dissimilarity methods for processing chemical structure databases. *The Computer Journal* **1980**, *41,* 547-558.

[50] J. W. Godden, L. Xue, J. Bajorath; Combinatorial preferences affect molecular similarity/diversity calculations using binary fingerprints and Tanimoto coefficients. *J. Chem. Inf. Comput. Sci.* **2000**, *40,* 163-166.

# PARTE EXPERIMENTAL

## Índice de la Parte Experimental.

## 5.0. Instrumentación.

Los **espectros de infrarrojo** (IR) han sido regristrados en un espectrofotómetro *Nicolet Magna 560* en el departamento de Química Orgánica del IQS por la Sra. M. C. Meca, bajo la dirección del Dr. X. Batllori. El número de onda se expresa en $cm^{-1}$. La notación empleada es: *t* (tensión), *f* (flexión), p. KBr (pastilla de bromuro potásico), film (film evaporado de cloroformo).

Los **espectros de resonancia magnética nuclear** ($^1$H-RMN y $^{13}$C-RMN) se han registrado en el aparato *Varian Gemini 300HC* ($^1$H-RMN de 300 MHz y $^{13}$C-RMN de 75.5 MHz) y *Varian 400-MR* ($^1$H-RMN de 400 MHz y $^{13}$C-RMN de 100.6 MHz) por el Dr. X. Batllori y la Sra. N. Ruiz en el departamento de Química Orgánica del IQS, bajo la dirección del Dr. X. Batllori. El desplazamiento químico se expresa en escala $\delta$ en ppm. Para los espectros de $^1$H-RMN se ha tomado como referencia la señal de tretrametilsilano (TMS) o 2,2,3,3-tetradeutero-3-(trimetilsilil)-propionato sódico (TSPNa). Para los espectros de $^{13}$C-RMN se ha tomado como referencia la señal del disolvente: $CDCl_3$ a 77.0 ppm, d-TFA a 163.8 ppm, $CD_3OD$ a 49.0 ppm. La notación empleada es: s (singlete), d (doblete), t (triplete), q (cuarteto), quint (quinteto), m (multiplete), sa (singlete ancho), sc (señal compleja). Se indican con * las señales de asignación intercambiable.

Los **análisis elementales orgánicos** (AEO) se han realizado en un instrumento *Carlo-Erba CHNS-O/EA1108* y *EuroVector EuroEA3000* en el departamento de Química Orgánica del IQS por la Sra. N. Ruiz, bajo la dirección del Dr. X. Batllori.

Los **espectros de masas** de baja y alta resolución (MS y HRMS) han sido realizados bajo la dirección del Dr. E. Gutián en el Servicio de Espectrometría de Masas de la Universidad de Santiago de Compostela. Los MS realizados mediante la técnica de impacto electrónico (70 eV) de baja resolución han sido registrados en un espectrómetro de masas *Hewlett.Packard-5988-A* de tipo cuadrupolar, los de alta resolución y los FAB han sido realizados en un espectrómetro de masas *VG AutoSpec (Micromass Instruments) Trisector EBE* de alta resolución. Los MS de ionización por electrospray (ESI) con analizador tipo TOF de baja y de alta resolución se han realizado en un espectrómetro de masas modelo *Biotof II* de la casa *Bruker*.

A todos ellos, mi más sincero agradecimiento.

## 5.1. Síntesis de aminas simétricas.

### 5.1.1. Síntesis de *N*-(4-((2-(pirrolidin-1-il)etilamino)metil)bencil)-2-(pirrolidin-1-il)etanamina (32{*4,4*}).

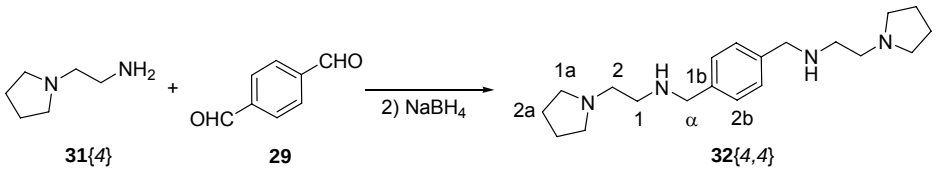


**31**{*4*} **29** **32**{*4,4*}

Se disuelven 0.61 g (4.5 mmol) de tereftalaldehído (**29**) y 1.04 g (9.0 mmol) de amina **31**{*4*} en 30 mL de MeOH anhidro. Se añade tamiz molecular de 4 Å y se agita a temperatura de reflujo bajo atmósfera de nitrógeno durante 24 h. Se filtra el tamiz molecular y se adicionan 0.34 g (9.0 mmol) de $NaBH_4$. Se deja reaccionar a temperatura ambiente durante 16 h. Transcurrido este tiempo se añade agua y se extrae con $CH_2Cl_2$. La fase orgánica se lava con salmuera y se seca sobre $MgSO_4$ anhidro. Se elimina el disolvente a presión reducida y se obtienen 1.32 g (4.0 mmol, 89% rendimiento) de un aceite amarillo **32**{*4,4*}.

**Datos espectroscópicos:**

**IR** (film): $\nu$ ($cm^{-1}$) 3310 (*t* N-H), 2962, 2928, 2874, 2794 (*t* $Csp^3$-H), 1485, 1444 (*f* $Csp^3$-H).

**$^1$H-RMN** (300 MHz, $CDCl_3$): δ (ppm) 7.27 (s, 4H, Ph), 3.79 (s, 4H, H-Cα), 2.73 (t, $^3J_{H,H}$=6.0 Hz, 4H, H-C1), 2.59 (t, $^3J_{H,H}$=6.0 Hz, 4H, H-C2), 2.47 (m, 8H, H-C1a), 2.20 (sa, 2H, deuterable, NH), 1.75 (quint, $^3J_{H,H}$=3.3 Hz, 8H, H-C2a).

**$^{13}$C-RMN** (75.5 MHz, $CDCl_3$): δ (ppm) 138.8 (C1b), 128.0 (C2b), 55.9 (Cα), 54.2 (C1a), 53.8 (C2), 47.8 (C1), 23.5 (C2a).

**MS** (FAB): m/z 331.3 (100) $[M+H]^+$, 330.3 (18), 329.3 (77).

**HRMS** (FAB): ($C_{20}H_{35}N_4$) $[M+H]^+$ Calculado: 331.2862. Obtenido: 331.2867.

## 5.1.2. Síntesis de *N*-(4-((3-(pirrolidin-1-il)propilamino)metil)bencil)-3-(pirrolidin-1-il)propan-1-amina (32{*5,5*}).

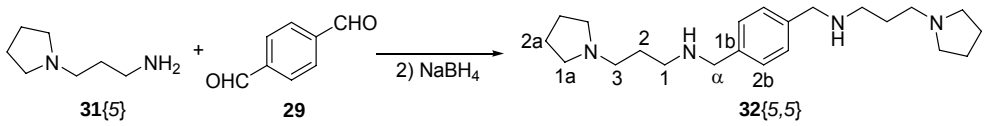


**31**{*5*} **29** **32**{*5,5*}

Se sigue el mismo procedimiento que para **32**{*4,4*} pero utilizando 0.75 g (5.5 mmol) de tereftalaldehído (**29**), 1.47 g (11.1 mmol) de amina **31**{*5*} y 0.43 g (11.1 mmol) de $NaBH_4$. Se obtienen 1.98 g (5.5 mmol, 99% rendimiento) de un aceite amarillo **32**{*5,5*}.

**Datos espectroscópicos:**

**IR** (film): $\nu$ ($cm^{-1}$) 3282 (*t* N-H), 2936, 2789 (*t* $Csp^3$-H), 1458 (*f* $Csp^3$-H).

**$^1$H-RMN** (300 MHz, $CDCl_3$): δ (ppm) 7.26 (s, 4H, Ph), 3.77 (s, 4H, H-Cα), 2.69 (t, $^3J_{H,H}$=7.0 Hz, 4H, H-C1), 2.49 (m, 12H, H-C3, H-C1a), 2.08 (sa, 2H, deuterable, NH), 1.75 (m, 12H, H-C2, H-C2a).

**$^{13}$C-RMN** (75.5 MHz, $CDCl_3$): δ (ppm) 138.5 (C1b), 128.0 (C2b), 54.6 (Cα), 54.1 (C1a), 53.5 (C3), 47.9 (C1), 28.8 (C2), 23.4 (C2a).

**MS** (IE): m/z 359.2 (1) $[M+H]^+$, 232.0 (55), 231.0 (11), 230.0 (59), 161.0 (27), 127.0 (11), 98.0 (18), 84.0 (100).

**HRMS** (ESI): ($C_{22}H_{39}N_4$) $[M+H]^+$ Calculado: 359.3169. Obtenido: 359.3158.

## 5.1.3. Síntesis de *N*-(4-((3-(1*H*-imidazol-1-il)propilamino)metil)bencil)-3-(1*H*-imidazol-1-il)propan-1-amina (32{*6,6*}).

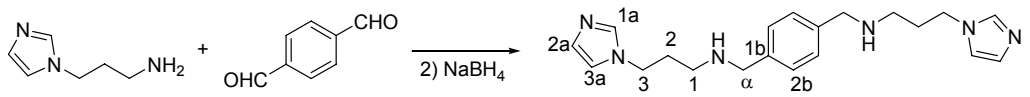


**31**{*6*} **29** **32**{*6,6*}

Se sigue el mismo procedimiento que para **32**{*4,4*} pero utilizando 0.54 g (3.9 mmol) de tereftalaldehído (**29**), 1.00 g (7.8 mmol) de amina **31**{*6*} y 0.30 g (7.8 mmol) de $NaBH_4$. Se obtienen 1.38 g (3.9 mmol, rendimiento cuantitativo) de un aceite amarillo **32**{*6,6*}.

**Datos espectroscópicos:**

**IR** ($CHCl_3$): $\nu$ ($cm^{-1}$) 3277(*t* N-H), 3103 (*t* $Csp^2$-H), 2935, 2815 (*t* $Csp^3$-H), 1508 (*t* esqueleto heteroaromático), 1453 (*f* $Csp^3$-H).

**$^1$H-RMN** (300 MHz, $CDCl_3$): δ (ppm) 7.41 (s, 2H, H-C1a), 7.26 (s, 4H, Ph), 7.02 (s, 2H, H-C2a), 6.88 (s, 2H, H-C3a), 4.04 (t, $^3J_{H,H}$=6.9 Hz, 4H, H-C3), 3.74 (s, 4H, H-C$\alpha$), 2.60 (t, $^3J_{H,H}$=6.9 Hz, 4H, H-C1), 2.05 (s, 2H, deuterable, NH), 1.92 (quint, $^3J_{H,H}$=6.9 Hz, 4H, H-C2).

**$^{13}$C-RMN** (75.5 MHz, $CDCl_3$): δ (ppm) 138.8 (C1a), 137.1 (C1b), 129.2 (C3a), 128.2 (C2b), 118.7 (C2a), 53.6 (C$\alpha$), 45.6 (C3), 44.6 (C1), 31.3 (C2).

**MS** (IE): m/z 353.0 (1) $[M+H]^+$, 257.0 (26), 228.9 (100), 188.9 (29), 138.0 (22), 124.0 (42), 104.0 (94), 81.0 (52).

**HRMS** (ESI): ($C_{20}H_{28}N_6$) $[M+H]^+$ Calculado: 353.2448. Obtenido: 353.2456.

## 5.1.4. Síntesis de *N*-(4-((2-(piperidin-1-il)etilamino)metil)bencil)-2-(piperidin-1-il)etanamina (32{*7,7*}).

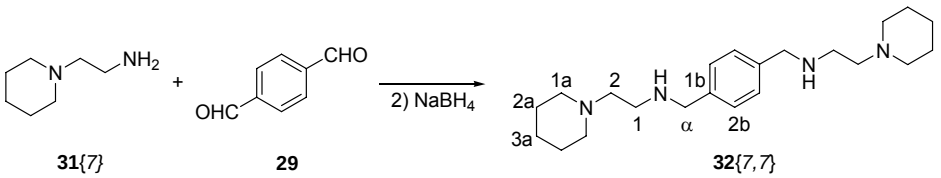


**31**{*7*} **29** **32**{*7,7*}

Se sigue el mismo procedimiento que para **32**{*4,4*} pero utilizando 0.29 g (2.1 mmol) de tereftalaldehído (**29**), 0.56 g (4.3 mmol) amina **31**{*7*} y 0.16 g (4.3 mmol) de $NaBH_4$. Se obtienen 0.76 g (2.1mmol, rendimiento cuantitativo) de un aceite amarillo **32**{*7,7*}.

**Datos espectroscópicos:**

**IR** (film): $\nu$ ($cm^{-1}$) 3310 (*t* N-H).

**$^{1}$H-RMN** (300MHz, $CDCl_3$): δ (ppm) 7.32 (s, 4H, Ph), 3.75 (s, 4H, H-Cα), 2.69 (t, $^{3}J_{H,H}$=7.0 Hz, 4H, H-C1), 2.47 (t, $^{3}J_{H,H}$=7.0 Hz, 4H, H-C2), 2.39 (m, 8H, H-C1a), 1.62-1.39 (m, 12H, H-C2a, H-C3a).

**$^{13}$C-RMN** (75.5MHz, $CDCl_3$): δ (ppm) 139.4 (C1b), 129.6 (C2b), 59.0 (Cα), 55.7 (C1a), 54.1 (C2), 46.1 (C1), 26.7 (C2a), 25.2 (C3a).

**AEO**: Calculado ($C_{22}H_{38}N_4$): C 73.69%, H 10.68%, N 15.63%. Obtenido: C 73.78%, H 10.56%, N 15.45%.

## 5.1.5. Síntesis de *N*-(4-((3-(2-metilpiperidin-1-il)propilamino)metil)bencil)-3-(2-metilpiperidin-1-il)propan-1-amina (32{*8,8*}).

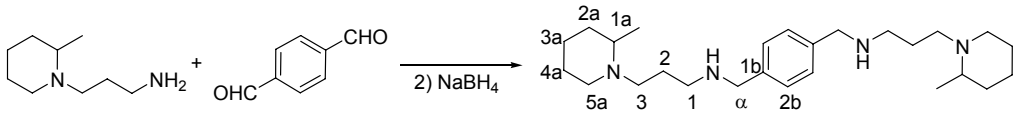


**31**{*8*} **29** **32**{*8,8*}

Se sigue el mismo procedimiento que para **32**{*4,4*} pero utilizando 0.43 g (3.2 mmol) de tereftalaldehído (**29**), 1.04 g (6.4 mmol) de amina **31**{*8*} y 0.25 g (6.4 mmol) de $NaBH_4$. Se obtienen 1.33 g (3.2 mmol, rendimiento cuantitativo) de un aceite marrón pálido **32**{*8,8*}.

**Datos espectroscópicos:**

**IR** (film): $\nu$ ($cm^{-1}$) 3282 (*t* N-H), 2929, 2854, 2793 (*t* $Csp^3$-H), 1449, 1372 (*f* $Csp^3$-H).

**$^1$H-RMN** (300 MHz, $CDCl_3$): δ (ppm) 7.27 (s, 4H, Ph), 3.77 (s, 4H, H-Cα), 2.87 (m, 2H, $H_{eq}$-C5a), 2.73 (m, 2H, $H_{eq}$-C3), 2.63 (t, $^3J_{H,H}$=6.9 Hz, 4H, H-C1), 2.36 (m, 2H, $H_{ax}$-C3), 2.26 (m, 2H, H-C1a), 2.14 (sa, 2H, deuterable, NH), 2.11 (m, 2H, $H_{ax}$-C5a),1.68 (quint, $^3J_{H,H}$=6.9 Hz, 4H, H-C2), 1.61 (m, 2H, $H_{eq}$-C4a), 1.58* (m, 2H, $H_{eq}$-C2a), 1.52* (m, 2H, $H_{eq}$-C3a), 1.44 (m, 2H, $H_{ax}$-C4a), 1.28 (m, 4H, $H_{ax}$-C2a, $H_{ax}$-C3a), 1.05 (d, $^3J_{H,H}$=6.3 Hz, 6H, $CH_3$).

**$^{13}$C-RMN** (75.5 MHz, $CDCl_3$): δ (ppm) 138.8 (C1b), 128.0 (C2b), 55.9 (C1a), 53.7 (Cα), 52.3 (C3), 52.1 (C5a), 48.3 (C1), 34.7* (C2a), 26.2 (C4a), 25.7 (C2), 24.0* (C3a), 19.1 ($CH_3$).

**AEO**: Calculado ($C_{26}H_{46}N_4$): C 75.31%, H 11.18%, N 13.51%. Obtenido: C 75.20%, H 10.93%, N 13.60%.

**MS** (IE): m/z 415.4 (0.4) $[M+H]^+$, 112.1 (100).

## 5.1.6. Síntesis de *N*-(4-((3-(4-metilpiperazin-1-il)propilamino)metil)bencil)-3-(4-metilpiperazin-1-il)propan-1-amina (32{*9,9*}).

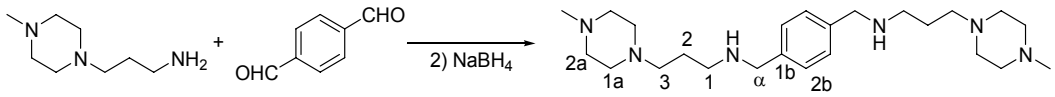


**31**{*9*} **29** **32**{*9,9*}

Se sigue el mismo procedimiento que para **32**{*4,4*} pero utilizando 0.48 g (3.5 mmol) de tereftalaldehído (**29**), 1.14 g (7.0 mmol) de amina **31**{*9*} y 0.27 g (7.0 mmol) de $NaBH_4$. Se obtienen 1.28 g (3.1 mmol, 87% rendimiento) de un aceite marrón **32**{*9,9*}.

**Datos espectroscópicos:**

**IR** (film): $\nu$ ($cm^{-1}$) 3281 (*t* N-H), 2935, 2793 (*t* $Csp^3$-H), 1458 (*f* $Csp^3$-H).

**$^1$H-RMN** (300 MHz, $CDCl_3$): δ (ppm) 7.26 (s, 4H, Ph), 3.76 (s, 4H, H-Cα), 2.66 (t, $^3J_{H,H}$=6.9 Hz, 4H, H-C1), 2.42 (m, 22H, H-C3, H-C1a, H-C2a, NH), 2.27 (s, 6H, $CH_3$), 1.70 (quint, $^3J_{H,H}$=6.9 Hz, 4H, H-C2).

**$^{13}$C-RMN** (75.5 MHz, $CDCl_3$): δ (ppm) 138.8 (C1b), 128.0 (C2b), 57.0 (Cα), 55.1 (C2a), 53.7 (C3), 53.2 (C1a), 48.1 (C1), 46.0 ($CH_3$), 26.9 (C2).

**MS** (IE): m/z 417.1 (9) $[M+H]^+$, 416.1 (28) $[M]^+$, 289.0 (6), 260.0 (14), 259.0 (58), 156.0 (8), 155.0 (30), 141.0 (14), 127.0 (39), 113.0 (100), 70 (29) .

**HRMS** (ESI): ($C_{24}H_{44}N_6$) $[M+H]^+$ Calculado: 417.3700. Obtenido: 417.3702.

## 5.1.7. Síntesis de *N*-(4-((2-morfolinoetilamino)metil)bencil)-2-morfolinoetilamina (32{*10,10*}).

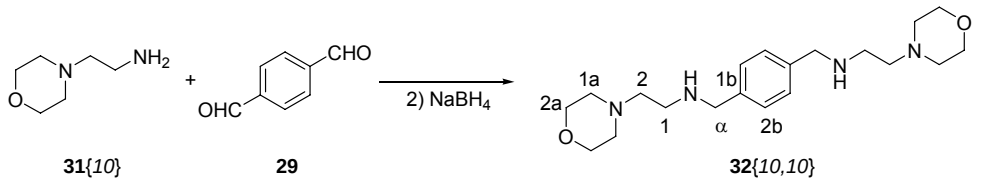


**31**{*10*} **29** **32**{*10,10*}

Se sigue el mismo procedimiento que para **32**{*4,4*} pero utilizando 0.54 g (4.0 mmol) de tereftalaldehído (**29**), 1.05 g (8.0 mmol) de amina **31**{*10*} y 0.31 g (8.0 mmol) de $NaBH_4$. Se obtienen 0.93 g (2.6 mmol, 64% rendimiento) de un sólido blanquecino **32**{*10,10*}.

**Datos espectroscópicos:**

**IR** (film): $\nu$ ($cm^{-1}$) 3341 (*t* N-H), 2968, 2930, 2817 (*t* $Csp^3$-H), 1446 (*f* $Csp^3$-H), 1117 (*t as* C-O-C), 830 (*t sim* C-O-C).

**$^1$H-RMN** (300 MHz, $CDCl_3$): δ (ppm) 7.27 (s, 4H, Ph), 3.79 (s, 4H, H-C$\alpha$), 3.69 (t, $^3J_{H,H}$=4.6 Hz, 8H, H-C2a), 2.70 (t, $^3J_{H,H}$=6.0 Hz, 4H, H-C1), 2.50 (t, $^3J_{H,H}$=6.0 Hz, 4H, H-C2), 2.403 (t, $^3J_{H,H}$=4.6 Hz, 8H, H-C1a), 1.82 (s, 2H, deuterable, NH).

**$^{13}$C-RMN** (75.5 MHz, $CDCl_3$): δ (ppm) 139.0 (C1b), 128.0 (C2b), 67.0 (C2a), 58.3 (C$\alpha$), 53.7 (C2, C1a), 45.3 (C1).

**AEO**: Calculado ($C_{20}H_{34}N_4O_2$): C 66.26%, H 9.45%, N 15.46%, O 8.83%. Obtenido: C 66.38%, H 9.67%, N 15.42%.

**MS** (IE): m/z 363.4 (5) $[M+H]^+$, 362.4 (6) $[M]^+$, 262.3 (38), 233.2 (20), 232.2 (45), 100.0 (100).

## 5.1.8. Síntesis de *N*-(4-((3-morfolinopropilamino)metil)bencil)-3-morfolinopropan-1-amina (32{*11,11*}).

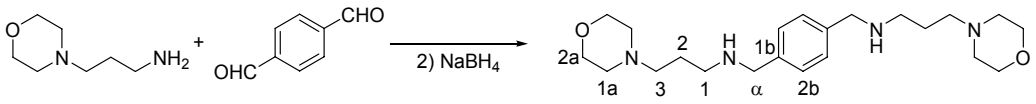


**31**{*11*} **29** **32**{*11,11*}

Se sigue el mismo procedimiento que para **32**{*4,4*} pero utilizando 0.47 g (3.5 mmol) de tereftalaldehído (**29**), 1.00 g (7.0 mmol) de amina **31**{*11*} y 0.27 g (7.0 mmol) de $NaBH_4$. Se obtienen 1.16 g (3.0 mmol, 85% rendimiento) de un aceite amarillo **32**{*11,11*}.

**Datos espectroscópicos:**

**IR** (film): $\nu$($cm^{-1}$) 3301 (*t* N-H), 2948, 2852, 2806 (*t* $Csp^3$-H), 1456 (*f* $Csp^3$-H), 1118 (*t as* C-O-C), 862 (*t sim* C-O-C).

**$^1$H-RMN** (300 MHz, $CDCl_3$): δ (ppm) 7.27 (s, 4H, Ph), 3.79 (s, 4H, H-C$\alpha$), 3.70 (t, $^3J_{H,H}$=4.6 Hz, 8H, H-C2a), 2.68 (t, $^3J_{H,H}$=7.0 Hz, 4H, H-C1), 2.41 (m, 12H, H-C3, H-C1a), 1.81 (s, 2H, deuterable, NH), 1.70 (quint, $^3J_{H,H}$=7.0 Hz, 4H, H-C2).

**$^{13}$C-RMN** (75.5 MHz, $CDCl_3$): δ (ppm) 138.9 (C1b), 128.0 (C2b), 67.0 (C2a), 57.4 (C$\alpha$), 53.8 (C1a, C3), 48.0 (C1), 26.8 (C2).

**MS** (IE): m/z 390.3 (2) $[M]^+$, 247.2 (2), 100.0 (100).

**HRMS** (IE): ($C_{22}H_{38}N_4O_2$) Calculado: 390.2995. Obtenido: 390.3007.

## 5.1.9. Síntesis de *N*-(4-((4-(piperidin-1-il)fenillimino)metil)benciliden)-4-(piperidin-1-il)bencenamina (32{*16,16*}).

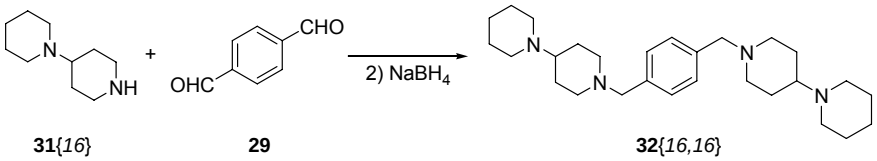


**31**{*16*} **29** **32**{*16,16*}

Se disuelven 0.50 g (3.0 mmol) de amina **31**{*16*} y 0.20 g (1.5 mmol) de tereftaldeído (**29**) en 30 mL de MeOH anhidro. Se calienta a reflujo durante 9 h bajo atmósfera de nitrógeno. Se deja enfriar a temperatura ambiente y se añaden 0.11 g (3.0 mmol) de $NaBH_4$. Se deja reaccionar a temperatura ambiente durante 6 h. Se añade agua, se filtra el sólido formado, se lava con agua y se seca sobre $P_2O_5$. Se obtienen 0.30 g (0.7 mmol, 46% rendimiento) de un sólido blanquecino **32**{*16,16*}.

**Datos espectroscópicos:**

**$^1$H-RMN** (300 MHz, d-TFA): δ (ppm) 7.59 (s, 4H, Ph), 4.44 (s, 4H, $\underline{CH_2}$-Ph), 3.86 (m, 4H, $CH_2$), 3.66 (m, 6H, $CH_2$, CH), 3.28 (m, 4H, $CH_2$), 3.05 (m, 4H, $CH_2$), 2.52 (m, 4H, $CH_2$), 2.30 (m, 4H, $CH_2$), 2.07 (m, 4H, $CH_2$), 1.89 (m, 6H, $CH_2$), 1.52 (m, 2H, $CH_2$).

## 5.1.10. Síntesis de *N*-(4-((3-(piperidin-1-il)propilamino)metil)bencil)-3-(piperidin-1-il)propan-1-amina (32{*19,19*}).

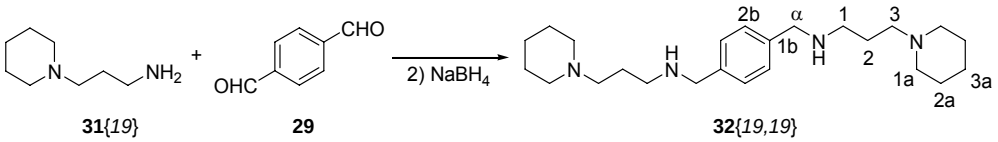


**31**{*19*} **29** **32**{*19,19*}

Se disuelven 0.47 g (3.5 mmol) de tereftaldeído (**29**) y 1.01 g (6.9 mmol) de amina **31**{*19*} en 10 mL de MeOH anhidro. Se añade $Na_2SO_4$ anhidro y se calienta en el microondas a 100 ºC durante 2 h. Se filtra y se adicionan 20 mL de MeOH anhidro y 0.26 g (6.9 mmol) de $NaBH_4$. Se deja reaccionar a temperatura ambiente durante 12 h. Se añade agua y se extrae con $CH_2Cl_2$. La fase orgánica se lava con salmuera y se seca sobre $MgSO_4$ anhidro. Se elimina el disolvente a presión reducida y se obtienen 1.21 g (3.1 mmol, 91% rendimiento) de un aceite amarillo pálido **32**{*19,19*}.

**Datos espectroscópicos:**

**IR** (film): $\nu$ ($cm^{-1}$) 3285 (*t* N-H), 2933, 2852, 2802 (*t* $Csp^3$-H), 1445 (*f* $Csp^3$-H).

**$^1$H-RMN** (300 MHz, $CDCl_3$): δ (ppm) 7.26 (s, 4H, Ph), 3.76 (s, 4H, H-Cα), 2.66 (t, $^3J_{H,H}$=6.9 Hz, 4H, H-C1), 2.37-2.32 (m, 12H, H-C3, H-C1a), 2.22 (sa, 2H, deuterable, NH), 1.71 (quint, $^3J_{H,H}$=6.9 Hz, 4H, H-C2), 1.56 (quint, $^3J_{H,H}$=5.7 Hz, 8H, H-C2a), 1.42 (m, 4H, H-C3a).

**$^{13}$C-RMN** (75.5 MHz, $CDCl_3$): δ (ppm) 138.8 (C1b), 128.0 (C2b), 57.8* (Cα), 54.7 (C1a), 53.6* (C3), 48.3 (C1), 26.0 (C2a), 24.5 (C3c).

**AEO**: Calculado ($C_{24}H_{42}N_4$): C 74.56%, H 10.95%, N 14.49%. Obtenido: C 74.77%, H 10.98%, N 14.30%.

**MS** (FAB): m/z 387.4 (100) $[M+H]^+$, 385.3 (23), 126.1 (19), 112.1 (39).

**HRMS** (FAB): ($C_{24}H_{43}N_4$) $[M+H]^+$ Calculado: 387.3488. Obtenido: 387.3487.

## 5.1.11. Síntesis de *N*-(3-((3-(2-metilpiperidin-1-il)propilamino)metil)bencil)-3-(2-metilpiperidin-1-il)propan-1-amina (50{*8,8*}).

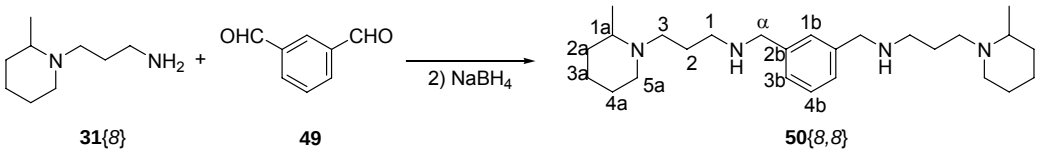


**31**{*8*} **49** **50**{*8,8*}

Se sigue el mismo procedimiento que para **32**{*4,4*} pero utilizando 0.40 g (2.9 mmol) de isoftaldehído (**49**), 0.95 g (5.8 mmol) de amina **31**{*8*} y 0.22 g (5.8 mmol) de $NaBH_4$. Se obtienen 1.04 g (2.5 mmol, 81% rendimiento) de un aceite amarillo **50**{*8,8*}.

**Datos espectroscópicos:**

**IR** (film): $\nu$ ($cm^{-1}$) 3277 (*t* N-H), 2929, 2854, 2793 (*t* $Csp^3$-H), 1448, 1372 (*f* $Csp^3$-H).

**$^1$H-RMN** (300 MHz, $CDCl_3$): δ (ppm) 7.25 (m, 4H, Ph), 3.77 (s, 4H, H-Cα), 2.86 (m, 2H, $H_{eq}$-C5a), 2.73 (m, 2H, $H_{eq}$-C3), 2.64 (t, $^3J_{H,H}$=6.9 Hz, 4H, H-C1), 2.36 (m, 2H, $H_{ax}$-C3), 2.25 (m, 2H, H-C1a), 2.11 (m, 2H, $H_{ax}$-C5a), 2.00 (sa, 2H, deuterable, NH), 1.68 (quint, $^3J_{H,H}$=6.9 Hz, 4H, H-C2), 1.60 (m, 8H, $H_{eq}$-C2a, $H_{eq}$-C3a, H-C4a), 1.28 (m, 4H, $H_{ax}$-C2a, $H_{ax}$-C3a), 1.05 (d, $^3J_{H,H}$=6.3 Hz, 6H, $CH_3$).

**$^{13}$C-RMN** (75.5 MHz, $CDCl_3$): δ (ppm) 140.4 (C2b), 128.3* (C1b), 127.8* (C4b), 126.6 (C3b), 55.9 (C1a), 54.1 (Cα), 52.3 (C3), 52.1 (C5a), 48.4 (C1), 34.7** (C2a), 26.2 (C4a), 25.8 (C2), 24.0** (C3a), 19.2 ($CH_3$).

**AEO**: Calculado ($C_{26}H_{46}N_4$): C 75.31%, H 11.18%, N 13.51%. Obtenido: C 75.10%, H 11.18%, N 13.62%

**MS** (IE): m/z 415.5 (2) $[M+1]^+$, 414.5 (6) $[M]^+$, 260.3 (22), 161.2 (15), 112.2 (100).

**HRMS** (IE): ($C_{26}H_{46}N_4$) Calculado: 414.3722. Obtenido: 414.3718.

## 5.1.12. Síntesis de *N*-(1-(4-(1-(3-morfolinopropilamino)etil)fenil)etil)-3-morfolinopropan-1-amina (56{*11,11*}).

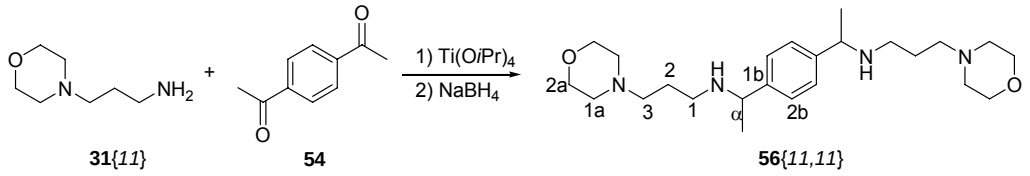


**31**{*11*}  **54**  **56**{*11,11*}

Se disuelven 0.41 g (2.5 mmol) de 1,4-diacetilbenceno (**54**), 0.72 g (5.0 mmol) de amina **31**{*11*} y 2.84 g (10.0 mmol) de Ti(O*i*Pr)$_4$ en 15 mL de MeOH anhidro. Se calienta la disolución a 60 ºC y bajo atmósfera de nitrógeno durante 6 h 30 min. A continuación se deja enfriar a temperatura ambiente y se añaden 0.19 g (5.0 mmol) de $NaBH_4$ y se deja reaccionar a temperatura ambiente durante 12 h. A la mezcla se le añaden 15 mL de $H_2O$ y se filtra. El filtrado se extrae con $CH_2Cl_2$ (2×50 mL). La fase orgánica se lava con salmuera y se seca sobre $MgSO_4$ anhidro. Se elimina el disolvente a presión reducida y el crudo obtenido se purifica por cromatografía de columna (fase estacionaria alúmina y gradiente de eluyente de $CH_2Cl_2$ a $CH_2Cl_2$/MeOH 50:1). Se obtienen 0.61 g (1.5 mmol, 58% rendimiento) de **56**{*11,11*} como semisólido amarillento.

**Datos espectroscópicos:**

**IR** (film): $\nu$(cm$^{-1}$) 3293 (*t* N-H), 2956, 2853, 2807 (*t* Csp$^3$-H), 1456, 1368 (*f* Csp$^3$-H), 1118 (*t as* C-O-C), 863 (*t sim* C-O-C).

**$^1$H-RMN** (300 MHz, $CDCl_3$): δ (ppm) 7.27 (m, 4H, Ph), 3.73 (q, $^3J_{H,H}$=6.6 Hz, 2H, H-C$\alpha$), 3.68 (t, $^3J_{H,H}$=4.6 Hz, 8H, H-C2a), 2.68-2.33 (sc, 16H, H-C1, H-C3, H-C1a), 1.65 (quint, $^3J_{H,H}$=7.0 Hz, 4H, H-C2), 1.34 (d, $^3J_{H,H}$=6.6 Hz, 6H, $CH_3$).

**$^{13}$C-RMN** (75.5 MHz, $CDCl_3$): δ (ppm) 144.1 (C1b), 126.4 (C2b), 67.0 (C2a), 58.1 (C$\alpha$), 57.4 (C3), 53.8 (C1a), 46.5 (C1), 26.8 (C2), 24.3 ($CH_3$).

**MS** (ESI): m/z 419.3 [M+H]$^+$, 247.2 (2), 100.0 (100).

**HRMS** (ESI): ($C_{24}H_{43}N_4O_2$) [M+H]$^+$ Calculado: 419.3381. Obtenido: 419.3382.

## 5.2. Síntesis de hidrazonas simétricas.

### 5.2.1. Síntesis de ((4-(*N*-(piperidin-1-il)imino)metil)fenil)-*N*-(piperidin-1-il)metanimina (33{*1,1*}).

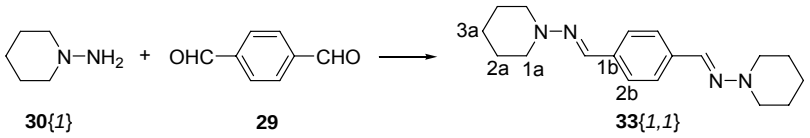


**30**{*1*} **29** **33**{*1,1*}

Se disuelven 1.51 g (14.7 mmol) de hidrazina **30**{*1*} en 30 mL de MeOH anhidro. Acto seguido se adicionan 0.992 g (7.33mmol) de tereftalaldehído (**29**). La solución restante se calienta a reflujo durante 16 h bajo atmósfera de nitrógeno y en presencia de tamiz molecular de 4 Å. A continuación se filtra en caliente el tamiz molecular. Se recoge el filtrado y se elimina parcialmente el disolvente hasta casi sequedad y se introduce en la nevera. Se filtra el sólido y se lava con de MeOH frío. El sólido obtenido se seca sobre pentóxido de fósforo. Se obtienen 1.42 g (4.8 mmol, rendimiento 65%) de un sólido fino amarillo **33**{*1,1*}.

**Datos espectroscópicos:**

**IR** (film): $\nu$ ($cm^{-1}$) 1576 (*t* C=N).

**$^{1}$H-RMN** (300 MHz, $CDCl_3$): δ (ppm) 7.55 (s, 4H, Ph), 7.53 (s, 2H, CH=N), 3.16 (m, 8H, H-C1a), 1.79-1.71 (m, 8H, H-C2a), 1.58-1.50 (m, 4H, H-C3a).

**$^{13}$C-RMN** (75.5 MHz, $CDCl_3$): δ (ppm) 136.0 (C1b), 134.3 (C=N), 125.9 (C2b), 52.1 (C1a), 25.3 (C2a), 24.2 (C3a).

**AEO**: Calculado ($C_{18}H_{26}N_4$): C 72.44%, H 8.78%, N 18.77%. Obtenido: C 72.40%, H 8.81%, N 18.83%.

## 5.2.2. Síntesis de ((4-(*N*-(2,6-dimetilpiperidin-1-il)imino)metil)fenil)-*N*-(2,6-dimetilpiperidin-1-il)metanimina (33{*2,2*}).

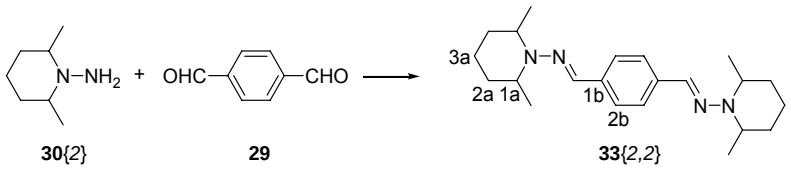


**30**{*2*} **29** **33**{*2,2*}

Se sigue el mismo procedimiento que para **33**{*1,1*} pero utilizando 1.20 g (8.4 mmol) de amina **30**{*2*} y 0.57 g (4.2 mmol) de tereftalaldehído (**29**). Se obtienen 1.05 g (3.0 mmol, rendimiento 65%) de un sólido amarillo **33**{*2,2*}.

**Datos espectroscópicos:**

**IR** (film): $\nu$ ($cm^{-1}$) 1684 (*t* C=N).

**$^{1}$H-RMN** (300MHz, $CDCl_3$): δ (ppm) 7.87 (s, 2H, CH=N), 7.64 (s, 4H, Ph), 3.31-3.27 (m, 4H, H-C1a), 1.83-1.51 (m, 12H, H-C2a, H-C3a), 1.03 (d, $^{3}J_{H,H}$=6.0 Hz, 12H, $CH_3$).

**$^{13}$C-RMN** (75.5MHz, $CDCl_3$): δ (ppm) 146.6 (C=N), 136.0 (C1b), 126.8 (C2b), 56.1 (C1a), 32.4 (C2a), 20.0 ($CH_3$), 19.9 (C3a).

**AEO**: Calculado ($C_{22}H_{34}N_4$): C 74.53%, H 9.67%, N 15.80%. Obtenido: C 74.30%, H 9.35%, N 15.84%.

## 5.2.3. Síntesis de ((4-(*N*-(4-metilpiperazin-1-il)imino)metil)fenil)-*N*-(4-metilpiperazin-1-il)metanimina (33{*3,3*}).

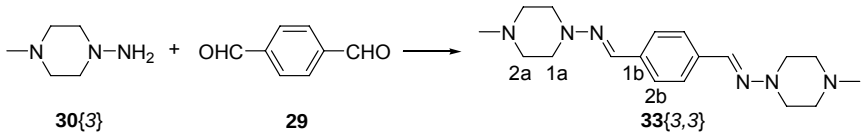


**30**{*3*} **29** **33**{*3,3*}

Se sigue el mismo procedimiento que para **33**{*1,1*} pero utilizando 0.64 g (5.4 mmol) de amina **30**{*3*} y 0.37 g (2.7 mmol) de tereftalaldehído (**29**). Se obtienen 0.67 g (2.0 mmol, rendimiento 75%) de sólido amarillento **33**{*3,3*}.

**Datos espectroscópicos:**

**IR** (film): $\nu$ ($cm^{-1}$) 1579 (*t* C=N).

**$^{1}$H-RMN** (300MHz, $CDCl_3$): δ (ppm) 7.57 (s, 4H, Ph), 7.53 (s, 2H, CH=N), 3.23 (m, 8H, H-C1a), 2.62 (m, 8H, H-C2a), 2.36 (s, 6H, $CH_3$).

**$^{13}$C-RMN** (75.5MHz, $CDCl_3$): δ (ppm) 135.8 (C1b), 135.4 (C=N), 126.2 (C2b), 54.5 (C1a), 51.0 (C2a), 46.0 ($CH_3$).

**AEO**: Calculado ($C_{18}H_{28}N_6$): C 65.82%, H 8.59%, N 25.59%. Obtenido: C 65.51%, H 8.72%, N 25.17%.

## 5.2.4. Síntesis de *N,N'*-(1,4-fenilendimetilidin)bis-morfolino-4-amina (33{*12,12*}).

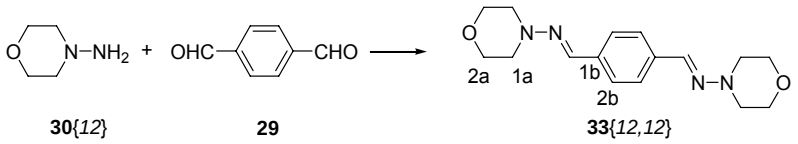


**30**{*12*} **29** **33**{*12,12*}

Se sigue el mismo procedimiento que para **33**{*1,1*} pero utilizando 1.00 g (9.8 mmol) de amina **30**{*12*} y 0.66 g (4.9 mmol) de tereftalaldehído (**29**). Se obtienen 1.16 g (3.8 mmol, rendimiento 78%) de sólido amarillento **33**{*12,12*}.

**Datos espectroscópicos:**

**IR** (p. KBr): $\nu$ ($cm^{-1}$) 1574 (*t* C=N).

**$^{1}$H-RMN** (300MHz, d-TFA): δ (ppm) 8.98 (s, 2H, CH=N), 7.99 (s, 4H, H-C2b), 4.34 (sa, 8H, H-C1a), 3.87 (as, 8H, H-C2a).

**$^{13}$C-RMN** (75.5MHz, d-TFA): δ (ppm) 169.3 (CH=N), 136.4 (C1b), 132.1 (C2b), 64.6 (C2a), 57.8 (C1a).

**AEO**: Calculado ($C_{16}H_{22}N_4O_2$): C 63.55%, H 7.33%, N 18.53%, O 10.58%. Obtenido: C 63.54%, H 7.23%, N 18.23%.

**MS** (IE): m/z 303.0 (20) $[M+1]^+$, 302.0 (100) $[M]^+$, 245.0 (27), 216.0 (7).

## 5.2.5. Síntesis de *N,N'*-(1,4-fenilendimetilidin)bis-4*H*-1,2,4-triazol-4-amina (33{*17,17*}).

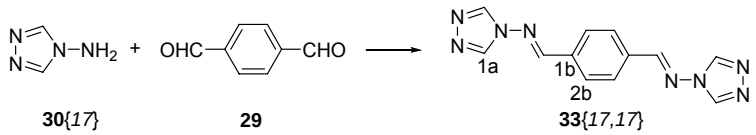


**30**{*17*} **29** **33**{*17,17*}

Se disuelven 1.00 g (11.8 mmol) de amina **30**{*17*} y 0.79 g (5.9 mmol) de tereftalaldehído (**29**) en 30 mL de MeOH anhidro. La mezcla se calienta a reflujo durante 8 h bajo atmósfera de nitrógeno. Se deja enfriar a temperatura ambiente, se filtra y se lava el sólido obtenido con MeOH frío. Se obtienen 1.17 g (4.4 mmol, rendimiento 75%) de sólido blanco **33**{*17,17*}.

**Datos espectroscópicos:**

**IR** (p. KBr): $\nu$ ($cm^{-1}$) 1608 (*t* C=N).

**$^{1}$H-RMN** (300MHz, d-TFA): δ (ppm) 9.61 (s, 4H, H-C1a), 9.16 (s, 2H, CH=N), 8.14 (s, 4H, H-C2b).

**$^{13}$C-RMN** (75.5MHz, d-TFA): δ (ppm) 166.8 (CH=N), 140.9 (C1a), 136.9 (C1b), 132.4 (C2b).

**MS** (IE): m/z 266.1 (7) $[M]^+$, 68.1 (12), 54.1 (14), 43.1 (100).

**HRMS** (IE): ($C_{12}H_{10}N_8$) Calculado: 266.1028. Obtenido: 266.1032.

## 5.3. Síntesis de intermedios amino-aldehído.

### 5.3.1. Síntesis de 4-((2-(pirrolidin-1-il)etilamino)metil)benzaldehído (35{*4*}).

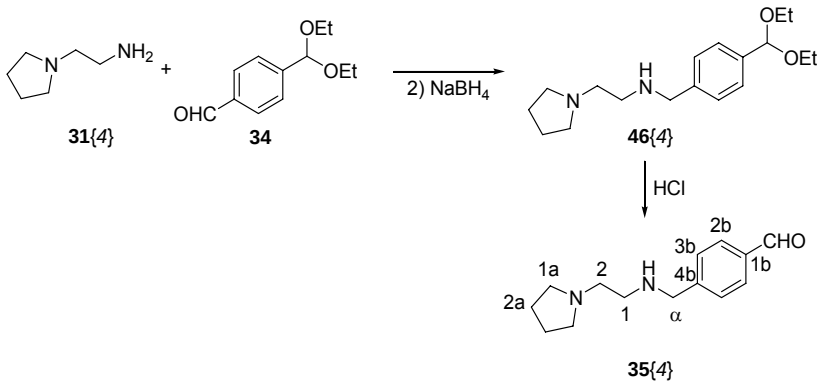


**31**{*4*} **34** **46**{*4*} **35**{*4*}

Se disuelven 2.01 g (9.3 mmol) de monoacetal dietílico del tereftalaldehído (**34**) y 1.09 g (9.3 mmol) de 2-(pirrolidin-1-il)etilamina **31**{*4*} en 30 mL de MeOH anhidro. Se añade tamiz molecular de 4 Å y se agita a temperatura de reflujo y bajo atmósfera de nitrógeno durante 36 h. Se filtra el tamiz molecular y se adicionan 0.36 g (9.3 mmol) de $NaBH_4$. Se deja reaccionar a temperatura ambiente durante 5 h. Se añade agua y se extrae con $CH_2Cl_2$. La fase orgánica se lava con salmuera y se seca sobre $MgSO_4$ anhidro. Se elimina el disolvente a presión reducida y se obtienen 2.66 g (8.7 mmol, 93%) de un aceite amarillo del correspondiente acetal **46**{*4*}. A 2.64 g (8.6 mmol) de este acetal **46**{*4*} se le añaden 20 mL de HCl 2M y se agita a temperatura ambiente 2 h. Se basifica con NaOH y se extrae con $CH_2Cl_2$. La fase orgánica se lava con salmuera y se seca sobre $MgSO_4$ anhidro. Se elimina el disolvente a presión reducida y se obtienen 1.79 g (7.7 mmol, 89% rendimiento) de un aceite marronoso **35**{*4*}.

**Datos espectroscópicos:**

**IR** (film): $\nu$ ($cm^{-1}$) 3309 (*t* N-H), 2961, 2930, 2875, 2799 (*t* $Csp^3$-H, $Csp^2$-H), 1700 (*t* C=O), 1606 (*t* $Csp^2$-$Csp^2$), 1459, 1446 (*f* $Csp^3$-H).

**$^1$H-RMN** (300 MHz, $CDCl_3$): δ (ppm) 10.00 (s, 1H, CHO), 7.84 (d, $^3J_{H,H}$=8.1 Hz, 2H, H-C2b), 7.51 (d, $^3J_{H,H}$=8.1 Hz, 2H, H-C3b), 3.90 (s, 2H, H-C$\alpha$), 2.75 (t, $^3J_{H,H}$=6.0 Hz, 2H, H-C1), 2.64 (t, $^3J_{H,H}$=6.0 Hz, 2H, H-C2), 2.51 (m, 4H, H-C1a), 2.01 (sa, 1H, deuterable, NH), 1.77 (m, 4H, H-C2a).

**$^{13}$C-RMN** (75.5 MHz, $CDCl_3$): δ (ppm) 191.8 (CHO), 147.6 (C4b), 135.1 (C1b), 129.7 (C2b), 128.4 (C3b), 55.8 (C$\alpha$), 54.2 (C1a), 53.7 (C2), 47.8 (C1), 23.5 (C2a).

**MS** (IE): m/z 233.2 (1) $[M+1]^+$, 232.2 (22) $[M]^+$, 148.1 (2), 119.0 (12), 84.1 (100).

**HRMS** (IE): ($C_{14}H_{20}N_2O$) Calculado: 232.1576. Obtenido: 232.1572.

## 5.3.2. Síntesis de 4-((3-(pirrolidin-1-il)propilamino)metil)benzaldehído (35{5}).

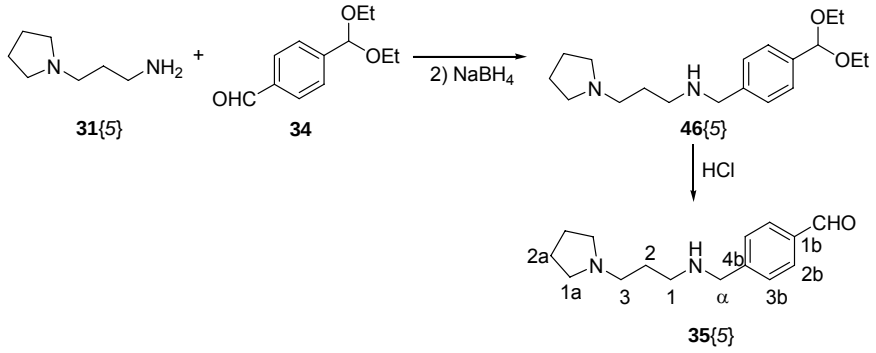


**31**{*5*} **34** **46**{*5*} **35**{*5*}

Se sigue el mismo procedimiento que para **35**{*4*} pero utilizando 6.01 g (28.0 mmol) de monoacetal dietílico del tereftalaldehído (**34**), 3.70 g (28.0 mmol) de amina **31**{*5*} y 1.07 g (28.0 mmol) de $NaBH_4$. Se obtienen 8.01 g (25.0 mmol, 89% rendimiento) de un aceite amarillento del correspondiente acetal **46**{*5*}.

7.98 g (24.9 mmol) de este acetal **46**{*5*} se hidrolizan y se obtienen 4.59 g (18.6 mmol, 75% rendimiento) de un aceite rojizo **35**{*5*}.

**Datos espectroscópicos:**

**IR** (film): $\nu$ ($cm^{-1}$) 3276 (*t* N-H), 2934, 2874, 2790 (*t* $Csp^3$-H, $Csp^2$-H), 1700 (*t* C=O), 1606 (t $Csp^2$-$Csp^2$), 1458 (*f* $Csp^3$-H).

**$^1$H-RMN** (300 MHz, $CDCl_3$): δ (ppm) 10.00 (s, 1H, CHO), 7.84 (d, $^3J_{H,H}$=8.1 Hz, 2H, H-C2b), 7.50 (d, $^3J_{H,H}$=8.1 Hz, 2H, H-C3b), 3.88 (s, 2H, H-C$\alpha$), 2.70 (t, $^3J_{H,H}$=7.0 Hz, 2H, H-C1), 2.51 (m, 6H, H-C3, H-C1a), 1.87 (sa, 1H, deuterable, NH), 1.75 (m, 6H, H-C2, H-C2a).

**$^{13}$C-RMN** (75.5 MHz, $CDCl_3$): δ (ppm) 191.8 (CHO), 147.7 (C4b), 135.2 (C1b), 129.8 (C2b), 128.3 (C3b), 54.7 (C$\alpha$), 54.3 (C1a), 53.7 (C3), 48.2 (C1), 29.2 (C2), 23.5 (C2a).

**AEO**: Calculado ($C_{15}H_{22}N_2O$): C 73.13%, H 9.00%, N 11.37%, O 6.49%. Obtenido: C 72.77%, H 9.64%, N 11.32%.

**MS** (IE): m/z 247.2 (2) $[M+1]^+$, 246.2 (21) $[M]^+$, 127.2 (10), 119.0 (22), 84.1 (100).

## 5.3.3. Síntesis de 4-((3-(1*H*-imidazol-1-il)propilamino)metil)benzaldehído (35{*6*}).

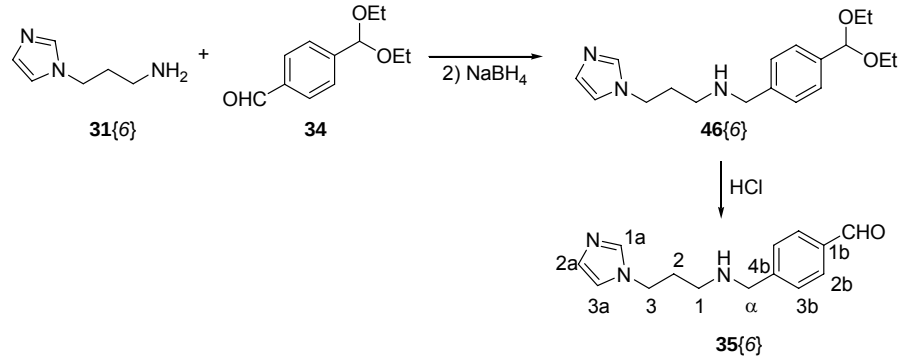


**31**{*6*} **34** **46**{*6*} **35**{*6*}

Se sigue el mismo procedimiento que para **35**{*4*} pero utilizando 2.01 g (9.3 mmol) de monoacetal dietílico del tereftalaldehído (**34**), 1.20 g (9.3 mmol) de amina **31**{*6*} y 0.36 g (9.3 mmol) de $NaBH_4$. Se obtienen 2.68 g (8.4 mmol, 90% rendimiento) de un aceite amarillento del correspondiente acetal **46**{*6*}.

2.68 g (8.4 mmol) de este acetal **46**{*6*} se hidrolizan y se obtienen 1.76 g (7.2 mmol, 86% rendimiento) de un aceite amarillento **35**{*6*}.

**Datos espectroscópicos:**

**IR (**film): $\nu$ ($cm^{-1}$) 3268 (*t* N-H), 3108 (*t* $Csp^2$-H), 2936, 2831, 2738 (*t* $Csp^3$-H, $Csp^2$-H), 1696 (*t* C=O), 1606 (*t* $Csp^2$-$Csp^2$), 1508 (*f* $Csp^3$-H).

**$^1$H-RMN** (300 MHz, $CDCl_3$): δ (ppm) 10.00 (s, 1H, CHO), 7.85 (d, $^3J_{H,H}$=8.1 Hz, 2H, H-C2b), 7.48 (d, $^3J_{H,H}$=8.1 Hz, 2H, H-C3b), 7.46 (s, 1H, H-C1a), 7.05 (s, 1H, H-C2a), 6.90 (s, 1H, H-C3a), 4.07 (t, $^3J_{H,H}$=6.9 Hz, 2H, H-C3), 3.85 (s, 2H, H-Cα), 2.62 (t, $^3J_{H,H}$=6.9 Hz, 2H, H-C1), 1.95 (quint, $^3J_{H,H}$=6.9 Hz, 2H, H-C2), 1.75 (sa, 1H, deuterable, NH).

**$^{13}$C-RMN** (75.5 MHz, $CDCl_3$): δ (ppm) 191.7 (CHO), 147.2 (C4b), 137.0 (C1a), 135.3 (C1b), 129.8 (C2b), 129.3 (C3a), 128.4 (C3b), 118.7 (C2a), 53.6 (Cα), 45.8 (C3), 44.6 (C1), 31.3 (C2).

**MS** (IE): m/z 244.1 (17) $[M+1]^+$, 243.1 (65) $[M]^+$, 174.1 (28), 148.1 (43), 134.0 (72), 119.0 (100).

**HRMS** (IE): ($C_{14}H_{17}N_3O$) Calculado: 243.1372. Obtenido: 243.1366.

## 5.3.4. Síntesis de 4-((2-(piperidin-1-il)etilamino)metil)benzaldehído (35{*7*}).

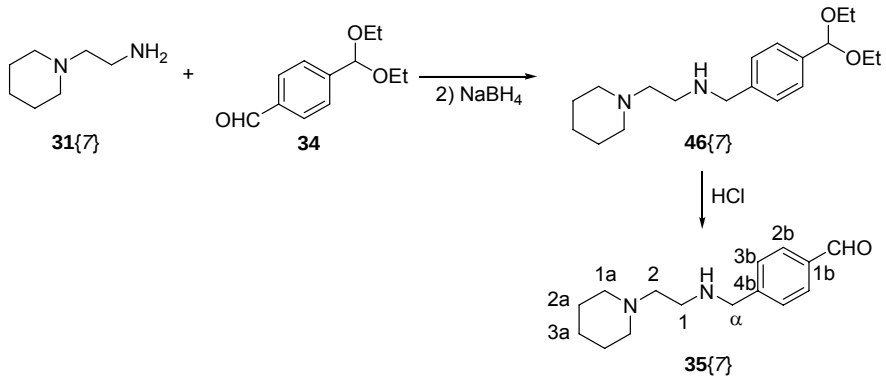


**31**{*7*} **34** **46**{*7*} **35**{*7*}

Método A:

Se sigue el mismo procedimiento que para **35**{*4*} pero utilizando 2.01 g (9.4 mmol) de monoacetal dietílico del tereftalaldehído (**34**), 1.23 g (9.4 mmol) de amina **31**{*7*} y 0.36 g (9.4 mmol) de $NaBH_4$. Se obtienen 2.79 g (8.7 mmol, 93% rendimiento) de un aceite amarillento del correspondiente acetal **46**{*7*}.

2.75 g (8.6 mmol) de este acetal **46**{*7*} se hidrolizan y se obtienen 2.11 g (8.6 mmol, rendimiento cuantitativo) de un sólido aceitoso amarillo **35**{*7*}.

Método B:

Se disuelven 0.91 g (4.2 mmol) de monoacetal dietílico del tereftalaldehído (**34**) y 0.55 g (4.2 mmol) de amina **31**{*7*} en 3 mL de MeOH anhidro. Se añade $Na_2SO_4$ anhidro y se calienta en el microondas a 100 ºC durante 2 h. Se filtra y se elimina el disolvente a presión reducida. Se obtienen 1.35 g (4.2 mmol, rendimiento cuantitativo) de un aceite rojizo correspondiente a la imina **45**{*7*}.

1.32 g (4.1 mmol) de este aceite rojizo **45**{*7*} se disuelven en 30 mL de MeOH anhidro. Se añaden 0.16 g (4.1 mmol) de $NaBH_4$ en pequeñas porciones y se deja reaccionar a temperatura ambiente durante 5 h. Se añade agua y se extrae con $CH_2Cl_2$. La fase orgánica se lava con salmuera y se seca sobre $MgSO_4$ anhidro. Se elimina el disolvente a presión reducida y se obtienen 1.23 g (3.8 mmol, 92 % rendimiento) de un aceite amarillento del correspondiente acetal **46**{*7*}.

A 1.21 g (3.8 mmol) de este acetal **46**{*7*} se le añaden 20 mL de HCl 2M y se agita a temperatura ambiente 2 h. Se basifica con NaOH y se extrae con $CH_2Cl_2$. La fase orgánica se lava con salmuera y se seca sobre $MgSO_4$ anhidro. Se elimina el disolvente a presión reducida y se obtienen 0.87 g (3.5 mmol, 94% rendimiento) de un sólido aceitoso amarillo **35**{*7*}.

**Datos espectroscópicos:**

**IR** (film): $\nu$ ($cm^{-1}$) 3308 (*t* N-H), 3050 (*t* $Csp^2$-H), 2934, 2851, 2809 (*t* $Csp^3$-H, $Csp^2$-H), 1701 (*t* C=O), 1606 (*t* $Csp^2$-$Csp^2$), 1453 (*f* $Csp^3$-H).

**$^1$H-RMN** (300 MHz, $CDCl_3$): δ (ppm) 10.00 (s, 1H, CHO), 7.84 (d, $^3J_{H,H}$=8.1 Hz, 2H, H-C2b), 7.50 (d, $^3J_{H,H}$=8.1 Hz, 2H, H-C3b), 3.89 (s, 2H, H-C$\alpha$), 2.70 (t, $^3J_{H,H}$=6.2 Hz, 2H, H-C1), 2.47 (t, $^3J_{H,H}$=6.2 Hz, 2H, H-C2), 2.36 (sa, 4H, H-C1a), 2.18 (sa, 1H, deuterable, NH), 1.57 (quint, $^3J_{H,H}$=5.7 Hz, 4H, H-C2a), 1.43 (m, 2H, H-C3a).

**$^{13}$C-RMN** (75.5 MHz, $CDCl_3$): δ (ppm) 191.8 (CHO), 147.7 (C4b), 135.2 (C1b), 129.8 (C2b), 128.4 (C3b), 58.4 (C$\alpha$), 54.7 (C1a), 53.7 (C2), 45.9 (C1), 25.9 (C2a), 24.4 (C3a).

**AEO**: Calculado ($C_{15}H_{22}N_2O$): C 73.13%, H 9.00%, N 11.37%, O 6.49%. Obtenido: C 73.11%, H 9.15%, N 11.22%.

**MS** (IE): m/z 246.2 (8) $[M]^+$, 119.1 (5), 98.1 (100).

**HRMS** (IE): ($C_{15}H_{22}N_2O$) Calculado: 246.1732. Obtenido: 246.1731.

## 5.3.5. Síntesis de 4-((3-(2-metilpiperidin-1-il)propilamino)metil)benzaldehído (35{*8*}).

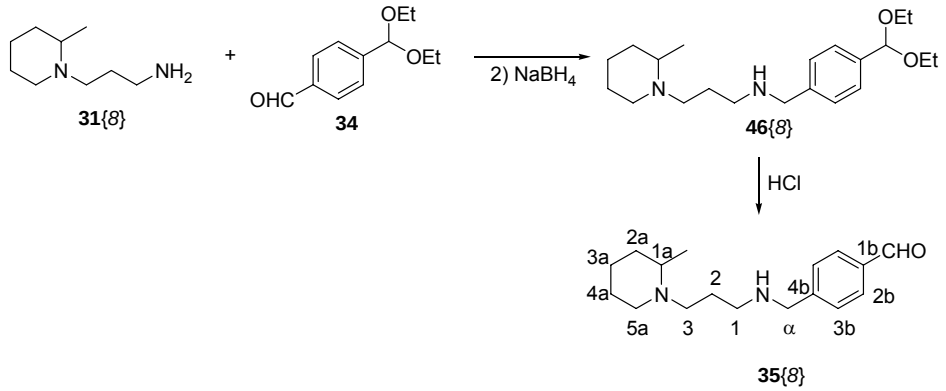


**31**{*8*} **34** **46**{*8*} **35**{*8*}

Se sigue el mismo procedimiento que para **35**{*4*} pero utilizando 2.01 g (9.3 mmol) de monoacetal dietílico del tereftalaldehído (**34**), 1.52 g (9.3 mmol) de amina **31**{*8*} y 0.36 g (9.3 mmol) de $NaBH_4$. Se obtienen 3.18 g (9.1 mmol, 98% rendimiento) de un aceite amarillento del correspondiente acetal **46**{*8*}.

3.18 g (9.1 mmol) de este acetal **46**{*8*} se hidrolizan y se obtienen 2.45 g (8.9 mmol, 98% rendimiento) de un aceite amarillento **35**{*8*}.

**Datos espectroscópicos:**

**IR** (film): $\nu$ ($cm^{-1}$) 3271 (*t* N-H), 2930, 2852, 2793, 2732 (*t* $Csp^3$-H, $Csp^2$-H), 1702 (*t* C=O), 1606 (*t* $Csp^2$-$Csp^2$), 1449, 1372 (*f* $Csp^3$-H).

**$^1$H-RMN** (300 MHz, $CDCl_3$): δ (ppm) 10.00 (s, 1H, CHO), 7.85 (d, $^3J_{H,H}$=8.1 Hz, 2H, H-C2b), 7.50 (d, $^3J_{H,H}$=8.1 Hz, 2H, H-C3b), 3.87 (s, 2H, H-C$\alpha$), 2.87 (m, 1H, $H_{eq}$-C5a), 2.77 (m, 1H, $H_{eq}$-C3), 2.65 (t, $^3J_{H,H}$=6.8 Hz, 2H, H-C1), 2.36 (m, 1H, $H_{ax}$-C3), 2.27 (m, 1H, H-C1a), 2.11 (m, 1H, $H_{ax}$-C5a), 2.00 (sa, 1H, deuterable, NH), 1.75-1.48 (m, 6H, H-C2, H-C4a, $H_{eq}$-C2a, $H_{eq}$-C3a), 1.29 (m, 2H, $H_{ax}$-C2a, $H_{ax}$-C3a), 1.06 (d, $^3J_{H,H}$=6.0 Hz, 3H, $CH_3$).

**$^{13}$C-RMN** (75.5 MHz, $CDCl_3$): δ (ppm) 191.8 (CHO), 147.7 (C4b), 135.2 (C1b), 129.8 (2b), 128.4 (C3b), 56.1 (C1a), 53.8 (C$\alpha$), 52.3 (C3), 52.0 (C5a), 48.5 (C1), 34.6* (C2a), 26.1 (C4a), 25.9 (C2), 23.9* (C3a), 19.0 ($CH_3$).

**MS** (IE): m/z 275.2 (9) $[M+1]^+$, 274.2 (37) $[M]^+$, 119.0 (18), 112.1 (100).

**HRMS** (IE): ($C_{17}H_{26}N_2O$) Calculado: 274.2045. Obtenido: 274.2046

## 5.3.6. Síntesis de 4-((3-(4-metilpiperazin-1-il)propilamino)metil)benzaldehído (35{*9*}).

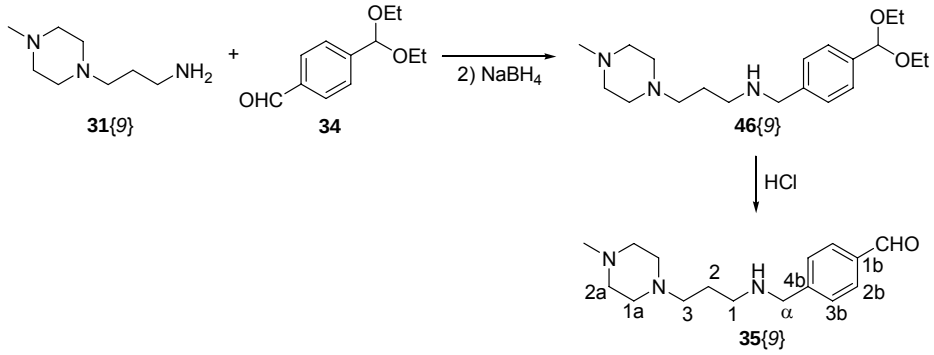


**31**{*9*} **34** **46**{*9*} **35**{*9*}

Se sigue el mismo procedimiento que para **35**{*4*} pero utilizando 2.00 g (9.3 mmol) de monoacetal dietílico del tereftalaldehído (**34**), 1.49 g (9.3 mmol) de amina **31**{*9*} y 0.36 g (9.3 mmol) de $NaBH_4$. Se obtienen 2.94 g (8.4 mmol, 90% rendimiento) de un aceite amarillento del correspondiente acetal **46**{*9*}.

2.93 g (8.4 mmol) de acetal este acetal **46**{*9*} se hidrolizan y se obtienen 2.31 g (8.4 mmol, rendimiento cuantitativo) de un aceite marrón **35**{*9*}.

**Datos espectroscópicos:**

**IR** (film): $\nu$ ($cm^{-1}$) 3276 (*t* N-H), 2936, 2875, 2794, 2769, 2740 (*t* $Csp^3$-H, $Csp^2$-H), 1700 (*t* C=O), 1606 (*t* $Csp^2$-$Csp^2$), 1458 (*f* $Csp^3$-H).

**$^1$H-RMN** (300 MHz, $CDCl_3$): δ (ppm) 10.00 (s, 1H, CHO), 7.85 (d, $^3J_{H,H}$=8.1 Hz, 2H, H-C2b), 7.50 (d, $^3J_{H,H}$=8.1 Hz, 2H, H-C3b), 3.87 (s, 2H, H-C$\alpha$), 2.69 (t, $^3J_{H,H}$=6.9 Hz, 2H, H-C1), 2.45 (sa, 8H, H-C1a, H-C2a), 2.42 (t, $^3J_{H,H}$=6.9 Hz, 2H, H-C3), 2.27 (s, 3H, $CH_3$), 2.08 (sa, 1H, deuterable, NH), 1.72 (quint, $^3J_{H,H}$=6.9 Hz, 2H, H-C2).

**$^{13}$C-RMN** (75.5 MHz, $CDCl_3$): δ (ppm) 191.8 (CHO), 147.7 (C4b), 135.2 (C1b), 129.8 (C2b), 128.3 (C3b), 57.0 (C$\alpha$), 55.1 (C2a), 53.7 (C3), 53.2 (C1a), 48.3 (C1), 46.0 ($CH_3$), 27.0 (C2).

**MS** (IE): m/z 276.2 (4) $[M+1]^+$, 275.2 (26) $[M]^+$, 231.2 (100), 205.1 (38), 174.1 (23), 119.0 (24), 113.1 (33).

**HRMS** (IE): ($C_{16}H_{25}N_3O$) Calculado: 275.1998. Obtenido: 275.2001.

## 5.3.7. Síntesis de 4-((2-morfolinoetilamino)metil)benzaldehído (35{*10*}).

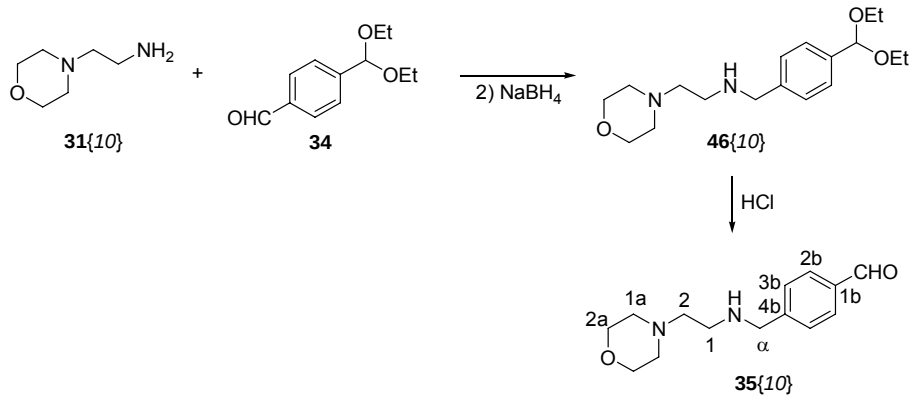


Se sigue el mismo procedimiento que para **35**{*4*} pero utilizando 2.00 g (9.3 mmol) de monoacetal dietílico del tereftalaldehído (**34**), 1.23 g (9.3 mmol) de amina **31**{*10*} y 0.36 g (9.3 mmol) de $NaBH_4$. Se obtienen 2.55 g (7.9 mmol, 85% rendimiento) de un aceite amarillo del correspondiente acetal **46**{*10*}.

2.52 g (7.8 mmol) de este acetal **46**{*10*} se hidrolizan y se obtienen 1.94 g (7.8 mmol, rendimiento cuantitativo) de un aceite amarillento **35**{*10*}.

**Datos espectroscópicos:**

**IR** (film): $\nu$ ($cm^{-1}$) 3309 (*t* N_H), 2954, 2917, 2894, 2852, 2818 (*t* $Csp^3$-H, $Csp^2$-H), 1698 (*t* C=O), 1607 (*t* $Csp^2$-$Csp^2$), 1455 (*f* $Csp^3$-H), 1117 (*t as* C-O-C), 852 (*t sim* C-O-C).

**$^1$H-RMN** (300 MHz, $CDCl_3$): δ (ppm) 10.00 (s, 1H, CHO), 7.86 (d, $^3J_{H,H}$=8.1 Hz, 2H, H-C2b), 7.50 (d, $^3J_{H,H}$=8.1 Hz, 2H, H-C3b), 3.90 (s, 2H, H-C$\alpha$), 3.70 (t, $^3J_{H,H}$=4.5 Hz, 4H, H-C2a), 2.71 (t, $^3J_{H,H}$=6.0 Hz, 2H, H-C1), 2.51 (t, $^3J_{H,H}$=6.0 Hz, 2H, H-C2), 2.42 (t, $^3J_{H,H}$=4.5 Hz, 4H, H-C1a), 1.93 (sa, 1H, deuterable, NH).

**$^{13}$C-RMN** (75.5 MHz, $CDCl_3$): δ (ppm) 191.7 (CHO), 147.5 (C4b), 135.2 (C1b), 129.8 (C2b), 128.4 (C3b), 66.9 (C2a), 58.2 (C$\alpha$), 53.7 (C1a, C2), 45.4 (C1).

**MS** (IE): m/z 248.2 (8) $[M]^+$, 133.0 (28), 119.0 (10), 100.0 (100), 83.9 (71).

**HRMS** (IE): ($C_{14}H_{20}N_2O_2$) Calculado: 248.1525. Obtenido: 248.1531.

## 5.3.8. Síntesis de 4-((3-morfolinopropilamino)metil)benzaldehído (35{*11*}).

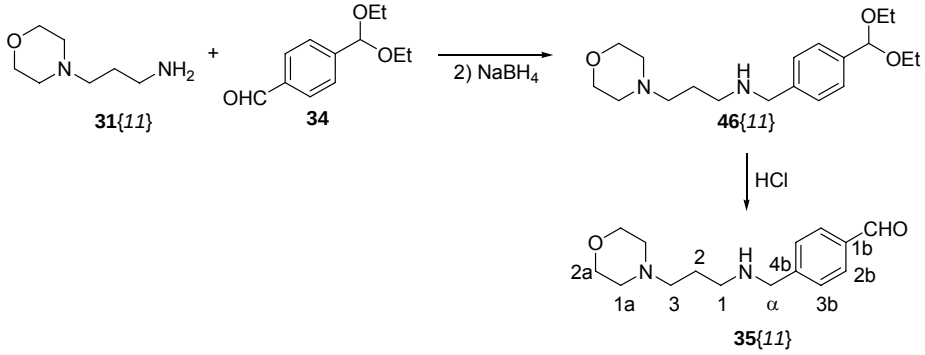


Se sigue el mismo procedimiento que para **35**{*4*} pero utilizando 2.01 g (9.3 mmol) de monoacetal dietílico del tereftalaldehído (**34**), 1.35 g (9.3 mmol) de amina **31**{*11*} y 0.36 g (9.3 mmol) de $NaBH_4$. Se obtienen 2.91 g (8.6 mmol, 92% rendimiento) de un aceite amarillo del correspondiente acetal **46**{*11*}.

2.86 g (8.5 mmol) de este acetal **46**{*11*} se hidrolizan y se obtienen 1.60 g (6.1 mmol, 72% rendimiento) de un aceite amarillo **35**{*11*}.

**Datos espectroscópicos:**

**IR** (film): $\nu$ ($cm^{-1}$) 3307 (*t* N-H*)*, 2950, 2892, 2853, 2814 (*t* $Csp^3$-H, $Csp^2$-H), 1698 (*t* C=O), 1607 (*t* $Csp^2$-$Csp^2$), 1457 (*f* $Csp^3$-H), 1117 (*t as* C-O-C), 861 (*t sim* C-O-C).

**$^1$H-RMN** (300 MHz, $CDCl_3$): δ (ppm) 10.00 (s, 1H, CHO), 7.85 (d, $^3J_{H,H}$=8.1 Hz, 2H, H-C2b), 7.50 (d, $^3J_{H,H}$=8.1 Hz, 2H, H-C3b), 3.88 (s, 2H, H-C$\alpha$), 3.70 (t, $^3J_{H,H}$=4.7 Hz, 4H, H-C2a), 2.70 (t, $^3J_{H,H}$=6.9 Hz, 2H, H-C1), 2.45-2.39 (m, 6H, H-C3, H-C1a), 1.81 (sa, 1H, deuterable, NH), 1.72 (quint, $^3J_{H,H}$=6.9 Hz, 2H, H-C2).

**$^{13}$C-RMN** (75.5 MHz, $CDCl_3$): δ (ppm) 191.2 (CHO), 147.6 (C4b), 135.2 (C1b), 129.8 (C2b), 128.3 (C3b), 66.9 (C2a), 57.3 (C$\alpha$), 53.8 (C1a), 53.7 (C3), 48.1 (C1), 26.7 (C2).

**MS** (IE): m/z 262.2 (3) $[M]^+$, 85.9 (71), 84.0 (100).

**HRMS** (IE): ($C_{15}H_{22}N_2O_2$) Calculado: 262.1681. Obtenido: 262.1682.

## 5.4. Síntesis de intermedios hidrazono-aldehído.

### 5.4.1. Síntesis de 4-((piperidin-1-ilimino)metil)benzaldehído (36{*1*}).

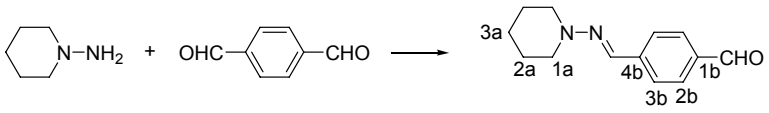


**30**{*1*} **29** **36**{*1*}

Se disuelven 1.00 g (7.4 mmol) de tereftalaldehído (**29**) en 30 mL de MeOH anhidro y se añade tamiz molecular de 4 Å. Se adiciona gota a gota y bajo atmósfera de nitrógeno una disolución de 0.38 g (3.7 mmol) de 1-aminopiperidina **30**{*1*} en 5 mL de MeOH anhidro. La mezcla se agita a temperatura de reflujo durante 36 h. Se elimina el disolvente a presión reducida y el sólido obtenido se purifica por cromatografía de columna (hexano/AcOEt 5:1). La fracción más pura se vuelve a cromatografiar utilizando como eluyente un gradiente de $CH_2Cl_2$/AcOEt 25:1 hasta $CH_2Cl_2$ 1:1). Se obtienen 0.48 g (2.2 mmol, 60% rendimiento) de un aceite amarillo **36**{*1*}.

**Datos espectroscópicos:**

**IR** (film): $\nu$ ($cm^{-1}$) 2938, 2854, 2818, 2731 (*t* $Csp^3$-H, $Csp^2$-H), 1694 (*t* C=O), 1605 (*t* $Csp^2$-$Csp^2$), 1579 (*t* C=N), 1549 (*t* $Csp^2$-$Csp^2$), 1448 (*f* $Csp^3$-H).

**$^1$H-RMN** (300 MHz, $CDCl_3$): δ (ppm) 9.96 (s, 1H, CHO), 7.83* (d, $^3J_{H,H}$=8.4 Hz, 2H, H-C2b), 7.71* (d, $^3J_{H,H}$=8.4 Hz, 2H, H-C3b), 7.48 (s, 1H, CH=N), 3.25 (t, $^3J_{H,H}$=5.7 Hz, 4H, H-C1a), 1.76 (quint, $^3J_{H,H}$=5.7 Hz, 4H, H-C2a), 1.61-1.54 (m, 2H, H-C3a).

**$^{13}$C-RMN** (75.5 MHz, $CDCl_3$): δ (ppm) 191.6 (CHO), 142.8 (C4b), 135.0 (C1b), 131.0 (C=N), 130.0 (C2b), 125.8 (C3b), 51.7 (C1a), 25.1 (C2a), 24.0 (C3a).

**AEO**: Calculado ($C_{13}H_{16}N_2O$): C 72.19%, H 7.46%, N 12.95%, O 7.40%. Obtenido: C 72.21%, H 7.55%, N 12.92%.

**MS** (IE): m/z 217.0 (17) $[M+1]^+$, 216.0 (100) $[M]^+$, 187.0 (3), 159.0 (38), 132.0 (19), 104.0 (23), 84.0 (34), 55 (58).

## 5.4.2. Síntesis de 4-((2,6-dimetilpiperidin-1-ilimino)metil)benzaldehído (36{*2*}).

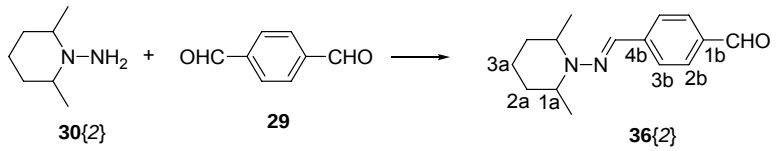


**30**{*2*} **29** **36**{*2*}

Se sigue el mismo procedimiento que para **36**{*1*} pero utilizando 3.82 g (28.2 mmol) de tereftalaldehído (**29**) y 2.01 g (14.1 mmol) de amina **30**{*2*} Se purifica por cromatografía de columna sobre gel de sílice (hexano/AcOEt 3:1) y se obtienen 2.71 g (11.1 mmol, 78% rendimiento) de un aceite amarillo **36**{*2*}.

**Datos espectroscópicos:**

**IR** (film): $\nu$ ($cm^{-1}$) 2967, 2935, 2869, 2820, 2728 (*t* $Csp^3$-H, $Csp^2$-H), 1693 (*t* C=O), 1604 (*t* $Csp^2$-$Csp^2$), 1572 (*t* C=N), 1539 (*t* $Csp^2$-$Csp^2$), 1468, 1372 (*f* $Csp^3$-H).

**$^1$H-RMN** (300 MHz, $CDCl_3$): δ (ppm) 9.95 (s, 1H, CHO), 7.81* (d, $^3J_{H,H}$=8.3 Hz, 2H, H-C2b), 7.69* (d, $^3J_{H,H}$=8.3 Hz, 2H, H-C3b), 7.35 (s, 1H, CH=N), 3.92 (m, 2H, H-C1a), 1.87-1.56 (m, 6H, H-C2a, H-C3a), 1.15 (d, $^3J_{H,H}$=6.6 Hz, 6H, $CH_3$).

**$^{13}$C-RMN** (75.5 MHz, $CDCl_3$): δ (ppm) 191.5 (CHO), 143.5 (C1b), 134.4 (C4b), 130.0 (C2b), 129.5 (C=N), 125.3 (C3b), 53.1 (C1a), 30.8 (C2a), 18.3 ($CH_3$), 15.6 (C3a).

**AEO**: Calculado ($C_{15}H_{20}N_2O$): C 73.74%, H 8.25%, N 11.47%, O 6.55%. Obtenido: C 73.37%, H 8.25%, N 11.41%.

**MS** (IE): m/z 245.2 (5) $[M+1]^+$, 244.2 (16) $[M]^+$, 229.2 (100), 89.0 (38), 55.0 (75).

## 5.4.3. Síntesis de 4-((4-metilpiperazin-1-ilimino)metil)benzaldehído (36{*3*}).

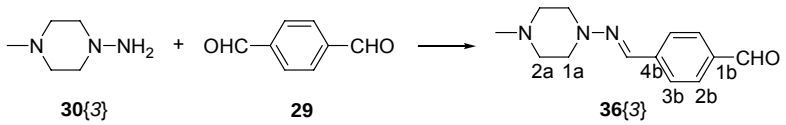


**30**{*3*} **29** **36**{*3*}

Se sigue el mismo procedimiento que para **36**{*1*} pero utilizando 1.14 g (8.4 mmol) de tereftalaldehído (**29**) y 0.50 g (4.2 mmol) de amina **30**{*3*}. Se purifica por cromatografía de columna sobre gel de sílice (gradiente de $CH_2Cl_2$ a $CH_2Cl_2$/MeOH 9:1). Se obtienen 0.80 g (3.5 mmol, 82% rendimiento) de un sólido amarillo **36**{*3*}.

**Datos espectroscópicos:**

**IR** (film): $\nu$ ($cm^{-1}$) 2941, 2843, 2799, 2728 (*t* $Csp^3$-H, $Csp^2$-H), 1692 (*t* C=O), 1605 (*t* $Csp^2$-$Csp^2$), 1581 (*t* C=N), 1551 (*t* $Csp^2$-$Csp^2$), 1451, 1364 (*f* $Csp^3$-H).

**$^1$H-RMN** (300MHz, $CDCl_3$): δ (ppm) 9.98 (s, 1H, CHO), 7.84 (d, $^3J_{H,H}$=7.7 Hz, 2H, H-C2b), 7.72 (d, $^3J_{H,H}$=7.7 Hz, 2H, H-C3b), 7.50 (s, 1H, CH=N), 3.30 (t, $^3J_{H,H}$=5.1 Hz, 4H, H-C1a), 2.62 (t, $^3J_{H,H}$=5.1 Hz, 4H, H-C2a), 2.37 (s, 3H, $CH_3$).

**$^{13}$C-RMN** (75.5 MHz, $CDCl_3$): δ (ppm) 191.6 (CHO), 142.1 (C1b), 135.3 (C4b), 132.6 (C=N), 130.0 (C2b), 126.1 (C3b), 54.3 (C1a), 50.6 (C2a), 46.0 ($CH_3$).

**MS** (IE): m/z 232.1 (2) $[M+1]^+$, 231.1 (12) $[M]^+$, 132.0 (2), 99.0 (100), 98.0 (66), 56.0 (53).

**HRMS** (IE): ($C_{13}H_{17}N_3O$) Calculado: 231.1372. Obtenido: 231.1376.

## 5.5. Síntesis de hidrazono/amino-aminas.

### 5.5.1. Síntesis de *N*-(4-((2,6-dimetilpiperidin-1-ilimino)metil)bencil)-2-(pirrolidin-1-il)etilamina (37{*2,4*}).

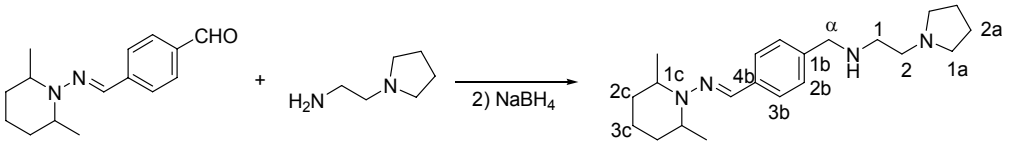


**36**{*2*} **31**{*4*} **37**{*2,4*}

Se disuelven 0.52 g (2.1 mmol) de **36**{*2*} y 0.25 g (2.1 mmol) de amina **31**{*4*} en 30 mL de MeOH anhidro. Se añade tamiz molecular de 4 Å y se agita a temperatura de reflujo y bajo atmósfera de nitrógeno durante 36 h. Se filtra el tamiz molecular y se adicionan 0.08 g (2.1 mmol) de $NaBH_4$. Se deja reaccionar a temperatura ambiente durante 16 h. Se añade agua y se extrae con $CH_2Cl_2$. La fase orgánica se lava con salmuera y se seca sobre $MgSO_4$ anhidro. Se elimina el disolvente a presión reducida y se obtienen 0.61 g (1.8 mmol, 85%) de un aceite amarillo **37**{*2,4*}.

**Datos espectroscópicos:**

**IR** (film): $\nu$ ($cm^{-1}$) 3311 (*t* N-N), 2962, 2931, 2872, 2794 (*t* $Csp^3$-H), 1624 (*t* $Csp^2$-$Csp^2$), 1584 (*t* C=N), 1556 (*t* $Csp^2$-$Csp^2$), 1459, 1447, 1369 (*f* $Csp^3$-H).

**$^1$H-RMN** (300 MHz, $CDCl_3$): δ (ppm) 8.07 (s, 1H, CH=N), 7.64 (d, $^3J_{H,H}$=8.1 Hz, 2H, H-C3b), 7.34 (d, $^3J_{H,H}$=8.1 Hz, 2H, H-C2b), 3.83 (s, 2H, H-C$\alpha$), 3.06 (m, 2H, H-C1c), 2.77 (t, $^3J_{H,H}$=6.0 Hz, 2H, H-C1), 2.63 (t, $^3J_{H,H}$=6.0 Hz, 2H, H-C2), 2.50 (m, 4H, H-C1a), 2.34 (sa, 1H, deuterable, NH), 1.77 (m, 8H, H-C2a, H-C2c), 1.50 (m, 2H, H-C3c), 1.00 (d, $^3J_{H,H}$=6.3 Hz, 6H, $CH_3$).

**MS** (IE): m/z 342.3 (0.5) $[M]^+$, 84.0 (100).

**HRMS** (IE): ($C_{21}H_{34}N_4$) Calculado: 342.2783. Obtenido: 342.2786.

## 5.5.2. Síntesis de *N*-(4-((2,6-dimetilpiperidin-1-ilimino)metil)bencil)-3-(1*H*-imidazol-1-il)propan-1-amina (37{*2,6*}).

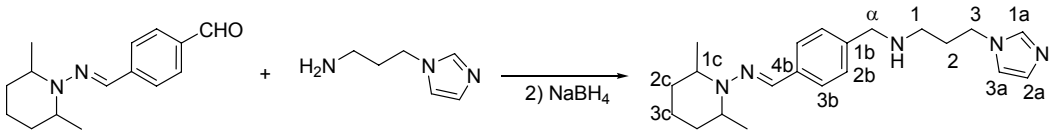


**36**{*2*} **31**{*6*} **37**{*2,6*}

Se sigue el mismo procedimiento que para **37**{*2,4*} pero utilizando 0.49 g (2.0 mmol) de **36**{*2*}, 0.26 g (2.0 mmol) de amina **31**{*6*} y 0.08 g (2.0 mmol) de $NaBH_4$. Se obtienen 0.70 g (2.0 mmol, rendimiento cuantitativo) de un aceite amarillo **35**{*2,6*}.

**Datos espectroscópicos:**

**IR** (film): $\nu$ ($cm^{-1}$) 3284 (*t* N-H), 3106 (*t* $Csp^2$-H), 2961, 2931, 2867, 2856, 2824 (*t* $Csp^3$-H, $Csp^2$-H), 1624 (*t* $Csp^2$-$Csp^2$), 1582 (*t* C=N), 1552(*t* $Csp^2$-$Csp^2$), 1508 (*t* esqueleto heteroaromático), 1449, 1369 (*f* $Csp^3$-H).

**$^1$H-RMN** (300 MHz, $CDCl_3$): δ (ppm) 8.04 (s, 1H, CH=N), 7.65 (d, $^3J_{H,H}$=8.1 Hz, 2H, H-C3b), 7.46 (s, 1H, H-C1a), 7.31 (d, $^3J_{H,H}$=8.1 Hz, 2H, H-C2b), 7.04 (s, 1H, H-C2a), 6.89 (s, 1H, H-C3a), 4.05 (t, $^3J_{H,H}$=6.9 Hz, 2H, H-C3), 3.77 (s, 2H, H-Cα), 3.10 (m, 2H, H-C1c), 2.61 (t, $^3J_{H,H}$=6.9 Hz, 2H, H-C1), 1.93 (quint, $^3J_{H,H}$=6.9 Hz, 2H, H-C2), 1.85 (sa, 1H, deuterable, NH), 1.77 (m, 4H, H-C2c), 1.51 (m, 2H, H-C3c), 1.00 (d, $^3J_{H,H}$=6.6 Hz, 6H, $CH_3$).

**$^{13}$C-RMN** (75.5 MHz, $CDCl_3$): δ (ppm) 151.7 (C=N), 141.4 (C1b), 137.0 (C1a), 134.0 (C4b), 129.2 (C3a), 128.2* (C3b), 127.3* (C2b), 118.7 (C2a), 57.2 (C1c), 53.7 (Cα), 45.7 (C3), 44.7 (C1), 32.8 (C2c), 31.4 (C2), 21.2 (C3c), 20.5 ($CH_3$).

**MS** (IE): m/z 354.2 (5) $[M+H]^+$, 243.1 (35), 242.1 (31), 241.0 (30), 215.0 (47), 112.1 (100), 81.0 (39), 55.0 (66).

**HRMS** (IE): ($C_{21}H_{32}N_5$) $[M+H]^+$ Calculado: 354.2658. Obtenido: 354.2666.

## 5.5.3. Síntesis de *N*-(4-((2,6-dimetilpiperidin-1-ilimino)metil)bencil)-3-(2-metilpiperidin-1-il)propan-1-amina (37{*2,8*}).

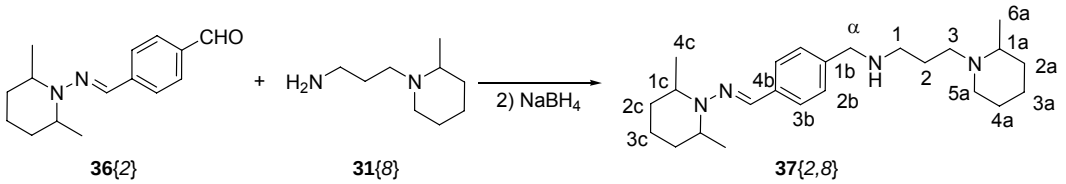


**36**{*2*} **31**{*8*} **37**{*2,8*}

Se sigue el mismo procedimiento que para **37**{*2,4*} pero utilizando 0.52 g (2.1 mmol) de **36**{*2*}, 0.35 g (2.1 mmol) de amina **31**{*8*} y 0.08 g (2.1 mmol) de $NaBH_4$. Se obtienen 0.77 g (2.0 mmol, 93% rendimiento) de un aceite amarillo **37**{*2,8*}.

**Datos espectroscópicos:**

**IR** (film): ν ($cm^{-1}$) 3281 (*t* N-H), 2961, 2930, 2855, 2808 (*t* $Csp^3$-H), 1625 (*t* $Csp^2$-$Csp^2$), 1584 (*t* C=N), 1554(*t* $Csp^2$-$Csp^2$), 1449, 1370 (*f* $Csp^3$-H).

**$^1$H-RMN** (300 MHz, $CDCl_3$): δ (ppm) 8.06 (s, 1H, CH=N), 7.64 (d, $^3J_{H,H}$=8.1 Hz, 2H, H-C3b), 7.34 (d, $^3J_{H,H}$=8.1 Hz, 2H, H-C2b), 3.81 (s, 2H, H-Cα), 3.08 (m, 2H, H-C1c), 2.88 (m, 1H, $H_{eq}$-C5a), 2.76 (m, 1H, $H_{eq}$-C3), 2.65 (t, $^3J_{H,H}$=6.8 Hz, 4H, H-C1), 2.35 (sa, 1H, deuterable, NH), 2.34 (m, 1H, $H_{ax}$-C3), 2.25 (m, 1H, H-C1a), 2.10 (m, 1H, $H_{ax}$-C5a), 1.79-1.32 (sc, 12H, H-C2, $H_{eq}$-C2a, $H_{eq}$-C3a, H-C4a, H-C2c, H-C3c), 1.27 (m, 2H, $H_{ax}$-C2a, $H_{ax}$-C3a), 1.06 (d, $^3J_{H,H}$=6.3 Hz, 3H, H-C6a), 1.00 (d, $^3J_{H,H}$=6.3 Hz, 6H, H-C4c).

**$^{13}$C-RMN** (75.5 MHz, $CDCl_3$): δ (ppm) 152.3 (C=N), 141.6 (C4b), 133.8 (C1b), 128.2 (C3b), 127.2 (C2b), 57.3 (C1c), 56.0 (C1a), 53.7 (Cα), 52.3 (C3), 52.0 (C5a), 48.3 (C1), 34.6* (C2a), 32.9 (C2c), 26.1 (C4a), 25.6 (C2), 23.9* (C3a), 21.4 (C3c), 20.6 (C4c), 19.0 (C6a).

**MS** (IE): m/z 385.4 (1) $[M+1]^+$, 384.4 (5) $[M]^+$, 244.2 (9), 229.2 (17), 126.2 (17), 112.2 (100), 98.1 (25).

**HRMS** (IE): ($C_{24}H_{40}N_4$) Calculado: 384.3253. Obtenido: 384.3250.

## 5.5.4. Síntesis de *N*-(4-((2,6-dimetilpiperidin-1-ilimino)metil)bencil)-3-(4-metilpiperazin-1-il)propan-1-amina (37{2,9}).

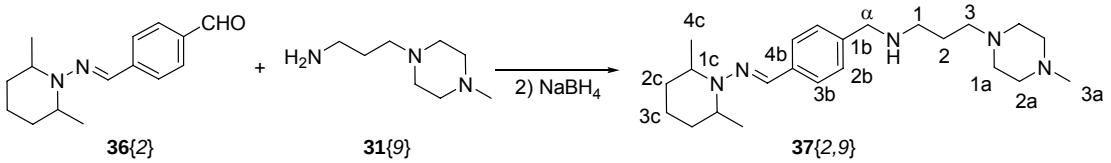


**36**{*2*} **31**{*9*} **37**{*2,9*}

Se sigue el mismo procedimiento que para **37**{*2,4*} pero utilizando 0.47 g (1.9 mmol) de **36**{*2*}, 0.31 g (1.9 mmol) de amina **31**{*9*} y 0.07 g (1.9 mmol) de $NaBH_4$. Se obtienen 0.72 g (1.9 mmol, 97% rendimiento) de un aceite amarillo **37**{*2,9*}.

**Datos espectroscópicos:**

**IR** (film): $\nu$ ($cm^{-1}$) 3286 (*t* N-H), 2932, 2872, 2837, 2794 (*t* $Csp^3$-H), 1625 (*t* $Csp^2$-$Csp^2$), 1584 (*t* C=N), 1554 (*t* $Csp^2$-$Csp^2$), 1458, 1370 (*f* $Csp^3$-H).

**$^1$H-RMN** (300 MHz, $CDCl_3$): δ (ppm) 8.05 (s, 1H, CH=N), 7.65* (d, $^3J_{H,H}$=8.1 Hz, 2H, H-C3b), 7.34* (d, $^3J_{H,H}$=8.1 Hz, 2H, H-C2b), 3.81 (s, 2H, H-C$\alpha$), 3.08 (m, 2H, H-C1c), 2.69 (t, $^3J_{H,H}$=6.9 Hz, 2H, H-C1), 2.44 (sa, 8H, H-C1a, H-C2a), 2.41 (t, $^3J_{H,H}$=6.9 Hz, 2H, H-C3), 2.30 (sa, 1H, deuterable, NH), 2.27 (s, 3H, H-C3a), 1.81-1.68 (m, 6H, H-C2c, H-C2), 1.51 (m, 2H, H-C3c), 1.00 (d, $^3J_{H,H}$=6.3 Hz, 6H, H-C4c).

**$^{13}$C-RMN** (75.5 MHz, $CDCl_3$): δ (ppm) 152.1 (C=N), 141.3 (C1b), 133.8 (C4b), 128.2* (C3b), 127.3* (C2b), 57.2 (C1c), 57.0 (C$\alpha$), 55.1 (C2a), 53.6 (C3), 53.2 (C1a), 48.1 (C1), 46.0 (C3a), 32.9 (C2c), 26.7 (C2), 21.4 (C3c), 20.6 (C4c).

**MS** (IE): m/z 386.3 (1) $[M+H]^+$, 385.3 (1) $[M]^+$, 273.2 (43), 229.1 (77), 113.0 (100), 70.0 (80).

**HRMS** (IE): ($C_{23}H_{39}N_5$) Calculado: 385.3205. Obtenido: 385.3211.

## 5.5.5. Síntesis de *N*-(4-((2,6-dimetilpiperidin-1-ilimino)metil)bencil)-3-morfolinopropan-1-amina (37{*2,11*}).

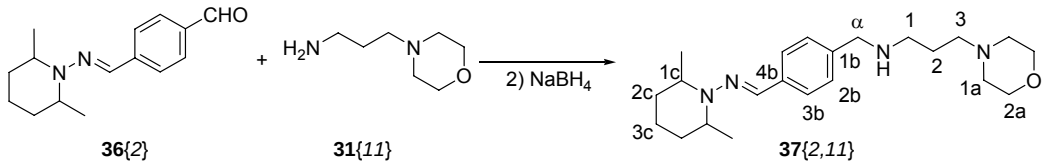


**36**{*2*} **31**{*11*} **37**{*2,11*}

Se sigue el mismo procedimiento que para **37**{*2,4*} pero utilizando 0.46 g (1.9 mmol) de **36**{*2*}, 0.27 g (1.9 mmol) de amina **31**{*11*} y 0.07 g (1.9 mmol) de $NaBH_4$. Se obtienen 0.63 g (1.7 mmol, 91% rendimiento) de un aceite amarillo **37**{*2,11*}.

**Datos espectroscópicos:**

**IR** (film): $\nu$ ($cm^{-1}$) 3293 (*t* N-H), 2930, 2854, 2808 (*t* $Csp^3$-H), 1625 (*t* $Csp^2$-$Csp^2$), 1584 (*t* C=N), 1554 (*t* $Csp^2$-$Csp^2$), 1456, 1369 (*f* $Csp^3$-H), 1118 (*t as* C-O-C), 863 (*t sim* C-O-C).

**$^1$H-RMN** (300 MHz, $CDCl_3$): δ (ppm) 8.06 (s, 1H, CH=N), 7.65 (d, $^3J_{H,H}$=8.1 Hz, 2H, H-C3b), 7.33 (d, $^3J_{H,H}$=8.1 Hz, 2H, H-C2b), 3.81 (s, 2H, H-C$\alpha$), 3.70 (t, $^3J_{H,H}$=4.7 Hz, 4H, H-C2a), 3.08 (m, 2H, H-C1c), 2.69 (t, $^3J_{H,H}$=6.9 Hz, 2H, H-C1), 2.45-2.38 (m, 6H, H-C3, H-C1a), 2.06 (sa, 1H, deuterable, NH), 1.81-1.66 (m, 6H, H-C2c, H-C2), 1.51 (m, 2H, H-C3c), 1.00 (d, $^3J_{H,H}$=6.3 Hz, 6H, $CH_3$).

**$^{13}$C-RMN** (75.5 MHz, $CDCl_3$): δ (ppm) 152.2 (C=N), 141.6 (C1b), 133.8 (C4b), 128.1 (C3b), 127.3 (C2b), 66.9 (C2a), 57.4 (C$\alpha$), 57.3 (C1c), 53.8 (C1a), 53.7 (C3), 47.9 (C1), 32.9 (C2c), 26.6 (C2), 21.4 (C3c), 20.6 ($CH_3$).

**MS** (IE): m/z 372.2 (2) $[M]^+$, 244.2 (24), 143.1 (8), 100.0 (100), 56.0 (26), 55.0 (24).

**HRMS** (IE): ($C_{22}H_{36}N_4O$) Calculado: 372.2889. Obtenido: 372.2895.

## 5.5.6. Síntesis de *N*-(4-((4-metilpiperazin-1-ilimino)metil)bencil)-2-(pirrolidin-1-il)etanamina (37{3,4}).

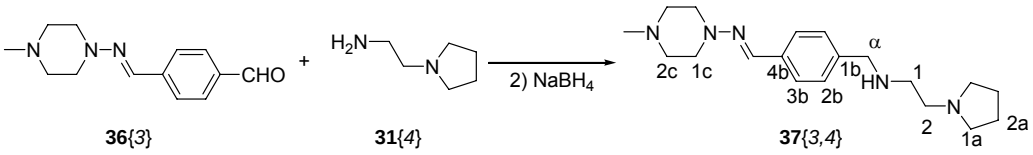


**36**{*3*} **31**{*4*} **37**{*3,4*}

Se sigue el mismo procedimiento que para **37**{*2,4*} pero utilizando 0.32 g (1.4 mmol) de **36**{*3*}, 1.16 g (1.4 mmol) de amina **31**{*4*} y 0.053 g (1.4 mmol) de $NaBH_4$. Se obtienen 0.42 g (1.3 mmol, 92% rendimiento) de un aceite amarillo **37**{*3,4*}.

**Datos espectroscópicos:**

**IR** (film evaporado $CHCl_3$): $\nu(cm^{-1})$ 3309 (*t* N-H), 2935, 2875, 2795 (*t* $Csp^3$-H), 1592 (*t* C=N), 1452 (*f* $Csp^3$-H).

**$^1$H-RMN** (300 MHz, $CDCl_3$): δ (ppm) 7.55 (d, 2H, $^3J_{H,H}$=8.0 Hz, H-C3b), 7.55 (s, 1H, CH=N), 7.29 (d, 2H, $^3J_{H,H}$=8.0 Hz, H-C2b), 3.80 (s, 2H, H-Cα), 3.21 (t, 4H, $^3J_{H,H}$=5.0 Hz, H-C1c), 2.73 (t, 2H, $^3J_{H,H}$=6.0 Hz, H-C1), 2.61 (m, 6H, H-C2, H-C2c), 2.48 (m, 4H, H-C1a), 2.36 (s, 3H, $CH_3$), 1.87 (s, 1H, deuterable, NH), 1.75 (m, 4H, H-C2a).

**$^{13}$C-RMN** (75.5 MHz, $CDCl_3$): δ (ppm) 140.4 (C1b), 135.8 (C=N), 134.8 (C4b), 128.2* (C3b), 126.0* (C2b), 55.9 (Cα), 54.5 (C1c), 54.2 (C1a), 53.8 (C2), 51.1 (C2c), 47.8 (C1), 46.0 ($CH_3$), 23.5 (C2a).

**AEO**: Calculado ($C_{19}H_{31}N_5$): C 69.26%, H 9.48%, N 21.26%. Obtenido: C 69.14%, H 9.67%, N 20.99%.

**MS** (IE): m/z 330.4 (4) $[M+1]^+$, 329.3 (12) $[M]^+$, 245.2 (6), 244.2 (30), 216.2 (29), 99.1 (57), 98.1 (59), 84.0 (100), 70.1 (18), 56.1 (35).

## 5.5.7. Síntesis de *N*-(4-((2-(pirrolidin-1-il)etilamino)metil)bencil)-3-(pirrolidin-1-il)propan-1-amina (32{*4,5*}).

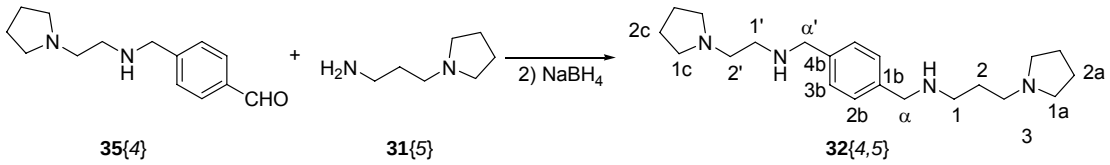


**35**{*4*} **31**{*5*} **32**{*4,5*}

Se sigue el mismo procedimiento que para **37**{*2,4*} pero utilizando 0.81 g (3.5 mmol) de **35**{*4*}, 0.46 g (3.5 mmol) de amina **31**{*5*} y 0.13 g (3.5 mmol) de $NaBH_4$. Se obtienen 1.11 g (3.2 mmol, 92% rendimiento) de un aceite amarillento **32**{*4,5*}.

**Datos espectroscópicos:**

**IR** (film): $\nu$ ($cm^{-1}$) 3281 (*t* N-H), 2961, 2930, 2874, 2790 (*t* $Csp^3$-H), 1458, 1445 (*f* $Csp^3$-H).

**$^1$H-RMN** (300 MHz, $CDCl_3$): δ (ppm) 7.27 (s, 4H, Ph), 3.79 (s, 2H, H-Cα'), 3.77 (s, 2H, H-Cα), 2.73 (m, 4H, H-C1, H-C1'), 2.61 (t, $^3J_{H,H}$=6.0 Hz, 2H, H-C2'), 2.49 (m, 10H, H-C3, H-C1a, H-C1c), 2.14 (sa, 2H, deuterable, NH), 1.79-1.71 (m, 10H, H-C2, H-C2a, H-C2c).

**$^{13}$C-RMN** (75.5 MHz, $CDCl_3$): δ (ppm) 139.0* (C4b), 138.8* (C1b), 128.1** (C3b), 128.0** (C2b), 55.9 (Cα'), 54.7 (Cα), 54.2 (C1a, C1c), 53.8*** (C2'), 53.7*** (C3), 48.0 (C1, C1'), 29.2 (C2), 23.5 (C2a, C2c).

**MS** (IE): m/z 345.3 (0.3) $[M+H]^+$, 260.2 (2), 84.1 (100).

**HRMS** (IE): ($C_{21}H_{37}N_4$) $[M+H]^+$ Calculado: 345.3018. Obtenido: 345.3022.

## 5.5.8. Síntesis de *N*-(4-((2-(pirrolidin-1-il)etilamino)metil)bencil)-3-(1*H*-imidazol-1-il)propan-1-amina (32{*4,6*}).

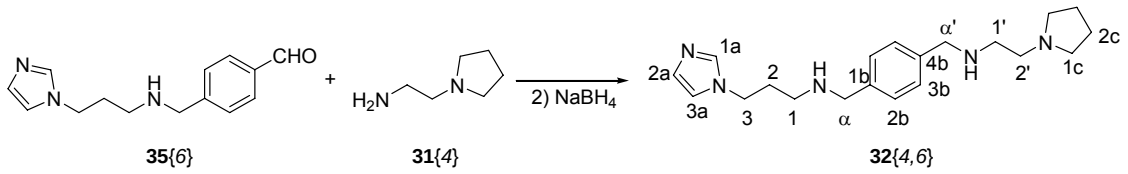


**35**{*6*} **31**{*4*} **32**{*4,6*}

Se sigue el mismo procedimiento que para **37**{*2,4*} pero utilizando 0.89 g (3.7 mmol) de **35**{*6*}, 0.43 g (3.7 mmol) de amina **31**{*4*} y 0.14 g (3.7 mmol) de $NaBH_4$. Se obtienen 1.14 g (3.3 mmol, 91% rendimiento) de un aceite amarillo **32**{*4,6*}.

**Datos espectroscópicos:**

**IR** (film): ν ($cm^{-1}$) 3279 (*t* N-H), 3104 (*t* $Csp^2$-H), 2929, 2875, 2799 (*t* C-$sp^3$-H), 1508 (*t* esqueleto heteroaromático), 1458, 1446 (*f* $Csp^3$-H).

**$^1$H-RMN** (300 MHz, $CDCl_3$): δ (ppm) 7.44 (s, 1H, H-C1a), 7.27 (s, 4H, Ph), 7.03 (s, 1H, H-C2a), 6.88 (s, 1H, H-C3a), 4.04 (t, $^3J_{H,H}$=6.9 Hz, 2H, H-C3), 3.79* (s, 2H, H-Cα), 3.73* (s, 2H, H-Cα'), 2.74 (t, $^3J_{H,H}$=5.9 Hz, 2H, H-C1'), 2.61 (m, 4H, H-C1, H-C2'), 2.48 (m, 4H, H-C1c), 2.18 (sa, 2H, deuterable, NH), 1.92 (quint, $^3J_{H,H}$=6.9 Hz, 2H, H-C2), 1.76 (quint, $^3J_{H,H}$=3.3 Hz, 4H, H-C2c).

**$^{13}$C-RMN** (75.5 MHz, $CDCl_3$): δ (ppm) 139.1* (C1b), 138.6* (C4b), 137.0 (C1a), 129.2 (C3a), 128.2** (C2b), 128.0** (C3b), 118.7 (C2a), 55.9 (Cα'), 54.2 (C1c), 53.8*** (C2'), 53.7*** (Cα), 47.9 (C1'), 45.6 (C3), 44.7 (C1), 31.4 (C2), 23.5 (C2c).

**MS** (IE): m/z 342.2 (4) $[M+H]^+$, 257.2 (100), 84.0 (64).

**HRMS** (IE): ($C_{20}H_{32}N_5$) $[M+H]^+$ Calculado: 342.2658. Obtenido: 342.2666.

## 5.5.9. Síntesis de *N*-(4-((2-(pirrolidin-1-il)etilamino)metil)bencil)-3-(4-metilpiperazin-1-il)propan-1-amina (32{*4,9*}).

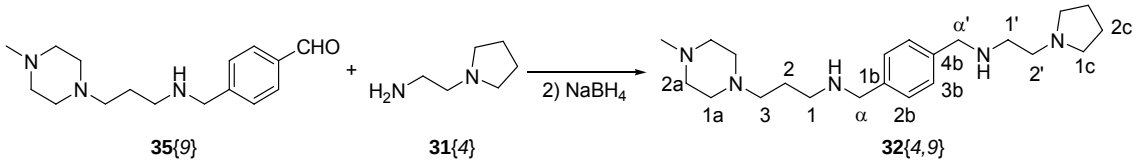


**35**{*9*} **31**{*4*} **32**{*4,9*}

Se sigue el mismo procedimiento que para **37**{*2,4*} pero utilizando 0.91 g (3.3 mmol) de **35**{*9*}, 0.39 g (3.3 mmol) de amina **31**{*4*} y 0.13 g (3.3 mmol) de $NaBH_4$. Se obtienen 0.96 g (2.6 mmol, 77% rendimiento) de un aceite amarillo **32**{*4,9*}.

**Datos espectroscópicos:**

**IR** (film): $\nu$ ($cm^{-1}$) 3288 (*t* N-H), 2934, 2875, 2793 (*t* $Csp^3$-H), 1458, 1447, 1372, 1354 (*f* $Csp^3$-H).

**$^1$H-RMN** (300 MHz, $CDCl_3$): δ (ppm) 7.27 (s, 4H, Ph), 3.79* (s, 2H, H-C$\alpha$), 3.76* (s, 2H, H-C$\alpha$'), 2.74 (t, $^3J_{H,H}$=6.5 Hz, 2H, H-C1'), 2.67 (t, $^3J_{H,H}$=6.9 Hz, 2H, H-C1), 2.61 (t, $^3J_{H,H}$=6.5 Hz, 2H, H-C2'), 2.50-2.38 (m, 14H, H-C3, H-C1a, H-C2a, H-C1c), 2.27 (s, 3H, $CH_3$), 2.11 (sa, 2H, deuterable, NH), 1.77-1.66 (m, 6H, H-C2, H-C2c).

**$^{13}$C-RMN** (75.5 MHz, $CDCl_3$): δ (ppm) 138.9* (C1b), 138.8* (C4b), 128.1** (C2b), 128.0** (C3b), 57.0 (C$\alpha$), 55.9 (C$\alpha$'), 55.1 (C2a), 54.2 (C1c), 53.8*** (C2'), 53.7*** (C3), 53.2 (C1a), 48.1 (C1), 47.9 (C1'), 46.0 ($CH_3$), 27.0 (C2), 23.5 (C2c).

**MS** (IE): m/z 374.3 (0.4) $[M+H]^+$, 303.2 (1), 289.2 (2), 113.1 (7), 84.0 (100).

**HRMS** (IE): ($C_{22}H_{40}N_5$) $[M+H]^+$ Calculado: 374.3284. Obtenido: 374.3276.

## 5.5.10. Síntesis de *N*-(4-((2-(pirrolidin-1-il)etilamino)metil)bencil)-3-morfolinopropan-1-amina (32{*4,11*}).

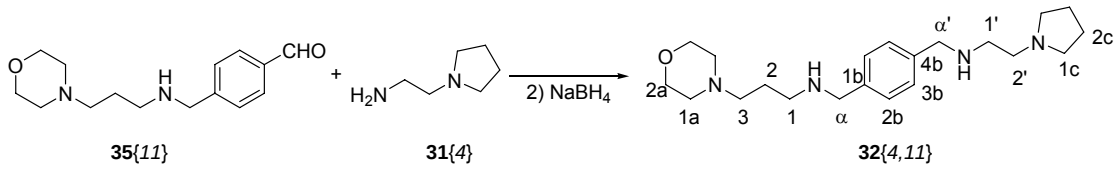


**35**{*11*} **31**{*4*} **32**{*4,11*}

Se sigue el mismo procedimiento que para **37**{*2,4*} pero utilizando 0.84 g (3.2 mmol) de **35**{*11*}, 0.37 g (3.2 mmol) de amina **31**{*4*} y 0.12 g (3.2 mmol) de $NaBH_4$. Se obtienen 1.05 g (2.9 mmol, 91% rendimiento) de un aceite amarillo **32**{*4,11*}.

**Datos espectroscópicos:**

**IR** (film): $\nu$ ($cm^{-1}$) 3305 (*t* N-H), 2953, 2932, 2872, 2852, 2802 (*t* $Csp^3$-H), 1457, 1446 (*f* $Csp^3$-H), 1118 (*t as* C-O-C), 862 (*t sim* C-O-C).

**$^1$H-RMN** (300 MHz, $CDCl_3$): δ (ppm) 7.27 (s, 4H, Ph), 3.79* (s, 2H, H-Cα), 3.77 (s, 2H, H-Cα'), 3.69 (t, $^3J_{H,H}$=4.7 Hz, 4H, H-C2a), 2.74 (t, $^3J_{H,H}$=5.9 Hz, 2H, H-C1'), 2.68 (t, $^3J_{H,H}$=6.9 Hz, 2H, H-C1), 2.61 (t, $^3J_{H,H}$=5.9 Hz, 2H, H-C2'), 2.50-2.37 (m, 10H, H-C3, H-C1a, H-C1c), 2.04 (sa, 2H, deuterable, NH), 1.80-1.68 (m, 6H, H-C2, H-C2c).

**$^{13}$C-RMN** (75.5 MHz, $CDCl_3$): δ (ppm) 139.0* (C1b), 138.7* (C4b), 128.1** (C2b), 128.0** (C3b), 67.0 (C2a), 57.4 (Cα), 55.9 (Cα'), 54.2 (C1c), 53.8 (C1a, C3), 53.7 (C2'), 48.0*** (C1'), 47.9*** (C1), 26.7 (C2), 23.5 (C2c).

**MS** (IE): m/z 361.2 (0.5) $[M+H]^+$, 276.2 (2), 216.2 (15), 100.0 (13), 84.0 (100).

**HRMS** (IE): ($C_{21}H_{37}N_4O$) $[M+H]^+$ Calculado: 361.2967. Obtenido: 361.2965.

## 5.5.11. Síntesis de *N*-(4-((3-(1*H*-imidazol-1-il)propilamino)metil)bencil)-3-(pirrolidin-1-il)propan-1-amina (32{*5,6*}).

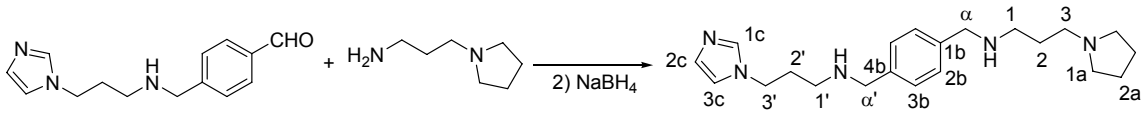


**35**{*6*} **31**{*5*} **32**{*5,6*}

Se sigue el mismo procedimiento que para **37**{*2,4*} pero utilizando 0.91 g (3.7 mmol) de **35**{*6*}, 0.49 g (3.7 mmol) de amina **31**{*5*} y 0.14 g (3.7 mmol) de $NaBH_4$. Se obtienen 1.33 g (3.7 mmol, rendimiento cuantitativo) de un aceite amarillento **32**{*5,6*}.

**Datos espectroscópicos:**

**IR** (film): $\nu$ ($cm^{-1}$) 3281 (*t* N-H), 3104 (*t* $Csp^2$-H), 2931, 2875, 2794 (*t* $Csp^3$-H), 1508 (*t* esqueleto heteroaromático), 1458 (*f* $Csp^3$-H).

**$^1$H-RMN** (300 MHz, $CDCl_3$): δ (ppm) 7.43 (s, 1H, H-C1c), 7.27 (s, 4H, Ph), 7.03 (s, 1H, H-C2c), 6.88 (s, 1H, H-C3c), 4.04 (t, $^3J_{H,H}$=6.9 Hz, 2H, H-C3'), 3.78* (s, 2H, H-Cα), 3.74* (s, 2H, H-Cα'), 2.70 (t, $^3J_{H,H}$=6.9 Hz, 2H, H-C1), 2.60 (t, $^3J_{H,H}$=6.6 Hz, 2H, H-C1'), 2.50 (m, 6H, H-C3, H-C1a), 2.05 (sa, 2H, deuterable, NH), 1.92 (quint, $^3J_{H,H}$=6.6 Hz, 2H, H-C2'), 1.79-1.10 (m, 6H, H-C2, H-C2a).

**$^{13}$C-RMN** (75.5 MHz, $CDCl_3$): δ (ppm) 139.1* (C1b), 138.6* (C4b), 137.0 (C1c), 129.2 (C3c), 128.1** (C2b), 128.0** (C3b), 118.7 (C2c), 54.7 (Cα), 54.2 (C1a), 53.7 (Cα', C3), 48.0 (C1), 45.6 (C3'), 44.7 (C1'), 31.4 (C2'), 29.2 (C2), 23.4 (C2a).

**MS** (IE): m/z 356.4 (1) $[M+H]^+$, 355.5 (0.3) $[M]^+$, 84.2 (100).

**HRMS** (IE): ($C_{21}H_{33}N_5$) Calculado: 355.2736. Obtenido: 355.2740.

## 5.5.12. Síntesis de *N*-(4-((2-(piperidin-1-il)etilamino)metil)bencil)-3-(pirrolidin-1-il)propan-1-amina (32{*5,7*}).

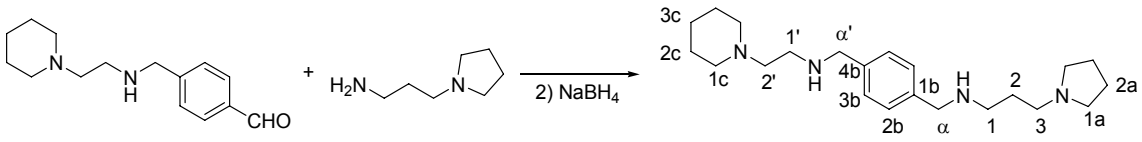


**35**{*7*} **31**{*5*} **32**{*5,7*}

Se sigue el mismo procedimiento que para **37**{*2,4*} pero utilizando 0.85 g (3.5 mmol) de **35**{*7*}, 0.46 g (3.5 mmol) de amina **31**{*5*} y 0.13 g (3.5 mmol) de $NaBH_4$. Se obtienen 1.13 g (3.2 mmol, 92% rendimiento) de un aceite amarillento **32**{*5,7*}.

**Datos espectroscópicos:**

**IR** (film): $\nu$ ($cm^{-1}$) 3298 (*t* N-H), 2933, 2876, 2851, 2792 (*t* $Csp^3$-H), 1454, 1443 (*f* $Csp^3$-H).

**$^1$H-RMN** (300 MHz, $CDCl_3$): δ (ppm) 7.27 (s, 4H, Ph),3.78* (s, 2H, H-Cα), 3.77* (s, 2H, H-Cα'), 2.69 (t, $^3J_{H,H}$=6.3 Hz, H-C1, 4H, H-C1'), 2.52 (m, 6H, H-C3, H-C1a), 2.44 (t, $^3J_{H,H}$=6.3 Hz, 2H, H-C2'), 2.33 (sa, 4H, H-C1c), 2.08 (sa, 2H, deuterable, NH), 1.79-1.70 (m, 6H, H-C2, H-C2a), 1.55 (m, 4H, H-C2c), 1.42 (m, 2H, H-C3c).

**$^{13}$C-RMN** (75.5 MHz, $CDCl_3$): δ (ppm) 138.9* (C1b), 138.7* (C4b), 128.0 (C2b, C3b), 58.5 (Cα'), 54.7 (Cα, C1c), 54.2 (C1a), 53.7** (C3), 53.6** (C2'), 48.0 (C1), 45.9 (C1'), 29.2 (C2), 26.0 (C2c), 24.5 (C3c), 23.4 (C2a).

**MS** (IE): m/z 359.3 (1) $[M+H]^+$, 260.2 (2), 231.2 (2), 98.2 (100), 84.1 (29).

**HRMS** (IE): ($C_{22}H_{39}N_4$) $[M+H]^+$ Calculado: 359.3175. Obtenido: 359.3175.

## 5.5.13. Síntesis de *N*-(4-((3-(pirrolidin-1-il)propilamino)metil)bencil)-3-(2-metilpiperidin-1-il)propan-1-amina (32{*5,8*}).

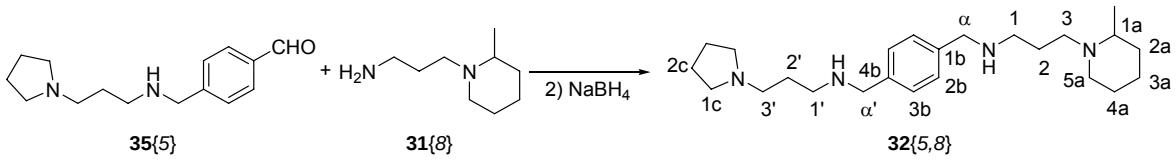


**35**{*5*} **31**{*8*} **32**{*5,8*}

Se sigue el mismo procedimiento que para **37**{*2,4*} pero utilizando 0.96 g (3.9 mmol) de **35**{*5*}, 0.63 g (3.9 mmol) de amina **31**{*8*} y 0.15 g (3.9 mmol) de $NaBH_4$. Se obtienen 1.24 g (3.2 mmol, 83% rendimiento) de un aceite amarillento **32**{*5,8*}.

**Datos espectroscópicos:**

**IR** (film): $\nu$ ($cm^{-1}$) 3281 (*t* N-H), 2930, 2874, 2855, 2790 (*t* $Csp^3$-H), 1448, 1372 (*f* $Csp^3$-H).

**$^1$H-RMN** (300 MHz, $CDCl_3$): δ (ppm) 7.27 (s, 4H, Ph), 3.77* (s, 2H, H-Cα), 3.76* (s, 2H, H-Cα'), 2.86 (m, 1H, $H_{eq}$-C5a), 2.68 (m, 5H, $H_{eq}$-C3, H-C1, H-C1'), 2.49 (m, 6H, H-C3', H-C1c), 2.36 (m, 1H, $H_{ax}$-C3), 2.26 (m, 1H, H-C1a), 2.11 (m, 1H, $H_{ax}$-C5a), 2.02 (sa, 2H, deuterable, NH), 1.79-1.58 (m, 12H, H-C2, $H_{eq}$-C2a, $H_{eq}$-C3a, H-C4a, H-C2', H-C2c), 1.27 (m, 2H, $H_{ax}$-C2a, $H_{ax}$-C3a), 1.05 (d, $^3J_{H,H}$=6.3 Hz, 3H, $CH_3$).

**$^{13}$C-RMN** (75.5 MHz, $CDCl_3$): δ (ppm) 138.9* (C1b), 138.8* (C4b), 128.1** (C2b), 128.0** (C3b), 56.0 (C1a), 54.8 (Cα'), 54.3 (C1c), 53.8** (Cα), 53.7** (C3'), 52.3 (C3), 52.1 (C5a), 48.3*** (C1), 48.0*** (C1'), 34.7**** (C2a), 29.3 (C2'), 26.2 (C4a), 25.8 (C2), 24.0**** (C3a), 23.5 (C2c), 19.1 ($CH_3$).

**MS** (IE): m/z 387.3 (8) $[M+H]^+$, 386.3 (6) $[M]^+$, 288.2 (12), 260.2 (50), 259.2 (21), 258.2 (87), 231.2 (13), 230.2 (58), 161.1 (35), 126.1 (38), 112.1 (100).

**HRMS** (IE): ($C_{24}H_{42}N_4$) Calculado: 386.3409. Obtenido: 386.3412.

## 5.5.14. Síntesis de *N*-(4-((3-(4-metilpiperazin-1-il)propilamino)metil)bencil)-3-(pirrolidin-1-il)propan-1-amina (32{*5,9*}).

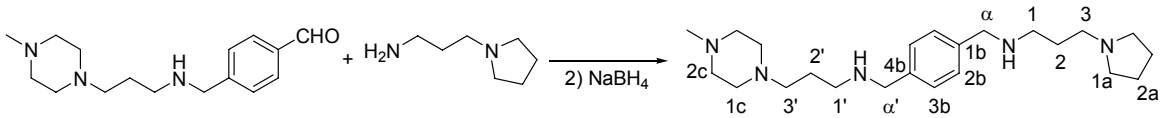


**35**{*9*} **31**{*5*} **32**{*5,9*}

Se sigue el mismo procedimiento que para **37**{*2,4*} pero utilizando 0.93 g (3.4 mmol) de **35**{*9*}, 0.45 g (3.4 mmol) de amina **31**{*5*} y 0.13 g (3.4 mmol) de $NaBH_4$. Se obtienen 1.25 g (3.2 mmol, 95% rendimiento) de un aceite amarillento **32**{*5,9*}.

**Datos espectroscópicos:**

**IR** (film): $\nu$ ($cm^{-1}$) 3284 (*t* N-H), 2935, 2875, 2792 (*t* $Csp^3$-H), 1458, 1372, 1353 (*f* $Csp^3$-H).

**$^1$H-RMN** (300 MHz, $CDCl_3$): δ (ppm) 7.27 (s, 4H, Ph), 3.77* (s, 2H, H-Cα), 3.76* (s, 2H, H-Cα'), 2.68 (m, 4H, H-C1, H-C1'), 2.53-2.38 (m, 16H, H-C3, H-C3', H-C1a, H-C1c, H-C2c), 2.27 (s, 3H, $CH_3$), 1.91 (sa, 2H, deuterable, NH), 1.79-1.68 (m, 8H, H-C2, H-C2', H-C2a).

**$^{13}$C-RMN** (75.5 MHz, $CDCl_3$): δ (ppm) 138.9 (C1b, C4b), 128.0 (C2b, C3b), 56.9 (Cα'), 55.1 (C2c), 54.7 (Cα), 54.2 (C1a), 53.7 (C3, C3'), 53.2 (C1c), 48.1* (C1), 48.0* (C1'), 46.0 ($CH_3$), 29.3 (C2), 27.0 (C2'), 23.5 (C2a).

**MS** (IE): m/z 387.4 (1) $[M]^+$, 315.2 (95), 303.3 (47), 289.3 (7), 272.3 (2), 260.2 (42), 259.2 (100), 231.3 (18), 230.2 (83), 113.1 (24), 84.1 (12).

**HRMS** (IE): ($C_{23}H_{41}N_5$) Calculado: 387.3362. Obtenido: 387.3347.

## 5.5.15. Síntesis de *N*-(4-((2-morfolinoetilamino)metil)bencil)-3-(pirrolidin-1-il)propan-1-amina (32{5,10}).

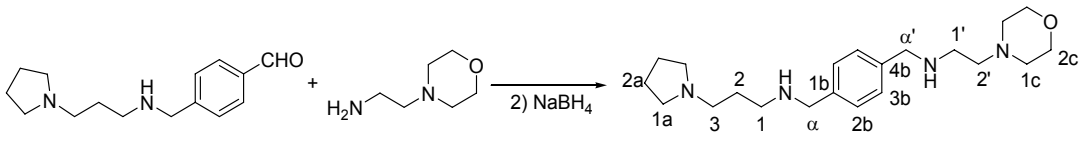


**35**{*5*} **31**{*10*} **32**{*5,10*}

Se sigue el mismo procedimiento que para **37**{*2,4*} pero utilizando 0.96 g (3.9 mmol) de **35**{*5*}, 0.51 g (3.9 mmol) de amina **31**{*10*} y 0.15 g (3.9 mmol) de $NaBH_4$. Se obtienen 1.27 g (3.5 mmol, 90% rendimiento) de un aceite amarillento **32**{*5,10*}.

**Datos espectroscópicos:**

**IR** (film): $\nu$ ($cm^{-1}$) 3304 (*t* N-H), 2935, 2872, 2852, 2800 (*t* $Csp^3$-H), 1454 (*f* $Csp^3$-H), 1118 (*t as* C-O-C), 868 (*t sim* C-O-C).

**$^1$H-RMN** (300 MHz, $CDCl_3$): δ (ppm) 7.28 (s, 4H, Ph), 3.79 (s, 4H, H-Cα, H-Cα'), 3.69 (t, $^3J_{H,H}$=4.5 Hz, 4H,H-C2c), 2.71 (m, 4H, H-C1, H-C1'), 2.51 (m, 8H, H-C3, H-C1a, H-C2'), 2.40 (t, $^3J_{H,H}$=4.5 Hz, 4H, H-C1c), 2.18 (sa, 2H, deuterable, NH), 1.78 (m, 6H, H-C2, H-C2a).

**$^{13}$C-RMN** (75.5 MHz, $CDCl_3$): δ (ppm) 139.0* (C1b), 138.6* (C4b), 128.1 (C2b, C3b), 67.0 (C2c), 58.2 (Cα'), 54.8 (Cα), 54.2 (C1a), 53.7 (C2', C1c), 53.6 (C3), 48.0 (C1), 45.3 (C1'), 28.9 (C2), 23.5 (C2a).

**MS** (IE): m/z 361.3 (3) $[M+H]^+$, 360.3 (4) $[M]^+$, 260.3 (89), 232.2 (79), 231.2 (22), 230.2 (100), 100.0 (54).

**HRMS** (IE): ($C_{21}H_{36}N_4O$) Calculado: 360.2889. Obtenido: 360.2879.

## 5.5.16. Síntesis de *N*-(4-((3-(pirrolidin-1-il)propilamino)metil)bencil)-3-morfolinopropan-1-amina (32{*5,11*}).

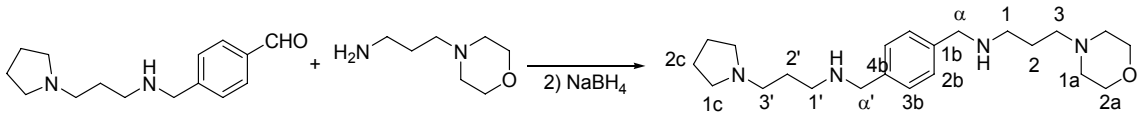


**35**{*5*} **31**{*11*} **32**{*5,11*}

Se sigue el mismo procedimiento que para **37**{*2,4*} pero utilizando 0.94 g (3.8 mmol) de **35**{*5*}, 0.55 g (3.8 mmol) de amina **31**{*11*} y 0.15 g (3.8 mmol) de $NaBH_4$. Se obtienen 1.33 g (3.5 mmol, 93% rendimiento) de un aceite amarillo **32**{*5,11*}.

**Datos espectroscópicos:**

**IR** (film): $\nu$ ($cm^{-1}$) 3288 (*t* N-H), 2935, 2872, 2853, 2802 (*t* $Csp^3$-H), 1457, 1447 (*f* $Csp^3$-H), 1118 (*t as* C-O-C), 862 (*t sim* C-O-C).

**$^1$H-RMN** (300 MHz, $CDCl_3$): δ (ppm) 7.27 (s, 4H, Ph), 3.78* (s, 2H, H-Cα), 3.77* (s, 2H, H-Cα'), 3.69 (t, $^3J_{H,H}$=4.8 Hz, 4H, H-C2a), 2.70 (m, 4H, H-C1, H-C1'), 2.51 (m, 6H, H-C3', H-C1c), 2.41 (m, 6H, H-C3, H-C1a), 2.04 (sa, 2H, deuterable, NH), 1.73 (m, 8H, H-C2, H-C2', H-C2c).

**$^{13}$C-RMN** (75.5 MHz, $CDCl_3$): δ (ppm) 138.9 (C1b, C4b), 128.0 (C2b, C3b), 67.0 (C2a), 57.4 (Cα), 54.8 (Cα'), 54.3 (C1c), 53.8* (C1a, C3), 53.7* (C3'), 48.1** (C1), 48.0** (C1'), 29.3 (C2'), 26.8 (C2), 23.5 (C2c).

**MS** (IE): m/z 374.3 (18) $[M]^+$, 246.2 (83), 231.2 (34), 230.2 (100), 186.2 (57), 185.2 (74), 184.2 (36), 100.1 (93).

**HRMS** (IE): ($C_{22}H_{38}N_4O$) $[M]^+$ Calculado: 374.3046. Obtenido: 374.3049.

## 5.5.17. Síntesis de *N*-(4-((2-(piperidin-1-il)etilamino)metil)bencil)-3-(1*H*-imidazol-1-il)propan-1-amina (32{*6,7*}).

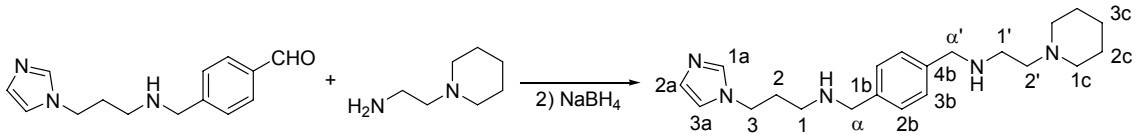


**35**{*6*} **31**{*7*} **32**{*6,7*}

Se sigue el mismo procedimiento que para **37**{*2,4*} pero utilizando 0.90 g (3.7 mmol) de **35**{*6*}, 0.48 g (3.7 mmol) de amina **31**{*7*} y 0.14 g (3.7 mmol) de $NaBH_4$. Se obtienen 1.23 g (3.5 mmol, 94% rendimiento) de un aceite amarillo **32**{*6,7*}.

**Datos espectroscópicos:**

**IR** (film): $\nu$ ($cm^{-1}$) 3279 (*t* N-H), 2935, 2850, 2793 (*t* $Csp^3$-H), 1508 (*t* esqueleto heteroaromático), 1446 (*f* $Csp^3$-H).

**$^1$H-RMN** (300 MHz, $CDCl_3$): δ (ppm) 7.43 (s, 1H, H-C1a), 7.28 (m, 4H, Ph), 7.03 (s, 1H, H-C2a), 6.89 (s, 1H, H-C3a), 4.04 (t, $^3J_{H,H}$=6.8 Hz, 2H, H-C3), 3.81* (s, 2H, H-C$\alpha$), 3.74* (s, 2H, H-C$\alpha$'), 2.73 (t, $^3J_{H,H}$=5.9 Hz, 2H, H-C1'), 2.60 (t, $^3J_{H,H}$=6.8 Hz, 2H, H-C1), 2.48 (t, $^3J_{H,H}$=5.9 Hz, 2H, H-C2'), 2.46 (sa, 2H, deuterable, NH), 2.37 (m, 4H, H-C1c), 1.92 (quint, $^3J_{H,H}$=6.8 Hz, 2H, H-C2), 1.56 (m, 4H, H-C2c), 1.43 (m, 2H, H-C3c).

**$^{13}$C-RMN** (75.5 MHz, DMSO-$d_6$): δ (ppm) 137.0 (C1a, C1b, C4b), 128.6* (C2b), 128.3* (C3b), 128.1 (C3a), 119.1 (C2a), 55.8* (C$\alpha$), 53.7 (C1c), 51.8* (C$\alpha$'), 51.3* (C2'), 44.8 (C3), 43.9 (C1'), 43.7 (C1), 29.9 (C2), 25.0 (C2c), 23.6 (C3c).

**MS** (IE): m/z 356.2 (0.05) $[M+1]^+$, 256.9 (50), 98.0 (100), 81.0 (4).

**HRMS** (ESI): ($C_{21}H_{34}N_5$) Calculado: 356.2809. Obtenido: 356.2823.

## 5.5.18. Síntesis de *N*-(4-((3-(1*H*-imidazol-1-il)propilamino)metil)bencil)-3-(2-metilpiperidin-1-il)propan-1-amina (32{*6,8*}).

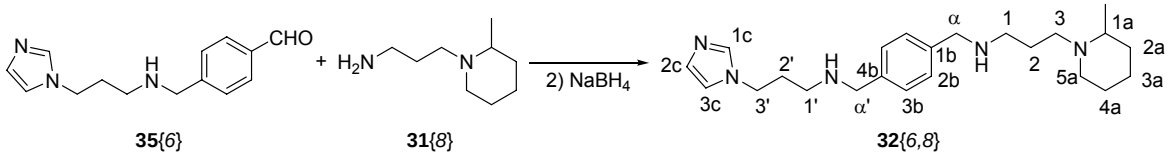


**35**{*6*} **31**{*8*} **32**{*6,8*}

Se sigue el mismo procedimiento que para **37**{*2,4*} pero utilizando 0.88 g (3.6 mmol) de **35**{*6*}, 0.59 g (3.6 mmol) de amina **31**{*8*} y 0.14 g (3.6 mmol) de $NaBH_4$. Se obtienen 1.20 g (3.1 mmol, 86% rendimiento) de un aceite amarillo **32**{*6,8*}.

**Datos espectroscópicos:**

**IR** (film): $\nu$ ($cm^{-1}$) 3277 (*t* N-H), 3104 (*t* $Csp^2$-H), 2929, 2853, 2802 (*t* $Csp^3$-H), 1508 (*t* esqueleto heteroaromático), 1450, 1373 (*f* $Csp^3$-H).

**$^1$H-RMN** (300 MHz, $CDCl_3$): δ (ppm) 7.44 (s, 1H, H-C1c), 7.27 (s, 4H, Ph), 7.03 (s, 1H, H-C2c), 6.89 (s, 1H, H-C3c), 4.04 (t, $^3J_{H,H}$=6.9 Hz, 2H, H-C3'), 3.77* (s, 2H, H-C$\alpha$), 3.74*(s, 2H, H-C$\alpha$'), 2.87 (m, 1H, $H_{eq}$-C5a), 2.74 (m, 1H, $H_{eq}$-C3), 2.65 (t, $^3J_{H,H}$=6.9 Hz, 2H, H-C1), 2.60 (t, $^3J_{H,H}$=6.9 Hz, 2H, H-C1'), 2.37 (m, 1H, $H_{ax}$-C3), 2.27 (m, 1H, H-C1a), 2.12 (m, 1H, $H_{ax}$-C5a), 2.09 (sa, 2H, deuterable, NH), 1.92 (quint, $^3J_{H,H}$=6.9 Hz, 2H, H-C2'), 1.72-1.53 (m, 6H, H-C2, $H_{eq}$-C2a, $H_{eq}$-C3a, H-C4a), 1.29 (m, 2H, $H_{ax}$-C2a, $H_{ax}$-C3a), 1.05 (d, $^3J_{H,H}$=6.3 Hz, 3H, $CH_3$).

**$^{13}$C-RMN** (75.5 MHz, $CDCl_3$): δ (ppm) 138.9* (C1b), 138.7* (C4b), 137.1 (C1c), 129.2 (C3c), 128.2** (C2b), 128.0** (C3b), 118.7 (C2c), 56.0 (C1a), 53.7 (C$\alpha$, C$\alpha$'), 52.3 (C3), 52.0 (C5a), 48.3 (C1), 45.7 (C3'), 44.7 (C1'), 34.6*** (C2a), 31.4 (C2'), 26.1 (C4a), 25.7 (C2), 23.9*** (C3a), 19.1 ($CH_3$).

**MS** (IE): m/z 383.3 (0.7) $[M]^+$, 243.1 (8), 229.1 (11), 155.2 (14), 124.2 (11), 112.2 (100).

**HRMS** (IE): ($C_{23}H_{37}N_5$) Calculado: 383.3049. Obtenido: 383.3048.

## 5.5.19. Síntesis de *N*-(4-((3-(4-metilpiperazin-1-il)propilamino)metil)bencil)-3-(1*H*-imidazol-1-il)propan-1-amina (32{*6,9*}).

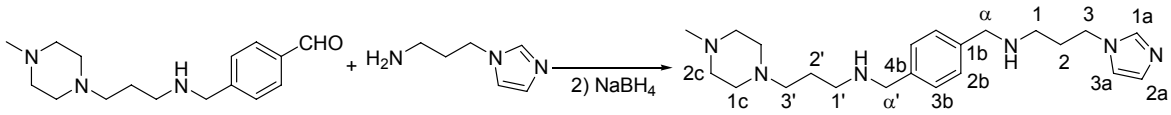


**35**{*9*} **31**{*6*} **32**{*6,9*}

Se sigue el mismo procedimiento que para **37**{*2,4*} pero utilizando 0.76 g (2.8 mmol) de **35**{*9*}, 0.35 g (2.8 mmol) de amina **31**{*6*} y 0.11 g (2.8 mmol) de $NaBH_4$. Se obtienen 0.36 g (0.9 mmol, 34% rendimiento) de un aceite amarillo **32**{*6,9*}.

**Datos espectroscópicos:**

**IR** (film): $\nu$ ($cm^{-1}$) 3278 (*t* N-H), 3102 (t $Csp^2$-H), 2934, 2875, 2795 (*t* $Csp^3$-H), 1508 (*t* esqueleto heteroaromático), 1458, 1372, 1356 (*f* $Csp^3$-H).

**$^1$H-RMN** (300 MHz, $CDCl_3$): δ (ppm) 7.43 (s, 1H, H-C1a), 7.27 (s, 4H, Ph), 7.03 (s, 1H, H-C2a), 6.88 (s, 1H, H-C3a), 4.04 (t, $^3J_{H,H}$=6.9 Hz, 2H, H-C3), 3.77* (s, 2H, H-C$\alpha$), 3.74* (s, 2H, H-C$\alpha$'), 2.68 (t, $^3J_{H,H}$=7.2 Hz, 2H, H-C1'), 2.61 (t, $^3J_{H,H}$=6.6 Hz, 2H, H-C1), 2.43 (sa, 8H, H-C1c, H-C2c), 2.41 (t, $^3J_{H,H}$=7.2 Hz, 2H, H-C3'), 2.27 (s, 3H, $CH_3$), 1.93 (sa, 2H, deuterable, NH), 1.92 (quint, $^3J_{H,H}$=6.6 Hz, 2H, H-C2), 1.71 (quint, $^3J_{H,H}$=7.2 Hz, 2H, H-C2').

**$^{13}$C-RMN** (75.5 MHz, $CDCl_3$): δ (ppm) 139.0* (C1b), 138.7* (C4b), 137.1 (C1a), 129.2 (C3a), 128.1** (C2b), 128.0** (C3b), 118.7 (C2a), 56.9 (C$\alpha$'), 55.1 (C2c), 53.7 (C$\alpha$, C3'), 53.2 (C1c), 48.1 (C1'), 46.0 ($CH_3$), 45.7 (C3), 44.7 (C1), 31.4 (C2), 26.9 (C2').

**MS** (IE): m/z 385.3 (2) $[M+H]^+$, 271.2 (15), 257.1 (24), 113.1 (76), 70.0 (100).

**HRMS** (IE): ($C_{22}H_{36}N_6$) Calculado: 384.3001. Obtenido: 384.3004.

## 5.5.20. Síntesis de *N*-(4-((2-morfolinoetilamino)metil)bencil)-3-(1*H*-imidazol-1-il)propan-1-amina (32{*6,10*}).

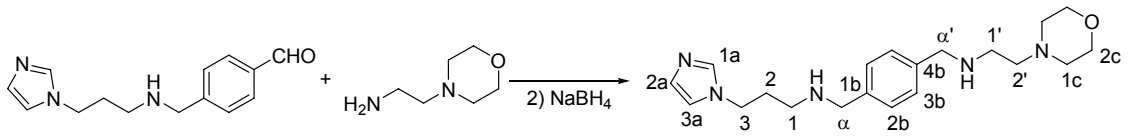


**35**{*6*} **31**{*10*} **32**{*6,10*}

Se sigue el mismo procedimiento que para **37**{*2,4*} pero utilizando 0.79 g (3.2 mmol) de **35**{*6*}, 0.43 g (3.2 mmol) de amina **31**{*10*} y 0.12 g (3.2 mmol) de $NaBH_4$. Se obtienen 1.11 g (3.1 mmol, 96% rendimiento) de un aceite amarillento **32**{*6,10*}.

**Datos espectroscópicos:**

**IR** (film): $\nu$ ($cm^{-1}$) 3299 (*t* N-H), 3105 (*t* $Csp^2$-H), 2934, 2890, 2851, 2811 (*t* $Csp^3$-H), 1508 (*t* esqueleto heteroaromático), 1454 (*f* $Csp^3$-H), 1117 (*t as* C-O-C), 854 (*t sim* C-O-C).

**$^1$H-RMN** (300 MHz, $CDCl_3$): δ (ppm) 7.43 (s, 1H, H-C1a), 7.28 (s, 4H, Ph), 7.03 (s, 1H, H-C2a), 6.88 (s, 1H, H-C3a), 4.05 (t, $^3J_{H,H}$=6.9 Hz, 2H, H-C3), 3.79* (s, 2H, H-C$\alpha$), 3.74* (s, 2H, H-C$\alpha$'), 3.69 (t, $^3J_{H,H}$=4.7 Hz, 4H, H-C2c), 2.71 (t, $^3J_{H,H}$=6.0 Hz, 2H, H-C1'), 2.60 (t, $^3J_{H,H}$=6.9 Hz, 2H, H-C1), 2.50 (t, $^3J_{H,H}$=6.0 Hz, 2H, H-C2'), 2.41 (t, $^3J_{H,H}$=4.7 Hz, 4H, H-C1c), 1.95 (sa, 2H, deuterable, NH), 1.93 (quint, $^3J_{H,H}$=6.9 Hz, 2H, H-C2).

**$^{13}$C-RMN** (75.5 MHz, $CDCl_3$): δ (ppm) 139.0* (C1b), 138.7* (C4b), 137.0 (C1a), 129.2 (C3a), 128.1** (C2b), 128.0** (C3b), 118.7 (C2a), 67.0 (C2c), 58.2 (C$\alpha$'), 53.7 (C$\alpha$, C2', C1c), 45.6 (C3), 45.3 (C1'), 44.6 (C1), 31.2 (C2).

**MS** (IE): m/z 358.2 (1) $[M+H]^+$, 257.0 (30), 100.0 (100), 56.0 (21).

**HRMS** (IE): ($C_{20}H_{31}N_5O$) Calculado: 357.2529. Obtenido: 357.2517.

## 5.5.21. Síntesis de *N*-(4-((3-morfolinopropilamino)metil)bencil)-3-(1*H*-imidazol-1-il)propan-1-amina (32{*6,11*}).

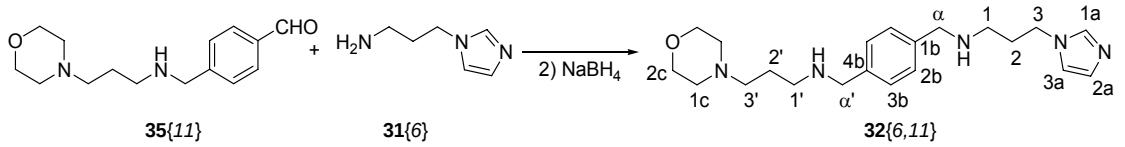


**35**{*11*} **31**{*6*} **32**{*6,11*}

Se sigue el mismo procedimiento que para **37**{*2,4*} pero utilizando 1.15 g (4.4 mmol) de **35**{*11*}, 0.56 g (4.4 mmol) de amina **31**{*6*} y 0.17 g (4.4 mmol) de $NaBH_4$. Se obtienen 1.36 g (3.7 mmol, 85% rendimiento) de un aceite amarillo **32**{*6,11*}.

**Datos espectroscópicos:**

**IR** (film): $\nu$ ($cm^{-1}$) 3282 (*t* N-H), 3104 (*t* $Csp^2$-H), 2935, 2852, 2808 (*t* $Csp^3$-H), 1509 (*t* esqueleto heteroaromático), 1456 (*f* $Csp^3$-H), 1117 (*t as* C-O-C), 861 (*t sim* C-O-C).

**$^1$H-RMN** (300 MHz, $CDCl_3$): δ (ppm) 7.42 (s, 1H, H-C1a), 7.27 (m, 4H, Ph), 7.03 (s, 1H, H-C2a), 6.88 (s, 1H, H-C3a), 4.04 (t, $^3J_{H,H}$=6.9 Hz, 2H, H-C3), 3.79 (s, 2H, H-Cα'), 3.74 (s, 2H, H-Cα), 3.69 (t, $^3J_{H,H}$=4.7 Hz, 4H, H-C2c), 2.71 (t, $^3J_{H,H}$=6.9 Hz, 2H, H-C1'), 2.60 (t, $^3J_{H,H}$=6.9 Hz, 2H, H-C1), 2.42 (m, 6H, H-C3', H-C1c), 1.92 (quint, $^3J_{H,H}$=6.9 Hz, 2H, H-C2), 1.88 (s, 2H, deuterable, NH), 1.72 (quint, $^3J_{H,H}$=6.9 Hz, 2H, H-C2').

**$^{13}$C-RMN** (75.5 MHz, $CDCl_3$): δ (ppm) 138.9* (C1b), 138.18* (C4b), 137.0 (C1a), 129.1 (C3a), 128.2 (C2b, C3b), 118.7 (C2a), 66.9 (C2c), 57.4 (Cα'), 53.7 (C1c), 53.6 (Cα), 53.4 (C3'), 48.0 (C1'), 45.5 (C3), 44.6 (C1), 31.3 (C2), 26.1 (C2').

**MS** (IE): m/z 372.0 (8) $[M+H]^+$, 114.0 (21), 100.0 (100), 95.0 (8), 81.0 (14), 56.1 (43).

**HRMS** (ESI): ($C_{21}H_{34}N_5O$) $[M+H]^+$ Calculado: 372.2758. Obtenido: 372.2772.

## 5.5.22. Síntesis de *N*-(4-((2-(piperidin-1-il)etilamino)metil)bencil)-3-(2-metilpiperidin-1-il)propan-1-amina (32{*7,8*}).

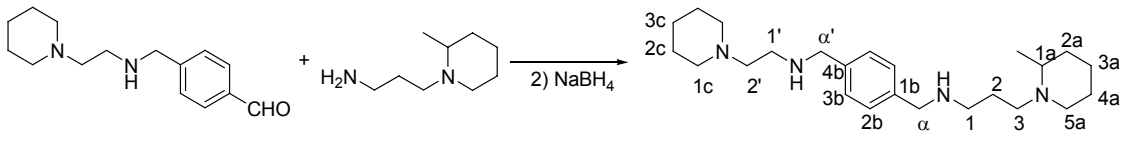


**35**{*7*} **31**{*8*} **32**{*7,8*}

Se disuelven 0.66 g (2.7 mmol) de **35**{*7*} y 0.44 g (2.7 mmol) de amina **31**{*8*} en 3 mL de MeOH anhidro. Se añade $Na_2SO_4$ anhidro y se calienta en el microondas a 100 ºC durante 2 h. Se filtra y se adicionan 10 mL de MeOH anhidro y 0.10 g (2.7 mmol) de $NaBH_4$. Se deja reaccionar a temperatura ambiente durante 4 h. Se añade agua y se extrae con $CH_2Cl_2$. La fase orgánica se lava con salmuera y se seca sobre $MgSO_4$ anhidro. Se elimina el disolvente a presión reducida y se obtienen 0.98 g (2.5 mmol, 95%) de un aceite amarillo **32**{*7,8*}.

**Datos espectroscópicos:**

**IR** (film): $\nu$ ($cm^{-1}$) 3301 (*t* N-H), 2932, 2852, 2802 (*t* $Csp^3$-H), 1467, 1443, 1373 (*f* $Csp^3$-H).

**$^1$H-RMN** (300 MHz, $CDCl_3$): δ (ppm) 7.27 (s, 4H, Ph), 3.78* (s, 2H, H-Cα), 3.77* (s, 2H, H-Cα'), 2.86 (m, 1H, $H_{eq}$-C5a), 2.78 (m, 1H, $H_{eq}$-C3), 2.69 (t, $^3J_{H,H}$=6.3 Hz, 2H, C1'), 2.63 (t, $^3J_{H,H}$=6.9 Hz, 4H, H-C1), 2.44 (t, $^3J_{H,H}$=6.3 Hz, 2H, C2'), 2.34 (m, 5H, $H_{ax}$-C3, C1c), 2.25 (m, 1H, H-C1a), 2.11 (m, 1H, $H_{ax}$-C5a), 2.07 (sa, 2H, deuterable, NH), 1.68 (quint, $^3J_{H,H}$=6.9 Hz, 2H, H-C2), 1.55 (m, H, $H_{eq}$-C2a, $H_{eq}$-C3a, H-C4a, H-C2c), 1.42 (m, 2H, H-C3c), 1.28 (m, 2H, $H_{ax}$-C2a, $H_{ax}$-C3a), 1.05 (d, $^3J_{H,H}$=6.3 Hz, 3H, $CH_3$).

**$^{13}$C-RMN** (75.5 MHz, $CDCl_3$): δ (ppm) 139.0* (C4b), 138.8* (C1b), 128.0 (C2b, C3b), 58.6 (Cα'), 55.9 (C1a), 54.7 (C1c), 53.7 (Cα, C2'), 52.3 (C3), 52.1 (C5a), 48.3 (C1), 45.9 (C1'), 34.7** (C2a), 26.2 (C4a), 26.1 (C2c), 25.7 (C2), 24.5 (C3c), 24.0** (C3a), 19.1 ($CH_3$).

**AEO**: Calculado ($C_{24}H_{42}N_4$): C 74.56%, H 10.95%, N 14.49%. Obtenido: C 74.61%, H 11.25%, N 14.49%.

**MS** (FAB): m/z 387.3 (32) $[M+H]^+$, 386.3 (3) $[M]^+$, 126.1 (13), 112.1 (100).

**HRMS** (FAB): ($C_{24}H_{43}N_4$) $[M+H]^+$ Calculado: 387.3488. Obtenido: 387.3492.

## 5.5.23. Síntesis de *N*-(4-((2-(piperidin-1-il)etilamino)metil)bencil)-3-(4-metilpiperazin-1-il)propan-1-amina (32{*7,9*}).

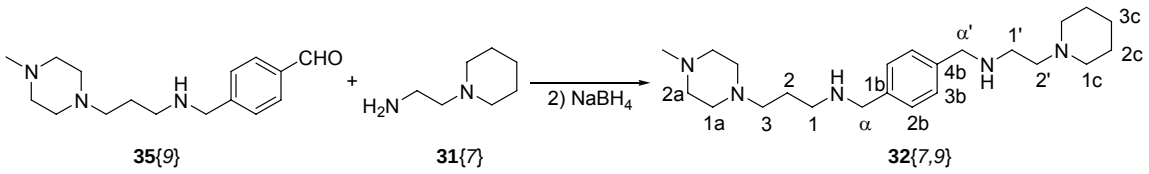


**35**{*9*} **31**{*7*} **32**{*7,9*}

Se sigue el mismo procedimiento que para **37**{*2,4*} pero utilizando 0.73 g (2.6 mmol) de **35**{*9*}, 0.34 g (2.6 mmol) de amina **31**{*7*} y 0.10 g (2.6 mmol) de $NaBH_4$. Se obtienen 0.48 g (1.2 mmol, 47% rendimiento) de un aceite amarillento **32**{*7,9*}.

**Datos espectroscópicos:**

**IR** (film): $\nu$ ($cm^{-1}$) 3285 (*t* N-H), 2934, 2878, 2849, 2794 (*t* $Csp^3$-H), 1457, 1446, 1372, 1349 (*f* $Csp^3$-H).

**$^1$H-RMN** (300 MHz, $CDCl_3$): δ (ppm) 7.27 (s, 4H, Ph), 3.78* (s, 2H, H-C$\alpha$), 3.77* (s, 2H, H-C$\alpha$'), 2.69 (m, 4H, H-C1', H-C1), 2.47-2.34 (m, 16H, H-C3, H-C1a, H-C2a, H-C2', H-C1c), 2.27 (s, 3H, $CH_3$), 2.22 (sa, 2H, deuterable, NH), 1.72 (quint, $^3J_{H,H}$=6.9 Hz, 2H, H-C2), 1.55 (m, 4H, H-C2c), 1.42 (m, 2H, H-C3c).

**$^{13}$C-RMN** (75.5 MHz, $CDCl_3$): δ (ppm) 139.0* (C1b), 138.5* (C4b), 128.1** (C2b), 128.0** (C3b), 58.5 (C$\alpha$'), 57.0 (C$\alpha$), 55.1 (C2a), 54.7 (C1c), 53.7*** (C3), 53.6*** (C2'), 53.2 (C1a), 48.1 (C1), 46.0 ($CH_3$), 45.9 (C1'), 26.8 (C2), 26.0 (C2c), 24.5 (C3c).

**MS** (FAB): m/z 388.2 (100) $[M+H]^+$, 387.2 (17) $[M]^+$, 230.1 (22), 132.9 (86), 127.1 (23), 113.1 (52), 112.1 (61).

**HRMS** (FAB): ($C_{21}H_{34}N_5O$) $[M+H]^+$ Calculado: 388.3440. Obtenido: 388.3454.

## 5.5.24. Síntesis de *N*-(4-((2-(piperidin-1-il)etilamino)metil)bencil)-3-morfolinopropan-1-amina (32{*7,11*}).

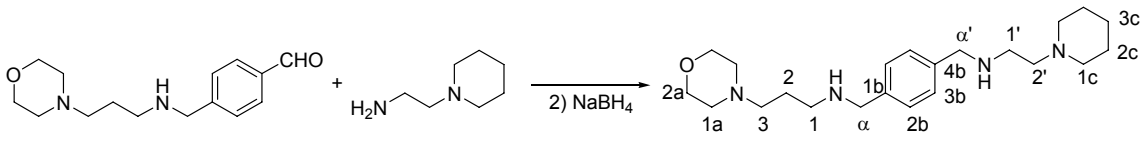


**35**{*11*} **31**{*7*} **32**{*7,11*}

Se sigue el mismo procedimiento que para **37**{*2,4*} pero utilizando 0.89 g (3.4 mmol) de **35**{*11*}, 0.44 g (3.4 mmol) de amina **31**{*7*} y 0.13 g (3.4 mmol) de $NaBH_4$. Se obtienen 1.24 g (3.3 mmol, 98% rendimiento) de un aceite amarillo **32**{*7,11*}.

**Datos espectroscópicos:**

**IR** (film): $\nu$ ($cm^{-1}$) 3304 (*t* N-H), 2933, 2852, 2806 (*t* $Csp^3$-H), 1454, 1444 (*f* $Csp^3$-H), 1119 (*t as* C-O-C), 862 (*t sim* C-O-C).

**$^1$H-RMN** (300 MHz, $CDCl_3$): δ (ppm) 7.27 (s, 4H, Ph), 3.78* (s, 2H, H-Cα), 3.77* (s, 2H, H-Cα'), 3.69 (t, $^3J_{H,H}$=4.7 Hz, 4H, H-C2a), 2.69 (m, 4H, H-C1, H-C1'), 2.47-2-34 (m, 12H, H-C3, H-C1a, H-C2', H-C1c), 2.11 (sa, 2H, deuterable, NH), 1.71 (quint, $^3J_{H,H}$=7.2 Hz, 2H, H-C2), 1.55 (m, 4H, H-C2c), 1.42 (m, 2H, H-C3c).

**$^{13}$C-RMN** (75.5 MHz, $CDCl_3$): δ (ppm) 139.0* (C1b), 138.6* (C4b), 128.1** (C2b), 128.0** (C3b), 66.9 (C2a), 58.5 (Cα'), 57.4 (Cα), 54.7 (C1c), 53.8 (C1a), 53.7 (C3, C2'), 48.0 (C1), 45.9 (C1'), 26.6 (C2), 26.0 (C2c), 24.5 (C3c).

**AEO**: Calculado ($C_{22}H_{38}N_4O$): C 70.54%, H 10.23%, N 14.96%, O 4.27%. Obtenido: C 70.97%, H 10.06%, N 14.98%.

**MS** (IE): m/z 373.3 (1) $[M-H]^+$, 98.0 (100).

## 5.5.25. Síntesis de *N*-(4-((3-(4-metilpiperazin-1-il)propilamino)metil)bencil)-3-(2-metilpiperidin-1-il)propan-1-amina (32{*8,9*}).

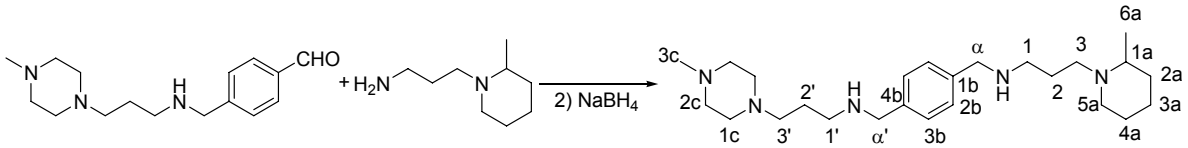


**35**{*9*} **31**{*8*} **32**{*8,9*}

Se sigue el mismo procedimiento que para **37**{*2,4*} pero utilizando 0.75 g (2.7 mmol) de **35**{*9*}, 0.45 g (2.7 mmol) de amina **31**{*8*} y 0.10 g (2.7 mmol) de $NaBH_4$. Se obtienen 0.45 g (1.1 mmol, 39% rendimiento) de un aceite amarillo **32**{*8,9*}.

**Datos espectroscópicos:**

**IR** (film): $\nu$ ($cm^{-1}$) 3280 (*t* N-H), 2931, 2875, 2852, 2793 (*t* $Csp^3$-H), 1458, 1448, 1372 (*f* $Csp^3$-H).

**$^1$H-RMN** (300 MHz, $CDCl_3$): δ (ppm) 7.28 (s, 4H, Ph), 3.77 (s, 4H, H-Cα, H-Cα'), 2.88 (m, 1H, $H_{eq}$-C5a), 2.75 (m, 1H, $H_{eq}$-C3), 2.67 (t, $^3J_{H,H}$=6.6 Hz, 2H, H-C1'), 2.65 (t, $^3J_{H,H}$=6.6 Hz, 2H, H-C1), 2.43 (sa, 12H, H-C3', H-C1c, H-C2c, $H_{ax}$-C3, H-C1a), 2.27 (s, 3H, H-C3c), 2.23 (sa, 2H, deuterable, NH), 2.12 (m, 1H, $H_{ax}$-C5a), 1.76-1.53 (m, 8H, H-C2, $H_{eq}$-C2a, $H_{eq}$-C3a, H-C4a, H-C2'), 1.32-1.21 (m, 2H, $H_{ax}$-C2a, $H_{ax}$-C3a), 1.05 (d, $^3J_{H,H}$=6.3 Hz, 3H, H-C6a).

**$^{13}$C-RMN** (75 MHz, $CDCl_3$): δ (ppm) 138.8* (C1b), 138.6* (C4b), 128.1** (C2b), 128.0** (C3b), 57.0 (Cα'), 56.0 (C1a), 55.1 (C2c), 53.7 (Cα, C3'), 53.2 (C1c), 52.3 (C3), 52.0 (C5a), 48.3 (C1), 48.1 (C1'), 46.0 (C3c), 34.5*** (C2a), 26.9 (C2'), 26.0 (C4a), 25.6 (C2), 23.9*** (C3a), 19.0 (C6a).

**MS** (IE): m/z 415.4 (0.3) $[M]^+$, 258.2 (35), 218.2 (4), 112.2 (100), 98.0 (27).

**HRMS** (IE): ($C_{25}H_{45}N_5$) Calculado: 415.3675. Obtenido: 415.3660.

## 5.5.26. Síntesis de *N*-(4-((2-morfolinoetilamino)metil)bencil)-3-(2-metilpiperidin-1-il)propan-1-amina (32{*8,10*}).

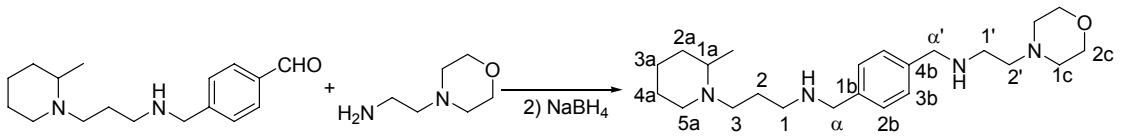


**35**{*8*} **31**{*10*} **32**{*8,10*}

Se sigue el mismo procedimiento que para **37**{*2,4*} pero utilizando 1.35 g (8.5 mmol) de **35**{*8*}, 1.12 g (8.5 mmol) de amina **31**{*10*} y 0.33 g (8.5mmol) de $NaBH_4$. Se obtienen 2.46 g (6.3 mmol, 74% rendimiento) de un aceite amarillento **32**{*8,10*}.

**Datos espectroscópicos:**

**IR** (film): $\nu$ ($cm^{-1}$) 3305 (*t* N-H), 2930, 2853, 2807 (*t* $Csp^3$-H), 1453 (*f* $Csp^3$-H), 1119 (*t as* C-O-C), 868 (*t sim* C-O-C).

**$^1$H-RMN** (300 MHz, $CDCl_3$): δ (ppm) 7.27 (s, 4H, Ph), 3.79* (s, 2H, H-Cα), 3.77* (s, 2H, H-Cα'), 3.69 (t, $^3J_{H,H}$=4.5 Hz, 4H, H-C2c), 2.86 (m, 1H, $H_{eq}$-C5a), 2.74 (m, 1H, $H_{eq}$-C3), 2.70 (t, $^3J_{H,H}$=6.0 Hz, 2H, H-C1'), 2.63 (t, $^3J_{H,H}$=6.9 Hz, 2H, H-C1), 2.49 (t, $^3J_{H,H}$=6.0 Hz, 2H, H-C2'), 2.40 (m, 4H, H-C1c), 2.34 (m, 1H, $H_{ax}$-C3), 2.25 (m, 1H, H-C1a), 2.11 (m, 1H, $H_{ax}$-C5a), 1.91 (sa, 2H, deuterable, NH), 1.68 (quint, $^3J_{H,H}$=6.9 Hz, 2H, H-C2), 1.63 (m, 4H, $H_{eq}$-C2a, $H_{eq}$-C3a, H-C4a), 1.27 (m, 2H, $H_{ax}$-C2a, $H_{ax}$-C3a), 1.05 (d, $^3J_{H,H}$=6.0 Hz, 3H, $CH_3$).

**$^{13}$C-RMN** (75.5 MHz, $CDCl_3$): δ (ppm) 139.0* (C1b), 138.9* (C4b), 128.0 (C2b, C3b), 67.0 (C2c), 58.3 (Cα'), 55.9 (C1a), 53.8 (Cα), 53.7 (C2', C1c), 52.3 (C3), 52.1 (C5a), 48.4 (C1), 45.3 (C1'), 34.7** (C2a), 26.2 (C4a), 25.8 (C2), 24.0** (C3a), 19.2 ($CH_3$).

**MS** (IE): m/z 389.3 (1) $[M+H]^+$, 155.2 (6), 126.2 (12), 112.1 (91), 100.0 (100), 98.0 (27).

**HRMS** (IE): ($C_{23}H_{40}N_4O$) Calculado: 388.3202. Obtenido: 388.3202.

## 5.5.27. Síntesis de *N*-(4-((3-morfolinopropilamino)metil)bencil)-3-(2-metilpiperidin-1-il)propan-1-amina (32{*8,11*}).

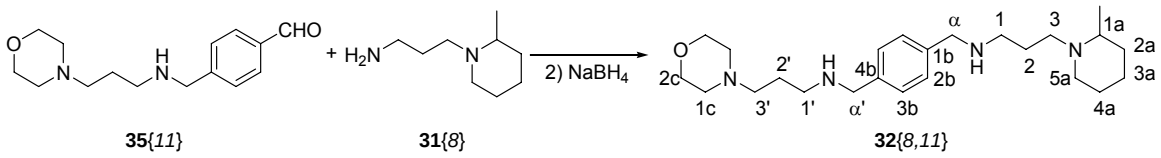


**35**{*11*} **31**{*8*} **32**{*8,11*}

Se sigue el mismo procedimiento que para **37**{*2,4*} pero utilizando 1.00 g (3.8 mmol) de **35**{*11*}, 0.62 g (3.8 mmol) de amina **31**{*8*} y 0.15 g (3.8 mmol) de $NaBH_4$. Se obtienen 1.54 g (3.8 mmol, rendimiento cuantitativo) de un aceite amarillo **32**{*8,11*}.

**Datos espectroscópicos:**

**IR** (film): ν ($cm^{-1}$) 3286 (*t* N-H), 2929, 2853, 2806 (*t* $Csp^3$-H), 1448, 1372 (*f* $Csp^3$-H), 1119 (*t as* C-O-C), 862 (*t sim* C-O-C).

**$^1$H-RMN** (300 MHz, $CDCl_3$): δ (ppm) 7.27 (s, 4H, Ph), 3.77 (s, 4H, H-Cα, H-Cα'), 3.70 (t, $^3J_{H,H}$=4.7 Hz, 4H, H-C2c), 2.87 (m, 1H, $H_{eq}$-C5a), 2.79-2.62 (m, 5H, H-C1, $H_{eq}$-C3, H-C1'), 2.43-2.32 (m, 7H, $H_{ax}$-C3, H-C3', H-C1c), 2.27 (m, 1H, H-C1a), 2.12 (sa, 2H, deuterable, NH), 2.11 (m, 1H, $H_{ax}$-C5a), 1.75-1.52 (m, 8H, H-C2, $H_{eq}$-C2a, $H_{eq}$-C3a, H-C4a, H-C2'), 1.30 (m, 2H, $H_{ax}$-C2a, $H_{ax}$-C3a), 1.05 (d, $^3J_{H,H}$=6.0 Hz, 3H, $CH_3$).

**$^{13}$C-RMN** (75.5 MHz, $CDCl_3$): δ (ppm) 138.9* (C1b), 138.7* (C4b), 128.1** (C2b), 128.0** (C3b), 67.0 (C2c), 57.4 (Cα'), 56.0 (C1a), 53.8 (C1c), 53.7 (C3', Cα), 52.3 (C3), 52.0 (C5a), 48.3 (C1), 48.0 (C1'), 34.6*** (C2a), 27.0 (C2'), 26.1 (C4a), 25.7 (C2), 23.9*** (C3a), 19.1 ($CH_3$).

**MS** (IE): m/z 403.4 (0.5) $[M+H]^+$, 112.0 (100), 100.0 (36).

**HRMS** (IE): ($C_{24}H_{42}N_4O$) Calculado: 402.3359. Obtenido: 402.3354.

## 5.5.28. Síntesis de *N*-(4-((2-morfolinoetilamino)metil)bencil)-3-(4-metilpiperazin-1-il)propan-1-amina (32{9,10}).

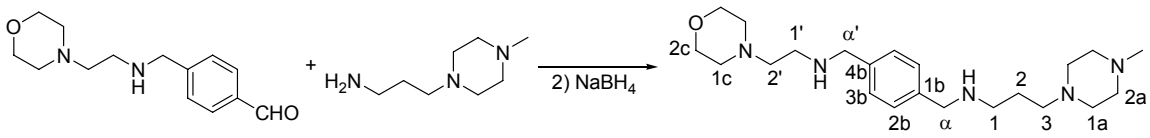


**35**{*10*} **31**{*9*} **32**{*9,10*}

Se sigue el mismo procedimiento que para **37**{*2,4*} pero utilizando 0.68 g (2.7 mmol) de **35**{*10*}, 0.44 g (2.7 mmol) de amina **31**{*9*} y 0.10 g (2.7 mmol) de $NaBH_4$. Se obtienen 0.92 g (2.4 mmol, 86% rendimiento) de un aceite amarillo **32**{*9,10*}.

**Datos espectroscópicos:**

**IR** (film): $\nu$ ($cm^{-1}$) 3300 (*t* N-H), 2935, 2872, 2796 (*t* $Csp^3$-H), 1456, 1372, 1355 (*f* $Csp^3$-H), 1118 (*t as* C-O-C), 868 (*t sim* C-O-C).

**$^1$H-RMN** (300 MHz, $CDCl_3$): δ (ppm) 7.27 (s, 4H, Ph), 3.79 (s, 2H, H-C$\alpha$'), 3.77 (s, 2H, H-C$\alpha$), 3.68 (t, $^3J_{H,H}$=4.7 Hz, 4H, H-C2c), 2.69 (m, 4H, H-C1', H-C1), 2.52-2.39 (m, 16H, H-C3, H.C1a, H-C2a, H-C2', H-C1c), 2.27 (s, 3H, $CH_3$), 2.11 (sa, 2H, deuterable, NH), 1.72 (quint, $^3J_{H,H}$=6.9 Hz, 2H, H-C2).

**$^{13}$C-RMN** (75.5 MHz, $CDCl_3$): δ (ppm) 138.9* (C1b), 138.7* (C4b), 128.0 (C2b, C3b), 67.0 (C2c), 58.2 (C$\alpha$'), 57.0 (C$\alpha$), 55.1 (C2a), 53.7 (C2', C1c, C3), 53.2 (C1a), 48.1 (C1), 46.0 ($CH_3$), 45.3 (C1'), 26.9 (C2).

**MS** (IE): m/z 389.4 (1) $[M]^+$, 100.1 (100), 70.0 (38), 56.0 (27).

**HRMS** (IE): ($C_{22}H_{39}N_5O$) Calculado: 389.3155. Obtenido: 389.3153.

## 5.5.29. Síntesis de *N*-(4-((3-morfolinopropilamino)metil)bencil)-3-(4-metilpiperazin-1-il)propan-1-amina (32{*9,11*}).

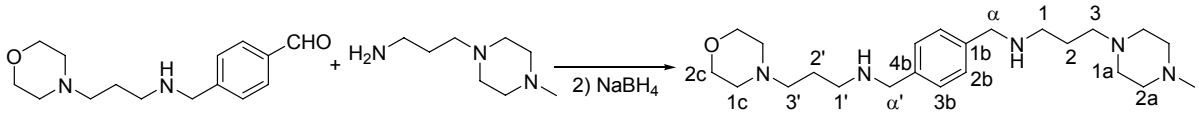


**35**{*11*} **31**{*9*} **32**{*9,11*}

Se sigue el mismo procedimiento que para **37**{*2,4*} pero utilizando 0.71 g (2.7 mmol) de **35**{*11*}, 0.43 g (2.7 mmol) de amina **31**{*9*} y 0.10 g (2.7 mmol) de $NaBH_4$. Se obtienen 0.91 g (2.3 mmol, 84% rendimiento) de un aceite amarillo **32**{*9,11*}.

**Datos espectroscópicos:**

**IR** (film): $\nu$ ($cm^{-1}$) 3288 (*t* N-H), 2935, 2872, 2851, 2795 (*t* $Csp^3$-H), 1476, 1372, 1356 (*f* $Csp^3$-H), 1118 (*t as* C-O-C), 862 (*t sim* C-O-C).

**$^1$H-RMN** (300 MHz, $CDCl_3$): δ (ppm) 7.27 (s, 4H, Ph), 3.77 (s, 4H, H-C$\alpha$, H-C$\alpha$'), 3.69 (t, $^3J_{H,H}$=4.8 Hz, 4H, H-C2c), 2.68 (t, $^3J_{H,H}$=6.9 Hz, 2H, H-C1'), 2.67 (t, $^3J_{H,H}$=6.9 Hz, 2H, H-C1), 2.45-2.37 (m, 16H, H-C3, H-C1a, H-C2a, H-C3', H-C1c), 2.27 (s, 3H, $CH_3$), 2.03 (sa, 2H, deuterable, NH), 1.71 (quint, $^3J_{H,H}$=6.9 Hz, 4H, H-C2, H-C2').

**$^{13}$C-RMN** (75.5 MHz, $CDCl_3$): δ (ppm) 138.8 (C1b, C4b), 128.0* (C2b), 127.9* (C3b), 66.9 (C2c), 57.3 (C$\alpha$'), 56.9 (C$\alpha$), 55.1 (C2a), 53.7 (C3', C1c, C3), 53.2 (C1a), 48.1 (C1'), 47.9 (C1), 46.0 ($CH_3$), 26.9 (C2), 26.7 (C2').

**MS** (IE): m/z 403.4 (4) $[M]^+$, 113.2 (52), 100.1 (100), 70.0 (97), 56.0 (49).

**HRMS** (IE): ($C_{23}H_{41}N_5O$) Calculado: 403.3311. Obtenido: 403.3311.

## 5.5.30. Síntesis de *N*-(4-((2-morfolinoetilamino)metil)bencil)-3-morfolinopropan-1-amina (32{10,11}).

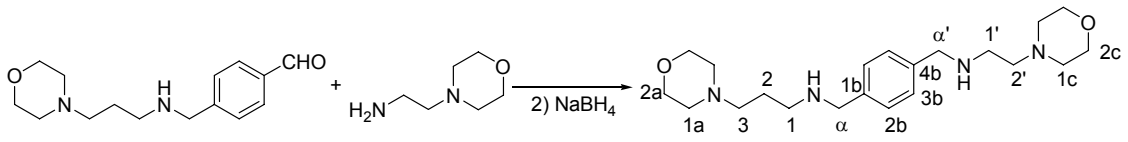


**35**{*11*} **31**{*10*} **32**{*10,11*}

Se sigue el mismo procedimiento que para **37**{*2,4*} pero utilizando 0.88 g (3.3 mmol) de **35**{*11*}, 0.44 g (3.3 mmol) de amina **31**{*10*} y 0.13 g (3.3 mmol) de $NaBH_4$. Se obtienen 1.16 g (3.1 mmol, 92% rendimiento) de un aceite naranja **32**{*10,11*}.

**Datos espectroscópicos:**

**IR** (film): $\nu$ ($cm^{-1}$) 3307 (*t* N-H), 2950, 2891, 2852, 2808 (*t* $Csp^3$-H), 1455 (*f* $Csp^3$-H), 1118 (*t as* C-O-C), 863 (*t sim* C-O-C).

**$^1$H-RMN** (300 MHz, $CDCl_3$): δ (ppm) 7.27 (s, 4H, Ph), 3.79* (s, 2H, H-C$\alpha$), 3.77* (s, 2H, H-C$\alpha$'), 3.69 (m, 8H, H-C2a, H-C2c), 2.69 (m, 4H, H-C1, H-C1'), 2.50 (t, $^3J_{H,H}$=6.0 Hz, 2H, H-C2'), 2.45-2.38 (m, 10H, H-C3, H-C1a, H-C1c), 1.96 (sa, 2H, deuterable, NH), 1.71 (quint, $^3J_{H,H}$=6.9 Hz, 2H, H-C2).

**$^{13}$C-RMN** (75.5 MHz, $CDCl_3$): δ (ppm) 138.9* (C1b), 138.8* (C4b), 128.1** (C2b), 128.0** (C3b), 67.0 (C2a, C2c), 58.2 (C$\alpha$'), 57.4 (C$\alpha$), 53.8 (C1a), 53.7 (C3, C2', C1c), 48.0 (C1), 45.3 (C1'), 26.7 (C2).

**MS** (IE): m/z 376.2 $[M]^+$, 276.2 (6), 100.0 (100), 56.0 (14).

**HRMS** (IE): ($C_{21}H_{36}N_4O_2$) Calculado: 376.2838. Obtenido: 376.2849.

## 5.6. Síntesis de hidrazono/amino-hidrazonas.

### 5.6.1. Síntesis de ((4-(*N*-(4-metilpiperazin-1-il)imino)metil)fenil)-*N*-(piperidin-1-il)metanamina (33{*1,3*}).

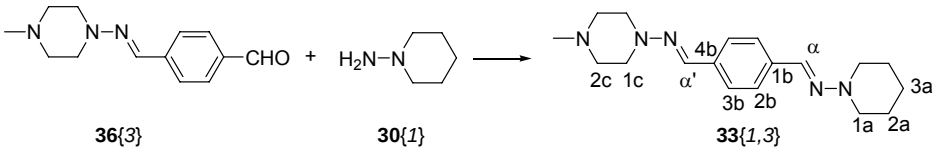


**36**{*3*} **30**{*1*} **33**{*1,3*}

Se disuelven 0.53 g (2.3 mmol) de **36**{*3*} y 0.24 g (2.3 mmol) de amina **30**{*1*} en 30 mL de MeOH anhidro. Se añade tamiz molecular de 4 Å y se agita a temperatura de reflujo y bajo atmósfera de nitrógeno durante 36 h. Se filtra el tamiz molecular y se elimina el disolvente a presión reducida y se obtienen 0.69 g (2.2 mmol, 95%) de un sólido amarillo **33**{*1,3*}.

**Datos espectroscópicos:**

**IR** (film): $\nu$ ($cm^{-1}$) 2934, 2837, 2798 (*t* $Csp^3$-H), 1577 (*t* C=N), 1452, 1365 (*f* $Csp^3$-H).

**$^1$H-RMN** (300 MHz, $CDCl_3$): δ (ppm) 7.56 (s, 4H, Ph), 7.53* (s, 1H, H-Cα), 7.52* (s, 1H, H-Cα'), 3.22 (t, $^3J_{H,H}$=5.1 Hz, 4H, H-C1c), 3.17 (t, $^3J_{H,H}$=5.6 Hz, 4H, H-C1a), 2.62 (t, $^3J_{H,H}$=5.1 Hz, 4H, H-C2c), 2.36 (s, 3H, $CH_3$), 1.75 (m, 4H, H-C2a), 1.54 (m, 2H, H-C3a).

**$^{13}$C-RMN** (75.5 MHz, $CDCl_3$): δ (ppm) 136.4* (C1b), 135.6 (Cα'), 135.5* (C4b), 134.0 (Cα), 126.2** (C2b), 126.0** (C3b), 54.6 (C1c), 52.1 (C1a), 51.0 (C2c), 46.0 ($CH_3$), 25.3 (C2a), 24.2 (C3a).

**MS** (IE): m/z 314.2 (22) $[M+1]^+$, 313.2 (100) $[M]^+$, 99.2 (33).

**HRMS** (IE): ($C_{18}H_{27}N_5$) Calculado: 313.2266. Obtenido: 313.2266.

## 5.6.2. Síntesis de *N*-(4-((piperidin-1-ilimino)metil)bencil)-3-(pirrolidin-1-il)propan-1-amina (37{*1,5*}).

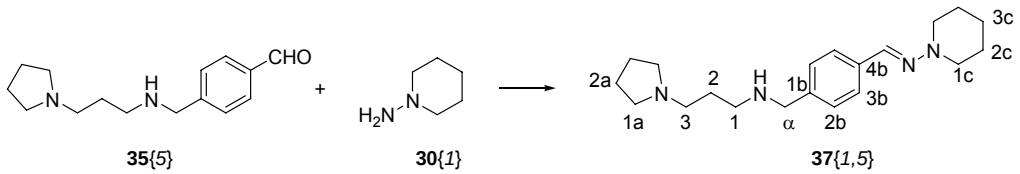


**35**{*5*} **30**{*1*} **37**{*1,5*}

Se sigue el mismo procedimiento que para **33**{*1,3*} pero utilizando 1.04 g (4.2 mmol) de **35**{*5*} y 0.44 g (4.2 mmol) de amina **30**{*1*}. Se obtienen 1.17 g (3.6 mmol, 84% rendimiento) de un aceite amarillo **37**{*1,5*}.

**Datos espectroscópicos:**

**IR** (film): $\nu$ ($cm^{-1}$) 3287 (*t* N-H), 2935, 2874, 2854, 2793 (*t* $Csp^3$-H), 1591 (*t* C=N), 1450 (*f* $Csp^3$-H).

**$^1$H-RMN** (300 MHz, $CDCl_3$): δ (ppm) 7.55 (d, $^3J_{H,H}$=8.1 Hz, 2H, H-C3b), 7.54 (s, 1H, CH=N), 7.27 (d, $^3J_{H,H}$=8.1 Hz, 2H, H-C2b), 3.78 (s, 2H, H-C$\alpha$), 3.15 (t, $^3J_{H,H}$=5.7 Hz, 4H, H-C1c), 2.28 (t, $^3J_{H,H}$=6.9 Hz, 2H, H-C1), 2.50 (m, 6H, H-C3, H-C1a), 2.03 (sa, 1H, deuterable, NH), 1.79-1.69 (m, 10H, H-C2, H-C2a, H-C2c), 1.55 (m, 2H, H-C3c).

**$^{13}$C-RMN** (75.5 MHz, $CDCl_3$): δ (ppm) 139.7 (C1b), 135.3 (C4b), 134.5 (C=N), 128.1 (C3b), 125.9 (C2b), 54.8 (C$\alpha$), 54.2 (C1a), 53.7 (C3), 52.1 (C1c), 48.0 (C1), 29.1 (C2), 25.2 (C2c), 24.2 (C3c), 23.5 (C2a).

**MS** (IE): m/z 328.3 (0.5) $[M]^+$, 244.2 (2), 201.2 (8), 84.1 (100).

**HRMS** (IE): ($C_{20}H_{32}N_4$) Calculado: 328.2627. Obtenido: 328.2624.

## 5.6.3. Síntesis de *N*-(4-((piperidin-1-ilimino)metil)bencil)-3-(1*H*-imidazol-1-il)propan-1-amina (37{*1,6*}).

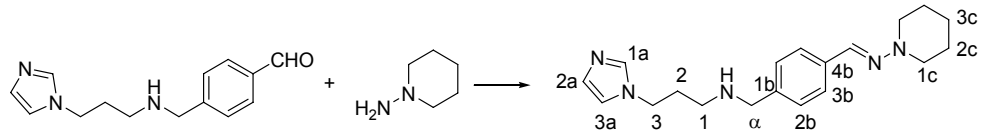


**35**{*6*} **30**{*1*} **37**{*1,6*}

Se sigue el mismo procedimiento que para **33**{*1,3*} pero utilizando 0.98 g (4.0 mmol) de **35**{*6*} y 0.42 g (4.0 mmol) de amina **30**{*1*}. Se obtienen 1.31 g (4.0 mmol, rendimiento cuantitativo) de un aceite rojizo **37**{*1,6*}.

**Datos espectroscópicos:**

**IR** (film): $\nu$ ($cm^{-1}$) 3282 (*t* N-H), 3105 (*t* $Csp^2$-H), 2935, 2853, 2809 (*t* $Csp^3$-H), 1590 (*t* C=N), 1508 (*t* esqueleto heteroaromático), 1450 (*f* $Csp^3$-H).

**$^1$H-RMN** (300 MHz, $CDCl_3$): δ (ppm) 7.56 (s, 1H, CH=N), 7.55 (d, $^3J_{H,H}$=8.1 Hz, 2H, H-C3b), 7.45 (s, 1H, H-C1a), 7.26 (d, $^3J_{H,H}$=8.1 Hz, 2H, H-C2b), 7.03 (s, 1H, H-C2a), 6.88 (s, 1H, H-C3a), 4.03 (t, $^3J_{H,H}$=6.9 Hz, 2H, H-C3), 3.74 (s, 2H, H-C$\alpha$), 3.15 (t, $^3J_{H,H}$=5.7 Hz, 4H, H-C1c), 2.60 (t, $^3J_{H,H}$=6.9 Hz, 2H, H-C1), 2.07 (sa, 1H, deuterable, NH), 1.92 (quint, $^3J_{H,H}$=6.9 Hz, 2H, H-C2), 1.75 (quint, $^3J_{H,H}$=5.7 Hz, 4H, H-C2c), 1.54 (quint, $^3J_{H,H}$=5.7 Hz, 2H, H-C3c).

**$^{13}$C-RMN** (75.5 MHz, $CDCl_3$): δ (ppm) 139.5 (C1b), 137.0 (C1a), 135.5 (C4b), 134.2 (C=N), 129.2 (C3a), 128.1 (C3b), 125.9 (C2b), 118.7 (C2a), 53.7 (C$\alpha$), 52.1 (C1c), 45.6 (C3), 44.7 (C1), 31.3 (C2), 25.2 (C2c), 24.2 (C3c).

**MS** (IE): m/z 326.2 (18) $[M+1]^+$, 243.2 (100), 242.2 (47), 241.1 (42), 215.1 (60), 173.1 (30), 147.0 (38), 91.0 (63), 55.0 (45).

**HRMS** (IE): ($C_{19}H_{27}N_5$) Calculado: 325.2266. Obtenido: 325.2277.

## 5.6.4. Síntesis de *N*-(4-((piperidin-1-ilimino)metil)bencil)-3-(2-metilpiperidin-1-il)propan-1-amina (37{*1,8*}).

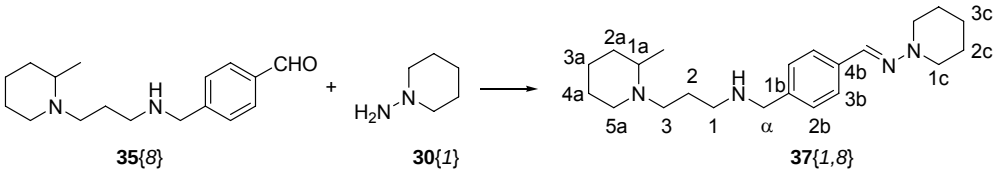


**35**{*8*} **30**{*1*} **37**{*1,8*}

Se sigue el mismo procedimiento que para **33**{*1,3*} pero utilizando 0.51 g (1.9 mmol) de **35**{*8*} y 0.19 g (1.9 mmol) de amina **30**{*1*}. Se obtienen 0.67 g (1.9 mmol, rendimiento cuantitativo) de un aceite rojizo **37**{*1,8*}.

**Datos espectroscópicos:**

**IR** (film): $\nu$ ($cm^{-1}$) 3282 (*t* N-H), 2932, 2854, 2804 (*t* $Csp^3$-H), 1591 (*t* C=N), 1450, 1364 (*f* $Csp^3$-H).

**$^1$H-RMN** (300 MHz, $CDCl_3$): δ (ppm) 7.55 (d, $^3J_{H,H}$=8.1 Hz, 2H, H-C3b), 7.54 (s, 1H, CH=N), 7.28 (d, $^3J_{H,H}$=8.1 Hz, 2H, H-C2b), 3.78 (s, 2H, H-C$\alpha$), 3.15 (t, $^3J_{H,H}$=5.4 Hz, 4H, H-C1c), 2.87 (m, 1H, $H_{eq}$-C5a), 2.74 (m, 1H, $H_{eq}$-C3), 2.65 (t, $^3J_{H,H}$=6.9 Hz, 2H, H-C1), 2.42 (sa, 1H, deuterable, NH), 2.37 (m, 1H, $H_{ax}$-C3), 2.28 (m, 1H, H-C1a), 2.13 (m, 1H, $H_{ax}$-C5a), 1.79-1.52 (m, 12H, H-C2, $H_{eq}$-C2a, $H_{eq}$-C3a, H-C4a, H-C2c, H-C3c), 1.29 (m, 2H, $H_{ax}$-C2a, $H_{ax}$-C3a), 1.05 (d, $^3J_{H,H}$=6.3 Hz, 3H, $CH_3$).

**$^{13}$C-RMN** (75.5 MHz, $CDCl_3$): δ (ppm) 139.5 (C1b), 135.4 (C4b), 134.4 (C=N), 128.2 (C3b), 125.9 (C2b), 56.0 (C1a), 53.7 (C$\alpha$), 52.3 (C3), 52.1 (C1c), 52.0 (C5a), 48.3 (C1), 34.6* (C2a), 26.1 (C4a), 25.5 (C2), 25.3 (C2c), 24.2 (C3c), 23.9* (C3a), 19.0 ($CH_3$).

**MS** (IE): m/z 356.2 (2) $[M]^+$, 216.0 (5), 201.0 (23), 155.1 (6), 112.0 (100), 84.0 (6).

**HRMS** (IE): ($C_{22}H_{36}N_4$) Calculado: 356.2940. Obtenido: 356.2942.

## 5.6.5. Síntesis de *N*-(4-((piperidin-1-ilimino)metil)bencil)-3-(4-metilpiperazin-1-il)propan-1-amina (37{*1,9*}).

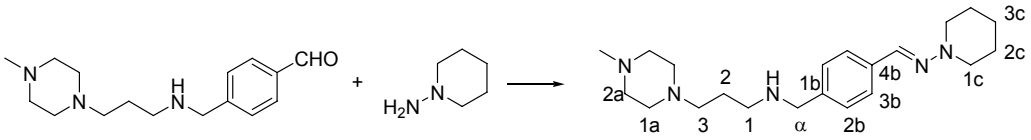


**35**{*9*} **30**{*1*} **37**{*1,9*}

Se sigue el mismo procedimiento que para **33**{*1,3*} pero utilizando 0.96 g (3.5 mmol) de **35**{*9*} y 0.36 g (3.5 mmol) de amina **30**{*1*}. Se obtienen 1.21 g (3.4 mmol, 97% rendimiento) de un aceite amarillo **37**{*1,9*}.

**Datos espectroscópicos:**

**IR** (film): $\nu$ ($cm^{-1}$) 3286 (*t*N-H), 2935, 2875, 2853, 2794 (*t* $Csp^3$-H), 1591 (*t* C=N), 1451, 1357 (*f* $Csp^3$-H).

**$^1$H-RMN** (300 MHz, $CDCl_3$): δ (ppm) 7.55 (d, $^3J_{H,H}$=8.1 Hz, 2H, H-C3b), 7.54 (s, 1H, CH=N), 7.27 (d, $^3J_{H,H}$=8.1 Hz, 2H, H-C2b), 3.77 (s, 2H, H-C$\alpha$), 3.15 (t, $^3J_{H,H}$=5.7 Hz, 4H, H-C1c), 2.67 (t, $^3J_{H,H}$=6.9 Hz, 2H, H-C1), 2.42 (sa, 8H, H-C1a, H-C2a), 2.40 (t, $^3J_{H,H}$=6.9 Hz, 2H, H-C3), 2.27 (s, 3H, $CH_3$), 2.16 (sa, 1H, deuterable, NH), 1.79-1.66 (m, 6H, H-C2, H-C2c), 1.54 (m, 2H, H-C3c).

**$^{13}$C-RMN** (75.5 MHz, $CDCl_3$): δ (ppm) 139.7 (C1b), 135.4 (C4b), 134.5 (C=N), 128.1 (C3b), 125.9 (C2b), 57.0 (C$\alpha$), 55.1 (C2a), 53.7 (C3), 53.2 (C1a), 52.1 (C1c), 48.1 (C1), 46.0 ($CH_3$), 26.9 (C2), 25.3 (C2c), 24.2 (C3c).

**MS** (IE): m/z 358.3 (2) $[M+H]^+$, 273.2 (70), 201.1 (100), 113.0 (77), 91.0 (51), 84.0 (18), 70 (77), 56.0 (37).

**HRMS** (IE): ($C_{21}H_{35}N_5$) Calculado: 357.2892. Obtenido: 357.2903.

## 5.6.6. Síntesis de *N*-(4-((piperidin-1-ilimino)metil)bencil)-3-morfolinopropan-1-amina (37{*1,11*}).

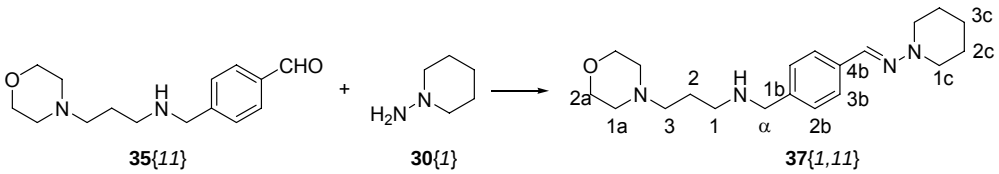


**35**{*11*} **30**{*1*} **37**{*1,11*}

Se sigue el mismo procedimiento que para **35**{*1,3*} pero utilizando 0.93 g (3.6 mmol) de **35**{*11*} y 0.37 g (3.6 mmol) de amina **30**{*1*}. Se obtienen 1.21 g (3.5 mmol, 99% rendimiento) de un aceite amarillo **37**{*1,11*}.

**Datos espectroscópicos:**

**IR** (film): $\nu$ ($cm^{-1}$) 3298 (*t* N-H), 2936, 2853, 2807 (*t* $Csp^3$-H), 1591 (*t* C=N), 1451 (*f* $Csp^3$-H), 1118 (*t as* C-O-C), 861 (*t sim* C-O-C).

**$^1$H-RMN** (300 MHz, $CDCl_3$): δ (ppm) 7.55 (d, $^3J_{H,H}$=8.1 Hz, 2H, H-C3b), 7.54 (s, 1H, CH=N), 7.27 (d, $^3J_{H,H}$=8.1 Hz, 2H, H-C2b), 3.77 (s, 2H, H-Cα), 3.69 (t, $^3J_{H,H}$=4.7 Hz, 4H, H-C2a), 3.15 (t, $^3J_{H,H}$=5.6 Hz, 4H, H-C1c), 2.67 (t, $^3J_{H,H}$=6.9 Hz, 2H, H-C1), 2.44-2.37 (m, 6H, H-C3, H-C1a), 1.99 (sa, 1H, deuterable, NH), 1.79-1.65 (m, 6H, H-C2, H-C2c), 1.54 (quint, $^3J_{H,H}$=5.7 Hz, 2H, H-C3c).

**$^{13}$C-RMN** (75.5 MHz, $CDCl_3$): δ (ppm) 139.8 (C1b), 135.4 (C4b), 134.4 (C=N), 128.1 (C3b), 125.9 (C2b), 67.0 (C2a), 57.4 (Cα), 53.8 (C3, C1a), 52.1 (C1c), 47.9 (C1), 26.6 (C2), 25.3 (C2c), 24.2 (C3c).

**MS** (IE): m/z 345.2 (2) $[M+H]^+$, 344.2 (3) $[M]^+$, 260.1 (3), 216.0 (29), 201.0 (28), 100.0 (100), 56.0 (20).

**HRMS** (IE): ($C_{20}H_{32}N_4O$) Calculado: 344.2576. Obtenido: 344.2580.

## 5.6.7. Síntesis de *N*-(4-((2,6-dimetilpiperidin-1-ilimino)metil)bencil)-3-(pirrolidin-1-il)propan-1-amina (37{*2,5*}).

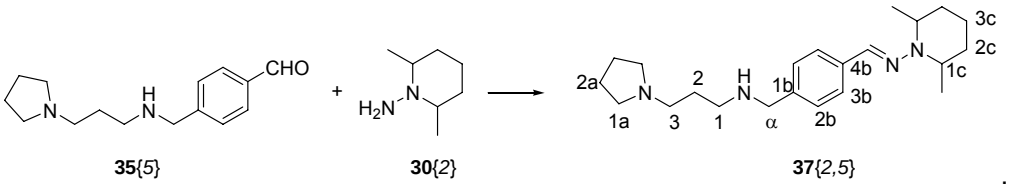


**35**{*5*} **30**{*2*} **37**{*2,5*}

Se sigue el mismo procedimiento que para **33**{*1,3*} pero utilizando 1.00 g (4.1 mmol) de **35**{*5*} y 0.58 g (4.1 mmol) de amina **30**{*2*}. Se obtienen 1.18 g (3.3 mmol, 81% rendimiento) de un aceite amarillo **37**{*2,5*}.

**Datos espectroscópicos:**

**IR** (film): $\nu$ ($cm^{-1}$) 3283 (*t* N-H), 2961, 2931, 2872, 2794 (*t* $Csp^3$-H), 1625 (*t* $Csp^2$-$Csp^2$), 1584 (*t* C=N), 1554 (*t* $Csp^2$-$Csp^2$), 1449, 1369 (*f* $Csp^3$-H).

**$^1$H-RMN** (300 MHz, $CDCl_3$): δ (ppm) 8.06 (s, 1H, CH=N), 7.64 (d, $^3J_{H,H}$=8.1 Hz, 2H, H-C3b), 7.33 (d, $^3J_{H,H}$=8.1 Hz, 2H, H-C2b), 3.81 (s, 2H, H-C$\alpha$), 3.07 (sa, 2H, H-C1c), 2.69 (t, $^3J_{H,H}$=6.9 Hz, 2H, H-C1), 2.51 (m, 6H, H-C3, H-C1a), 2.08 (sa, 1H, deuterable, NH), 1.79-1.69 (m, 10H, H-C2, H-C2a, H-C2c), 1.53 (m, 2H, H-C3c), 1.00 (d, $^3J_{H,H}$=6.3 Hz, 6H, $CH_3$).

**$^{13}$C-RMN** (75.5 MHz, $CDCl_3$): δ (ppm) 152.4 (C=N), 141.7 (C1b), 133.7 (C4b), 128.1 (C3b), 127.3 (C2b), 57.3 (C1c), 54.8 (C$\alpha$), 54.2 (C1a), 53.7 (C3), 48.0 (C1), 32.9 (C2c), 29.1 (C2), 23.5 (C2a), 21.5 (C3c), 20.6 ($CH_3$).

**MS** (IE): m/z 356.3 (1) $[M]^+$, 244.2 (11), 98.2 (14), 84.1 (100), 55.0 (23).

**HRMS** (IE): ($C_{22}H_{36}N_4$) Calculado: 356.2940. Obtenido: 356.2934.

## 5.6.8. Síntesis de *N*-(4-((4-metilpiperazin-1-ilimino)metil)bencil)-3-(pirrolidin-1-il)propan-1-amina (37{*3,5*}).

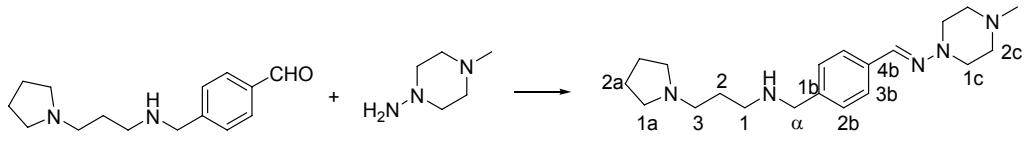


**35**{*5*} **30**{*3*} **37**{*3,5*}

Se sigue el mismo procedimiento que para **33**{*1,3*} pero utilizando 1.03 g (4.2 mmol) de **35**{*5*} y 0.50 g (4.2 mmol) de amina **30**{*3*}. Se obtienen 1.43 g (4.2 mmol, rendimiento cuantitativo) de un aceite marrón **37**{*3,5*}.

**Datos espectroscópicos:**

**IR** (film): $\nu$ ($cm^{-1}$) 3288 (*t* N-H), 2937, 2876, 2794 (*t* $Csp^3$-H), 1592 (*t* C=N), 1452, 1365, 1355 (*f* $Csp^3$-H).

**$^1$H-RMN** (300 MHz, $CDCl_3$): δ (ppm) 7.55 (d, $^3J_{H,H}$=8.1 Hz, 2H, H-C3b), 7.54 (s, 1H, CH=N), 7.28 (d, $^3J_{H,H}$=8.1 Hz, 2H, H-C2b), 3.78 (s, 2H, H-C$\alpha$), 3.21 (t, $^3J_{H,H}$=5.1 Hz, 4H, H-C1c), 2.70 (t, $^3J_{H,H}$=6.6 Hz, 2H, H-C1), 2.62 (t, $^3J_{H,H}$=5.1Hz, 4H, H-C2c), 2.49 (m, 6H, H-C3, H-C1a), 2.35 (s, 3H, $CH_3$), 2.02 (sa, 1H, deuterable, NH), 1.76 (m, 6H, H-C2, H-C2a).

**$^{13}$C-RMN** (75.5 MHz, $CDCl_3$): δ (ppm) 140.3 (C1b), 135.8 (C=N), 134.8 (C4b), 128.1 (C3b), 126.0 (C2b), 54.8 (C$\alpha$), 54.5 (C1c), 54.3 (C1a), 53.7 (C3), 51.0 (C2c), 48.0 (C1), 46.0 ($CH_3$), 29.2 (C2), 23.5 (C2a).

**MS** (IE): m/z 343.2 (1) $[M]^+$, 244.2 (3), 216.2 (4), 99.2 (34), 84.2 (100), 56.0 (39).

**HRMS** (IE): ($C_{20}H_{33}N_5$) Calculado: 343.2736. Obtenido: 343.2736.

## 5.6.9. Síntesis de *N*-(4-((4-metilpiperazin-1-ilimino)metil)bencil)-3-(1*H*-imidazol-1-il)propan-1-amina (37{*3,6*}).

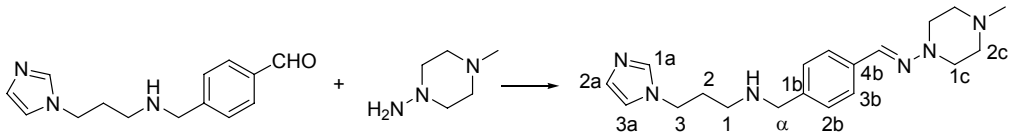


**35**{*6*} **30**{*3*} **37**{*3,6*}

Se sigue el mismo procedimiento que para **33**{*1,3*} pero utilizando 0.92 g (3.8 mmol) de **35**{*6*} y 0.45 g (3.8 mmol) de amina **30**{*3*}. Se obtienen 1.23 g (3.6 mmol, 96% rendimiento) de un aceite amarillo **37**{*3,6*}.

**Datos espectroscópicos:**

**IR** (film): $\nu$ ($cm^{-1}$) 3282 (*t* N-H), 3104 (*t* $Csp^2$-H), 2937, 2880, 2828, 2797 (*t* $Csp^3$-H), 1592 (*t* C=N), 1508 (t esqueleto heteroaromático), 1452, 1365, 1356 (*f* $Csp^3$-H).

**$^1$H-RMN** (300 MHz, $CDCl_3$): δ (ppm) 7.56 (d, $^3J_{H,H}$=8.1 Hz, 2H, H-C3b), 7.55 (s, 1H, CH=N), 7.45 (s, 1H, H-C1a), 7.27 (d, $^3J_{H,H}$=8.1 Hz, 2H, H-C2b), 7.04 (s, 1H, H-C2a), 6.89 (s, 1H, H-C3a), 4.04 (t, $^3J_{H,H}$=6.9 Hz, 2H, H-C3), 3.75 (s, 2H, H-C$\alpha$), 3.22 (t, $^3J_{H,H}$=5.1 Hz, 4H, H-C1c), 2.64-2.58 (m, 6H, H-C1, H-C2c), 2.36 (s, 3H, $CH_3$), 1.92 (quint, $^3J_{H,H}$=6.9 Hz, 2H, H-C2), 1.70 (sa, 1H, deuterable, NH).

**$^{13}$C-RMN** (75.5 MHz, $CDCl_3$): δ (ppm) 140.0 (C1b), 137.0 (C1a), 135.6 (C=N), 135.1 (C4b), 129.2 (C3a), 128.1 (C3b), 126.1 (C2b), 118.7 (C2a), 54.5 (C1c), 53.7 (C$\alpha$), 51.0 (C2c), 45.9 ($CH_3$), 45.6 (C3), 44.7 (C1), 31.4 (C2).

**MS** (IE): m/z 341.3 (2) $[M+H]^+$, 99.2 (82), 98.2 (100), 56.0 (76).

**HRMS** (IE): ($C_{19}H_{28}N_6$) Calculado: 340.2375. Obtenido: 340.2374.

## 5.6.10. Síntesis de *N*-(4-((4-metilpiperazin-1-ilimino)metil)benzil)-3-(2-metilpiperidin-1-il)propan-1-amina (37{*3,8*}).

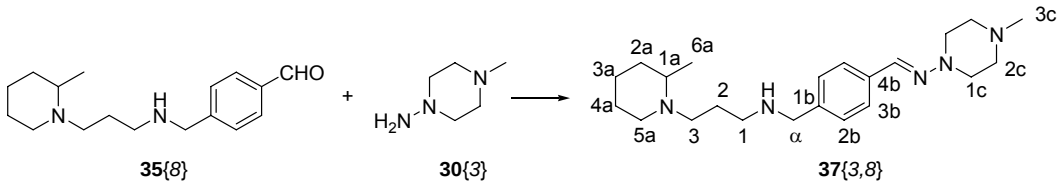


**35**{*8*} **30**{*3*} **37**{*3,8*}

Se sigue el mismo procedimiento que para **33**{*1,3*} pero utilizando 0.93 g (3.4 mmol) de **35**{*8*} y 0.40 g (3.4 mmol) de amina **30**{*3*}. Se obtienen 1.05 g (2.8 mmol, 84% rendimiento) de un aceite rojo **37**{*3,8*}.

**Datos espectroscópicos:**

**IR** (film): $\nu$ ($cm^{-1}$) 3279 (*t* N-H), 2932, 2881, 2841, 2795 (*t* $Csp^3$-H), 1593 (*t* C=N), 1452, 1366 (*f* $Csp^3$-H).

**$^1$H-RMN** (300 MHz, $CDCl_3$): δ (ppm) 7.56 (d, $^3J_{H,H}$=8.1 Hz, 2H, H-C3b), 7.55 (s, 1H, CH=N), 7.29 (d, $^3J_{H,H}$=8.1 Hz, 2H, H-C2b), 3.77 (s, 2H, H-Cα), 3.21 (t, $^3J_{H,H}$=5.1 Hz, 4H, H-C1c), 2.87 (m, 1H, $H_{eq}$-C5a), 2.73 (m, 1H, $H_{eq}$-C3), 2.65-2.60 (m, 6H, H-C1, H-C2c), 2.36 (s, 3H, H-C3c), 2.36 (m, 1H, $H_{ax}$-C3), 2.29 (m, 1H, H-C1a), 2.11 (m, 1H, $H_{ax}$-C5a), 1.95 (sa, 1H, deuterable, NH), 1.67 (quint, $^3J_{H,H}$=6.9 Hz, 2H, H-C2), 1.61-1.48 (m, 4H, $H_{eq}$-C2a, $H_{eq}$-C3a, H-C4a), 1.27 (m, 2H, $H_{ax}$-C2a, $H_{ax}$-C3a), 1.04 (d, $^3J_{H,H}$=6.0 Hz, 3H, H-C6a).

**$^{13}$C-RMN** (75.5 MHz, $CDCl_3$): δ (ppm) 140.3 (C1b), 135.8 (C=N), 134.8 (C4b), 128.2 (C3b), 126.1 (C2b), 56.0 (C1a), 54.5 (C1c), 53.8 (Cα), 52.3 (C3), 52.1 (C5a), 51.1 (C2c), 48.3 (C1), 46.0 (C3c), 34.7* (C2a), 26.2 (C4a), 25.8 (C2), 24.0* (C3a), 19.1 (C6a).

**MS** (IE): m/z 372.4 (1) $[M+H]^+$, 371.4 (2) $[M]^+$, 272.3 (2), 216.2 (7), 112.2 (100), 99.2 (39), 56.0 (56).

**HRMS** (IE): ($C_{22}H_{37}N_5$) Calculado: 371.3049. Obtenido: 371.3053.

## 5.6.11. Síntesis de *N*-(4-((4-metilpiperazin-1-ilimino)metil)bencil)-3-(4-metilpiperazin-1-il)propan-1-amina (37{*3,9*}).

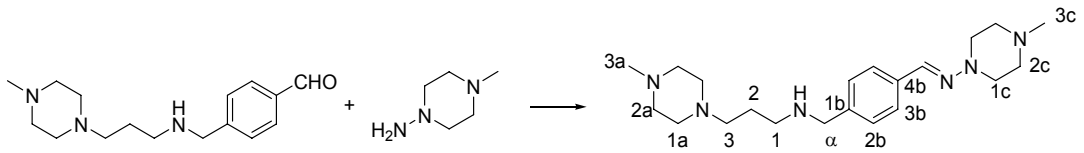


**35**{*9*} **30**{*3*} **37**{*3,9*}

Se sigue el mismo procedimiento que para **33**{*1,3*} pero utilizando 0.93 g (3.4 mmol) de **35**{*9*} y 0.40 g (3.4 mmol) de amina **30**{*3*}. Se obtienen 1.25 g (3.4 mmol, 99% rendimiento) de un aceite amarillento **37**{*3,9*}.

**Datos espectroscópicos:**

**IR** (film): $\nu$ ($cm^{-1}$) 3283 (*t* N-H), 2936, 2877, 2836, 2794, 2768 (*t* $Csp^3$-H), 1593 (*t* C=N), 1453, 1365, 1356 (*f* $Csp^3$-H).

**$^1$H-RMN** (300 MHz, $CDCl_3$): δ (ppm) 7.55 (d, $^3J_{H,H}$=8.1 Hz, 2H, H-C3b), 7.55 (s, 1H, CH=N), 7.28 (d, $^3J_{H,H}$=8.1 Hz, 2H, H-C2b), 3.77 (s, 2H, H-C$\alpha$), 3.21 (t, $^3J_{H,H}$=5.1 Hz, 4H, H-C1c), 2.66 (t, $^3J_{H,H}$=6.9 Hz, 2H, H-C1), 2.62 (t, $^3J_{H,H}$=5.1 Hz, 4H, H-C2c), 2.42 (sa, 8H, H-C1a, H-C2a), 2.40 (t, $^3J_{H,H}$=6.9 Hz, 2H, H-C3), 2.36 (s, 3H, H-C3c), 2.27 (s, 3H, H-C3a), 1.82 (sa, 1H, deuterable, NH), 1.70 (quint, $^3J_{H,H}$=6.9 Hz, 2H, H-C2).

**$^{13}$C-RMN** (75.5 MHz, $CDCl_3$): δ (ppm) 140.2 (C1b), 135.8 (C=N), 134.8 (C4b), 128.1 (C3b), 126.0 (C2b), 57.0 (C$\alpha$), 55.1 (C2a), 54.5 (C1c), 53.7 (C3), 53.2 (C1a), 51.0 (C2c), 48.0 (C1), 46.0* (C3a), 45.9* (C3c), 26.9 (C2).

**MS** (IE): m/z 373.4 (0.6) $[M+H]^+$, 372.3 (0.7) $[M]^+$, 273.3 (21), 216.2 (29), 113.2 (46), 99.2 (54), 70.0 (79), 56.0 (100).

**HRMS** (IE): ($C_{21}H_{36}N_6$) Calculado: 372.3001. Obtenido: 372.2990.

## 5.6.12. Síntesis de *N*-(4-((4-metilpiperazin-1-ilimino)metil)bencil)-3-morfolinopropan-1-amina (37{*3,11*}).

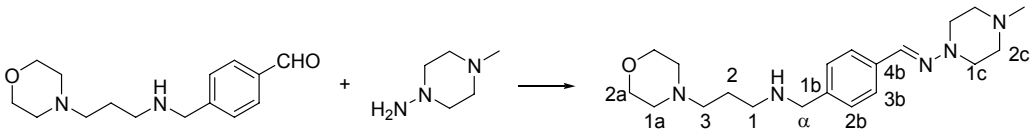


**35**{*11*} **30**{*3*} **37**{*3,11*}

Se sigue el mismo procedimiento que para **33**{*1,3*} pero utilizando 0.89 g (3.4 mmol) de **35**{*11*} y 0.40 g (3.4 mmol) de amina **30**{*3*}. Se obtienen 1.22 g (3.4 mmol, rendimiento cuantitativo) de un aceite amarillo **37**{*3,11*}.

**Datos espectroscópicos:**

**IR** (film): $\nu$ ($cm^{-1}$) 3293 (*t* N-H), 2939, 2888, 2844, 2799 (*t* $Csp^3$-H), 1592 (*t* C=N), 1453, 1364, 1356 (*f* $Csp^3$-H), 1118 (*t as* C-O-C), 806 (*t sim* C-O-C).

**$^1$H-RMN** (300 MHz, $CDCl_3$): δ (ppm) 7.56 (s, 1H, CH=N), 7.56 (d, $^3J_{H,H}$=8.1 Hz, 2H, H-C3b), 7.28 (d, $^3J_{H,H}$=8.1 Hz, 2H, H-C2b), 3.77 (s, 2H, H-C$\alpha$), 3.69 (t, $^3J_{H,H}$=4.7 Hz, 4H, H-C2a), 3.21 (t, $^3J_{H,H}$=5.1 Hz, 4H, H-C1c), 2.67 (t, $^3J_{H,H}$=6.9 Hz, 2H, H-C1), 2.62 (t, $^3J_{H,H}$=5.1 Hz, 4H, H-C2c), 2.44-2.37 (m, 6H, H-C3, H-C1a), 2.35 (s, 3H, $CH_3$), 2.05 (sa, 1H, deuterable, NH), 1.70 (quint, $^3J_{H,H}$=6.9 Hz, 2H, H-C2).

**$^{13}$C-RMN** (75.5 MHz, $CDCl_3$): δ (ppm) 140.2 (C1b), 135.7 (C=N), 134.9 (C4b), 128.1 (C3b), 126.1 (C2b), 66.9 (C2a), 57.4 (C$\alpha$), 54.5 (C1c), 53.8 (C3, C1a), 51.0 (C2c), 47.9 (C1), 45.9 ($CH_3$), 26.6 (C2).

**MS** (IE): m/z 359.2 (2) $[M]^+$, 260.2 (4), 231.2 (16), 100.0 (100), 99.0 (84), 98.0 (57), 56 (75).

**HRMS** (IE): ($C_{20}H_{33}N_5O$) Calculado: 359.2685. Obtenido: 359.2685.

## 5.7. Síntesis de monociclamos sustituidos y sus intermedios.

### 5.7.1. Síntesis de 4-(hidroximetil)-benzaldehído (92).[1]

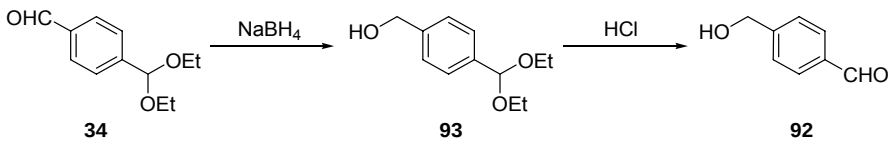


**34** **93** **92**

Se disuelven 3,01 g (14.0 mmol) de monoacetal dietílico del tereftalaldehído (**34**) en 50 mL de MeOH anhidro. Se enfría en un baño de agua-hielo y se añade $NaBH_4$ (0.54 g, 14.0 mmol) y se agita a temperatura ambiente durante 6 h. Se añaden 20 mL de agua y se extrae con $CH_2Cl_2$ (50 + 25 mL). Las fases orgánicas se combinan y se lavan con salmuera. La fase orgánica se seca con $MgSO_4$ anhidro y se elimina el disolvente a presión reducida. Se obtienen 2.79 g (13.3 mmol, 95%) de (4-(diethoxymethyl)fenil)metanol (**93**) como un aceite amarillo. **$^1$H-RMN** (300 MHz, $CDCl_3$): δ (ppm) 7.49 (d, $^3J$ (H,H)=8.0 Hz, 2H, H-C3, H-C5), 7.38 (d, $^3J$ (H,H)=8.0 Hz, H2H, -C2, H-C6), 5.53 (s, 1H, CH), 4.71 (d, $^3J$ (H,H)=6.0 Hz, 2H, $CH_2$), 3.60 (m, 4H, $OCH_2$), 1.83 (t, $^3J$ (H,H)=6.0 Hz, 1H, deuterable, OH), 1.26 (t, $^3J$ (H,H)=7.0 Hz, 6H, $CH_3$). 2.53 g (12.0 mmol) de este acetal **93** se hidrolizan con 25 mL de HCl 2M a temperatura ambiente durante 2 h. Se añade $K_2CO_3$ hasta pH 8-9. Se extrae con $CH_2Cl_2$. La fase orgánica se lava con salmuera y se seca sobre $MgSO_4$ anhidro. Se elimina el disolvente a presión reducida. El crudo obtenido se purifica por cromatografía de columna (hexano/AcOEt 1:1) y se obtienen 1.21 g (8.9 mmol, 74% rendimiento) de 4-(hidroximetil)-benzaldehído (**92**) como un sólido blanco.

**Datos espectroscópicos:**

**$^1$H-RMN** (300 MHz, $CDCl_3$): δ (ppm) 10.04 (s, 1H, CHO), 7.91 (d, $^3J_{H,H}$=8.0 Hz, 2H, H-C2, H-C6), 7.57 (d, $^3J_{H,H}$=8.0 Hz, 2H, H-C3, H-C5), 4.84 (s, 2H, $CH_2$), 1.87 (sa, 1H, deuterable, OH).

## 5.7.2. Síntesis de 4-(bromometil)benzaldehído (74).[1]

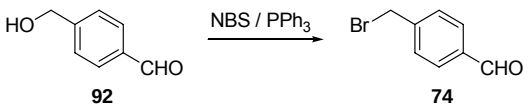


**92** **74**

Se disuelven 0.50 g (3.7 mmol) de 4-(hidroximetil)-benzaldehído (**92**) en 40 mL de $CH_2Cl_2$ anhidro, se añaden 1.93 g (7.3 mmol) de $PPh_3$ y 1.31 g (7.3 mmol) de NBS. Se calienta a reflujo durante 2 h. Transcurrido este tiempo se deja enfriar a temperatura ambiente y se añaden 40 mL de $H_2O$. Se separan las fases y se extrae la fase acuosa con $CH_2Cl_2$ (2×20 mL). Se combinan las fases orgánicas y se seca con $MgSO_4$ anhidro. Se elimina el disolvente a presión reducida y se obtiene un aceite marrón que cristaliza lentamente. Se purifica por cromatografía de columna (hexano/AcOEt con un gradiente de 20:1 a 10:1) y se obtiene 0.54 g (2.7 mmol, 73% rendimiento) de 4-(bromometil)benzaldehído (**74**) como sólido blanco.

**Datos espectroscópicos:**

**IR** (film): $\nu$ ($cm^{-1}$) 2855, 2844, 2753 (*t* $Csp^3$-H ), 1686 (*t* C=O), 1605, 1577 (*t* $Csp^2$-$Csp^2$), 1441, 1427 (*f* $Csp^3$-H), 833 (*ffp* $Csp^2$-H).

**$^1$H-RMN** (300 MHz, $CDCl_3$): δ (ppm) 10.04 (s, 1H, CHO), 7.90 (d, $^3J_{H,H}$=8.0 Hz, 2H, H-C2, H-C6), 7.59 (d, $^3J_{H,H}$=8.0 Hz, 2H, H-C3, H-C5), 4.54 (s, 2H, $CH_2$).

**$^{13}$C-RMN** (75.5 MHz, $CDCl_3$): δ (ppm) 191.3 (CHO), 144.1 (C4), 136.0 (C1), 130.1 (C2, C6), 129.6 (C3, C5), 32.0 ($CH_2$-Br).

**AEO**: Calculado ($C_8H_7BrO$): C 48.27%, H 3.54%, Br 40.14%, O 8.04%. Obtenido: C 48.34%, H 3.64%.

**MS** (IE): m/z 200.1 (57) $[M+2]^+$, 199.2 (7) $[M+1]^+$, 198.2 (58) $[M]^+$, 120.3 (45), 119.3 (100), 118.3 (56), 91.3 (100), 90.3 (89), 89.3 (88).

## 5.7.3. Síntesis de 1,4,8-tris(*tert*-butoxicarbonil)-1,4,8,11-tetraazaciclotetradecano (66).[2]

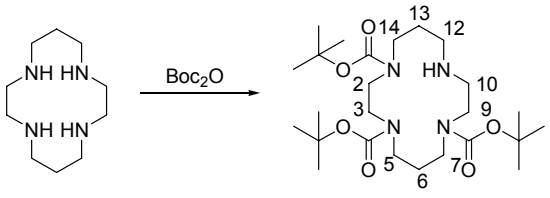


**57** **66**

Se disuelven 1.25 g (6.2 mmol) de 1,4,8,11-tetraazaciclotetradecano (**57**) en 300 mL de $CH_2Cl_2$ y se añade una disolución de 3.13 g (14.3 mmol) de bicarbonato de *tert*-butilo ($Boc_2O$) en 75 mL de $CH_2Cl_2$. Se agita a temperatura ambiente y bajo atmósfera de nitrógeno durante 6 h 30 min. Transcurrido este tiempo se elimina el disolvente a presión reducida. Se purifica por cromatografía de columna ($CH_2Cl_2$/MeOH 20:1) y se obtienen 1.81 g (3.67 mmol, 58% rendimiento) de 1,4,8-tris(*tert*-butoxicarbonil)-1,4,8,11-tetraazaciclotetradecano (**66**) como un sólido blanco espumoso.

**Datos espectroscópicos:**

**IR** (film): $\nu$ ($cm^{-1}$) 2974, 2931, 2815 (*t* $Csp^3$-H), 1692 (*t* C=O), 1479, 1466, 1365 (*f* $Csp^3$-H), 1243 (*t as* N-CO-O), 1169 (*t* C-N), 897 (*t sim* N-CO-O).

**$^1$H-RMN** (300 MHz, $CDCl_3$): δ (ppm) 3.42 (sa, 4H, H-C2, H-C3), 3.33 (m, 8H, H-C5, H-C7, H-C9, H-C14), 2.81 (t, $^3J_{H,H}$=5.0 Hz, 2H, H-C10), 2.64 (t, $^3J_{H,H}$=5.5 Hz, 2H, H-C12), 1.95 (sa, 2H, H-C6), 1.73 (sa, 2H, H-C13), 1.49 (s, 27H, $CH_3$).

**$^{13}$C-RMN** (75.5 MHz, $CDCl_3$): δ (ppm) 155.3 (Cq), 79.5 (Cq), 79.2 (Cq), 53.4 ($CH_2$), 50.8 ($CH_2$), 50.6 ($CH_2$), 50.0 ($CH_2$), 47.7 ($CH_2$), 45.9 ($CH_2$), 44.1 ($CH_2$), 28.6 ($CH_3$).

**AEO**: Calculado ($C_{25}H_{48}N_4O_6$): C 59.97%, H 9.66%, N 11.19%, O 19.17%. Obtenido: C 59.67%, H 9.36%, N 10.93%.

**MS** (ESI): m/z 501.4 (100) $[M+H]^+$.

**HRMS** (ESI): ($C_{25}H_{49}N_4O_6$) $[M+H]^+$ Calculado: 501.3647. Obtenido: 501.3645.

## 5.7.4. Síntesis de 1-[4-(carboxaldehído)fenilmetil]-4,8,11-tris(*tert*-butoxicarbonil)-1,4,8,11-tetraazaciclotetradecano (90).

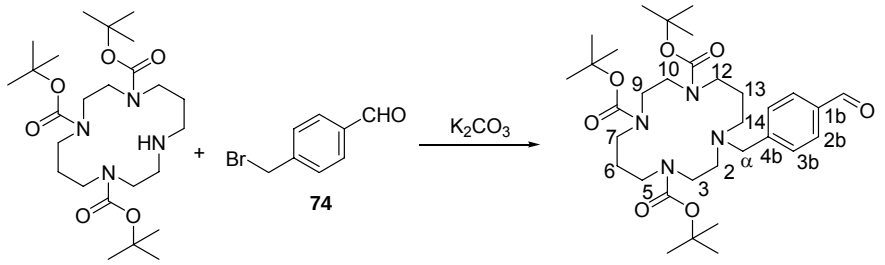


**66** **74** **90**

Se disuelven 0.49 g (2.4 mmol) de 4-(bromometil)-benzaldehído (**74**) en 25 mL de ACN y se añaden 0.67 g (4.8 mmol) de $K_2CO_3$ anhidro. A esta suspensión se le añade una disolución de 1.22 g (2.4 mmol) de 1,4,8-tris(*tert*-butoxicarbonil)-1,4,8,11-tetraazaciclotetradecano (**66**) en 25 mL de ACN y se calienta a reflujo y bajo atmósfera de nitrógeno durante 16 h. Se deja enfriar y se filtran las sales. Se elimina el disolvente del filtrado a presión reducida. Se purifica por cromatografía de columna ($CH_2Cl_2$/MeOH gradiente de 50:0 a 50:1). Se obtienen 1.33 g (2.2 mmol, 89% rendimiento) de 1-[4-(carboxaldehído)fenilmetil]-4,8,11-tris(*tert*-butoxicarbonil)-1,4,8,11-tetraazaciclotetradecano (**90**) como un sólido blanco espumoso.

**Datos espectroscópicos:**

**IR** (film): $\nu$ ($cm^{-1}$) 3004, 2975, 2932, 2870, 2817 (*t* $Csp^3$-H, $Csp^2$-H), 1695 (*t* C=O), 1607 (*t* $Csp^2$-$Csp^2$), 1478, 1465, 1390, 1366 (*f* $Csp^3$-H), 1247 (*t as* N-CO-O), 1165 (*t* C-N), 859 (*t sim* N-CO-O).

**$^1$H-RMN** (300 MHz, $CDCl_3$): δ (ppm) 9.99 (s, 1H, CHO), 7.82 (d, $^3J_{H,H}$=8.0 Hz, 2H, H-C2b), 7.45 (d, $^3J_{H,H}$=8.0 Hz, 2H, H-C3b), 3.61 (s, 2H, H-C$\alpha$), 3.30 (m, 12H, H-C3, H-C5, H-C7, H-C9, H-C10, H-C12), 2.63 (sa, 2H, H-C2), 2.39 (sa, 2H, H-C14), 1.90 (sa, 2H, H-C6), 1.69 (m, 2H, H-C13), 1.47 (s, 18H, $CH_3$), 1.43 (s, 9H, $CH_3$).

**$^{13}$C-RMN** (75.5 MHz, $CDCl_3$): δ (ppm) 191.7 (CHO), 155.4 (N-CO-O), 146.4 (C4b), 135.3 (C1b), 129.6 (C2b), 129.4 (C3b), 79.7 (Cq *t*-But), 79.6 (Cq *t*-But), 59.7 (C$\alpha$), 53.3 (C14), 51.9 (C2), 47.8* (C3), 47.2* (C9, C10), 46.2* (C5, C7, C12), 28.6 ($CH_3$), 28.5 ($CH_3$), 27.1 (C6, C13).

**AEO**: Calculado ($C_{33}H_{54}N_4O_7$): C 64.05%, H 8.80%, N 9.05%, O 18.10%. Obtenido: C 64.04%, H 8.77%, N 8.93%.

**MS** (IE): m/z 619.7 (5) $[M+H]^+$, 618.7 (14) $[M]^+$, 561.5 (6), 517.5 (2), 201.3 (18), 162.2 (42), 119.2 (27), 57.3 (100).

## 5.7.5. Síntesis de 1-[4-(bromometil)fenilmetil)]-4,8,11-tris(*tert*-butoxicarbonil)-1,4,8,11-tetraazaciclotetradecano (67).[3]

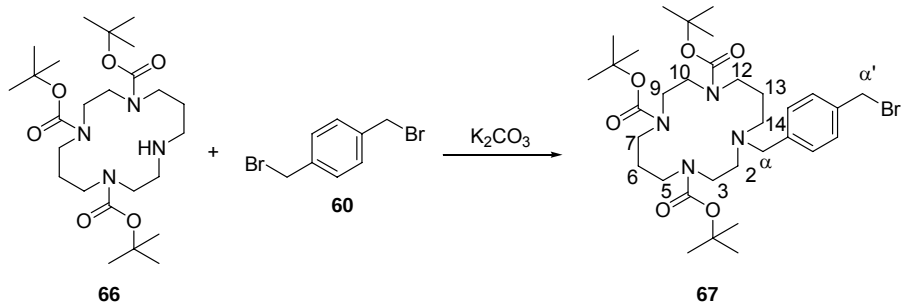


**66** **60** **67**

Se disuelven a 60 ºC, 2.81 g (10.6 mmol) de α,α'-dibromo-*p*-xileno (**60**) en 50 mL de ACN y se añaden 0.27 g (1.0 mmol) de $K_2CO_3$ anhidro. A esta suspensión se le añade gota a gota y bajo atmósfera de nitrógeno, una disolución de 0.48 g (9.7 mmol) de 1,4,8-tris(*tert*-butoxicarbonil)-1,4,8,11-tetraazaciclotetradecano (**66**) en 8 mL de ACN y se calienta a 60 ºC durante 5 h. Se deja enfriar y se filtran las sales. Se elimina parcialmente el disolvente del filtrado a presión reducida, hasta que empieza a precipitar el exceso de α,α'-dibromo-*p*-xileno (**60**). Se filtra otra vez y se elimina el resto del disolvente a presión reducida. Se purifica por cromatografía de columna ($CH_2Cl_2$/MeOH 50:1). Se obtienen 0.45 g (0.7 mmol, 70% rendimiento) de 1-[4-(bromometil)fenilmetil)]-4,8,11-tris(*tert*-butoxicarbonil)-1,4,8,11-tetraazaciclotetradecano (**67**) como un sólido blanco.

**Datos espectroscópicos:**

**$^1$H-RMN** (300 MHz, $CDCl_3$): δ (ppm) 7.30 (d, $^3J_{H,H}$=8.0 Hz, 2H,Ph), 7.22 (d, $^3J_{H,H}$=8.0 Hz, 2H, Ph), 4.46 (s, 2H, H-Cα'), 3.51 (s, 2H, H-Cα), 3.29 (m, 12H, H-C3, H-C5, H-C7, H-C9, H-C10, H-C12), 2.60 (sa, 2H, H-C2), 2.36 (sa, 2H, H-C14), 1.88 (sa, 2H, H-C6), 1.66 (m, 2H, H-C13), 1.46 (s, 18H, $CH_3$), 1.43 (s, 9H, $CH_3$).

## 5.7.6. Síntesis de 1-[4-(3-(2-metilpiperidin-1-il)propil-1-aminometil)fenilmetil]-4,8,11-tris(*tert*-butoxicarbonil)-1,4,8,11-tetraazaciclotetradecano (87{*8*}).

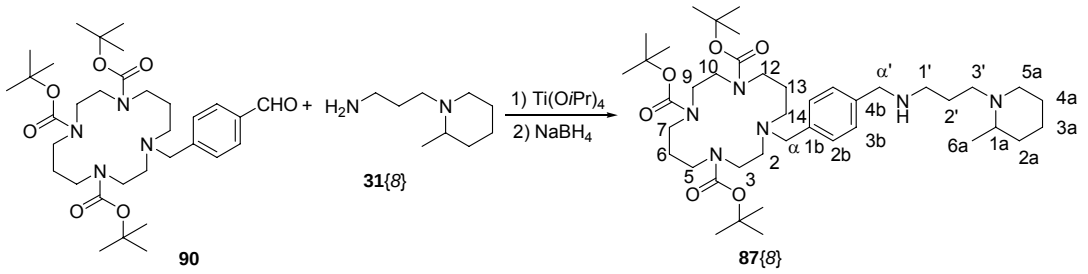


Se disuelven 1.26 g (2.0 mmol) de **90** y 0.33 g (2.0 mmol) de amina **31**{*8*} en 30 mL de EtOH absoluto. Se añaden 1.19 g (4.0 mmol) de Ti(O*i*Pr)$_4$ y se deja reaccionar a temperatura ambiente y bajo atmósfera de nitrógeno durante 36 h. Se añaden 0.08 g (2.0 mmol) de $NaBH_4$ y se deja reaccionar a temperatura ambiente 12 h. Se añaden 20 mL de $H_2O$ y se agita durante 1 h 30 min. Se filtra y se lava con $CH_2Cl_2$. Se separan las fases y la fase acuosa se extrae con 15 mL de $CH_2Cl_2$. Las fases orgánicas se combinan y se seca sobre $MgSO_4$ anhidro. El disolvente se elimina a presión reducida y el crudo se purifica por cromatografía de columna sobre alúmina neutra ($CH_2Cl_2$/MeOH 50:1). Se obtienen 1.17 g (1.5 mmol, 76% rendimiento) de **87**{*8*} como un aceite amarillo.

**Datos espectroscópicos:**

**IR** (film): $\nu$ (cm$^{-1}$) 2974, 2931, 2804 (*t* Csp$^3$-H), 1690 (*t* C=O), 1477,1465, 1413, 1366 (*f* Csp$^3$-H), 1166 (*t as* N-CO-O), 754 (*t sim* N-CO-O).

**$^1$H-RMN** (400 MHz, $CDCl_3$): δ (ppm) 7.22 (m, 4H, Ph), 3.75 (s, 2H, H-C$\alpha$'), 3.52 (s, 2H, H-C$\alpha$), 3.34-2.23 (sa, 12H, H-C3, H-C5, H-C7, H-C9, H-C10, H-C12), 2.87 (m, 1H, $H_{eq}$-C5a), 2.73 (m, 1H, $H_{eq}$-C3'), 2.64 (t, $^3J_{H,H}$=6.9 Hz, 2H, H-C1'), 2.62 (sa, 2H, H-C2), 2.37 (m, 3H, H-C14, $H_{ax}$-C3'), 2.26 (m, 2H, H-C1a), 2.11 (m, 1H, $H_{ax}$-C5a), 1.90 (sa, 2H, H-C6), 1.73-1.59 (sc, 9H, H-C13, H-C2', H-C2a, $H_{eq}$-C3a, H-C4a), 1.67 (sa, 2H, H-C13), 1.47 (s, 18H, $CH_3$), 1.44 (s, 9H, $CH_3$), 1.28 (m, 2H, $H_{ax}$-C2a, $H_{ax}$-C3a), 1.05 (d, $^3J_{H,H}$=6.3 Hz, 6H, $CH_3$).

**$^{13}$C-RMN** (100.6 MHz, $CDCl_3$): δ (ppm) 155.8 (N-CO-O), 139.3 (C4b), 137.5 (C1b), 129.4 (C2b), 128.2 (C3b), 79.8 (Cq *t*-But), 79.6 (Cq *t*-But), 59.7 (C$\alpha$), 56.2 (C1a), 54.0 (C$\alpha$'), 53.2 (C2), 52.5 (C3'), 52.3 (C5a), 51.5 (C14), 48.6 (C1'), 47.6-46.1 (C3, C5, C7, C9, C10, C12), 34.9 (C2a, C4a), 31.1 (C6), 28.7 ($CH_3$), 26.4 (C2'), 26.0 (C13), 24.2 (C3a), 19.3 (C6a).

**AEO**: Calculado ($C_{42}H_{74}N_6O_6$): C 66.46%, H 9.83%, N 11.07%, O 12.65%. Obtenido: C 66.47%, H 10.26%, N 10.93%.

**MS** (ESI): m/z 760.6 (55) $[M+H]^+$, 759.6 (60) $[M]^+$, 296.2 (100).

**HRMS** (ESI): ($C_{42}H_{75}N_6O_6$) Calculado: 759.5743. Obtenido: 759.5743.

## 5.7.7. Síntesis de 1-[4-(3-(2-metilpiperidin-1-il)propil-1-aminometil)fenilmetil]-1,4,8,11-tetraazaciclotetradecano·6HCl·7½$H_2O$ (70{*8*}).

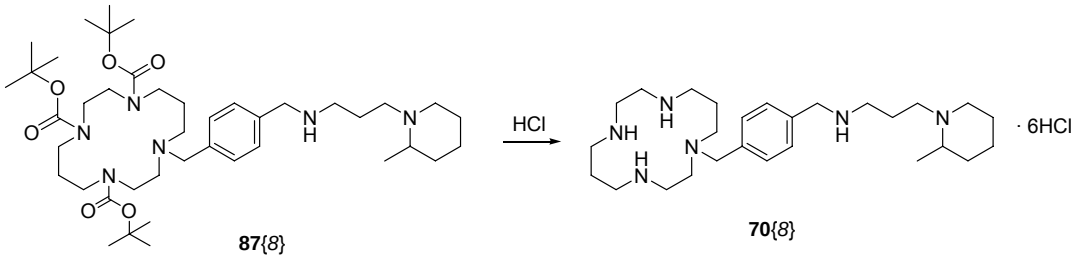


**87**{*8*} **70**{*8*}

A 1.07 g (1.4 mmol) de **87**{*8*} se le añaden 18 mL de HCl 1M en éter dietílico y se agita a temperature ambiente durante 12 h. Se elimina el disolvente a presión reducida y se obtienen 1.03 g (1.3 mmol, 90% rendimiento) de **70**{*8*} como un sólido blanco.

**Datos espectroscópicos:**

**IR** (film): $\nu$ ($cm^{-1}$) 2953, 2749, 2678 (*t* $Csp^3$-H), 1624, 1581 (*f* $NH_2^+$, $NH^+$), 1455 (*f* $Csp^3$-H).

**$^1$H-RMN** (400 MHz, $D_2O$): δ (ppm) 7.51 (m, 4H, Ph), 4.38* (s, 2H, H-C$\alpha$'), 4.21* (s, 2H, H-C$\alpha$), 3.51 (sc, 8H, $4CH_2$), 3.41 (m, 1H, HCH), 3.30 (sc, 9H, $4CH_2$, HCH), 3.09 (sc, 4H, $CH_2$, CH, HCH), 2.91 (m, 1H, HCH), 2.17-1.99 (sc, 6H, $3CH_2$), 1.86 (m, 2H, 2HCH), 1.71 (m, 1H, HCH), 1.59 (m, 1H, HCH), 1.44 (m, 2H, 2HCH), 1.24 (d, $^3J_{H,H}$=6.4 Hz, 3H, $CH_3$).

**$^{13}$C-RMN** (100.6 MHz, $D_2O$): δ (ppm) 132.9 ($C_q$), 132.0 (CH), 131.1 (CH), 130.6 ($C_q$), 60.3 ($CH_2$), 58.7 ($CH_2$), 56.8 (CH), 52.6 ($CH_2$), 50.9 ($CH_2$), 49.6 ($CH_2$), 48.3 ($CH_2$), 48.0 ($CH_2$), 44.9 ($CH_2$), 44.5 ($CH_2$), 42.0 ($CH_2$), 41.4 ($CH_2$), 38.1-37.6 ($CH_2$), 31.7 ($CH_2$), 23.2 ($CH_2$), 21.6 ($CH_2$), 20.3 ($CH_2$), 18.5 ($CH_2$), 17.4 ($CH_3$).

**AEO**: Calculado ($C_{25}H_{46}N_6O$·6HCl·7½$H_2O$): C 39.89%, H 8.82%, N 10.33%, O 14.76%, Cl 20.20%. Obtenido: C 39.91%, H 8.41%, N 10.00%.

**MS** (ESI): m/z 459.4 (100) $[M+H]^+$.

**HRMS** (ESI): ($C_{27}H_{51}N_6$) $[M+H]^+$ Calculado: 459.4170. Obtenido: 459.4163.

## 5.7.8. Síntesis de 1-[4-(3-morfolinopropil-1-aminometil)fenilmetil]-4,8,11-tris(*tert*-butoxicarbonil)-1,4,8,11-tetraazaciclotetradecano (87{*11*}).

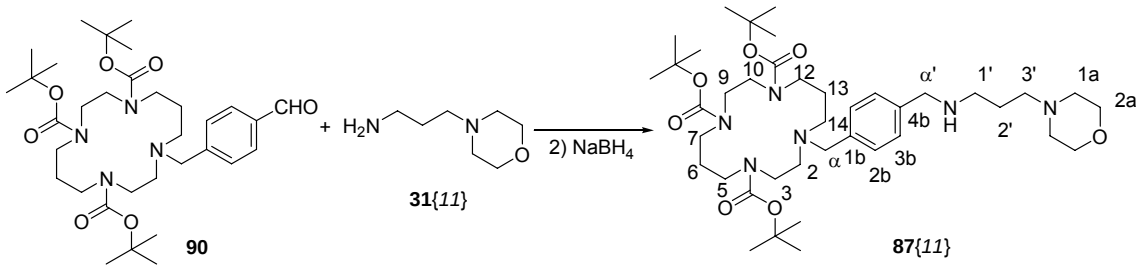


Se disuelven 1.26 g (2.0 mmol) de 1-[4-(carboxaldehído)fenilmetil]-4,8,11-tris(*tert*-butoxicarbonil)-1,4,8,11-tetraazaciclotetradecano (**90**) y 0.44 g (3.0 mmol) de amina **31**{*11*} en 15 mL de MeOH anhidro. Se añade $Na_2SO_4$ anhidro y se calienta en el microondas a 100 ºC durante 3 h. Se filtra, se añaden 0.08 g (2.0 mmol) de $NaBH_4$ y se deja reaccionar a temperatura ambiente 12 h. Se añaden 20 mL de $H_2O$ y se extrae con $CH_2Cl_2$. La fase orgánica se lava con salmuera y se seca sobre $MgSO_4$ anhidro. El disolvente se elimina a presión reducida y el crudo se purifica por cromatografía de columna ($CH_2Cl_2$/MeOH gradiente de 20:1 a 9:1). Se obtienen 0.48 g (0.6 mmol, 32% rendimiento) de 1-[4-(3-morfolinopropil-1-aminometil)fenilmetil]-4,8,11-tris(*tert*-butoxicarbonil)-1,4,8,11-tetraazaciclotetradecano **87**{*11*} como un aceite amarillo.

**Datos espectroscópicos:**

**IR** (film): $\nu$ ($cm^{-1}$) 2971, 2927, 2853, 2808 (*t* $Csp^3$-H), 1693 (*t* C=O), 1477,1464, 1365 (*f* $Csp^3$-H), 1165 (*t as* N-CO-O).

**$^1$H-RMN** (300 MHz, $CDCl_3$): δ (ppm) 7.29 (m, 4H, Ph), 3.86 (s, 2H, H-C$\alpha$'), 3.65 (t, $^3J_{H,H}$=4.5 Hz, 4H, H-C2a), 3.53 (s, 2H, H-C$\alpha$), 3.34-2.25 (sa, 12H, H-C3, H-C5, H-C7, H-C9, H-C10, H-C12), 2.84 (t, $^3J_{H,H}$=6.5 Hz, 2H, H-C1'), 2.62 (sa, 1H, NH), 2.46 (m, 6H, H-C3', H-C1a), 2.37 (sa, 2H, H-C14), 1.89 (sa, 2H, H-C6), 1.83 (t, $^3J_{H,H}$=6.5 Hz, 2H, H-C2'), 1.67 (sa, 2H, H-C13), 1.47 (s, 18H, $CH_3$), 1.44 (s, 9H, $CH_3$).

**$^{13}$C-RMN** (75.5 MHz, $CDCl_3$): δ (ppm) 155.4 (N-CO-O), 137.6 (C1b, C4b), 129.1 (C2b), 127.9 (C3b), 79.6 (Cq *t*-But), 79.4 (Cq *t*-But), 66.9 (C2a), 59.4 (C$\alpha$), 57.5 (C$\alpha$'), 53.7 (C1a), 53.4 (C3'), 51.3 (C2, C14), 48.0 (C1'), 47.3 (C3, C9, C10, C12), 45.9 (C5, C7), 29.7 (C6), 28.5 ($CH_3$), 26.0 (C13, C2').

## 5.7.9. Síntesis de 1-[4-(3-morfolinopropil-1-aminometil)fenilmetil]-1,4,8,11-tetraazaciclotetradecano·6HCl·3$H_2O$ (70{*11*}).

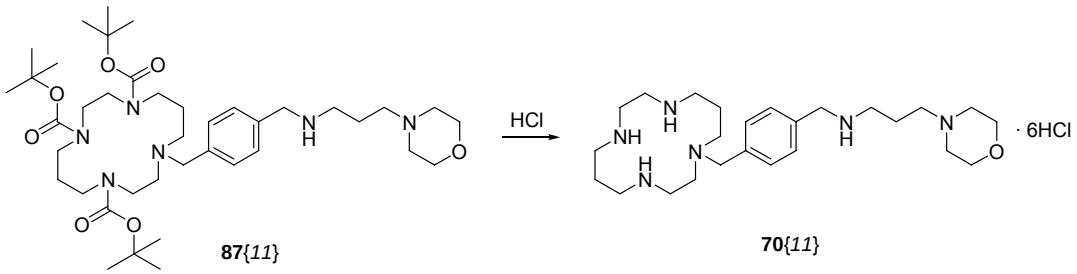


**87**{*11*} **70**{*11*}

A 0.46 g (0.6 mmol) de (**87**{*11*}) se le añaden 8 mL de HCl 1M en éter dietílico y se agita a temperature ambiente durante 12 h. Se elimina el disolvente a presión reducida y el sólido obtenido se recristaliza de metanol. Se obtienen 0.16 g (0.2 mmol, 37% rendimiento) de **70**{*11*} como un sólido blanco.

**Datos espectroscópicos:**

**IR** (p. KBr): ν ($cm^{-1}$) 2958, 2787 (*t* $Csp^3$-H), 1583 (*f* $NH_2^+$, $NH^+$), 1472, 1440 (*f* $Csp^3$-H), 1107 (*t as* C-O-C), 772 (*t sim* C-O-C).

**$^1$H-RMN** (400 MHz, $D_2O$): δ (ppm) 7.58 (m, 4H, Ph), 4.32 (s, 2H, $CH_2$), 4.27 (s, 2H, $CH_2$), 4.14 (m, 2H, $CH_2$), 3.82 (m, 2H, $CH_2$), 3.58-3.47 (m, 8H, $CH_2$), 3.38-3.28 (m, 10H, $CH_2$), 3.24-3.20 (m, 6H, $CH_2$), 2.26-2.07 (m, 6H, $CH_2$).

**$^{13}$C-RMN** (75.5 MHz, $D_2O$): δ (ppm) 132.5 (Cq), 132.0 (CH), 131.2 (CH), 64.3 ($CH_2$), 58.1 ($CH_2$), 56.2 ($CH_2$), 54.3 ($CH_2$), 52.2 ($CH_2$), 51.4 ($CH_2$), 50.3 ($CH_2$), 48.7 ($CH_2$), 46.9 ($CH_2$), 44.7 ($CH_2$), 43.2 ($CH_2$), 40.0 ($CH_2$), 21.1 ($CH_2$), 20.0 ($CH_2$).

**AEO**: Calculado ($C_{25}H_{46}N_6O$·6HCl·3$H_2O$): C 41.71%, H 8.14%, N 11.67%, O 8.89%, Cl 29.59%. Obtenido: C 41.57%, H 7.99%, N 11.44%.

**MS** (ESI): m/z 447.38 (100) $[M+H]^+$.

**HRMS** (ESI): ($C_{27}H_{47}N_6O$) $[M+H]^+$ Calculado: 447.3806. Obtenido: 447.3795.

## Bibliografía.

[1] E. Kawabata, K. Kikuchi, Y. Urano, H. Kojima, A. Odani, T. Nagano; Design and synthesis of zinc-selective chelators for extracellular applications. *J. Am. Chem. Soc.* **2005**, *127,* 818-819.

[2] B. Boitrel, B. Andrioletti, M. Lachkar, R. Guilard; Characterization and application of a new diprotected cyclam: a novel two-step synthesis of linked tetraazamacrocycles. *Tetrahedron Lett.* **1995**, *36,* 4995-4998.

[3] J. I. Luengo, A. T. Price, A. Shaw, K. Wiggall; CXCR-4 receptor antagonists-thrombopoietin mimetics. World Patent WO 00/66112 (filing date: 3-5-2000).

# CONCLUSIONES

## 6. Conclusiones.

- Se ha diseñado una quimioteca de inhibidores potenciales del correceptor CXCR4 que mantienen las principales características estructurales del AMD3100, un *linker p*-fenilenbismetilénico disustituido por sistemas heterocíclicos unidos a una cadena alquílica lineal de longitud variable. Estas sustituciones han dado lugar a diaminas **32**, dihidrazonas **33** y aminohidrazonas **37**.

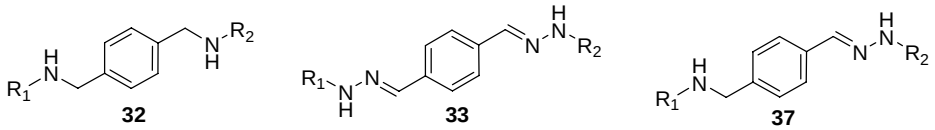


- Una selección de diversidad de los compuestos de la quimioteca diseñada ha permitido identificar diaminas **32**, dihidrazonas **33** y aminohidrazonas **37**, que han presentado un amplio rango de actividad anti-VIH, con valores de $EC_{50}$ desde 0.008 μg/mL hasta valores superiores a 25 μg/mL. En esta selección destaca la diamina **32**{*8,8*}, cuya $EC_{50}$ es 0.008 μg/mL, semejante a la del AMD3100 (0.001 μg/mL). También destacan las diaminas **32**{*6,8*} y **32**{*8,9*}, cuyos valores de $EC_{50}$ son de 0.03 μg/mL en ambos casos. El estudio del modo de acción de los compuestos más activos de la quimioteca diseñada de análogos no ciclámicos del AMD3100 ha permitido confirmar la hipótesis inicial del diseño: los compuestos actúan en el mismo tiempo del ciclo viral en que actúa el AMD3100, es decir, inhiben la unión del virus al correceptor CXCR4. Estos resultados demuestran que los ocho átomos de nitrógeno presentes en el AMD3100 no son necesarios para la interacción con el correceptor CXCR4, ya que compuestos con cuatro átomos de nitrógeno han permitido obtener elevada actividad antiviral.

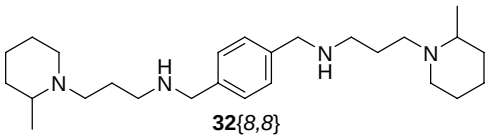


**32**{*8,8*}

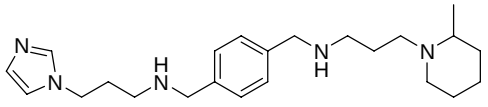


**32**{*6,8*}

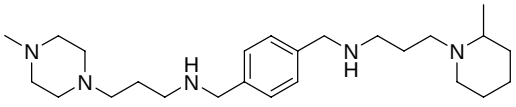


**32**{*8,9*}

- La comparación de los valores de actividad obtenidos para todos los compuestos sintetizados de la quimioteca permite concluir que las dihidrazonas **33** no son buenos candidatos como potenciales antivirales ya que ninguna de las moléculas sintetizadas de este grupo ha resultado activa. Los *building blocks* que han mostrado mayor actividad son las aminas 1-(3-aminopropil)-pirrolidina (**31**{*5*}) y 1-(3-aminopropil)-2-pipecolina (**31**{*8*}). También, se ha observado que una cadena alquílica trimetilénica

entre el átomo de nitrógeno en posición bencílica y el sistema heterocíclico confiere mayor actividad antiviral que una cadena etilénica. Por otra parte, la sustitución del *linker p*-fenilénico de **32**{*8,8*} por un *linker m*-fenilénico provoca la disminución de un orden de magnitud en la actividad, de manera que se concluye que el *linker p*-fenilénico permite una mejor interacción con el correceptor CXCR4. Además, la presencia de metilos sobre los átomos de carbono bencílicos del *linker p*-fenilénico (estructuras **56** respecto a estructuras **32**) varía según el caso estudiado: en uno se mantiene la actividad antiviral, en otro disminuye un orden de magnitud y en el último caso se pasa de un compuesto inactivo a uno ligeramente activo.

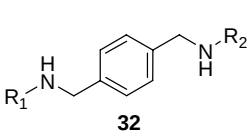


**32**

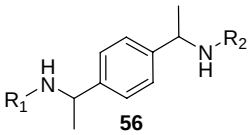


**56**

- Se ha desarrollado una metodología sintética que permite obtener monociclamos sustituidos de estructura general **70** a partir de un intermedio clave, el aldehído ciclámico **90**, y aminas primarias **31**. Este intermedio **90** ha permitido utilizar aminas primarias como reactivos en la obtención de los monociclamos sustituidos **70** con rendimientos elevados en presencia de isopropóxido de titanio (IV).

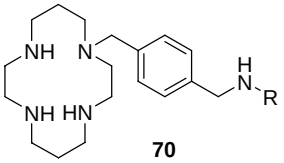


**70**

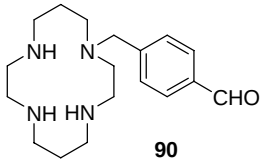


**90**

- Esta metodología se ha utilizado en la síntesis de dos monociclamos sustituidos, **70**{*8*} y **70**{*11*}, seleccionados mediante métodos computacionales de *docking* sobre el correceptor CXCR4, modelos QSAR y farmacofóricos, con valores de $EC_{50}$ de 0.022 y 0.058 μg/mL respectivamente. Ambos monociclamos presentan mejor actividad antiviral que los monociclamos sintetizados en AnorMed, excepto AMD3645. La comparación de la actividad de estos dos monociclamos con los compuestos de sustitución simétrica respecto al *linker p*-fenilenbismetilénico AMD3100 y **32**{*8,8*}, ambos más activos, muestra que la sustitución no simétrica no es favorable para la unión al correceptor CXCR4.

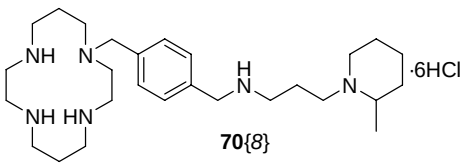


**70**{*8*}

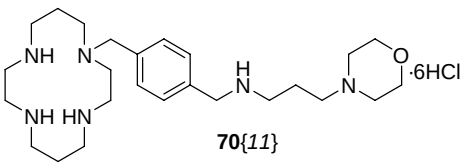


**70**{*11*}

- Se han calculado modelos QSAR y modelos de clasificación binarios (activos e inactivos) a partir de los valores de $EC_{50}$ de los compuestos sintetizados de la quimioteca de análogos al AMD3100. También se han modelado farmacóforos a partir de la estructura de ligandos conocidos de CXCR4, donde se han incluido los compuestos activos de la quimioteca diseñada. Estos modelos se han utilizado en un cribado virtual por consenso de diaminas **32**, dihidrazonas **33**, aminohidrazonas **37** y monociclamos **70** no sintetizados, donde se han seleccionado **37**{*2,8*}, **32**{*7,8*} y **70**{*8*}. Estos tres compuestos han presentado actividad antiviral en los ensayos biológicos.

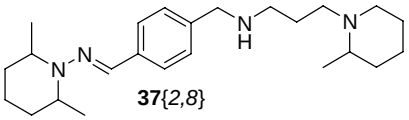

**37**{*2,8*}

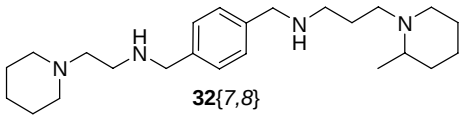

**32**{*7,8*}

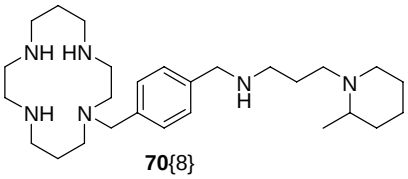

**70**{8}

# ANEXOS

## A.1. Descriptores moleculares.

***Tabla A.1.*** *Descriptores moleculares disponibles en MOE para la caracterización de moléculas.*

| **Descriptores 2D** | |
|---|---|
| **Propiedades físicas** | |
| *apol* | Suma de polarizabilidades atómicas |
| *bpol* | Suma del valor absoluto de la diferencia entre polarizabilidades atómicas de los átomos enlazados |
| *density* | *Weight* dividido por *vdw_vol* |
| *Fcharge* | Carga total de la molécula (suma de cargas formales) |
| *mr* | Refractividad molecular calculada a partir de un modelo lineal desarrollado por Labute para compuestos pequeños |
| *SMR* | Refractividad molecular calculada a partir de estructuras en estado de protonación correcto desarrollado por Crippen[1] |
| *Weight* | Peso molecular |
| *logP(o/w)* | Log del coeficiente de partición octanol/agua calculado a partir de un modelo desarrollado por Labute |
| *logS* | Log de la solubilidad acuosa |
| *reactive* | Indicador de la presencia de grupos reactivos |
| *SlogP* | Logaritmos del coeficiente de partición octanol/agua[1] |
| *TPSA* | Área de superficie polar[2] |
| *vdw_vol* | Volumen de van der Waals |
| *vdw_area* | Área de van der Waals |
| **Áreas de superficies subdivididas** | |
| Están basados en el área de la superficie de van der Waals para cada átomo, $\nu_i$, junto con alguna propiedad atómica, $p_i$. Estos descriptores se definen como la suma de $\nu_i$ sobre todos los átomos *i* que tienen $p_i$ en un rango (*a,b*].<br>En los siguientes descriptores $L_i$ se refiere a la contribución al logaritmo del coeficiente de partición octanol/agua del átomo *i* calculado en el descriptor *SlogP*. $R_i$ se refiere a la contribución a la refractividad molar del átomo *i* calculada en el descriptor *SMR*. | |
| *SlogP_VSA0* | Suma de $\nu_i$ tal que $L_i \leq -0.4$ |
| *SlogP_VSA1* | Suma de $\nu_i$ tal que $L_i$ esté en el intervalo (-0.4, -0.2] |
| *SlogP_VSA2* | Suma de $\nu_i$ tal que $L_i$ esté en el intervalo (-0.2, 0] |
| *SlogP_VSA3* | Suma de $\nu_i$ tal que $L_i$ esté en el intervalo (0, 0.1] |
| *SlogP_VSA4* | Suma de $\nu_i$ tal que $L_i$ esté en el intervalo (0.1, 0.15] |
| *SlogP_VSA5* | Suma de $\nu_i$ tal que $L_i$ esté en el intervalo (0.15, 0.20] |
| *SlogP_VSA6* | Suma de $\nu_i$ tal que $L_i$ esté en el intervalo (0.20, 0.25] |
| *SlogP_VSA7* | Suma de $\nu_i$ tal que $L_i$ esté en el intervalo (0.25, 0.30] |
| *SlogP_VSA8* | Suma de $\nu_i$ tal que $L_i$ esté en el intervalo (0.30, 0.40] |

| | |
|---|---|
| *SlogP_VSA9* | Suma de $v_i$ tal que $L_i > 0.4$ |
| *SMR_VSA0* | Suma de $v_i$ tal que $R_i$ esté en el intervalo [0, 0.11] |
| *SMR_VSA1* | Suma de $v_i$ tal que $R_i$ esté en el intervalo (0.11, 0.26] |
| *SMR_VSA2* | Suma de $v_i$ tal que $R_i$ esté en el intervalo (0.26, 0.35] |
| *SMR_VSA3* | Suma de $v_i$ tal que $R_i$ esté en el intervalo (0.35, 0.39] |
| *SMR_VSA4* | Suma de $v_i$ tal que $R_i$ esté en el intervalo (0.39, 0.44] |
| *SMR_VSA5* | Suma de $v_i$ tal que $R_i$ esté en el intervalo (0.44, 0.485] |
| *SMR_VSA6* | Suma de $v_i$ tal que $R_i$ esté en el intervalo (0.485, 0.56] |
| *SMR_VSA7* | Suma de $v_i$ tal que $R_i > 0.56$ |
| | **Cuentas de átomos y enlaces** |
| *a_aro* | Número de átomos aromáticos |
| *a_count* | Número de átomos (incluye H implícitos) |
| *a_heavy* | Número de átomos pesados |
| *a_ICM* | Índice de información o entropía de Shanon (media) |
| *a_IC* | Índice de información o entropía de Shanon (total) |
| *a_nH* | Número de átomos de H (incluye H implícitos) |
| *a_nB* | Número de átomos de B |
| *a_nC* | Número de átomos de C |
| *a_nN* | Número de átomos de N |
| *a_nO* | Número de átomos de O |
| *a_nF* | Número de átomos de F |
| *a_nP* | Número de átomos de P |
| *a_nS* | Número de átomos de S |
| *a_nCl* | Número de átomos de Cl |
| *a_nBr* | Número de átomos de Br |
| *a_nI* | Número de átomos de I |
| *b_1rotN* | Número de enlaces simples rotables |
| *b_1rotR* | Fracción de enlaces simples rotables |
| *b_ar* | Número de enlaces aromáticos |
| *b_count* | Número de enlaces (incluye H implícitos) |
| *b_double* | Número de enlaces dobles |
| *b_heavy* | Número de enlaces entre átomos pesados |
| *b_rotN* | Número de enlaces rotables |
| *b_rotR* | Fracción de enlaces rotables |
| *b_single* | Número de enlaces simples (incluye H implícitos) |
| *b_triple* | Número de enlaces triples |
| *rings* | Número de anillos |
| *VAdjMa* | Índice de contenido medio de información de magnitud de adyacencia |
| *VAdjEq* | Índice de contenido medio de información de igualdad de adyacencia |

| **Topológicos** | |
|---|---|
| *chi0, chi0_C, chi1, chi1_C* | Índices de conectividad Kier & Hall de órdenes 0 y 1 ([3] |
| *chi0v, chi0v_C, chi1v, chi1v_C* | Índices de conectividad de valencia atómica de Kier & Hall de órdenes 0 y 1 [3] |
| *Kier1, Kier2, Kier3* | Índices de Kier & Hall kappa shape de órdenes 1-3[4] |
| *KierA1, KierA2, KierA3* | Índices Kier & Hall atom modified shapede órdenes 1-3 |
| *KierFlex* | Índice de flexibilidad molecular de Kier |
| *zagreb* | Índice de Zagreb |
| *balabanJ* | Índice de conectividad topológica de Balaban[5] |
| *radius* | Menor excentricidad atómica del grafo de la molécula sin H |
| *diameter* | Mayor valor en la matriz de distancias[6] |
| *petitjeanSC* | Coeficiente de forma de grafo de Petitjean[6] |
| *petitjean* | Valor de *(diameter-radius)/diameter* |
| *VDistEq* | Índice de contenido medio de información de igualdad de distancia |
| *VDistMa* | Índice de contenido medio de información de magnitud de distancia |
| *weinerPol* | número de polaridad de Wiener[7] |
| *weinerPath* | índice de Wiener[7,8] |

| **Características farmacofóricas** | |
|---|---|
| *a_acc* | Número de átomos aceptores de puente de H |
| *a_acid* | Número de átomos ácidos |
| *a_base* | Número de átomos básicos |
| *a_don* | Número de átomos dadores de puente de H |
| *a_hyd* | Número de átomos hidrofóbicos |
| *vsa_acc* | Suma de áreas de la superficie de van der Waals de aceptores de puente de H |
| *vsa_acid* | Suma de áreas de la superficie de van der Waals de átomos ácidos |
| *vsa_base* | Suma de áreas de la superficie de van der Waals de átomos básicos |
| *vsa_don* | Suma de áreas de la superficie de van der Waals de dadores de puente de H |
| *vsa_hyd* | Suma de áreas de la superficie de van der Waals de átomos hidrofóbicos |
| *vsa_other* | Suma de áreas de la superficie de van der Waals de otros átomos |
| *vsa_pol* | Suma de áreas de la superficie de van der Waals de átomos polares |

**Cargas parciales**

Los descriptores *PEOE* utilizan las cargas parciales calculadas mediante el método PEOE, mientras que los descriptores *Q* utilizan las cargas parciales guardadas con la estructura generalmente son las del *forcefield,* calculadas al minimizar la energía.

Sea $q_i$ la carga parcial de un átomo *i* y $v_i$, el área de la superficie de van der Waals para cada átomo, se definen los siguientes descriptores.

| | |
|---|---|
| *Q_PC+, PEOE_PC+* | Total de carga parcial positiva |
| *Q_PC-, PEOE_PC-* | Total de carga parcial negativa |
| *Q_RPC+ PEOE_RPC+* | Carga parcial relativa positiva |
| *Q_RPC- PEOE_RPC-* | Carga parcial relativa negativa |

| | |
|---|---|
| *Q_VSA_POS*<br>*PEOE_VSA_POS* | Área positiva total de la superficie de van der Waals.<br>Suma de todos los $\nu_i$ cuya $q_i > 0$ |
| *Q_VSA_NEG*<br>*PEOE_VSA_NEG* | Área negativa total de la superficie de van der Waals con $q_i$ negativa.<br>Suma de todos los $\nu_i$ cuya $q_i < 0$ |
| *Q_VSA_PPOS*<br>*PEOE_VSA_PPOS* | Área positiva polar total de la superficie de van der Waals.<br>Suma de todos los $\nu_i$ cuya $q_i > 0.2$ |
| *Q_VSA_PNEG*<br>*PEOE_VSA_PNEG* | Área negativa polar total de la superficie de van der Waals.<br>Suma de todos los $\nu_i$ cuya $q_i < -0.2$ |
| *Q_VSA_HYD*<br>*PEOE_VSA_HYD* | Área hidrofóbica total de la superficie de van der Waals.<br>Suma de $\nu_i$ cuya $\|q_i\| \leq 0.2$ |
| *Q_VSA_POL*<br>*PEOE_VSA_POL* | Área polar total de la superficie de van der Waals.<br>Suma de $\nu_i$ cuya $\|q_i\| > 0.2$ |
| *Q_VSA_FPOS*<br>*PEOE_VSA_FPOS* | Fraccional del área positiva de la superficie de van der Waals |
| *Q_VSA_FNEG*<br>*PEOE_VSA_FNEG* | Fraccional del área negativa de la superficie de van der Waals |
| *Q_VSA_FPPOS*<br>*PEOE_VSA_FPOS* | Fraccional del área positiva polar de la superficie de van der Waals con $q_i > 0.2$ |
| *Q_VSA_FPNEG*<br>*PEOE_VSA_FPNEG* | Fraccional del área negativa polar de superficie de van der Waals con $q_i < -0.2$ |
| *Q_VSA_FHYD*<br>*PEOE_VSA_FHYD* | Fraccional del área de superficie de van der Waals hidrofóbica.<br>Suma de $\nu_i$ tal que $\|q_i\| \leq 0.2$ |
| *Q_VSA_FPOL*<br>*PEOE_VSA_FPOL* | Fraccional del área polar de la superficie de van der Waals.<br>Suma de $\nu_i$ tal que $\|q_i\| > 0.2$ |
| *PEOE_VSA+6* | Suma de $\nu_i$ si $q_i > 0.3$ |
| *PEOE_VSA+5* | Suma de $\nu_i$ si $q_i$ está en el intervalo [0.25, 0.30) |
| *PEOE_VSA+4* | Suma de $\nu_i$ si $q_i$ está en el intervalo [0.20, 0.350) |
| *PEOE_VSA+3* | Suma de $\nu_i$ si $q_i$ está en el intervalo [0.15, 0.20) |
| *PEOE_VSA+2* | Suma de $\nu_i$ si $q_i$ está en el intervalo [0.10, 0.15) |
| *PEOE_VSA+1* | Suma de $\nu_i$ si $q_i$ está en el intervalo [0.05, 0.10) |
| *PEOE_VSA+0* | Suma de $\nu_i$ si $q_i$ está en el intervalo [0.00, 0.05) |
| *PEOE_VSA-0* | Suma de $\nu_i$ si $q_i$ está en el intervalo [-0.05, 0.00) |
| *PEOE_VSA-1* | Suma de $\nu_i$ si $q_i$ está en el intervalo [-0.10, -0.05) |
| *PEOE_VSA-2* | Suma de $\nu_i$ si $q_i$ está en el intervalo [-0.15, -0.10) |
| *PEOE_VSA-3* | Suma de $\nu_i$ si $q_i$ está en el intervalo [-0.20, -0.15) |
| *PEOE_VSA-4* | Suma de $\nu_i$ si $q_i$ está en el intervalo [-0.25, -0.20) |
| *PEOE_VSA-5* | Suma de $\nu_i$ si $q_i$ está en el intervalo [-0.30, -0.25) |
| *PEOE_VSA-6* | Suma de $\nu_i$ si $q_i < -0.30$ |
| **Descriptores 3D** | |
| **Energía potencial** | |
| *E* | Valor de la energía potencial |
| *E_ang* | Energía potencial de flexión del ángulo |
| *E_ele* | Componente electrostática de la energía potencial |
| *E_nb* | Energía potencial con los términos enlazados inactivos |

| | |
|---|---|
| *E_oop* | Energía potencial fuera del plano |
| *E_sol* | Energía de solvatación |
| *E_stb* | Energía potencial de tensión-flexión de enlace |
| *E_str* | Energía potencial de tensión de enlace |
| *E_strain* | Energía de tensión local |
| *E_tor* | Energía potencial de torsión |
| *E_vdw* | Componente de van der Waals de la energía potencial |
| *E_rele* | Energía de interacción electrostática |
| *E_rnb* | Energía de interacción de ligando y receptor |
| *E_rsol* | Energía de solvatación entre ligando y receptor |
| *E_rvdw* | Energía d einteracción de van der Waals entre ligando y receptor |
| | **Superficie, forma y volumen** |
| *ASA* | Área de superficie accesible al agua |
| *vol* | Volumen de Van der Waals |
| *rgyr* | Radio de giro |
| *pmi*<br>*pmiX, pmiY, pmiZ* | Momento de inercia principal y sus componentes *x, y* y *z* |
| *glob* | Globularidad |
| *dens* | Densidad |
| *VSA* | Área de superficie de van der Waals |
| | **Carga dependientes de la conformación** |
| El área de superficie accesible al agua se ha calculado considerando un radio de 1.4 Å para la molécula de agua.<br>$q_i$ representa la carga parcial del átomo *i*. | |
| *ASA+* | Área de superficie accesible al agua para todos los átomos con carga parcial positiva |
| *ASA-* | Área de superficie accesible al agua para todos los átomos con carga parcial negativa |
| *ASA_H* | Área de superficie accesible al agua de los átomo hidrofóbicos, $\|q_i\| < 0.2$ |
| *ASA_P* | Área de superficie accesible al agua de los átomos polares $\|q_i\| \geq 0.2$ |
| *DASA* | Valor absoluto de la diferencia entre el *ASA+* y el *ASA-* |
| *CASA+* | Área de superficie ponderada con carga positiva[9] |
| *CASA-* | Área de superficie ponderada con carga negativa[9] |
| *DCASA* | Valor absoluto de la diferencia entre *CASA+* y *CASA-*[9] |
| *FASA+* | Fraccional de *ASA+* |
| *FASA-* | Fraccional *ASA-* |
| *FCASA+* | Fraccional de *CASA+* |
| *FCASA-* | Fraccional de *CASA-* |
| *FASA_H* | Fraccional de *ASA_H* |
| *FASA_P* | Fraccional *ASA_P* |
| *dipole* | Momento dipolar y sus componentes *z, y* y *z* |

## Bibliografía.


[1] S. A. Wildman, G. M. Crippen; Prediction of physiochemical parameters by atomic contributions. *J. Chem. Inf. Comput. Sci.* **1999**, *39,* 868-873.

[2] P. Ertl, B. Rohde, P. Selzer; Fast calculation of molecular polar surface area as a sum of fragment-based contributions and its application to the prediction of drug transport porperties. *J. Med. Chem.* **2000**, *43,* 3714-3717.

[3] L. H. Hall, L. B. Kier; The nature of structure-activity relationships and their relation to molecular connectivity. *Eur. J. Med. Chem.* **1977**, *12,* 307-312.

[4] L. B. Kier; A shape index from molecular graphs. *Quant. Struct. -Act. Relat.* **1985**, *4,* 109-116.

[5] A. T. Balaban; Highly discriminationg distance-based topological index. *Chem. Phys. Lett.* **1982**, *89,* 399-404.

[6] M. Petitjean; Applications of the radius-diameter diagram to the classification of topological and geometrical shapes of chemical compounds. *J. Chem. Inf. Comput. Sci.* **1992**, *32,* 331-337.

[7] A. T. Balaban; Five new topological indices for the branchig of tree-like graphs. *Theor. Chim. Acta* **1979**, *53,* 355-375.

[8] H. Wiener; Structural determination of paraffin boiling points. *J. Am. Chem. Soc.* **1947**, *69,* 17-20.

[9] D. T. Stanton, P. C. Jurs; Development and use of charged partial surface area structural descriptors in computer-assisted quantitative structure-property relationship studies. *Anal. Chem.* **1990**, *62,* 2323-2329.

## A.2. *Training set* utilizado en los QSAR.

***Tabla A.2.*** Training set *utilizado para calcular los modelos QSAR. Se muestra también el valor de la actividad de cada uno de los compuestos, $pEC_{50}$.*

| # | Estructura | Nombre | $pEC_{50}$ |
|---|---|---|---|
| 1 | 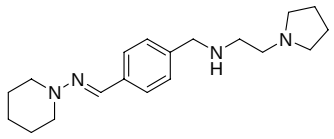 | **37**{*1,11*} | 4.512 |
| 2 | 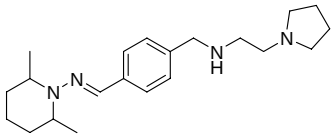 | **37**{*2,4*} | 4.367 |
| 3 | 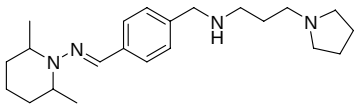 | **37**{*2,5*} | 5.251 |
| 4 | 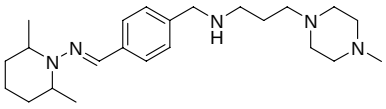 | **37**{*2,9*} | 5.005 |
| 5 | 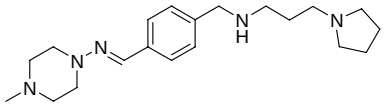 | **37**{*3,5*} | 5.281 |
| 6 | 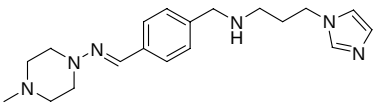 | **37**{*3,6*} | 4.483 |

| # | Estructura | Nombre | $pEC_{50}$ |
|---|---|---|---|
| 7 | 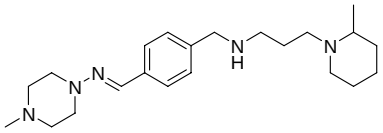 | **37**{*3,8*} | 5.424 |
| 8 | 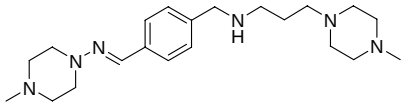 | **37**{*3,9*} | 4.503 |
| 9 | 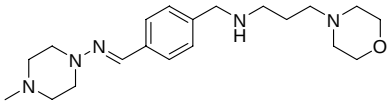 | **37**{*3,11*} | 4.647 |
| 10 | 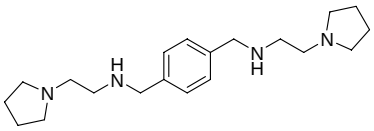 | **32**{*4,4*} | 4.511 |
| 11 | 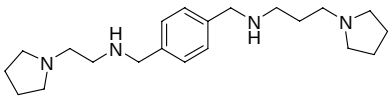 | **32**{*4,5*} | 5.299 |
| 12 | 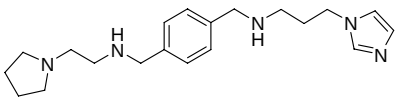 | **32**{*4,6*} | 4.852 |
| 13 | 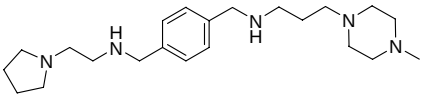 | **32**{*4,9*} | 4.659 |

| # | Estructura | Nombre | $pEC_{50}$ |
|---|---|---|---|
| 14 | 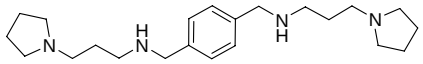 | **32**{*5,5*} | 5.600 |
| 15 | 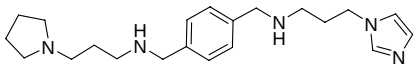 | **32**{*5,6*} | 6.250 |
| 16 | 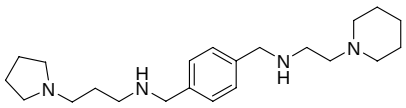 | **32**{*5,7*} | 5.327 |
| 17 | 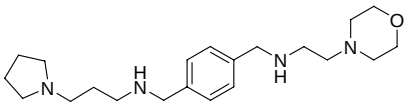 | **32**{*5,10*} | 5.177 |
| 18 | 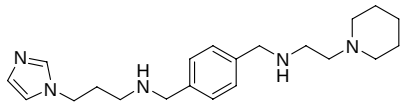 | **32**{*6,7*} | 5.254 |
| 19 | 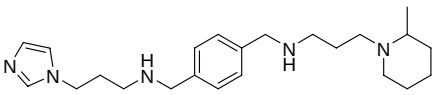 | **32**{*6,8*} | 7.106 |
| 20 | 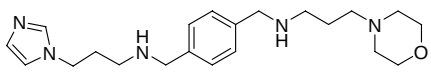 | **32**{*6,11*} | 4.305 |

| # | Estructura | Nombre | $pEC_{50}$ |
|---|---|---|---|
| 21 | 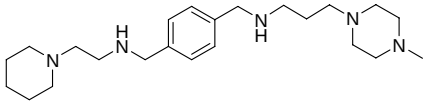 | **32**{*7,9*} | 5.190 |
| 22 | 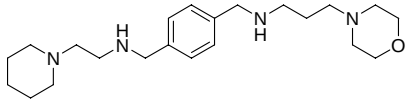 | **32**{*7,11*} | 5.142 |
| 23 | 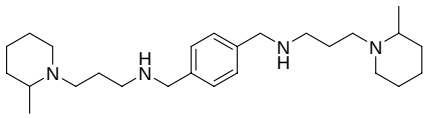 | **32**{*8,8*} | 7.715 |
| 24 | 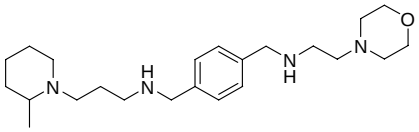 | **32**{*8,10*} | 5.987 |
| 25 | 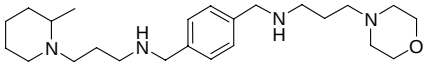 | **32**{*8,11*} | 5.906 |
| 26 | 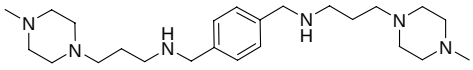 | **32**{*9,9*} | 4.642 |
| 27 | 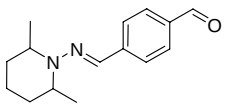 | **36**{*2*} | 4.432 |

| # | Estructura | Nombre | $pEC_{50}$ |
|---|---|---|---|
| 28 | 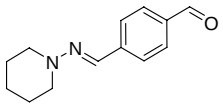 | **36**{*1*} | 4.235 |
| 29 | 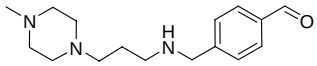 | **35**{*9*} | 4.233 |
| 30 | 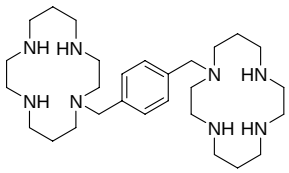 | AMD3100 | 8.688 |

## A.3. *Test set* utilizado en los QSAR.

***Tabla A.3.*** Test set *utilizado para calcular los modelos QSAR. Se muestra también el valor de la actividad de cada uno de los compuestos, $pEC_{50}$.*

| # | Estructura | Nombre | $pEC_{50}$ |
|---|---|---|---|
| 1 | 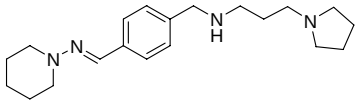 | **37**{*1,5*} | 5.079 |
| 2 | 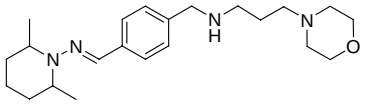 | **37**{*2,11*} | 4.375 |
| 3 | 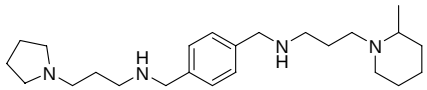 | **32**{*5,8*} | 6.357 |
| 4 | 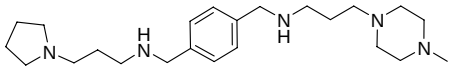 | **32**{*5,9*} | 5.889 |
| 5 | 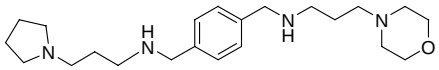 | **32**{*5,11*} | 5.369 |
| 6 | 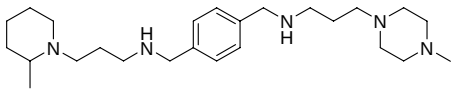 | **32**{*8,9*} | 7.142 |

| # | Estructura | Nombre | $pEC_{50}$ |
|---|---|---|---|
| 7 | 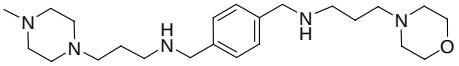 | **32**{*9,11*} | 4.647 |
| 8 | 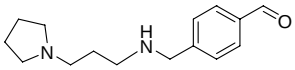 | **35**{*5*} | 4.337 |
| 9 | 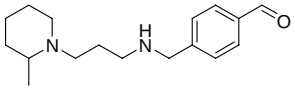 | **35**{*8*} | 5.183 |

## A.4. *Training set* utilizado en los árboles de clasificación.

***Tabla A.4.*** Training set *utilizado para construir los árboles de clasificación. Se muestra también el valor de la actividad anti-VIH de cada uno de los compuestos, $EC_{50}$, así como la clase a la que pertenece, 0 para los compuestos inactivos y 1 para los compuestos activos.*

| # | Estructura | Nombre | $EC_{50}$ / $\mu g \cdot mL^{-1}$ | Clase |
|---|---|---|---|---|
| 1 | 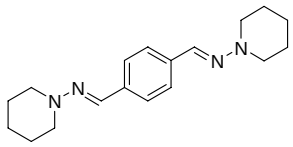 | **33**{*1,1*} | >25 | 0 |
| 2 | 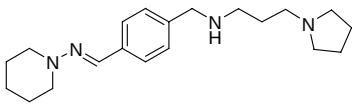 | **37**{*1,5*} | 2.7 | 1 |
| 3 | 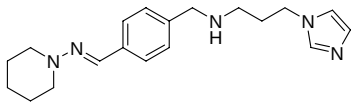 | **37**{*1,6*} | >25 | 0 |
| 4 | 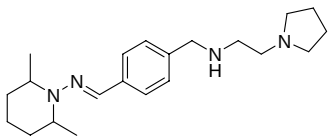 | **37**{*1,11*} | 10.6 | 1 |
| 5 | 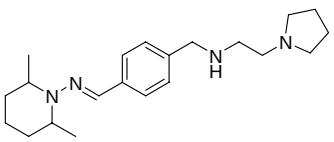 | **37**{*2,4*} | 14.7 | 1 |
| 6 | 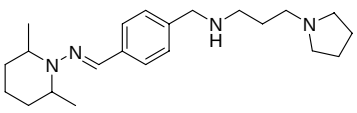 | **37**{*2,5*} | 2.0 | 1 |

| # | Estructura | Nombre | $EC_{50}$ / $\mu g \cdot mL^{-1}$ | Clase |
|---|---|---|---|---|
| 7 | 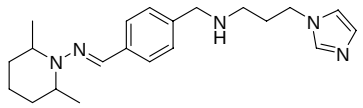 | **37**{*2,6*} | >25 | 0 |
| 8 | 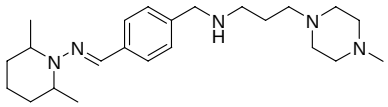 | **37**{*2,9*} | 3.8 | 1 |
| 9 | 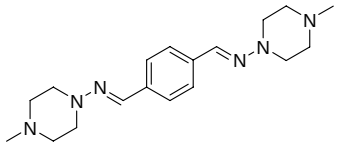 | **33**{*3,3*} | >25 | 0 |
| 10 | 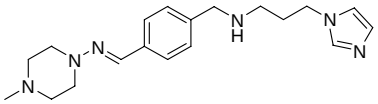 | **37**{*3,6*} | 11.2 | 1 |
| 11 | 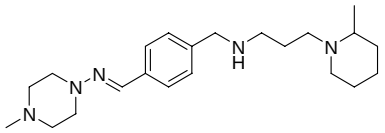 | **37**{*3,8*} | 1.4 | 1 |
| 12 | 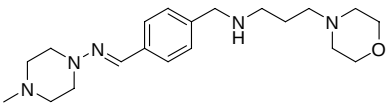 | **37**{*3,11*} | 8.1 | 1 |
| 13 | 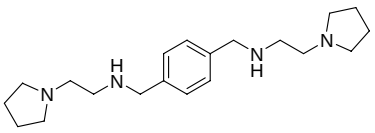 | **32**{*4,4*} | 10.2 | 1 |

| # | Estructura | Nombre | $EC_{50}$ / $\mu g \cdot mL^{-1}$ | Clase |
|---|---|---|---|---|
| 14 | 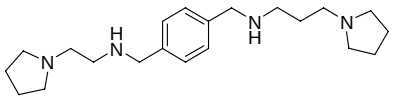 | **32**{*4,5*} | 1.7 | 1 |
| 15 | 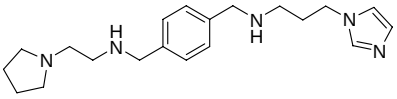 | **32**{*4,6*} | 4.8 | 1 |
| 16 | 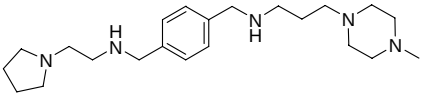 | **32**{*4,9*} | 8.2 | 1 |
| 17 | 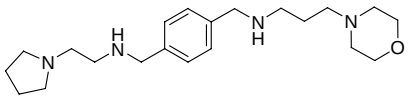 | **32**{*4,11*} | >25 | 0 |
| 18 | 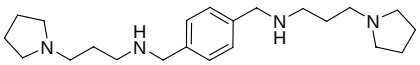 | **32**{*5,5*} | 0.9 | 1 |
| 19 | 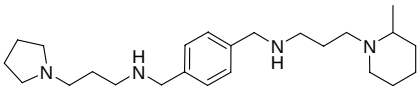 | **32**{*5,8*} | 0.2 | 1 |
| 20 | 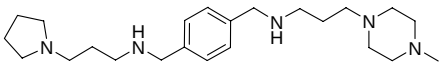 | **32**{*5,9*} | 0.5 | 1 |

| # | Estructura | Nombre | $EC_{50}$ / $\mu g \cdot mL^{-1}$ | Clase |
|---|---|---|---|---|
| 21 | 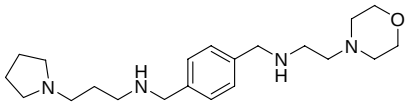 | **32**{*5,10*} | 2.4 | 1 |
| 22 | 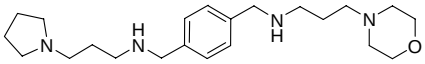 | **32**{*5,11*} | 1.6 | 1 |
| 23 | 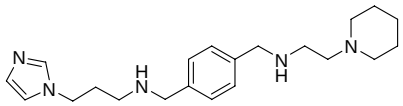 | **32**{*6,7*} | 2.0 | 1 |
| 24 | 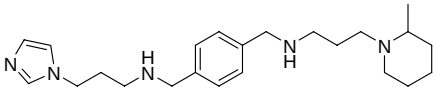 | **32**{*6,8*} | 0.03 | 1 |
| 25 | 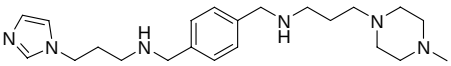 | **32**{*6,9*} | >25 | 0 |
| 26 | 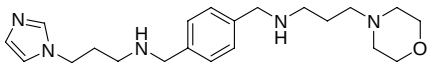 | **32**{*6,11*} | 18.4 | 1 |
| 27 | 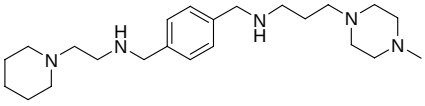 | **32**{*7,9*} | 2.5 | 1 |

| # | Estructura | Nombre | $EC_{50}$ / $\mu g \cdot mL^{-1}$ | Clase |
|---|---|---|---|---|
| 28 | 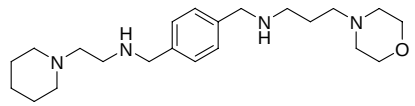 | **32**{*7,11*} | 2.7 | 1 |
| 29 | 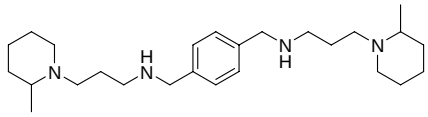 | **32**{*8,8*} | 0.008 | 1 |
| 30 | 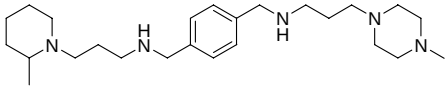 | **32**{*8,9*} | 0.03 | 1 |
| 31 | 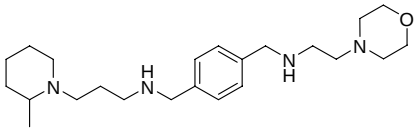 | **32**{*8,10*} | 0.4 | 1 |
| 32 | 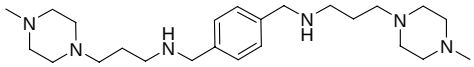 | **32**{*9,9*} | 9.5 | 1 |
| 33 | 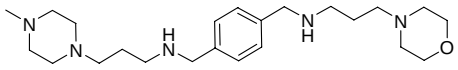 | **32**{*9,11*} | 9.1 | 1 |
| 34 | 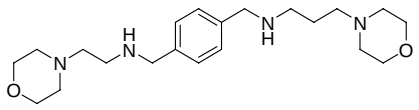 | **32**{*10,11*} | >25 | 0 |

| # | Estructura | Nombre | $EC_{50}$ / $\mu g \cdot mL^{-1}$ | Clase |
|---|---|---|---|---|
| 35 | 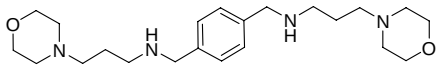 | **32**{*11,11*} | >25 | 0 |
| 36 | 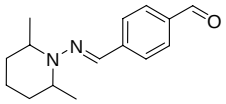 | **36**{*2*} | 9.0 | 1 |
| 37 | 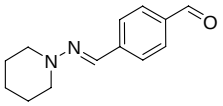 | **36**{*1*} | 12.6 | 1 |
| 38 | 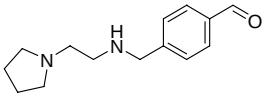 | **35**{*4*} | >25 | 0 |
| 39 | 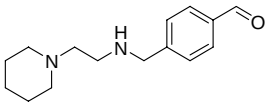 | **35**{*7*} | >25 | 0 |
| 40 | 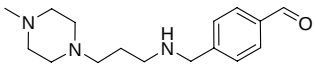 | **35**{*9*} | 16.1 | 1 |
| 41 | 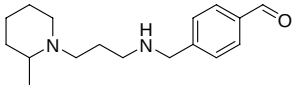 | **35**{*8*} | 1.8 | 1 |

| # | Estructura | Nombre | $EC_{50}$ / $\mu g \cdot mL^{-1}$ | Clase |
|---|---|---|---|---|
| 42 | 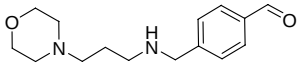 | **35**{*11*} | >25 | 0 |
| 43 | 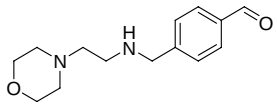 | **35**{*10*} | >25 | 0 |
| 44 | 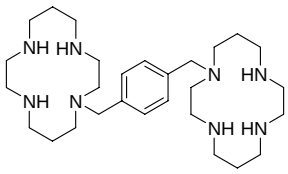 | AMD3100 | 0.001 | 1 |

## A.5. *Test set* utilizado en los árboles de clasificación.

***Tabla A.5.*** Test set *utilizado para construir los árboles de clasificación. Se muestra también el valor de la actividad anti-VIH de cada uno de los compuestos, $EC_{50}$, así como la clase a la que pertenece, 0 para los compuestos inactivos y 1 para los compuestos activos.*

| # | Estructura | Nombre | $EC_{50}$ / μg·mL$^{-1}$ | Clase |
|---|---|---|---|---|
| 1 | 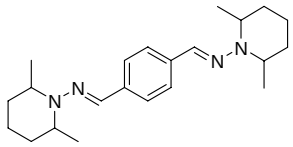 | **33**{*2,2*} | >25 | 0 |
| 2 | 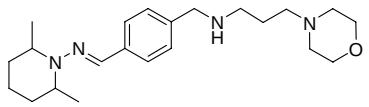 | **37**{*2,11*} | 15.7 | 1 |
| 3 | 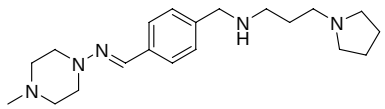 | **37**{*3,5*} | 1.8 | 1 |
| 4 | 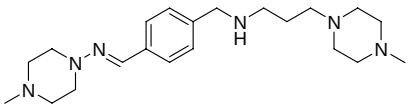 | **37**{*3,9*} | 11.7 | 1 |
| 5 | 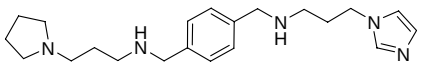 | **32**{*5,6*} | 0.2 | 1 |
| 6 | 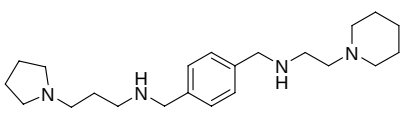 | **32**{*5,7*} | 1.7 | 1 |

| # | Estructura | Nombre | $EC_{50}$ / $\mu g \cdot mL^{-1}$ | Clase |
|---|---|---|---|---|
| 7 | 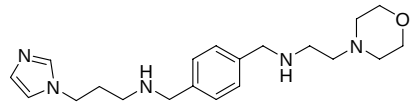 | **32**{*6,10*} | >25 | 0 |
| 8 | 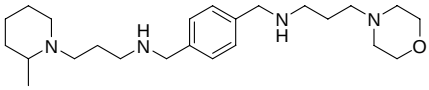 | **32**{*8,11*} | 0.5 | 1 |
| 9 | 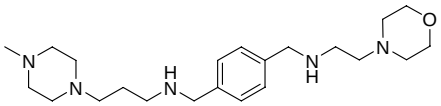 | **32**{*9,10*} | >25 | 0 |
| 10 | 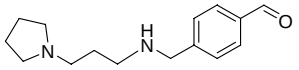 | **35**{*5*} | 11.3 | 1 |
| 11 | 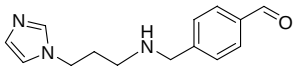 | **35**{*6*} | >25 | 0 |

## A.6. Base de datos de activos utilizada en los farmacóforos.

***Tabla A.6.*** *Base de datos de inhibidores de entrada del correceptor CXCR4 y su actividad expresada como $EC_{50}$ en nM.*

| # | Estructura | Familia | $EC_{50}$ / μM |
|---|---|---|---|
| 1 | 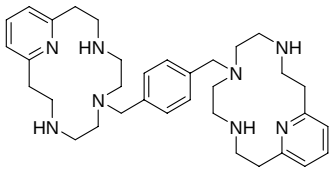 | azamacrociclo **105** | $0.8 \cdot 10^{-3}$ |
| 2 | 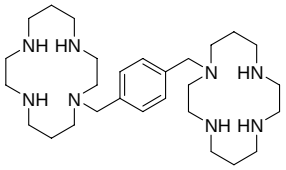 | azamacrociclo **24** | $4.2 \cdot 10^{-3}$ |
| 3 | 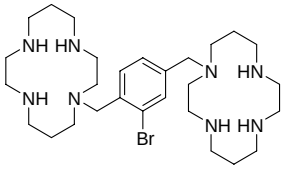 | azamacrociclo | $6.0 \cdot 10^{-3}$ |
| 4 | 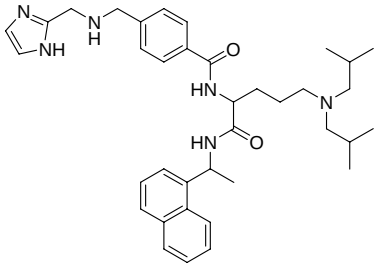 | KRH **106** | $6.7 \cdot 10^{-3}$ |
| 5 | 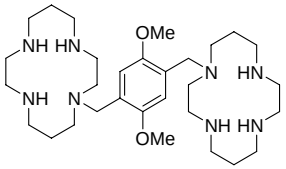 | azamacrociclo | $7.1 \cdot 10^{-3}$ |
| 6 | 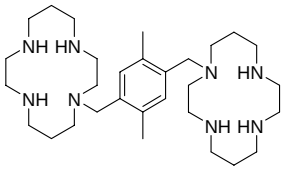 | azamacrociclo | $7.6 \cdot 10^{-3}$ |

| # | Estructura | Familia | $EC_{50}$ / μM |
|---|---|---|---|
| 7 | 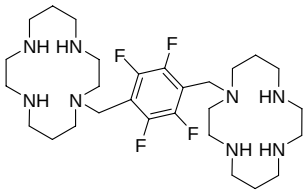 | azamacrociclo | $7.9 \cdot 10^{-3}$ |
| 8 | 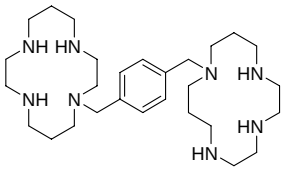 | azamacrociclo | $7.9 \cdot 10^{-3}$ |
| 9 | 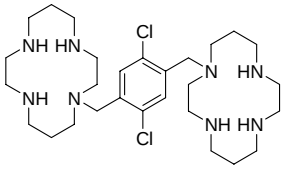 | azamacrociclo | 0.011 |
| 10 | 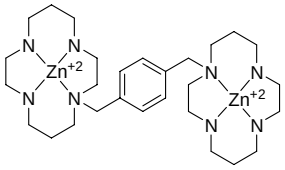 | azamacrociclo | 0.011 |
| 11 | 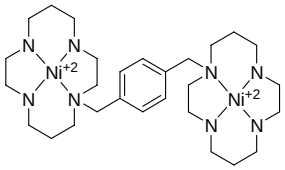 | azamacrociclo | 0.013 |
| 12 | 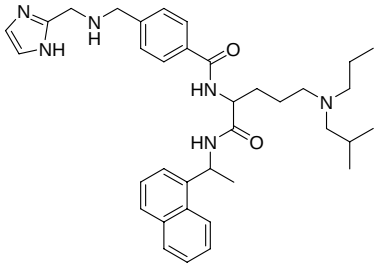 | KRH | 0.015 |
| 13 | 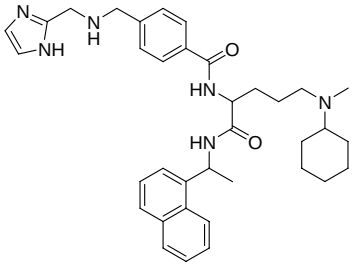 | KRH | 0.015 |

| # | Estructura | Familia | $EC_{50}$ / μM |
|---|---|---|---|
| 14 | 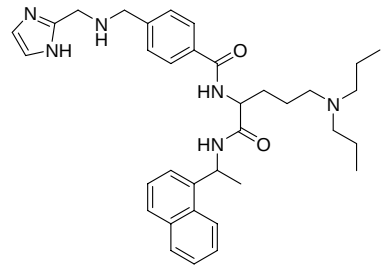 | KRH | 0.015 |
| 15 | 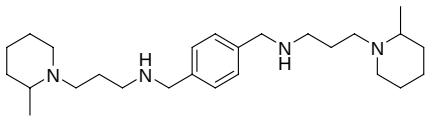 | poliamina **32**{*8,8*} | 0.019 |
| 16 | 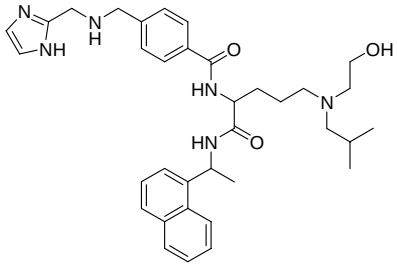 | KRH | 0.020 |
| 17 | 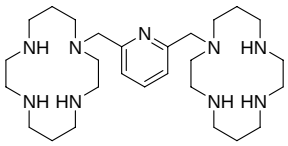 | azamacrociclo | 0.025 |
| 18 | 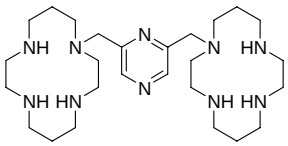 | azamacrociclo | 0.026 |
| 19 | 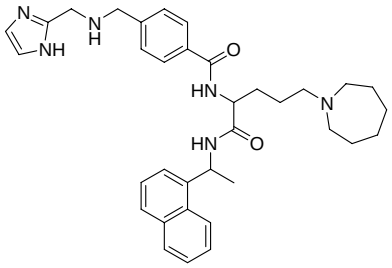 | KRH | 0.029 |

| # | Estructura | Familia | $EC_{50}$ / μM |
|---|---|---|---|
| 20 | 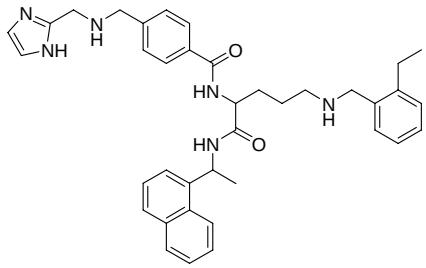 | KRH | 0.030 |
| 21 | 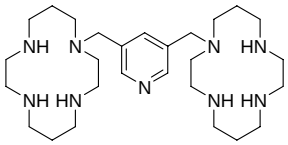 | azamacrociclo | 0.032 |
| 22 | 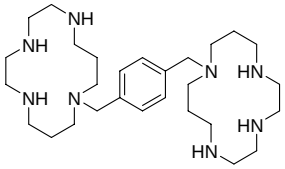 | azamacrociclo | 0.034 |
| 23 | 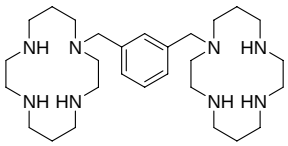 | azamacrociclo | 0.034 |
| 24 | 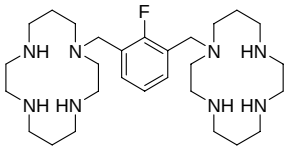 | azamacrociclo | 0.035 |
| 25 | 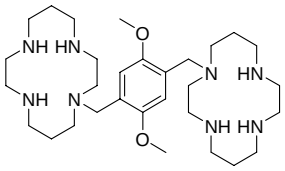 | azamacrociclo | 0.035 |
| 26 | 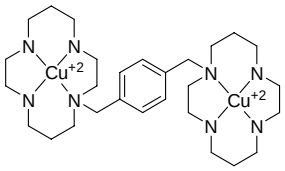 | azamacrociclo | 0.037 |
| 27 | 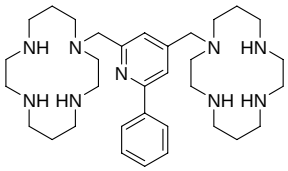 | azamacrociclo | 0.040 |

| # | Estructura | Familia | $EC_{50}$ / μM |
|---|---|---|---|
| 28 | 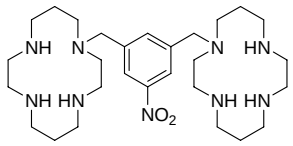 | azamacrociclo | 0.041 |
| 29 | 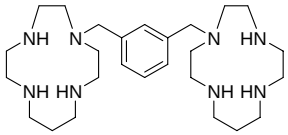 | azamacrociclo | 0.041 |
| 30 | 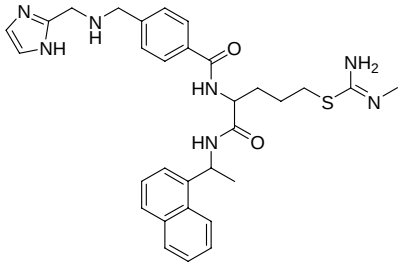 | KRH | 0.046 |
| 31 | 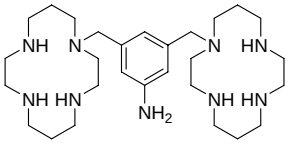 | azamacrociclo | 0.047 |
| 32 | 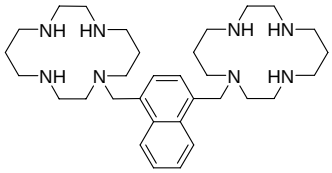 | azamacrociclo | 0.055 |
| 33 | 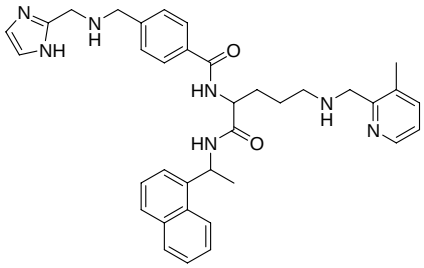 | KRH | 0.055 |
| 34 | 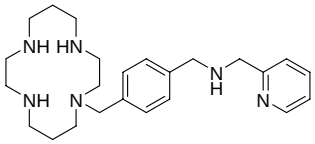 | azamacrociclo | 0.058 |

| # | Estructura | Familia | $EC_{50}$ / μM |
|---|---|---|---|
| 35 | 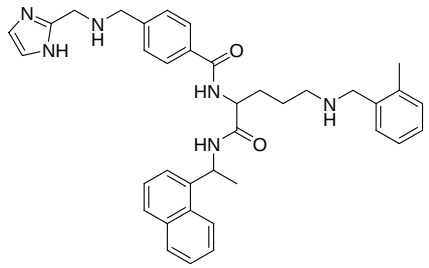 | KRH | 0.058 |
| 36 | 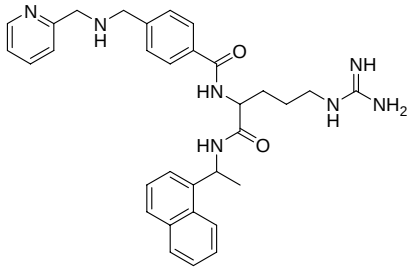 | KRH | 0.060 |
| 37 | 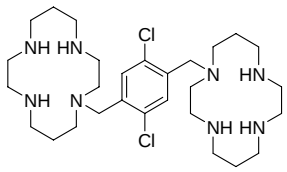 | azamacrociclo | 0.063 |
| 38 | 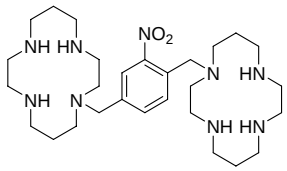 | azamacrociclo | 0.065 |
| 39 | 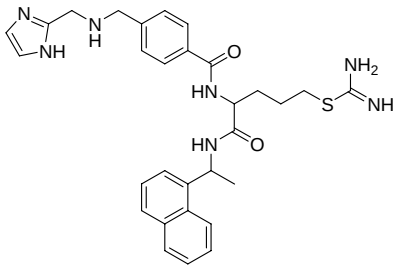 | KRH | 0.069 |
| 40 | 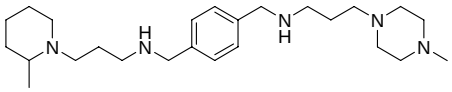 | poliamina **32**{*8,9*} | 0.072 |
| 41 | 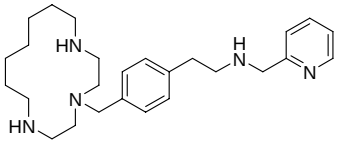 | azamacrociclo | 0.075 |

| # | Estructura | Familia | $EC_{50}$ / μM |
|---|---|---|---|
| 42 | 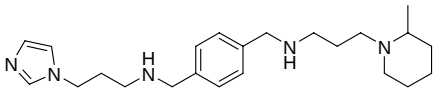 | poliamina<br>**32**{*6,8*} | 0.078 |
| 43 | 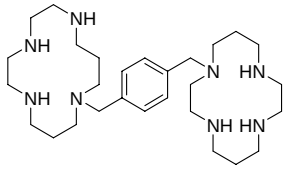 | azamacrociclo | 0.081 |
| 44 | 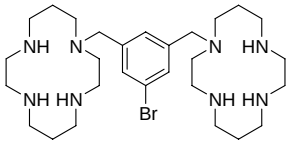 | azamacrociclo | 0.085 |
| 45 | 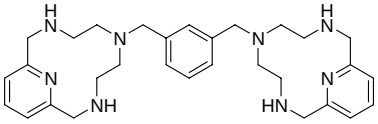 | azamacrociclo | 0.097 |
| 46 | 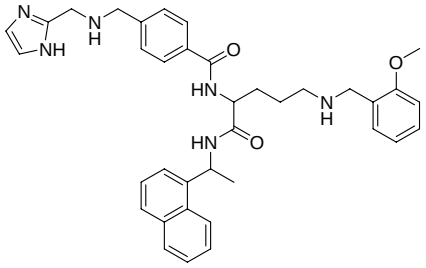 | KRH | 0.100 |
| 47 | 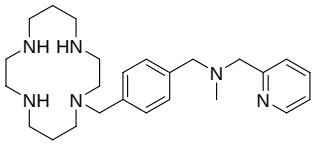 | azamacrociclo | 0.100 |
| 48 | 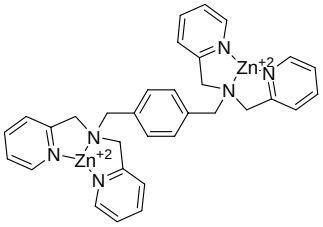 | Dpa<br>**107** | 0.100 |

| # | Estructura | Familia | $EC_{50}$ / μM |
|---|---|---|---|
| 49 | 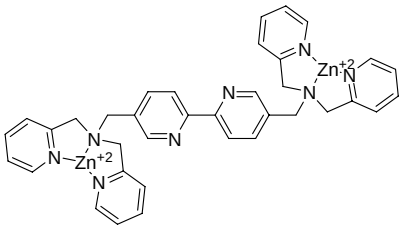 | Dpa | 0.100 |
| 50 | 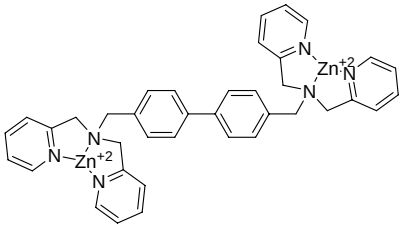 | Dpa | 0.120 |
| 51 | 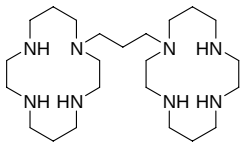 | azamacrociclo | 0.138 |
| 52 | 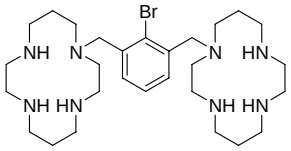 | azamacrociclo | 0.138 |
| 53 | 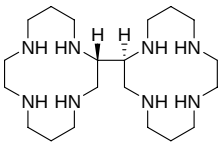 | azamacrociclo | 0.144 |
| 54 | 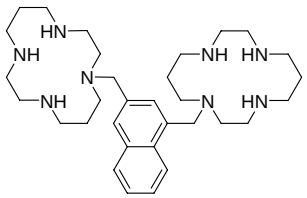 | azamacrociclo | 0.158 |
| 55 | 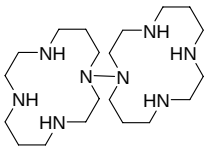 | azamacrociclo | 0.158 |
| 56 | 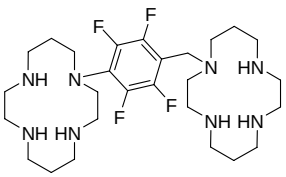 | azamacrociclo | 0.159 |

| # | Estructura | Familia | $EC_{50}$ / μM |
|---|---|---|---|
| 57 | 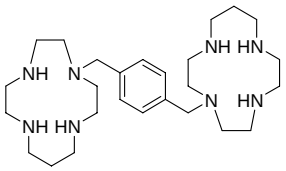 | azamacrociclo | 0.166 |
| 58 | 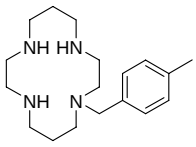 | azamacrociclo | 0.170 |
| 59 | 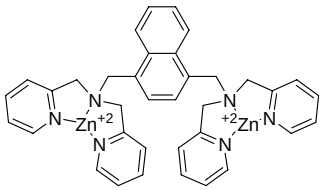 | Dpa | 0.180 |
| 60 | 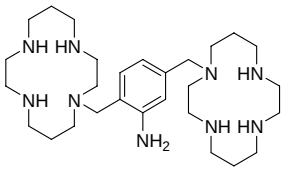 | azamacrociclo | 0.187 |
| 61 | 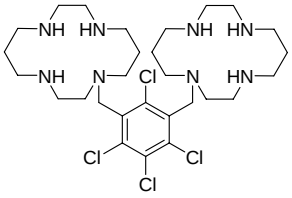 | azamacrociclo | 0.200 |
| 62 | 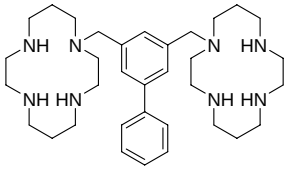 | azamacrociclo | 0.204 |
| 63 | 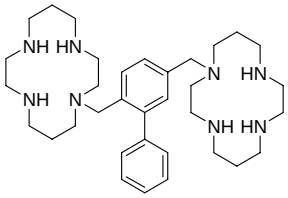 | azamacrociclo | 0.230 |
| 64 | 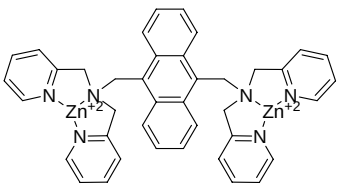 | Dpa | 0.240 |

| # | Estructura | Familia | $EC_{50}$ / μM |
|---|---|---|---|
| 65 | 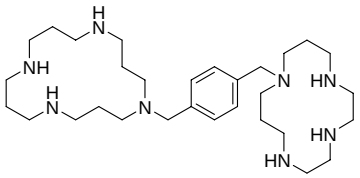 | azamacrociclo | 0.312 |
| 66 | 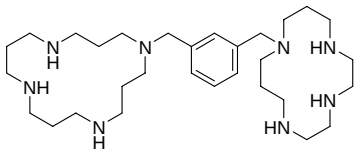 | azamacrociclo | 0.324 |
| 67 | 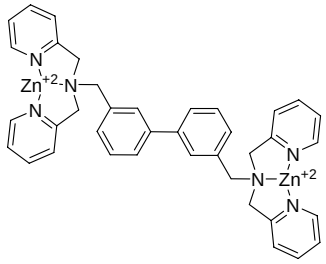 | Dpa | 0.350 |
| 68 | 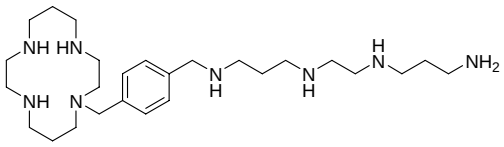 | azamacrociclo | 0.372 |
| 69 | 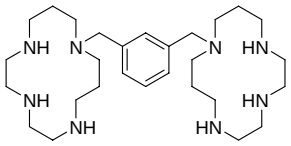 | azamacrociclo | 0.395 |
| 70 | 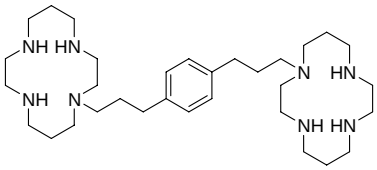 | azamacrociclo | 0.398 |
| 71 | 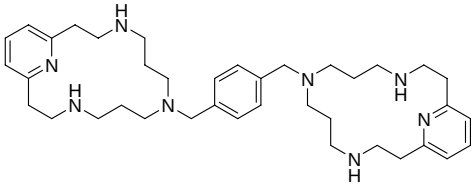 | azamacrociclo | 0.421 |
| 72 | 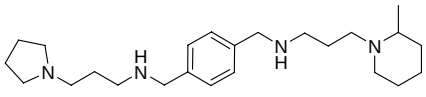 | poliamina<br>**32**{*5,8*} | 0.440 |

| # | Estructura | Familia | $EC_{50}$ / μM |
|---|---|---|---|
| 73 | 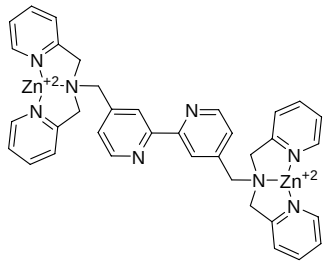 | Dpa | 0.460 |
| 74 | 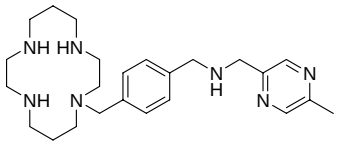 | azamacrociclo | 0.468 |
| 75 | 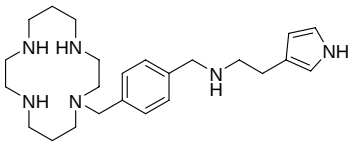 | azamacrociclo | 0.481 |
| 76 | 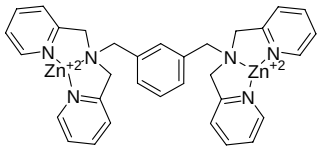 | Dpa | 0.490 |
| 77 | 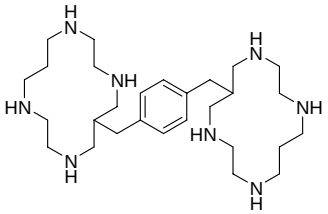 | azamacrociclo | 0.501 |
| 78 | 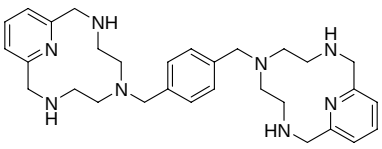 | azamacrociclo | 0.524 |
| 79 | 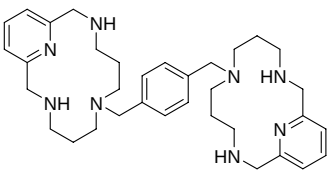 | azamacrociclo | 0.534 |

| # | Estructura | Familia | $EC_{50}$ / μM |
|---|---|---|---|
| 80 | 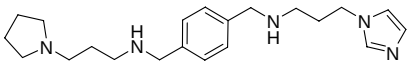 | poliamina<br>**32**{*5,6*} | 0.563 |
| 81 | 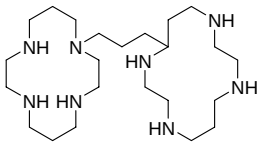 | azamacrociclo | 0.650 |
| 82 | 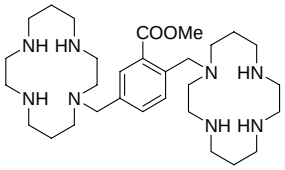 | azamacrociclo | 0.683 |
| 83 | 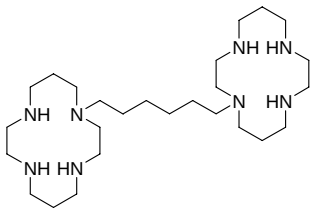 | azamacrociclo | 0.692 |
| 84 | 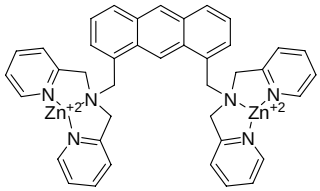 | Dpa | 0.750 |
| 85 | 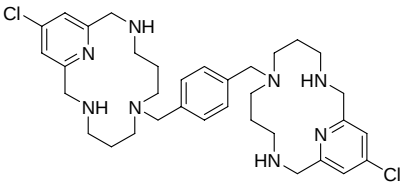 | azamacrociclo | 0.751 |
| 86 | 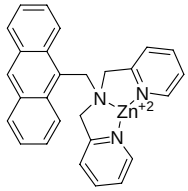 | Dpa | 0.770 |
| 87 | 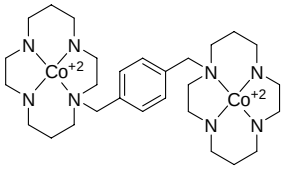 | azamacrociclo | 0.810 |

| # | Estructura | Familia | $EC_{50}$ / μM |
|---|---|---|---|
| 88 | 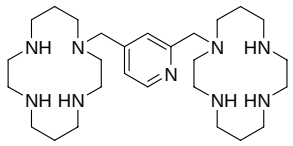 | azamacrociclo | 0.850 |
| 89 | 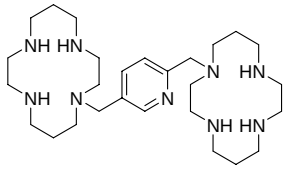 | azamacrociclo | 0.908 |
| 90 | 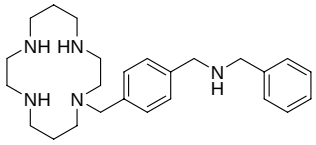 | azamacrociclo | 0.972 |
| 91 | 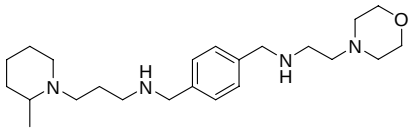 | poliamina **32**{*8,10*} | 1.02 |
| 92 | 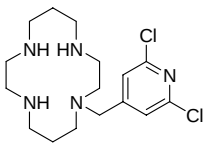 | azamacrociclo | 1.20 |
| 93 | 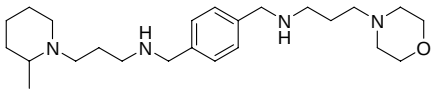 | poliamina **32**{*8,11*} | 1.23 |
| 94 | 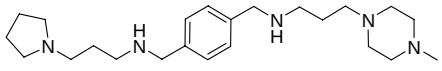 | poliamina **32**{*5,9*} | 1.28 |
| 95 | 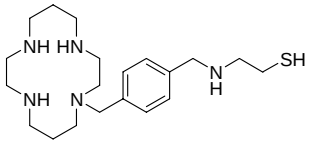 | azamacrociclo | 1.31 |

| # | Estructura | Familia | $EC_{50}$ / μM |
|---|---|---|---|
| 96 | 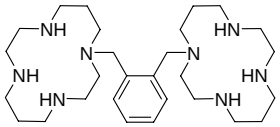 | azamacrociclo | 1.35 |
| 97 | 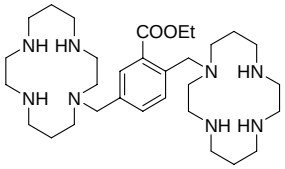 | azamacrociclo | 1.43 |
| 98 | 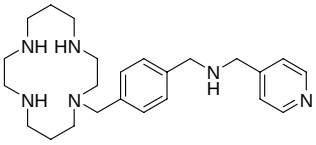 | azamacrociclo | 1.45 |
| 99 | 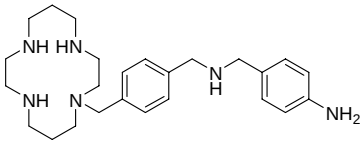 | azamacrociclo | 1.64 |
| 100 | 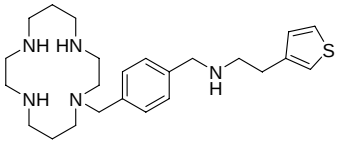 | azamacrociclo | 1.68 |
| 101 | 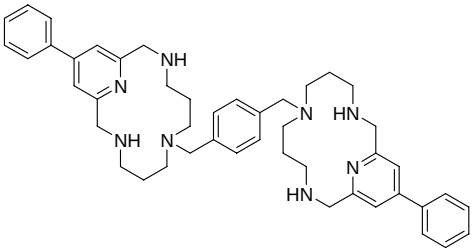 | azamacrociclo | 1.75 |
| 102 | 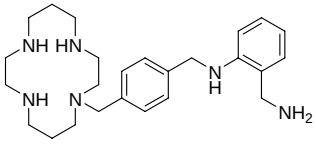 | azamacrociclo | 1.88 |
| 103 | 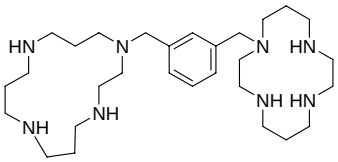 | azamacrociclo | 2.40 |

| # | Estructura | Familia | $EC_{50}$ / μM |
|---|---|---|---|
| 104 | 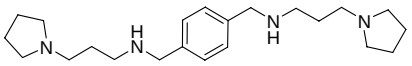 | poliamina **32**{*5,5*} | 2.48 |
| 105 | 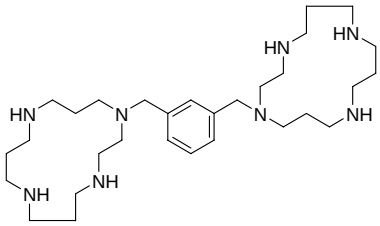 | azamacrociclo | 2.75 |
| 106 | 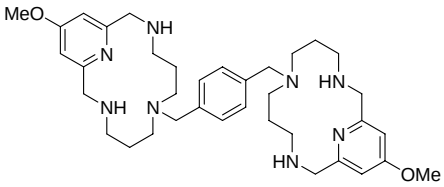 | azamacrociclo | 3.10 |
| 107 | 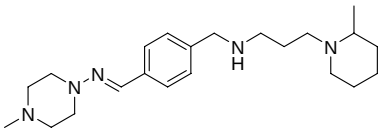 | poliamina **37**{*3,8*} | 3.74 |
| 108 | 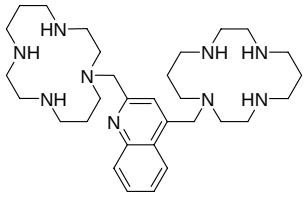 | azamacrociclo | 3.77 |
| 109 | 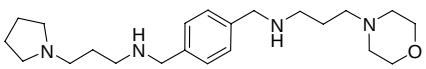 | poliamina **32**{*5,11*} | 4.23 |
| 110 | 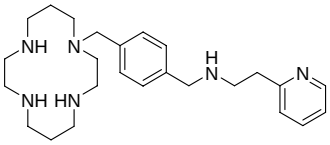 | azamacrociclo | 4.24 |
| 111 | 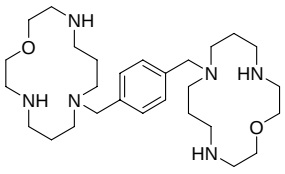 | azamacrociclo | 4.49 |

| # | Estructura | Familia | $EC_{50}$ / μM |
|---|---|---|---|
| 112 | 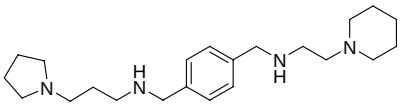 | poliamina **32**{*5,7*} | 4.67 |
| 113 | 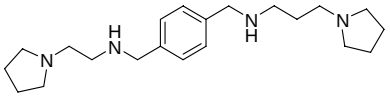 | poliamina **32**{*4,5*} | 4.98 |
| 114 | 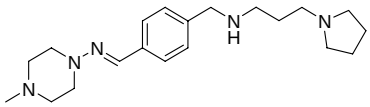 | poliamina **32**{*3,5*} | 5.19 |
| 115 | 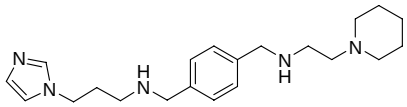 | poliamina **32**{*6,7*} | 5.54 |
| 116 | 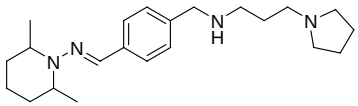 | poliamina **37**{*2,5*} | 5.58 |
| 117 | 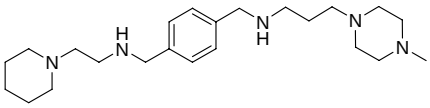 | poliamina **32**{*7,9*} | 6.40 |
| 118 | 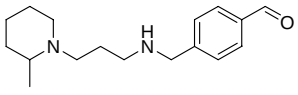 | poliamina **35**{*8*} | 6.51 |
| 119 | 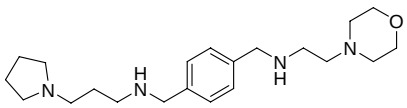 | poliamina **32**{*5,10*} | 6.60 |

| # | Estructura | Familia | $EC_{50}$ / μM |
|---|---|---|---|
| 120 | 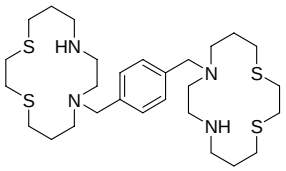 | azamacrociclo | 6.84 |
| 121 | 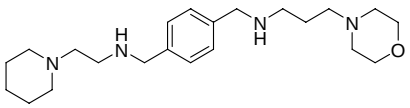 | poliamina **32**{*7,11*} | 7.15 |
| 122 | 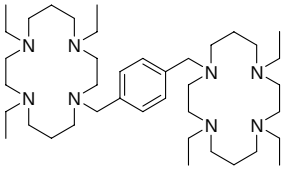 | azamacrociclo | 7.76 |
| 123 | 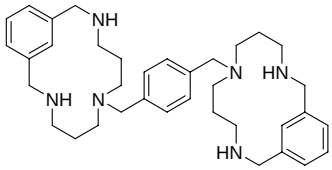 | azamacrociclo | 7.96 |
| 124 | 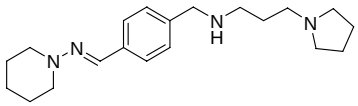 | poliamina **37**{*1,5*} | 8.29 |
| 125 | 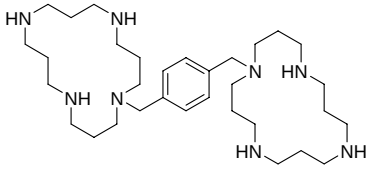 | azamacrociclo | 9.12 |
| 126 | 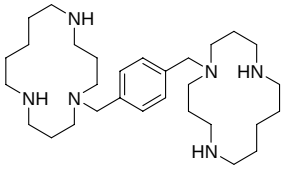 | azamacrociclo | 9.61 |
| 127 | 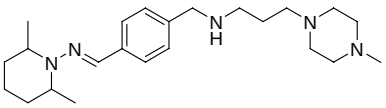 | poliamina **37**{*2,9*} | 9.83 |

| # | Estructura | Familia | $EC_{50}$ / μM |
|---|---|---|---|
| 128 | 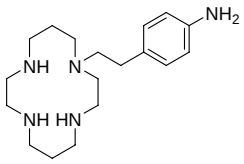 | azamacrociclo | 9.95 |
| 129 | 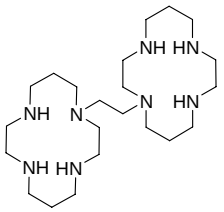 | azamacrociclo | 11.2 |
| 130 | 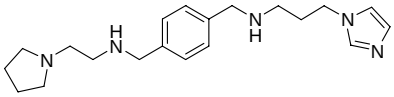 | poliamina **32**{*4,6*} | 14.0 |
| 131 | 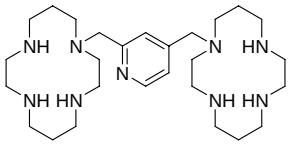 | azamacrociclo | 16.4 |
| 133 | 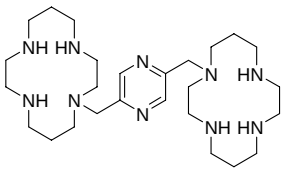 | azamacrociclo | 20.9 |
| 133 | 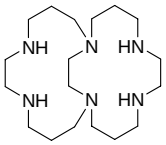 | azamacrociclo | 21.1 |
| 134 | 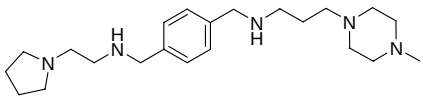 | poliamina **32**{*4,9*} | 21.8 |
| 135 | 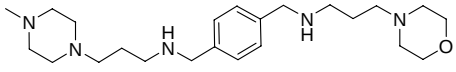 | poliamina **32**{*9,11*} | 22.3 |

| # | Estructura | Familia | $EC_{50}$ / μM |
|---|---|---|---|
| 136 | 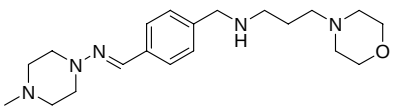 | poliamina **37**{*3,11*} | 22.4 |
| 137 | 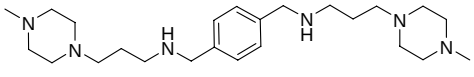 | poliamina **32**{*9,9*} | 22.6 |
| 138 | 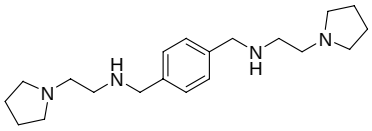 | poliamina **32**{*4,4*} | 30.6 |
| 139 | 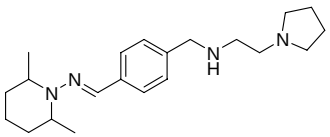 | poliamina **37**{*2,4*} | 30.6 |
| 140 | 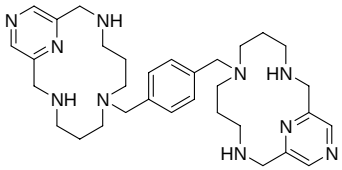 | azamacrociclo | 30.9 |
| 141 | 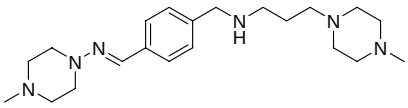 | poliamina **37**{*3,9*} | 31.2 |
| 142 | 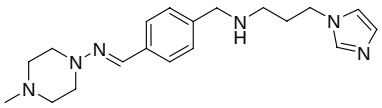 | poliamina **37**{*3,6*} | 32.7 |
| 143 | 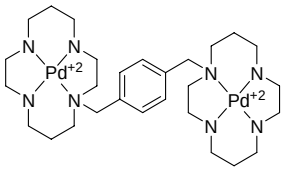 | azamacrociclo | 36.2 |

| # | Estructura | Familia | $EC_{50}$ / μM |
|---|---|---|---|
| 144 | 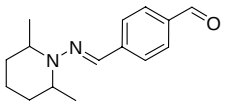 | poliamina **36**{*2*} | 37.0 |
| 145 | 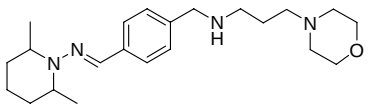 | poliamina **37**{*2,11*} | 41.9 |
| 146 | 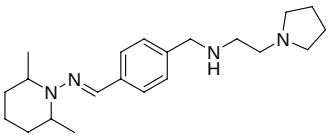 | poliamina **37**{*2,4*} | 42.7 |
| 147 | 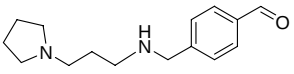 | poliamina **35**{*5*} | 45.5 |
| 148 | 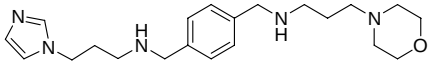 | poliamina **32**{*6,11*} | 49.1 |
| 149 | 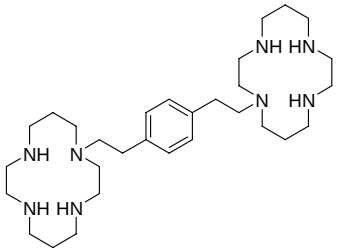 | azamacrociclo | 56.8 |
| 150 | 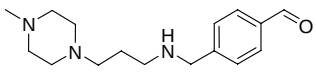 | poliamina **35**{*9*} | 58.0 |
| 151 | 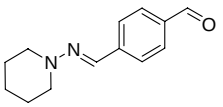 | poliamina **36**{*1*} | 58.3 |

## A.7. Base de datos de inactivos reales utilizada en los farmacóforos.

***Tabla A.7.*** *Base de datos de compuestos inactivos como inhibidores del VIH-1 a concentraciones inferiores a 25 μg/mL.*

| # | Estructura | Nombre |
|---|---|---|
| 1 | 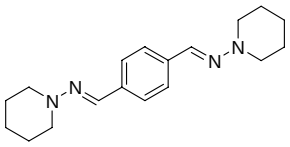 | **33**{*1,1*} |
| 2 | 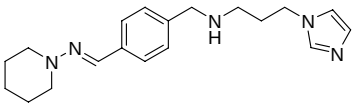 | **37**{*1,6*} |
| 3 | 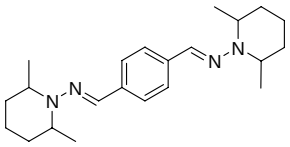 | **33**{*2,2*} |
| 4 | 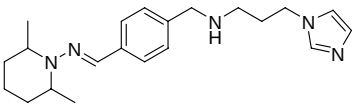 | **37**{*2,6*} |
| 5 | 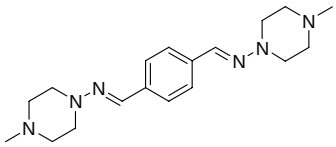 | **33**{*3,3*} |
| 6 | 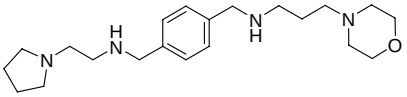 | **32**{*4,11*} |

| # | Estructura | Nombre |
|---|---|---|
| 7 | 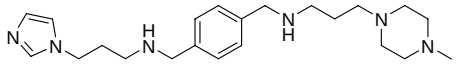 | **32**{*6,9*} |
| 8 | 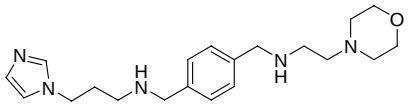 | **32**{*6,10*} |
| 9 | 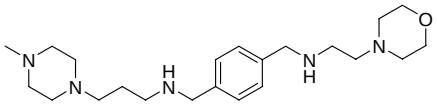 | **32**{*9,10*} |
| 10 | 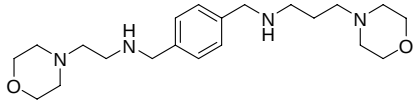 | **32**{*10,11*} |
| 11 | 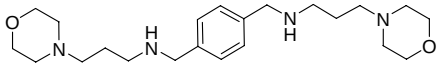 | **32**{*11,11*} |
| 12 | 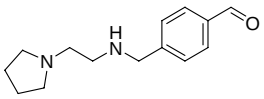 | **35**{*4*} |
| 13 | 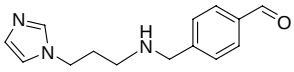 | **35**{*6*} |

| # | Estructura | Nombre |
|---|---|---|
| 14 | 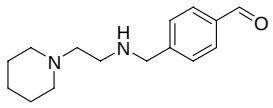 | **35**{*7*} |
| 15 | 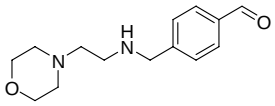 | **35**{*10*} |
| 16 | 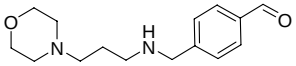 | **35**{*11*} |

## A.8. Publicaciones.

Los resultados de la presente tesis han dado lugar a las siguientes publicaciones:

- S. Pettersson, I. Clotet-Codina, J. A. Esté, J. I. Borrell; Recent advances in combinatorial chemistry applied to development of anti-HIV drugs. *Mini Rev. Med. Chem.* **2006**, *6*, 91-108.
- S. Pettersson, V. I. Pérez-Nueno, L. Ros-Blanco, R. Puig de la Bellacasa, M. O. Rabal, X. Batllori, B. Clotet, I. Clotet-Codina, M. Armand-Ugón, J. Esté, J. I. Borrell, J. Teixidó; Discovery of novel non-cyclam polynitrogenated CXCR4 coreceptor inhibitors. *ChemMedChem* **2008**, *3*, 1549-1557.
- V.I. Pérez-Nueno, S. Pettersson, D. W. Ritchie, J. I. Borrell, J. Teixidó; Discovery of novel HIV entry inhibitors for the CXCR4 receptor by prospective virtual screening. *J. Chem. Inf. Model.* **2009**, *49*, 810-823.

A partir de los resultados obtenidos también se ha publicado la siguiente patente:

- J. Teixidó, J. I. Borrell, S. Nonell, X. Batllori, S. Pettersson, L. Ros-Blanco, R. Puig de la Bellacasa, M. O. Rabal, V. I. Pérez-Nueno, J. Esté, I. Clotet-Codina, M. Armand-Ugón; Nuevos sistemas polinitrogenados como agentes anti-VIH. Patente española ES2298077B1 (fecha de presentación 26-10-2006). También publicada como WO 2008/049950 A1 (PCT/ES2007/000613).

Además se ha presentado el trabajo realizado en los siguientes congresos:

- S. Pettersson, J. I. Borrell, X. Batllori, L. Ros, R. Puig de la Bellacasa, M. O. Rabal, V. Pérez, J. Esté, I. Clotet-Codina, M. Armand-Ugón, J. Teixidó; Discovery of highly active novel HIV entry inhibitors. 6th AFMC International Medicinal Chemistry Symposium (AIMECS07), **2007**, Estambul (Turquía). *Póster.*
- V. I. Pérez-Nueno, S. Pettersson, O. Rabal, L. Ros-Blanco, R. Puig de la Bellacasa, J. Esté, I. Clotet-Codina, M. Armand-Ugón, X. Batllori, J. I. Borrell, J. Teixidó; Virtual Screening tools applied to HIV entry inhibitors. Virtual Discovery Europe. Computer-Aided Drug Design and Screening, **2007**, Londres (Reino Unido). *Póster.*
- S. Pettersson, J. I. Borrell, J. Teixidó; Nous inhibidors del coreceptor CXCR4 d'entrada del VIH. Cinquena Trobada de Joves Investigadors dels Països Catalans, **2008**, Vic (España). *Comunicación oral.*
- S. Pettersson, V. Pérez-Nueno, L. Ros-Blanco, B. Clotet, I. Clotet-Codina, M. Armand-Ugón, J. Esté, J. Teixidó, J. I. Borrell; Discovery of novel non-cyclam polynitrogenated CXCR4 coreceptor inhibitors. Ehrlich II – 2$^{nd}$ World Conference on Magic Bullets, **2008**, Nürnberg (Alemania). *Comunicación oral.*

# Recent Advances in Combinatorial Chemistry Applied to Development of Anti-HIV Drugs

S. Pettersson[a], I. Clotet-Codina[b], J.A. Esté[b], J.I. Borrell[a] and J. Teixidó[*,a]

[a]*Grup d'Enginyeria Molecular (GEM), Institut Químic de Sarriá (IQS), Universitat Ramon Llull, Vía Augusta 390, E-08017 Barcelona, Spain*

[b]*Laboratori de Retrovirologia IrsiCaixa, Hospital Universitari Germans Trias i Pujol, Universitat Autònoma de Barcelona, Badalona 08916, Spain*

**Abstract:** A compilation of combinatorial chemistry techniques applied to anti-HIV drug development is presented in this review. This synthetic strategy together with high throughput screening assays has allowed the discovery and optimization of novel lead anti-HIV compounds.

**Keywords:** Combinatorial chemistry, synthesis, anti-HIV drugs, high throughput screening.

## INTRODUCTION

The World Health Organization (WHO) estimates that about 40 million people were living with the human immunodeficiency virus (HIV) and AIDS by the end of 2004 [1].

Studies in HIV biology have provided deep knowledge of the molecular events in the HIV life cycle, which consists of several steps: viral entry [2-8], reverse transcription [9-15], integration [11,16-22], gene expression [23,24], gene assembly [25], budding [26] and maturation [27], see Fig. (**1**). These stages serve as potential targets for designing anti-HIV drugs [28].

This sequential fragmentation of the viral cycle has been used in this review for the classification of the synthesized anti-HIV libraries of compounds in accordance with the original intended target.

Current antiretroviral therapy consists of combinations of three families of compounds: reverse transcriptase inhibitors (RTI) and protease inhibitors (PI), both directed to enzymes produced by HIV, and entry inhibitors (ENI) that target the HIV envelope glycoprotein gp41 and prevent virus-cell fusion. Reverse transcriptase inhibitors (RTI) are classified in nucleoside (NRTI) and non-nucleoside (NNRTI) types. Within the group of the NRTI, the current FDA approved drugs used for anti-HIV therapy are [29]: in 1987 Zidovudine (AZT) [30,31], in 1991 Didanosine (ddl) [32,33], in 1992 Zalcitabine (ddC) [33,34], in 1994 Stavudine (d4T) [34-36], in 1995 Lamivudine (3TC) [37], in 1997 Zidovudine/Lamivudine (combines AZT and 3TC) [38], in 1998 Abacavir [39-41], in 2000 Zidovudine/Lamivudine/Abacavir (combines AZT, 3TC and Abacavir), in 2001 Tenofovir (bis-poc PMPA) [42,43], in 2003 Emtricitabine (FTC), in 2004 Abacavir/Lamivudine (combines Abacavir and 3TC) and also in 2004 Emtricitabine/Tenofovir (combines FTC and bis-poc PMPA). Within the NNRTI, the second group of reverse transcriptase inhibitors (RTI), those actually approved by the FDA are [29]: in 1996 Nevirapine (NVP) [44-46], in 1997 Delavirdine (DLV) [47,48] and in 1998 Efavirenz (EFV) [49].

In the other family of compounds used for antiretroviral therapy, the PI, the drugs approved by the FDA are [29]: in 1995 Saquinavir (SQV) [50-52], in 1996 Ritonavir (RTV) [53-55] and Indinavir (IDV) [56], in 1997 Nelfinavir (NFV) [57,58], in 1999 Amprenavir (APV) [59-61], in 2000 Lopinavir (ABT-378/r) [62], in 2003 Atazanavir (BMS-232632) and Fosamprenavir (GW433908).

No integrase inhibitors have been approved yet but there are already compounds in early human clinical trials [63].

The only approved fusion inhibitor is Enfuvirtide (Fuseon, T-20) [64], in 2003, but there are several compounds in different clinical trial stages, such as AMD070, UK,427,857 and TAK-220 [8,29].

Nevertheless, new strategies against HIV infection have been, and are still, determ inant in controlling the emergence of HIV resistance, improving the efficacy of antiretroviral treatment and expanding the arsenal necessary to combat HIV.

Combinatorial chemistry allows the obtention of a large population of molecules in a short period of time. Therefore, it has been a useful tool for the discovery and optimization of new lead compounds in medicinal chemistry research.

Obviously, the search for new potential anti-HIV drugs has taken advantage of the benefits of such combinatorial strategy [65]. Subsequently, the synthesized libraries must be examined for specific target activity in high throughput screening (HTS). These systems are designed to identify molecules with specific properties and allow the screening of thousands of compounds per day [66-68].

A compilation of the combinatorial techniques applied to the development of anti-HIV agents is presented in this review. Some references might be missed because, especially in patents, it is difficult to discern if the libraries of the synthesized compounds were really combinatorial due to the intrinsic combinatorial nature of the general formula depicted in Markush structures. In these cases the initial virtual

*Address correspondence to this author at the Grup d'Enginyeria Molecular (GEM), Institut Químic de Sarriá (IQS), Universitat Ramon Llull, Vía Augusta 390, E-08017 Barcelona, Spain; E-mail: j.teixido@iqs.url.edu

**1389-5575/06 $50.00+.00** 

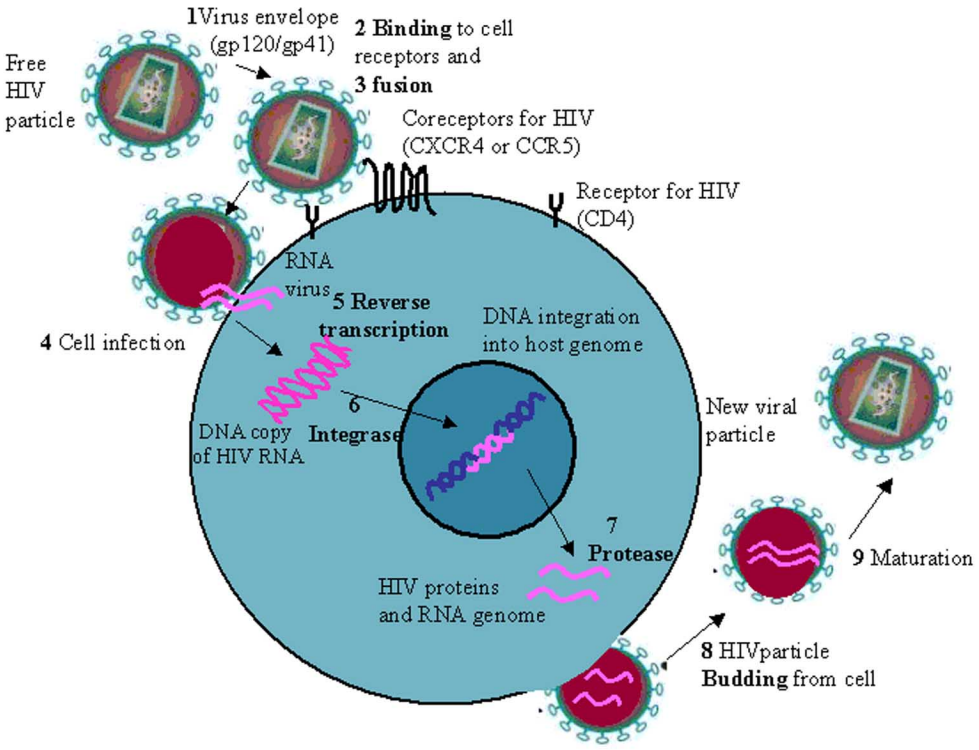


**Fig. (1).** The different steps of the HIV-1 life cycle. The text in bold refers to targets inhibited by existing agents approved by the FDA or that are likely to be inhibited in the future by new anti-HIV drugs.

library of compounds could be originally combinatorial, but a subsequent reduction of its size (i.e. using computational tools in virtual screening techniques followed by a cherry picking or sparse array selection) leads to a reduced library to be synthesized with loss of the combinatorial perception in the published work [69].

## VIRAL ENTRY

Nucleoside phosphorothioates are isoelectronic analogs of natural nucleotides in which a non bridging oxygen atom of the phosphate group is replaced by a sulfur atom [70]. This kind of compounds have shown to block the cytopathic effect of HIV-1 in uninfected ATH8 cells. These findings suggested that nucleoside phosphorothioates and their oligonucleotide analogues may represent class of experimental chemotherapeutic agents against AIDS [71].

With this background, a library of phosphorothioate oligonucleotides that contained all possible sequences of eight nucleotides divided into 16 sets, each consisting of 4,096 sequences (4 nucleotides: A, G, C, T; 8 positions; $4^8$ = 65,536 compounds), was synthesized in 1990 in solid-phase using 3*H*-1,2-benzodithiol-3-one 1,1-dioxide as sulfur-transfer reagent. The combinatorial screening of this library identified the phosphorothioate oligonucleotide $T_2G_4T_2$ as inhibitor of HIV envelope-mediated cell fusion [72]. Nevertheless, research on this oligonucleotide family has been discontinued in early clinical phases.

Another approach was finding small molecule inhibitors that bind to the coiled-coil core of gp41 subunit of HIV

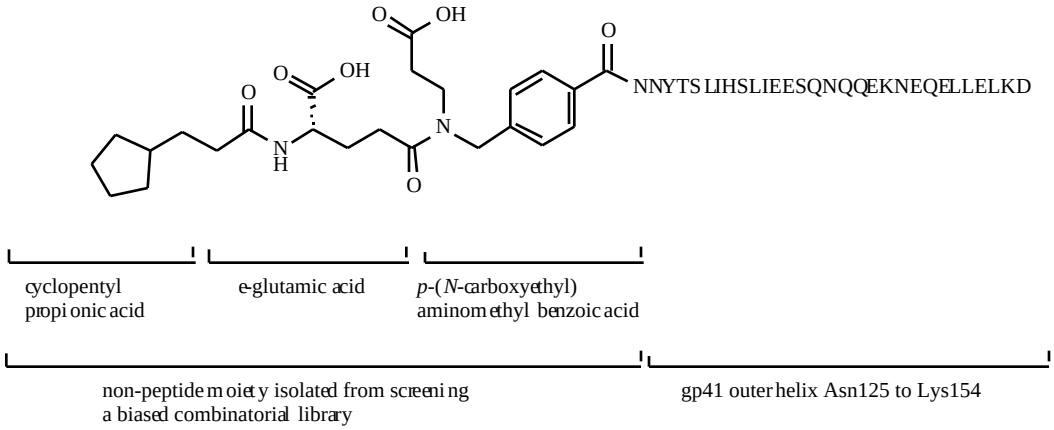


**Fig. (2).** Chemical structure of the nonpeptide moiety derived from the combinatorial library attached to the HIV-1 peptide, Asn-125 to Lys-154. The individual components from the combinatorial library are labeled in brackets.

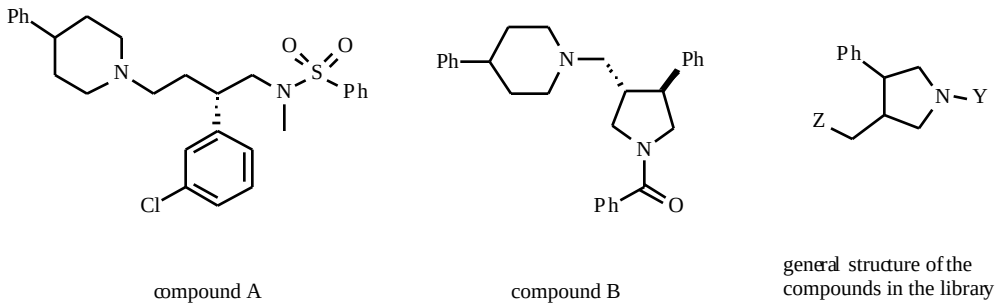


**Fig. (3).** Structure of compounds A and B and general structure of the compounds in the library generated from the SAR study around both the acyclic (A) and cyclic (B) scaffolds.

envelope and block membrane fusion, which has led to the discovery of a synthetic moiety that binds the coiled-coil when attached to the N-terminus of a 30-mer outer-layer peptide. This molecule, Fig. (**2**), was targeted by synthesizing a combinatorial library of three building blocks linked to the N-terminus of an outer-layer peptide lacking the first two α-helical turns, resulting in 61,275 of the 62,500 potential ligands from all possible combinations of 50 building blocks at the first two positions and 25 different building blocks at the third [73] (building blocks in Fig. (**4**) of the reference [74]).

A different strategy was inhibiting the binding of the virus to the CCR5 chemokine receptor. A combinatorial library was designed from a classical medicinal chemistry SAR study around compounds A and B (Fig. **3**).

The selected scaffold, see Fig. (**4**), was treated with 1,3-diisopropylcarbodimide (DIC) to form the symmetrical anhydride and then coupled to polystyrene bound arylsulfonamide in presence of DMAP. A portion of each resin was archived and the remaining resin was mixed and split into 39 equal pools. The Boc group was removed by treatment with TFA and then an acylating agent (39 different Y subunits from a variety of acid chlorides, sulfonyl chlorides and isocyanates based on the previously performed SAR study) [75-80] was added. A portion of resin from each pool was archived and the remaining resin was mixed and split into 100 equal portions. Each portion was alkylated with trimethylsilyl diazomethane followed by displacement with 2 equivalents of the amine Z subunits (selection also based on the previously performed SAR study [75-80]).

Such procedure afforded 100 pools with 117 compounds/pool. The excess amine was removed by scavenging with polystyryl isothiocyanate resin. Then, the pools were treated with borane-methyl sulfide complex to reduce the amide bonds. The desired products were obtained by treating the pools with HCl/MeOH. LC/MS analysis was performed to evaluate the composition of each pool.

The 100 mixtures were assayed for CCR5 binding affinity leading to the discovery of compound in Fig. (**5**), a potent receptor binding and with moderate anti-viral activity [81].

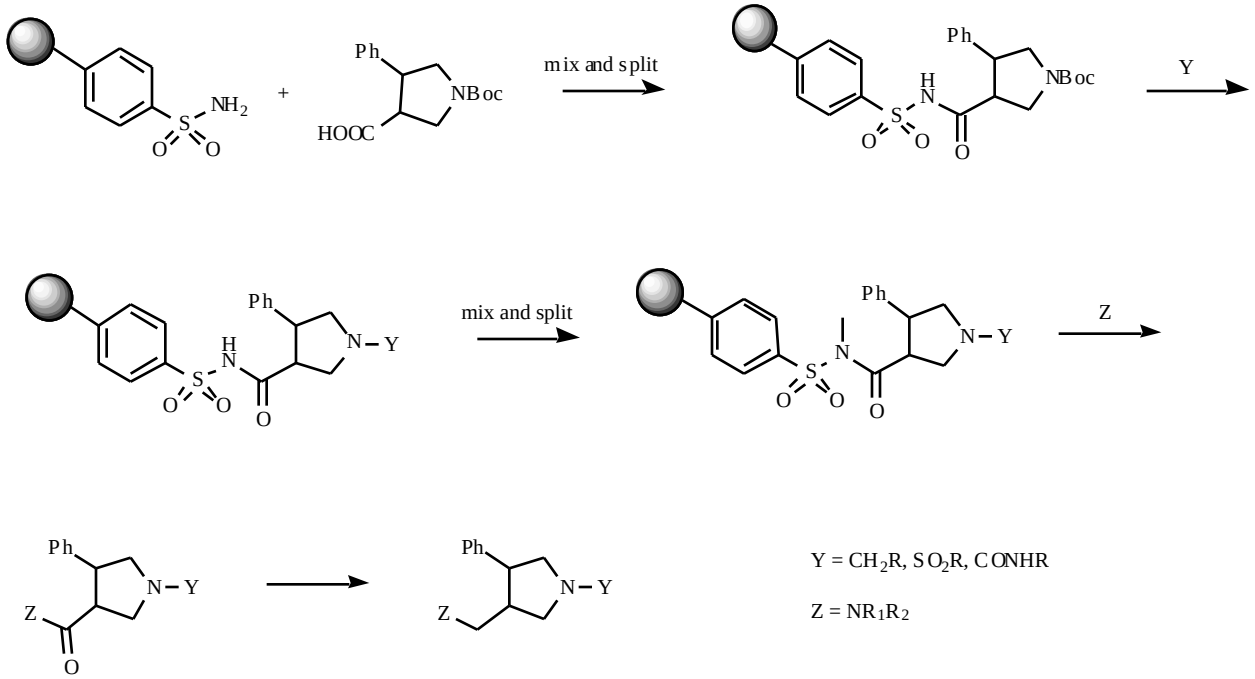


**Fig. (4).** Solid-phase synthetic route for the CCR5 antagonist library designed by Willoughby *et al.* [81] with 39 different Y subunits and 100 different Z subunits.

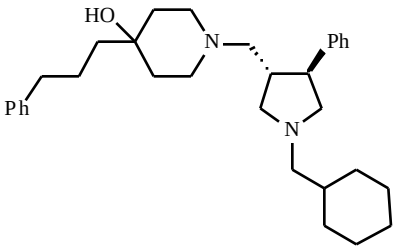


**Fig. (5).** Structure of the most potent compound in the synthesized library of CCR5 antagonists.

This compound was used for further investigations by Hale *et al*., who discovered that the incorporation of appropriate acid functional groups increased the effect on the anti HIV-1 properties of these molecules [82].

The CCR5 chemokine receptor was also used as target for a thiazolidinone library (Fig. **6**) prepared in solution phase synthesis. The first step of the synthesis was the preparation of the 4-thiazolidinone reagent pool from the corresponding arylaldehyde and 3-chloropropylamine generating an intermediate imine, which was reacted with a cyclizing agent such as mercaptoacetic acid to afford the substituted 4-thiazolidinone. These compounds were treated with NaI to afford the desired 4-thiazolidinone reagent pool, which was used for the combinatorial synthesis in array format. Each 4-thiazolidinone was treated with ten amines in separate wells and after reaction the content of each well was split into 4 new plates and treated with 4 different aldehydes [83].

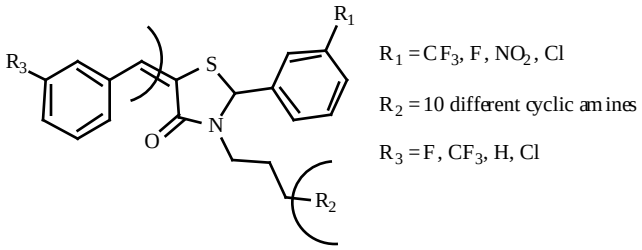


**Fig. (6).** General structure for the compounds in the library of 4-thiazolidinone. The curved lines show the different building blocks used for these structures.

Peptide libraries have been designed as possible gp120/cell membrane receptor interaction inhibitors on the basis of the crystal structure of a gp120/CD4/Fab17b complex. The synthesized libraries were H-Phe-X-X-Arg-$NH_2$ (X = Gly, Ser, Val, Phe, Lys), H-Glu-$X_1$-Glu-$X_2$-Asp-$NH_2$ (where $X_1$ = Gly, Phe, Ala, Ser, Asp, Asn and $X_2$ = Tyr, Asp, Leu, Gly, Lys, Ser; library of 36 peptides) and H-Phe-X-Arg-$NH_2$ (X = Arg, Asp, Gln, Gly, Lys, Phe, Pro, Ser, Trp, Val, None). They were prepared via both large batch and parallel split synthesis techniques.

Fmoc deprotection of the pre-swollen Rink amide resin was followed by coupling of the next amino acid using TBTU/HOBT methodology. The sequences were constructed using successive Fmoc deprotection/amino acid coupling steps. Deprotection of the final Fmoc group followed by TFA mediated cleavage from the resin and removal of acid labile side chain protecting groups afforded the desired peptides as C-terminal protected amides (Fig. **7**). The first peptide library showed a relatively good binding inhibition but no anti-viral activity. The second library was more active than the tetrapeptide library, but no clear correlation between activity and nature of the X substituent was found, and cellular assays against HIV-infected cells gave no significant activity. The third library was also not active [84].

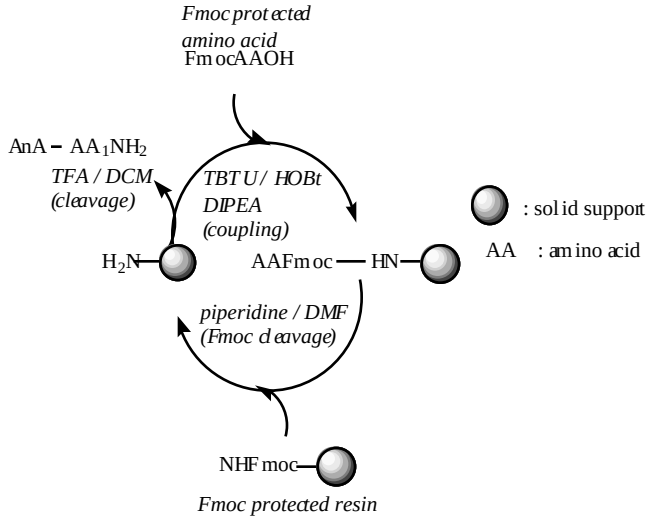


**Fig. (7).** General peptide synthesis scheme for the libraries H-Phe-X-X-Arg-$NH_2$, H-Glu-$X_1$-Glu-$X_2$-Asp-$NH_2$ and H-Phe-X-Arg-$NH_2$ reported by Boussard *et al*. [84].

## REVERSE TRANSCRIPTION

As stated in the introduction, there are two different classes of reverse transcriptase (RT) inhibitors: the nucleoside (NRTIs) and the non nucleoside (NNRTIs) inhibitors.

1-aryl-1*H*,3*H*-thiazolo[3,4-*a*]benzimidazoles (TBZs) have shown high activity as HIV-1 NNRTIs [85-87]. Structure-activity studies on these compounds suggested that the substitution on the C-1 atom of the thiazolo[3,4-*a*]benzimidazole moiety played a crucial role in the interaction of TBZs with the HIV-1 RT, especially when a 2,6-dihalo-substituted phenyl ring was present.

Therefore 2,3-diaryl-1,3-thiazolidin-4-one derivatives have been synthesized as new NNRTIs by treatment of a 2,6-

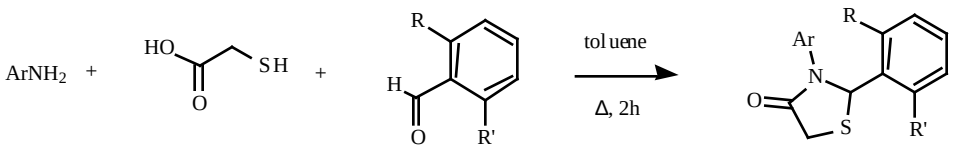


**Fig. (8).** General synthesis scheme for 2,3-diaryl-1,3-thiazolidin-4-one derivatives reported by Barreca *et al*. [88]. Where Ar = phenyl, pyridin-(2,3 or 4)-yl, 3-Me-pyridin-2-yl, 4-Me-pyridin-2-yl, 5-(Cl, Br or Me)-pyridin-2-yl, 6-(Br or Me)-pyridin-2-yl or 4,6-di-Me-pyridin-2-yl; and R,R' = Cl,Cl, F,F or Cl,F.

dihalo-substituted benzaldehyde with an equimolar amount of an (hetero)aromatic amine in the presence of an excess of mercaptoacetic acid in refluxing toluene (Fig. **8**).

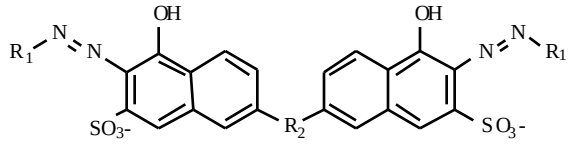

**Fig. (9).** General structures for the aryl diazo derivatives.

These compounds were up to 10-fold more potent inhibitors of replication of HIV-1 ($III_B$) or HIV-2 (ROD) in MT-4 cells than the TBZ lead compound [88].

Skillman *et al.* have used a structure-based design scheme to identify HIV-1 RT inhibitors and subsequently designed combinatorial analog libraries. A general procedure has been used for diazotization reaction and coupling to the corresponding acid.

Different aryl diazo derivatives (Fig. **9**) were synthesized with this methodology and the central urea was also replaced with a variety of linkers including thiourea, oxalyl, squarate, chelidonate, chelidamate, 2,6-pyridine dicarboxylate and terephthalate groups.

therapy (HAART) for treating neurological aspects of HIV infection [91].

A library of analogs of the natural product mappicine (Fig. **11**) has been synthesized and their activity has been tested in an HIV RNase H (ribonuclease H) assay, one of the activities of the retroviral enzyme RT.

The synthesis was performed using parallel techniques that allowed the combinatorialization of three building blocks [92].

One of the building blocks in the library, the pyridone D-ring was synthesized from a formyl pyridine where the aldehyde was reduced to a methyl group, the resulting compound was treated with *i*PrMgCl, then a TMS-iodine exchange was performed and after demethylation the iodopyridone building block was obtained.

This first building block, with associated fluorous tag, was alkylated with a propargylating agent (the second building block) and then a cascade radical annulation with the third building block, an isonitrile bearing the A-ring substituent, provided the desired mappicine analog.

This methodology was used for the synthesis of a 560-member library [93], see Fig. (**12**).

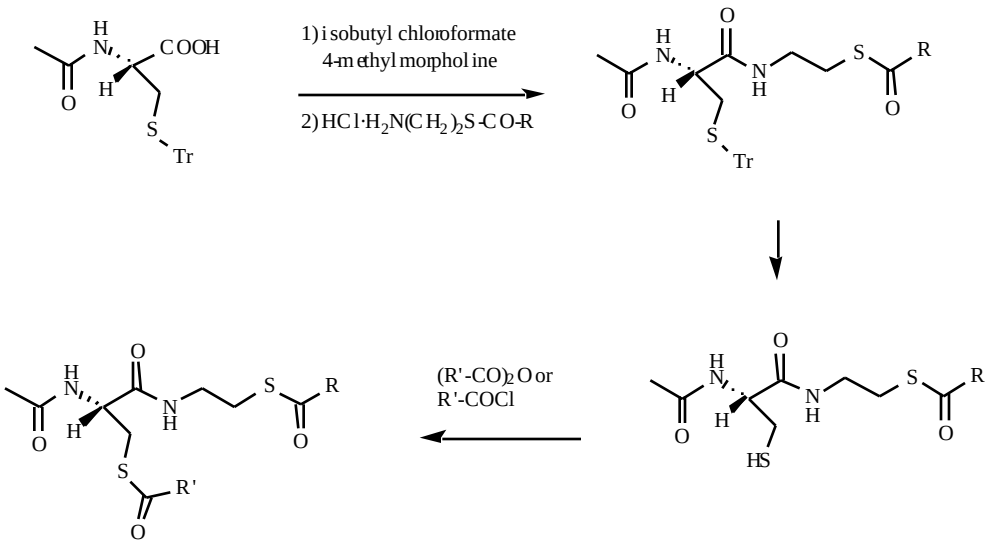


**Fig. (10).** Synthesis scheme for *N*-(*N*-acetyl-L-cysteinyl)-*S*-acetylcystemine analogs reported by Oiry *et al.* [91], where R and R' = $CH_3$, $CH(CH_3)_2$, $C(CH_3)_3$.

The most active compounds against HIV-1 RT were the urea-linked with acidic aryl diazo side-chains [89,90].

Recently a series of *N*-(*N*-acetyl-L-cysteinyl)-*S*-acetylcystemine analogs have been synthesized from commercially available *N*-acetyl-*S*-trityl-L-cysteine. The library was designed with a combinatorial approach although the synthesis was not performed with this methodology Fig. (**10**).

Compounds were tested by quantifying reverse transcriptase activity and pro-glutathione (GSH) antioxidant properties. Results showed that none of these compounds had higher values than the *N*-(*N*-acetyl-L-cysteinyl)-*S*-acetylcystemine, but they could be used as adjuvant therapies in conjunction with highly active antiretroviral

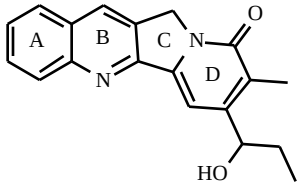

**Fig. (11).** Structure of mappicine.

## INTEGRATION

A synthetic peptide combinatorial library approach has been used for the synthesis of hexapeptides with an N-terminal free amine group and a C-terminal amide group

consisting of natural L-amino acids. This library was screened for HIV integrase inhibition in an iterative way. In the first selection step, the two N-terminal positions of the hexapeptides were defined; therefore 400 peptide mixtures were screened. Once an active peptide mixture was identified, in the second step the third position in the peptide mixtures was defined. This process continued until all positions were defined. The sequence of the most inhibiting hexapeptide was determined, His-Cys-Lys-Phe-Trp-Trp, which inhibits IN-mediated 3'-processing and integration with an $IC_{50}$ of 2 μM [94].

Structure-based computer modeling and combinatorial chemistry have been used to identify new inhibitors of HIV-1 IN, the Carbonyl J derivatives [89]; these compounds were also studied as HIV-1 RT inhibitors [90] where their structures and synthesis is detailed.

## NUCLEOCAPSID PROTEIN

Another possible target for the development of new antiviral agents is the p7 nucleocapsid protein (NCp7) of HIV-1, which is required for the functioning of the integrase enzyme as for the reverse transcriptase and protease enzymes. A series of *S*-acyl-2-mercaptobenzamide thioester derivatives were designed using a combinatorial chemistry approach. An amino acid amide was coupled with *N*,*N*'-disuccinimidyl-2,2'-dithiosalicylate, prepared from 2,2'-dithiosalicylic acid, *N*-hydroxysuccinimide and DIC. The disulfide benzamides were reduced to thiols using tris-(2-carboxyethyl)phosphine hydrochloride (TCEP·HCl) and the resulting compounds were acylated with an acid chloride to yield the desired thioesters, see Fig. (**13**).

A repertoire of 40 acyl ($R_aC$=O) groups, 6 $R_S$ substitutions on the mercaptobenzoyl substructure and 19 $NHR_L$ groups were used to render compounds with a broad anti-HIV activity. Generally good anti-HIV activity was compatible with nearly all of the acyl groups and most of the halogen substitutions on the benzoyl ring and best results were obtained with ligands that were simple amino acid primary amides as those of glycine, β-alanine, and D- or L-alanine [95].

## REV AND TAT-TAR RNA INTERACTION

A strategy for designing anti-HIV drugs is the inhibition of RNA Rev responsive element (RRE). In this context, Park *et al*. have used a one-pot Ugi-type multiple component condensation for constructing a library of

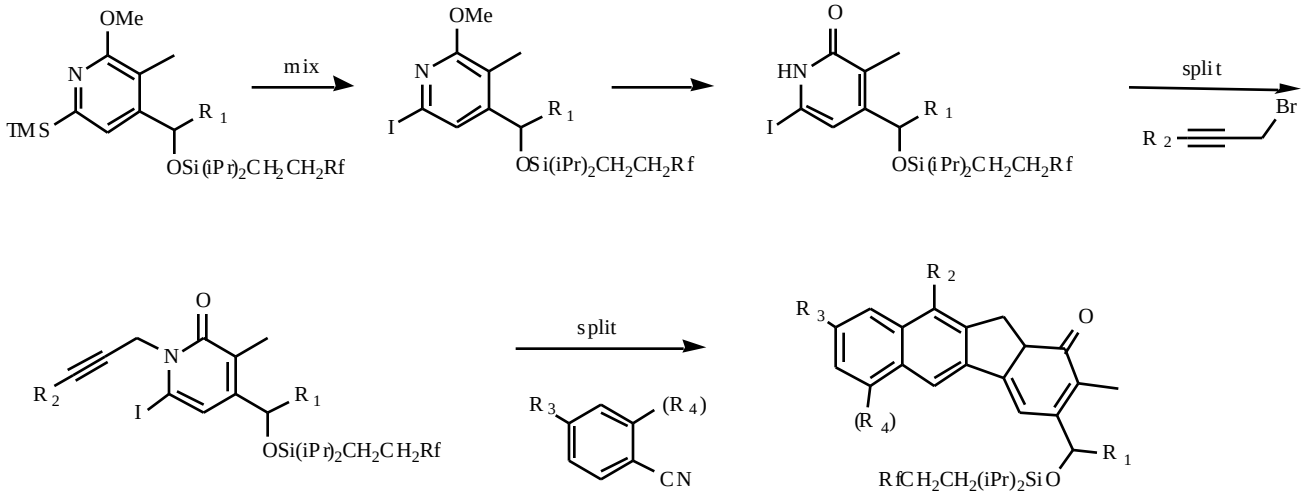


| Rf | | $R_1$ | | $R_2$ | | $R_3$ (a) | | |
|---|---|---|---|---|---|---|---|---|
| 1. $C_3F_7$ | 5. $C_8F_{17}$ | 1. Me | 5. i-Pr | 1. H | 5. Pr | 1. H | 5. p-Et | 9. p-Me |
| 2. $C_4F_9$ | 6. $C_9F_{19}$ | 2. Pr | 6. c-$C_6H_{11}$ | 2. m-MeOPh | 6. Bu | 2. p-F | 6. p-Cl | 10. p-SMe |
| 3. $C_6F_{15}$ | 7. $C_{10}F_{21}$ | 3. Et | 7. $C_2H_4$-c-$C_6H_{11}$ | 3. Me | 7. $C_5H_{11}$ | 3. p-OMe | 7. p-$OCF_3$ | |
| 4. $C_7F_{15}$ | | 4. s-Bu | | 4. Et | 8. Ph | 4. p-$CF_3$ | 8. o-F (b) | |

(a) for 1-7, 9, 10, $R_4$ = H

(b) for 8, $R_4$ = F and $R_3$ = H

**Fig. (12).** Synthetic scheme for the 560-membered mappicine analogs library with associated fluorous tags performed by Curran *et al.* [93].

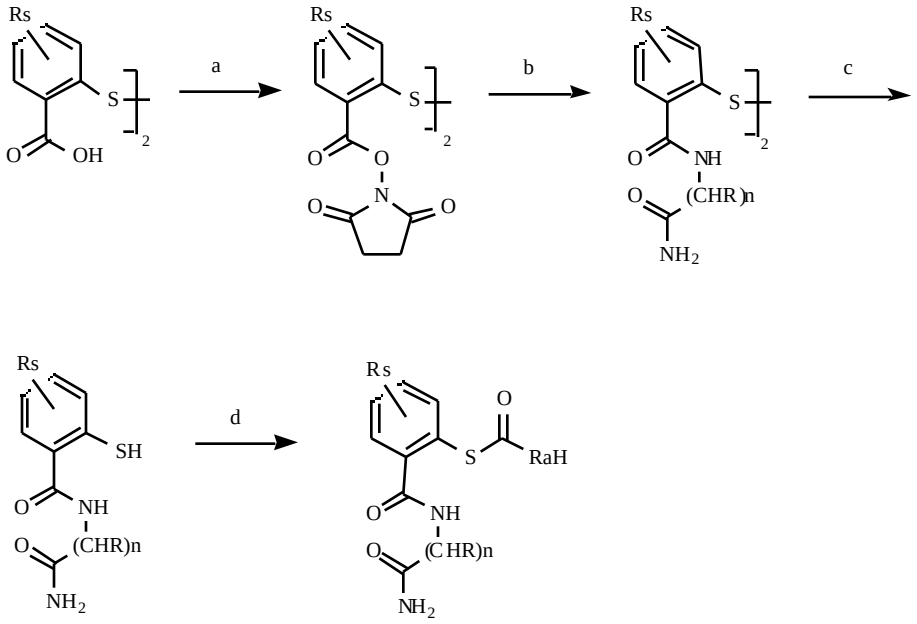


**Fig. (13).** Synthesis scheme for the 2-mercaptoamide thioesters developed by Srivastava *et al*. [95]. (a) *N*-hydroxysuccinimide/DIC/THF-*i*PrOH(7:3)/25ºC; (b) $H_2N(CHR)_nC(=O)NH_2$/DMF/25ºC; (c) TCEP·HCl/$Et_3N$/DMF-$H_2O$(9:1)/25ºC; (d) $R_aCOCl$/DMA/25ºC.

neomycin B mimetics. The starting materials were a neamine-derived aldehyde, *tert*-butyl isocyanide or isocyanoacetic acid methyl ester, a glycine-conjugated polyethylene glycol (PEG) methyl ether, and various Cbz-N-protected amino acids. Products were cleaved from PEG, hydrolyzed with basic catalysis, de-O-acetylated, and finally hydrogenated (Fig. **14** and Fig. **15**).

The peptidoaminoglycoside with X and R = H, R' = *tert*-butyl and R'' = HOOC-$CH_2$- was the most active

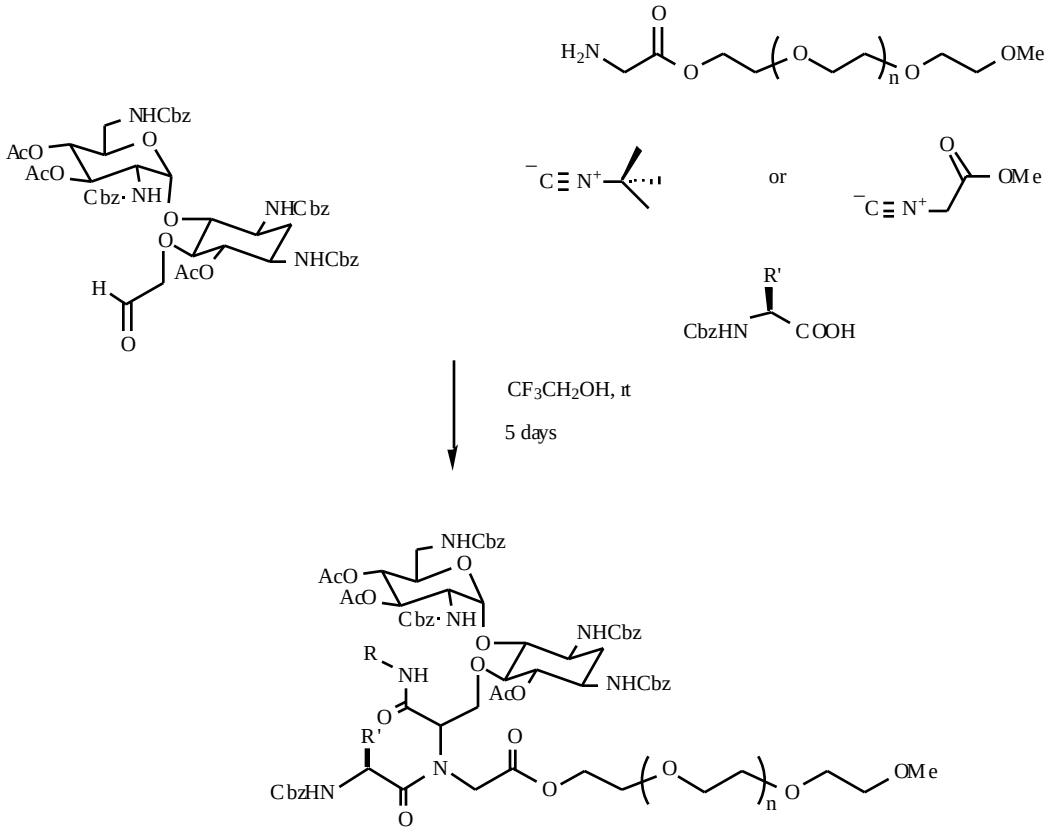


**Fig. (14).** Synthesis of neomycin B mimetics by Park *et al.* [96] using four-component condensation, where R' = Gly, Ala, Val, Phe, Trp, His, Tyr, Thr, Ser, Asp, Gln, Lys and Arg; R = *tert*-butyl, $CH_2C(O)OCH_3$ and n = ca. 113.

compound in the library and with higher activity than neomycin B [96].

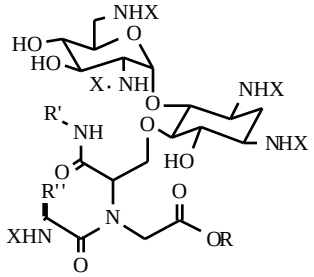

**Fig. (15).** General structure of the peptidoaminoglycosides as neomycin B mimetics, where X = Cbz and H (after removal of Cbz by hydrogenation); R = H, $CH_3$; R' = *tert*-butyl, $CH_2C(O)OCH_3$; R'' = corresponds to R' in the previous figures.

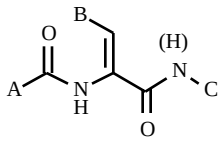

**Fig. (16).** General structure of the arylidenediamides in the library where A, B and C are different substituents (straight or branched alkyl chain, carbocyclic aryl and substituted or heterocyclic derivatives).

This strategy has also been used for the combinatorial synthesis of arylidenediamides in array format with the general structure shown in Fig. (**16**). The synthetic strategy is shown in Fig. (**17**).

An example was the synthesis of a 10,240 component array, which were synthesized from 8 oxazolones (A), 32 aldehydes (B) and 40 amines (C) [97].

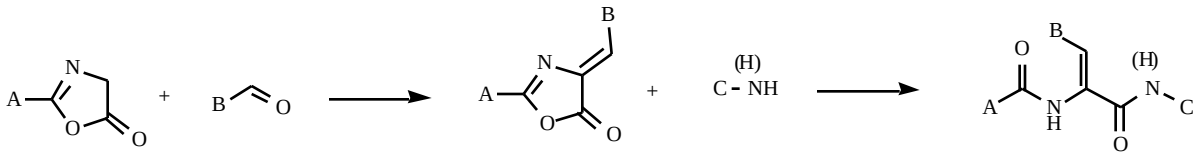

**Fig. (17).** General synthetic scheme for the compounds in the arylidenediamide library reported by Zambias *et al.* [97]. Substituents A, B and C on the molecular core are straight or branched alkyl chains, carbocyclic aryl and substituted or heterocyclic derivatives, which may also contain functional groups replacing hydrogen atoms, as tertiary amine, amide, ester, ether and halogen.

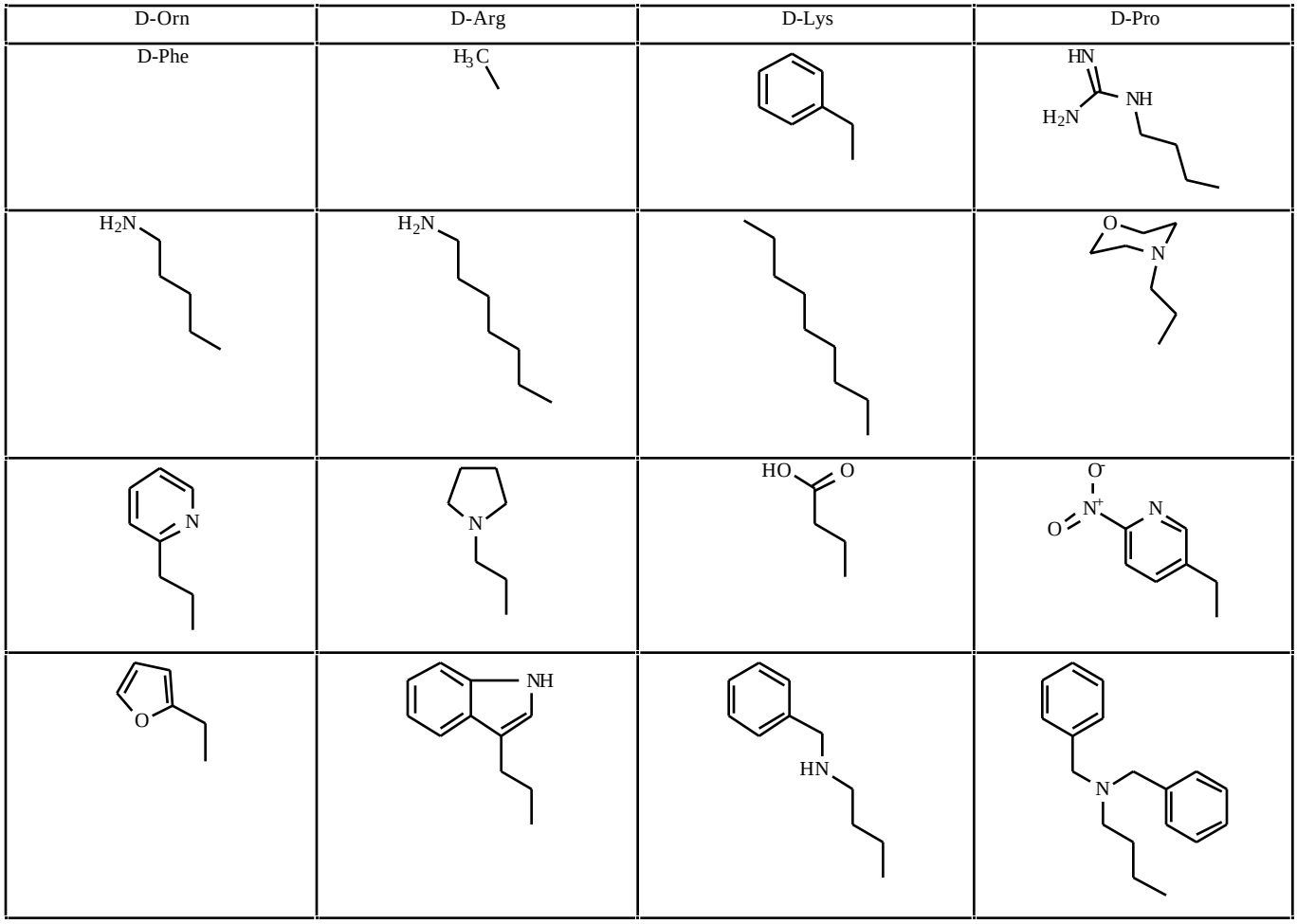


**Fig. (18).** Structure of the building blocks Hamy *et al.* [98] used to create the combinatorial peptoid library.

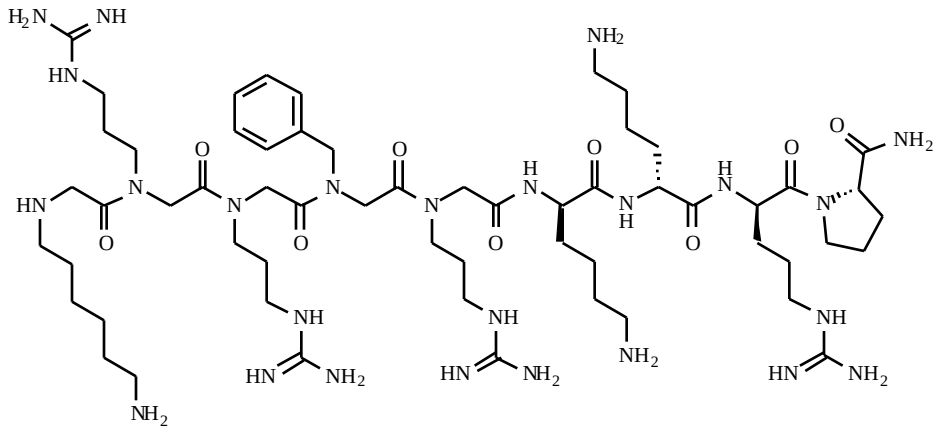

**Fig. (19).** Structure of compound CGP64222.

Another target for anti HIV-1 drugs is the inhibition of the Tat/TAR RNA interaction.

For this purpose, Hamy *et al*. synthesized a combinatorial peptoid library containing 3.2 x $10^6$ compounds divided into 20 sublibraries of 160,000 compounds each.

To limit the complexity of the library and to maintain high concentrations of individual components in the sublibraries, the four C-terminal residues were always a sequence composed of D-amino acids, D-Lys-D-Lys-D-Arg-D-Pro-amide. Five positions (residues A to E) were randomized by introducing a set of 20 building blocks carrying a wide range of functional groups (Fig. **18**).

The synthesis was accomplished by a split and mix process on a 1 % crosslinked polystyrene resin bearing the fluorenylmethoxycarbonyl-protected acid Rink amide linker.

One of the oligomers of the library specifically inhibited the Tat/TAR RNA interaction, both *in vitro* and *in vivo* (CGP64222, (Fig. **19**)) [98].

Neomycin B mimetics, arylidenediamides and the previous peptoid library have been recently proved to inhibit viral activity in the step of viral entry by acting as CXCR4 antagonist instead of the original target for which they were designed, inhibition of Tat/TAR RNA interaction [99].

An *et al*. have synthesized four unsymmetric piperazinyl polyazacyclophane scaffolds (Fig. **20**).

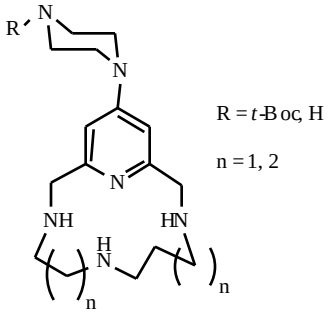


**Fig. (20).** Structure of piperazinyl polyazacyclophane scaffolds.

These scaffolds were utilized for the generation of twenty-six chemical libraries (total of 16,000 compounds) using the solution-phase simultaneous addition of functionalities (SPSAF) combinatorial approach with thirty-eight different functionalities (Fig. **21**) grouped into fourteen functionality sets A-N.

Set A included functionalities $R_1$-$R_{10}$; set B functionalities $R_{11}$-$R_{16}$; set C functionalities $R_{14}$-$R_{19}$; set D functionalities $R_{20}$-$R_{25}$; set E functionalities $R_{11}$-$R_{13}$, $R_{17}$-$R_{19}$; set F functionalities $R_{23}$, $R_{26}$-$R_{30}$; set G functionalities $R_2$, $R_8$, $R_{16}$, $R_{31}$-$R_{33}$; set H functionalities $R_{11}$-$R_{15}$, $R_{32}$; set I functionalities $R_{17}$-$R_{19}$, $R_{34}$-$R_{36}$; set J functionalities $R_{12}$, $R_{19}$, $R_{27}$, $R_{29}$, $R_{30}$, $R_{37}$; set K functionalities $R_{11}$-$R_{13}$, $R_{15}$, $R_{32}$; set L functionalities $R_9$, $R_{17}$-$R_{19}$, $R_{33}$; set M functionalities $R_{12}$, $R_{26}$, $R_{27}$, $R_{29}$, $R_{30}$; and set N functionalities $R_{12}$, $R_{19}$, $R_{28}$, $R_{29}$, $R_{38}$.

The combinatorial library was obtained by substitution of the H atoms in the NH groups of the piperazinyl polyazacyclophane scaffolds by the previously defined sets of functionalities.

These libraries were tested in HIV-1 tat/TAR protein-RNA disrupting assay using high throughput screening. Guanidine libraries 32 and 34 in the reference (with the piperazinyl polyazacyclophane scaffold with n = 1 and N substituted with set K and set M respectively) were potent inhibitors of HIV-1 tat/TAR protein-RNA interaction [100].

Recently a combinatorial library of 39,304 unnatural small molecules has been synthesized in solid phase using a set of 34 monomers and three consecutive cycles of split and pool. Monomers were selected to cover a broad range of the chemical space by varying charge, aromaticity, hydrogen bonding potential, flexibility, size, length of side chain and hydrophobicity.

The library had the general structure $NH_2$-M3-M2-M1-$NH(CH_2)_2$-O-TentaGel and was synthesized using standard Fmoc solid-phase synthetic methods, and encoded using 18 photocleavable tags. TR87 (Fig. **22**) was identified as Tat-TAR inhibitor [101].

## PROTEASE INHIBITORS

The first HIV protease inhibitor library was published by Owens *et al*. in 1991 and they identified a potent inhibitor through the screening of tetrapeptide mixtures [102].

These mixtures were synthesized as acetylated tetrapeptide amides where only one position was unique and the remaining positions contained a mixture of different amino acids; 22 amino acids plus statine (Sta) were used.

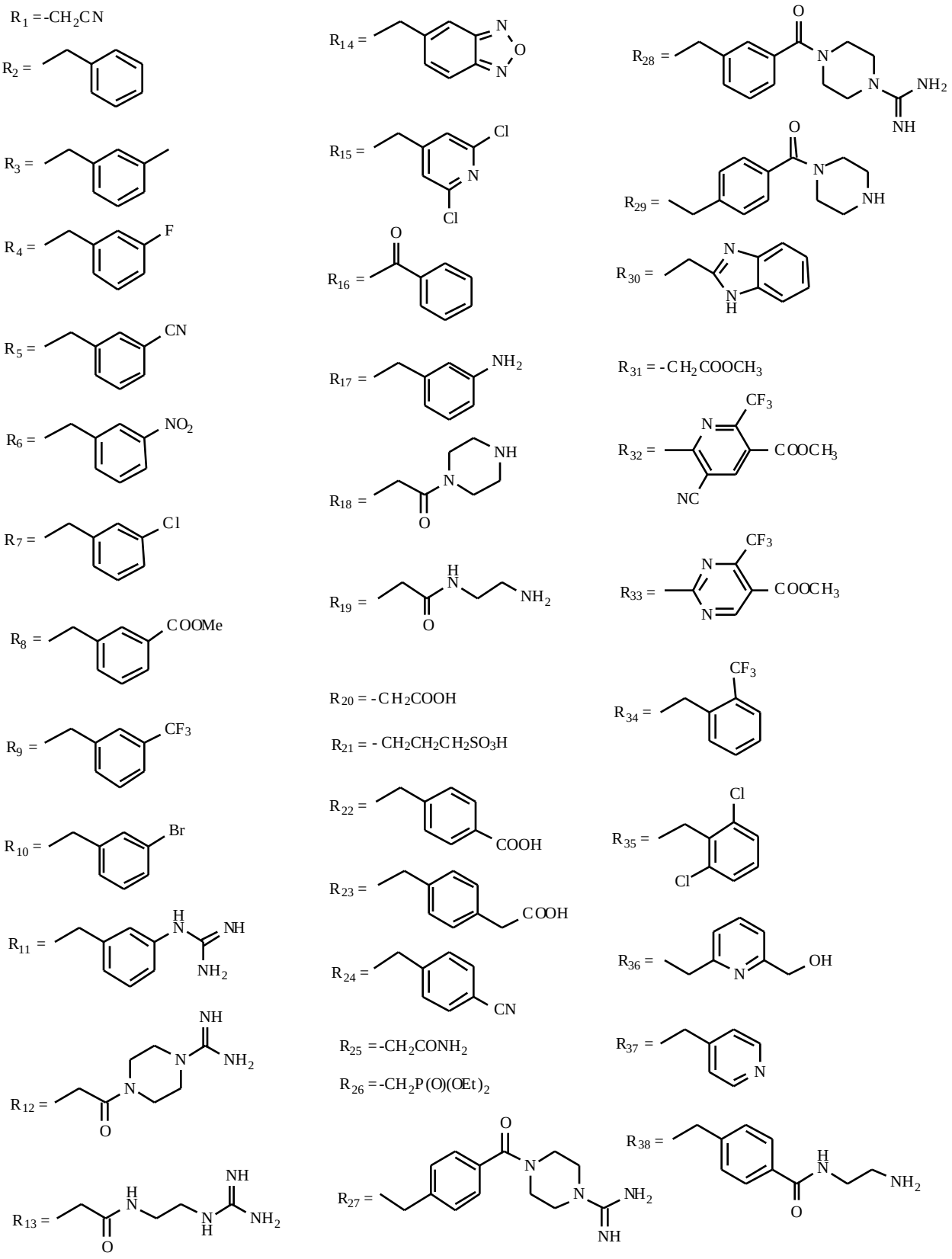


**Fig. (21).** Functionalities used for the generation of the SPSAF combinatorial library.

In the first step 22 separate Boc-amino acid-MBHA resins were prepared. The resins were combined to give Boc-$X_1$-MBHA. Then, 23 unique Boc-amino acid-$X_1$- MBHA dipeptide resins were prepared using the 22 Boc-amino acids and Boc-statine. These 23 dipeptide resins were combined to generate a new mixed resin, Boc-$Z_2$-$X_1$-MBHA, were Z is equal to X plus statine. The same procedure was used for preparing a new tripeptide resin, Boc-$X_3$-$Z_2$-$X_1$-MBHA.

Finally, 22 separate additional couplings were performed to yield 22tetrapeptide resins, Boc-$X_4$-$X_3$-$Z_2$-$X_1$-MBHA, where now the fourth $X_4$ position is defined. The peptide mixtures were cleaved from the resin with HF, and subsequently lyophilized to give 22 separate mixtures which contained 11,132 different tetrapeptide amides each.

L-ArgCar-4ABP-D-LysCar TR87

ArgCar and Lys Car: represent Arg and Lys carbamates

4ABP:

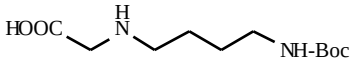


**Fig. (22).** Structure of Tat-TAR inhibitor TR87.

Positional scanning deconvolution was performed evaluating the ability to inhibit HIV protease. The most potent identified tetrapeptide was Ac-Phe-Ile-Sta-D-Leu-$NH_2$ with an $IC_{50}$ of 1.4 μM [102].

Indinavir is a protease inhibitor approved by the U.S. Federal Drug Administration as therapeutic agent for the treatment of HIV infection, whose synthesis was described in 1994 [103].

In order to improve potency and physical properties, such as short half-life and increasing viral resistance, Cheng *et al*. designed in 2000 a combinatorial library and for this purpose a solid phase synthesis route was established.

These analogues of indinavir were based on the division of the molecule into three main fragments, the aminoindanol

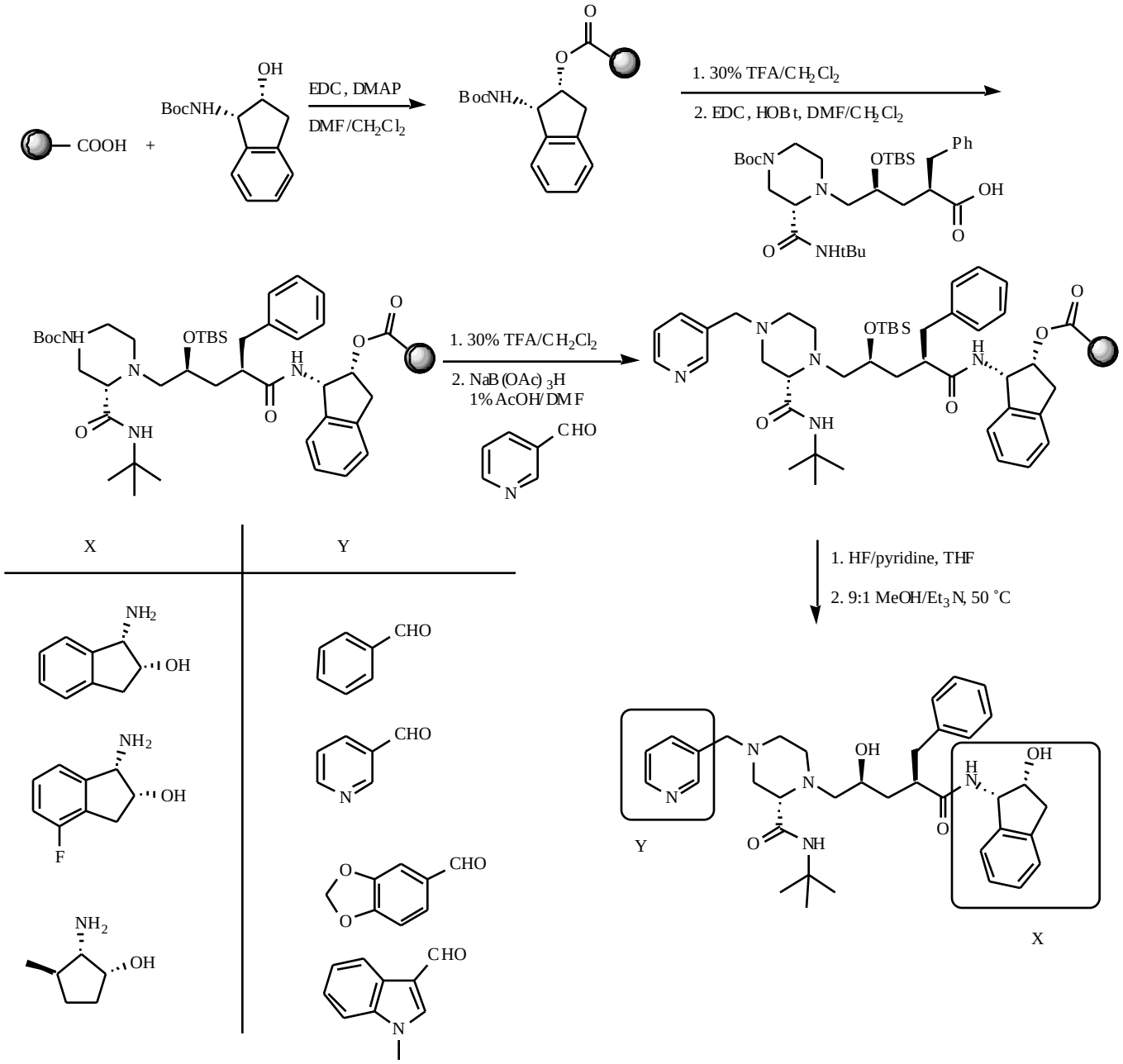


**Fig. (23).** Solid phase synthesis of indinavir reported by Cheng *et al.* [104], who follow the same methodology for the synthesis of their combinatorial library of indinavir analogs.

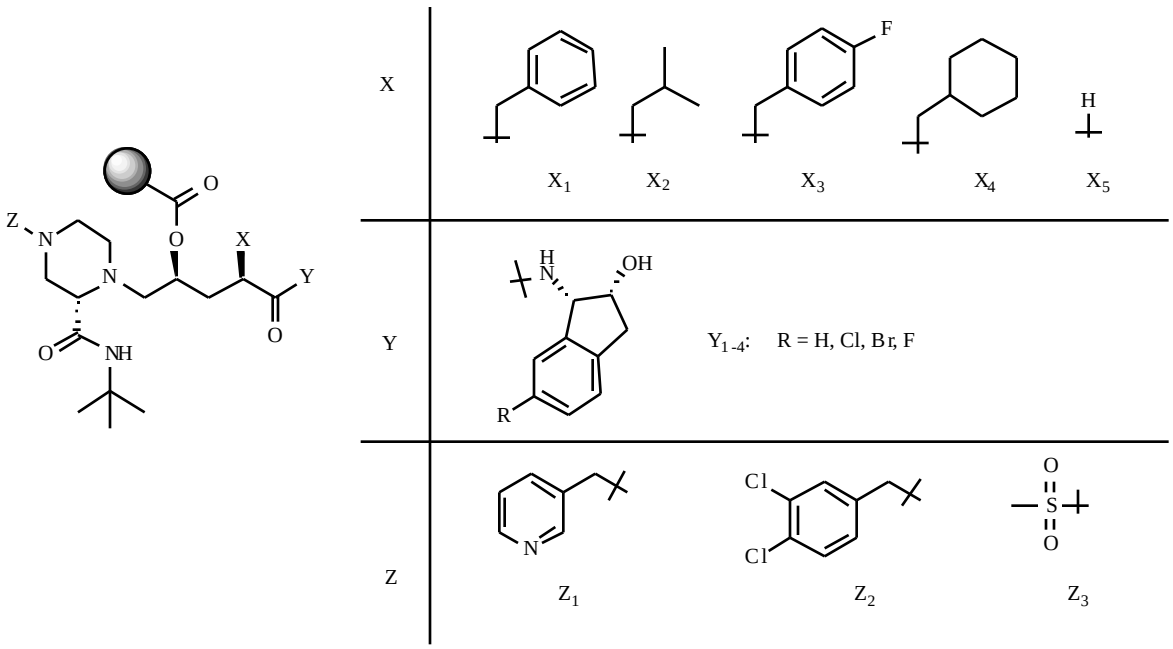


**Fig. (24).** General structure for the compounds in the library and subunits X, Y and Z synthesized by Rano *et al.* [105].

moiety, the hydroxyethylene unit and the pyridylmethyl group. The hydroxyl group on the aminoindanol was used for binding to the resin (Rapp TentaGel S COOH) *via* an ester linkage. The hydroxyethylene and pyridylmethyl fragments were coupled sequentially through amide formation and reductive amination. The final product was cleaved from the resin by transesterification with mild base (Fig. **23**) [104].

Another 'indinavir-based' combinatorial library (Fig. **24**) was designed by Rano *et al.* in order to improve the pharmacokinetic properties and *in vivo* potencies of indinavir.

A mix and split approach was used for the synthesis of these indinavir analogs diversifying the X, Y and Z subunits in (Fig. **24**). First, the resin bound hydroxyethylene isostere fragments containing 5 different X subunits were archived and mixed. The allyl group was removed and this material was split into 4 separate pools. Then, the Y subunits were attached and the pools were archived, mixed and the Boc group was removed. This resin was split into 2 separate pools followed by reductive amination with the carboxaldehyde Z subunits. Finally, the protease inhibitors were released from the resin by gentle warming in 10% TEA/MeOH. Biological activities for compounds of this library were lower than indinavir's [105].

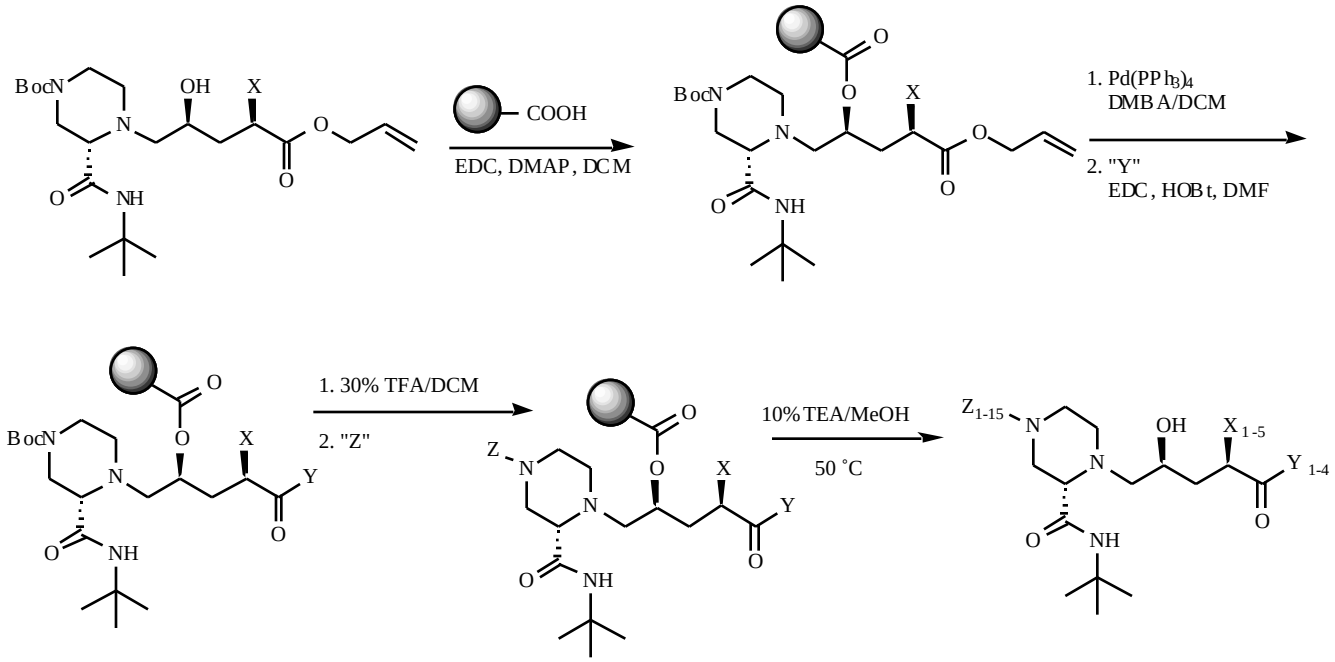


**Fig. (25).** Solid phase synthesis of the indinavir analogues library reported by Cheng *et al.* [106].

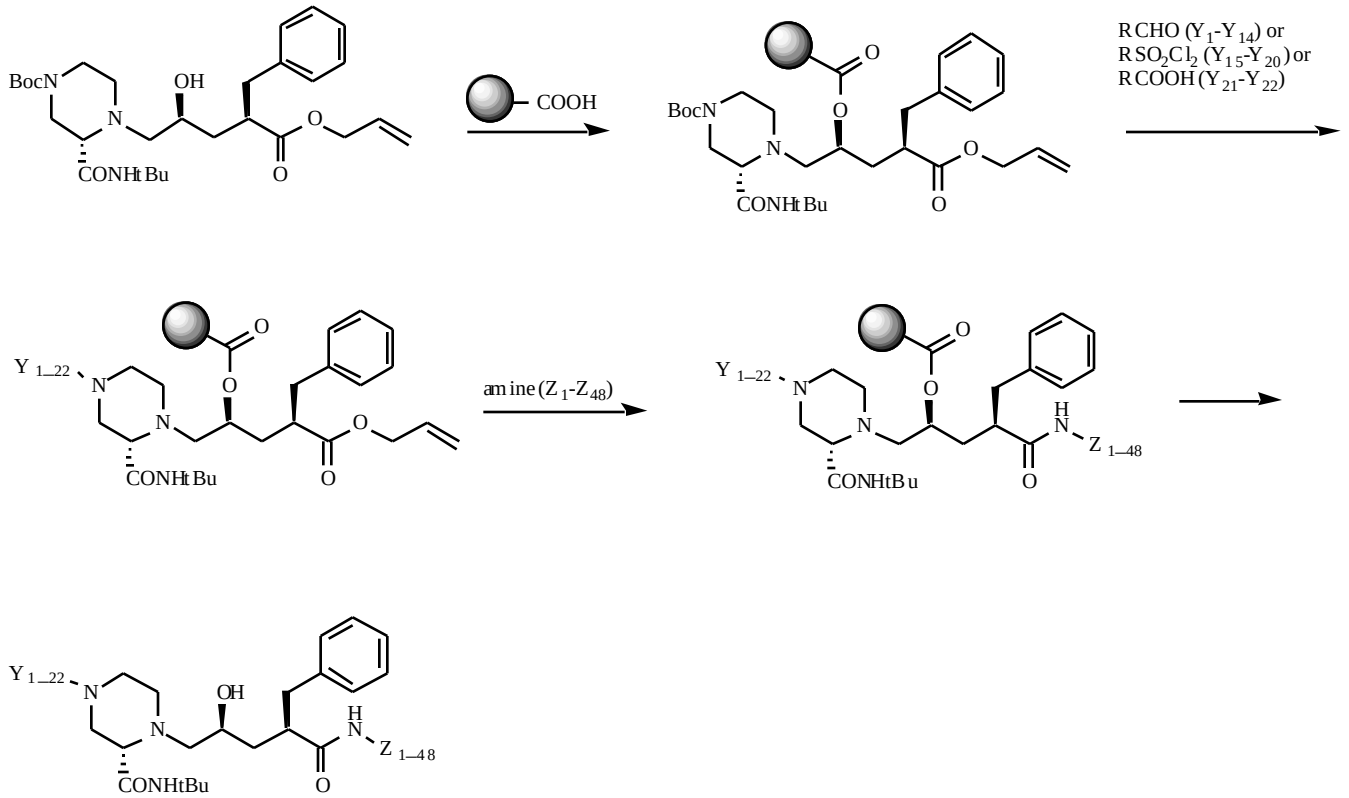


**Fig. (26).** Synthetic scheme of the library of indinavir analogues performed by Rahgavan *et al.* [107].

The aforementioned studies led to the design of another combinatorial library of indinavir analogues in 2002.

The synthesis was performed using a solid-phase mix and split protocol. The protected X subunit was anchored to the resin through the hydroxyl group via an ester linkage. Five resin bound X fragments were archived and mixed. Then, the allyl group was removed and the resulting material was split into four pools. Y subunits were attached and the four pools were archived and mixed, the Boc group being removed under acidic conditions. Then the resin was split into 15 pools and the Z subunits were attached by reductive amination, amide coupling or sulfonylation. Final products were released from the resin (Fig. **25**). The size of the library was 5 x 4 x 15 ($X_{1\text{-}5}$, $Y_{1\text{-}4}$ and $Z_{1\text{-}15}$). Their biological activity was tested as the ability to inhibit cleavage of a substrate by the wild-type HIV-1 protease enzyme, to inhibit the spread of viral infection in MT4 human T-lymphoid cells infected by the IIIb isolate and also with A-44 mutant enzyme variant PI-resistant HIV virus. Results showed that compounds X1-Y1-Z9, X1-Y1-Z10 and X1-Y1-Z15 were more potent than indinavir against both wild-type and mutant enzymes [106].

Based on the same approach, Rahgavan *et al*. synthesized a 1 x 22 x 48 combinatorial library of indinavir analogs varying the X, Y and Z subunits. The X-dimension comprised a single subunit, the hydroxyl ethylene core structure; the Y-dimension comprised 22 different subunits where aldehydes, sulfonyl chlorides and acids were included; and the Z-dimension was selected by molecular modeling with the criteria of fitting in the $S_2$ binding pocket and

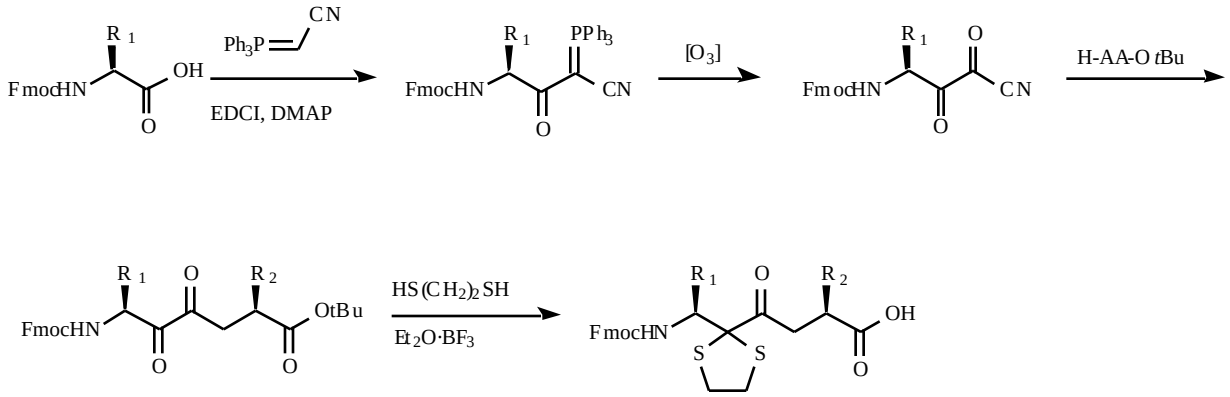


**Fig. (27).** Synthesis scheme of the α-keto amide dipeptidyl building blocks and protection of their α-keto functionality as 1,3-dithiolane with simultaneous cleavage of the *tert*-butyl ester reported by Papanikos *et al.* [109].

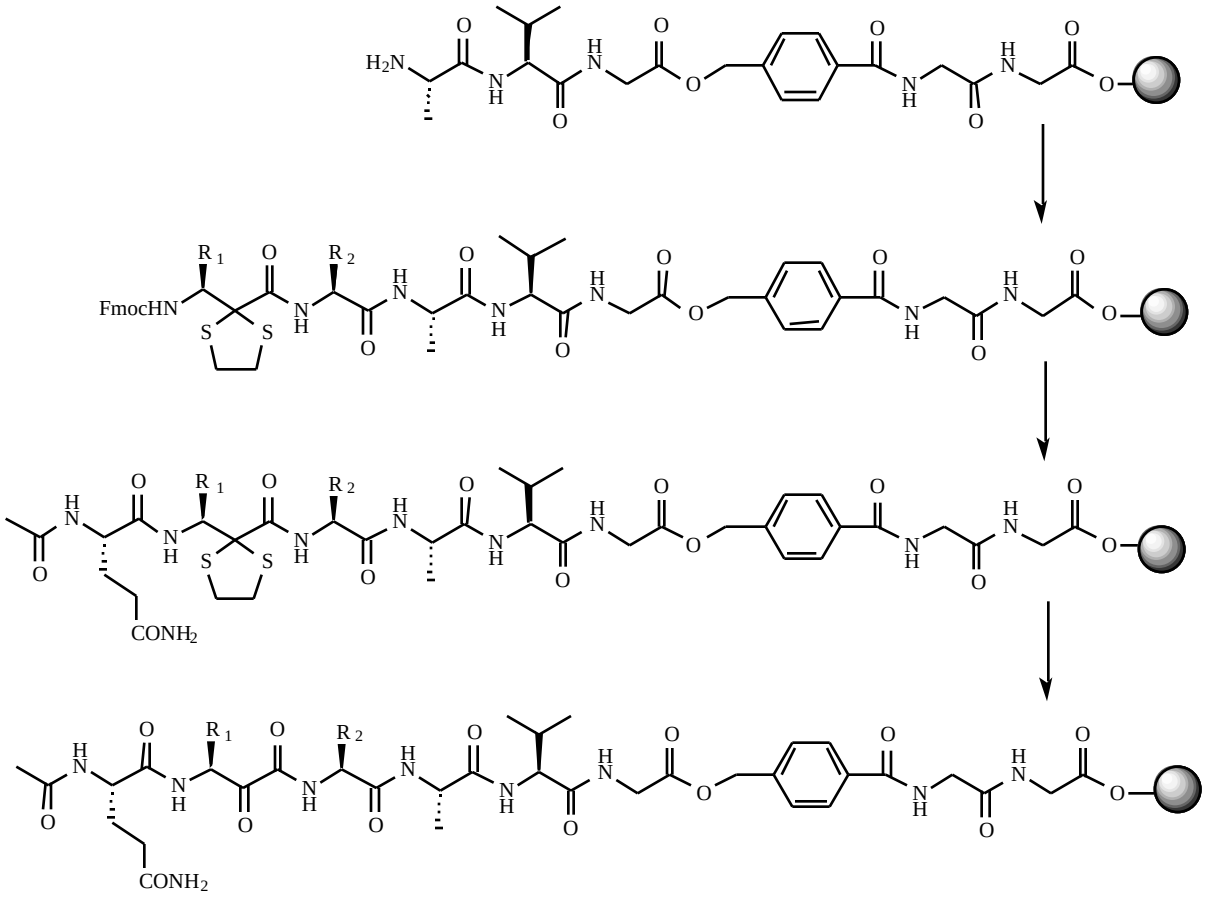

**Fig. (28).** Synthetic strategy used by Papanikos *et al.* [109] for the formation of resin-bound internal α-keto amide peptides using solid-phase peptide synthesis with the α-keto amide building blocks. $R_1$ = $CH_3$, $CH_2CH(CH_3)_2$, $CH_2Ph$ and $R_2$ = $CH_2CH(CH_3)_2$, $CH_2CH_2Ph$.

making the same kind of interactions with HIV protease enzyme as aminoindanol, therefore Z included a diverse set of aliphatic and aromatic amino alcohols and amines, some sulfones, phenols and basic amines and aminoindanol and 3-methyl-cyclopentyl amino alcohol were used as control pools. The structures of subunits X, Y and Z are shown in the reference [107].

The library was synthesized on solid support using the mix and split strategy (Fig. **26**). 2,6-dimethyl-4-hydroxy phenol was discovered to be a good replacement for aminoindanol [107].

A different strategy for HIV-1 protease inhibitors is the synthesis of α-keto amide peptides [108]. A solid-phase peptide synthetic methodology was used for this purpose. Dipeptidyl building blocks were accessible with the acylcyanophosphorane methodology and then converted into α-keto amides. Then the α-keto functionality was protected with 1,2-ethanedithiol (Fig. **27**), the resulting building blocks were assembled onto the resin to yield the desired dithiolane derivatives after Fmoc deprotection. The α-keto functionality was recovered by 1,3-dithiolane deprotection (Fig. **28**) [109].

De Michelis *et al*. have synthesized a focused library of 18 compounds incorporating the 1,3-(*N,N'*-dibenzyl)diamino-2-propanol motif based on a previous work [110] that showed that this motif elicited anti-HIV activity. The library, based on this motif, was substituted at the two end positions by various mono- or polyaminated substituted chains Fig. (**29**) [28].

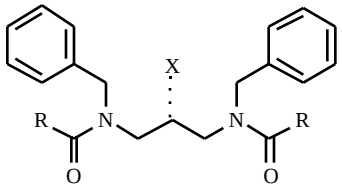

**Fig. (29).** General structure of the compounds in the library, where X = O, OH.

A different approach was the use of constrained macrocyclic templates equivalent to a tripeptide. Such templates may allow independent regioselective optimization of protease/enzyme inhibitors via focused combinatorial libraries.

The first step involved the conversion of the cyclic acid to an epoxide, which was the precursor of the desired N-terminal macrocyclic protease inhibitors, Fig (**30**). Such epoxide was regioselectively opened by primary amines to give a library of hydroxyethylamine derivatives, which were acylated by a range of sulfonyl chlorides to give a sulfonamide library or by series of isocyanates to give an urea library, see Fig. (**31**). These compounds were proved to be competitive inhibitors of HIV-1 protease [111].

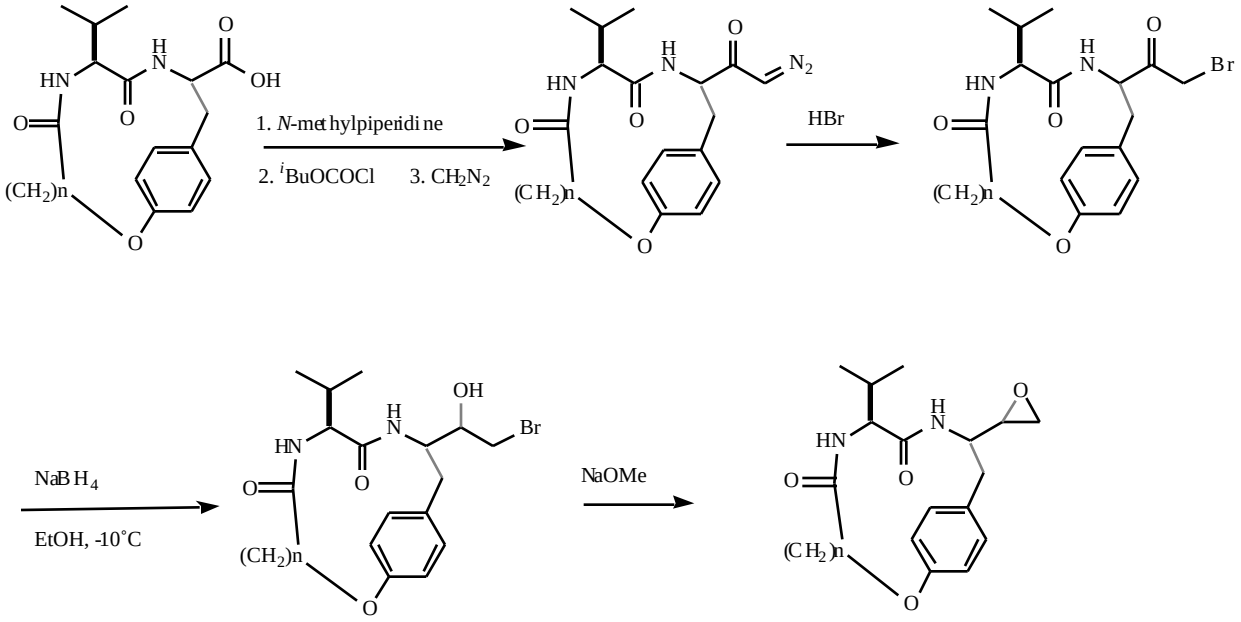


**Fig. (30).** Synthesis of the macrocyclic epoxides reported by Reid *et al.* [111].

Leroux *et al*. used a combinatorial liquid-phase strategy for the synthesis of a library of diPNA-arginine conjugates. The biological assays have not been performed, therefore their activity values, targets and modes of action have not been determined. Their design was based on the anti-HIV activity some diPNA-arginine conjugates had displayed. In the synthesis of the library diversification, see Fig. (**32**), can be achieved by varying the nature of the nucleobases $B_1$ and $B_2$ (adenine, cytosine, guanine, thymine, uracil plus the universal base analog 5-nitroindole), the length of the spacer (n) linking the arginine residue to the PNA dimer backbone (spacers composed of 2, 3, 4 and 5 methylene units were used) and, finally, the nature of *C*-extremity of arginine (carboxylic acid and methyl ester forms). Considering these variations the size of the library was $6^2$ x 4 x 2 = 288 compounds.

To synthesize this library a fully protected backbone (FPB) strategy was used. The fully protected di(aminoethylglycinamide) was selectively deprotected on the $P_1$-protected amino function, which was then stochiometrically condensed with an equimolar mixture of the six nucleobase units.

Then, the second $P_2$-amino protecting group was cleaved and another nucleobase unit was introduced. The library of diPNA-arginine conjugates was obtained by deprotection of nucleobases and the guanidinium group of arginine followed by hydrolysis [112].

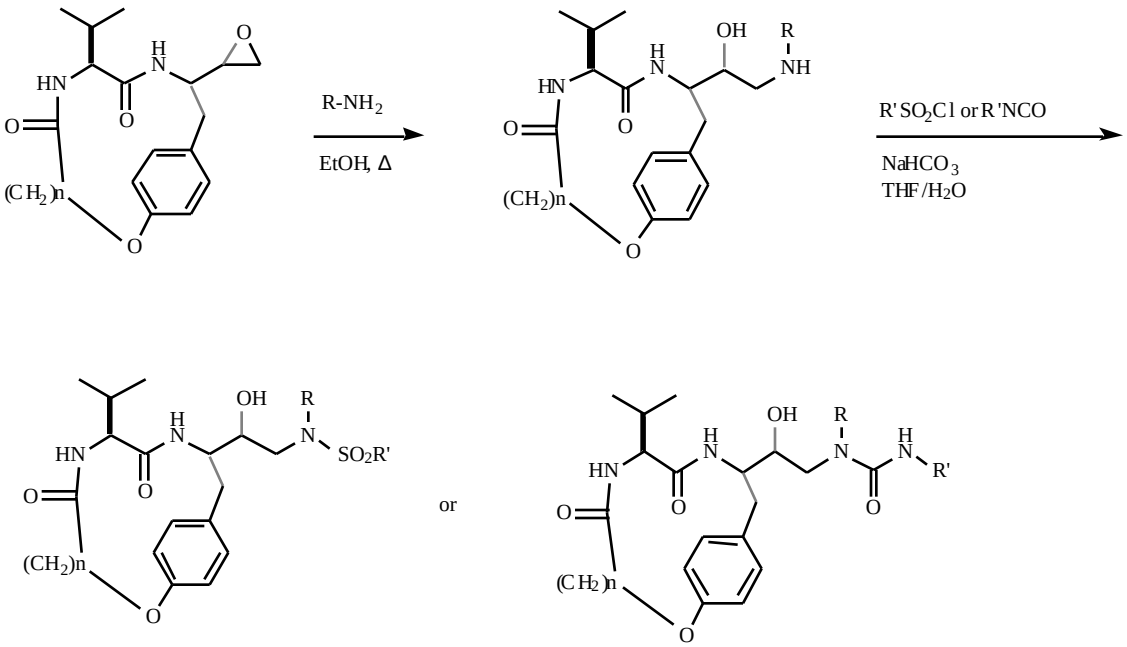


**Fig. (31).** Synthesis of N-terminal macrocyclic inhibitors developed by Reid *et al.* [111].

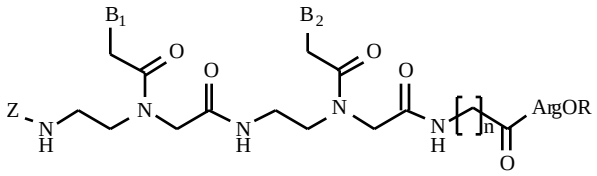


**Fig. (32).** Structure of the diPNA-arginine conjugates in the library, where $B_1$ and $B_2$ correspond to the five natural nucleobases, adenine, cytosine, guanine, thymine, uracil, and the universal base analog 5-nitroindole, n is a spacer composed of 2, 3, 4 and 5 methylenes, R is H or Me and Z represents the benzyloxycarbonyl group.

## CONCLUDING REMARKS

We have reported several combinatorial synthetic techniques, which have been applied for the discovery and generation of potential anti-HIV drugs. These synthetic techniques are mainly used in the first steps of drug discovery such as hit and lead finding. Therefore, combinatorial chemistry has proved to be a powerful tool for early stages in drug development. However, single compound syntheses are still preferred in more advanced steps although we are confident that combinatorial approach will find its place also for lead optimization purposes [69].

## ACKNOWLEDGEMENTS

This work was supported in part by the Fundació Marató de TV3 project 020930 and the Spanish Ministerio de Educación y Ciencia project BFI-2003-00405. I Clotet-Codina holds a FI scholarship from Generalitat de Catalunya and S. Pettersson from IQS.

## ABBREVIATIONS

A = Adenine

Ac = Acetyl

Ala = Alanine

Arg = Arginine

Asn = Asparagine

Asp = Aspartic acid

Boc = *tert*-butoxycarbonyl

C = cytosine

Cbz = Carbobenzyloxy

Cys = Cysteine

DCM = Dichloromethane

DIC = 1,3-diisopropylcarbodimide

DIPEA = *N*,*N*-diisopropylethylamine

DMA = Dimethylacetamide

DMAP = 4-dimethylaminopyridine

DMBA = *N*,*N*-dimethylbenzylamine

DMF = *N*,*N*-dimethylformamide

EDC = 1-ethyl-3-(3-dimethylaminopropyl)carbodiimide

EDCI = 1-ethyl-3-[3-(dimethylamino)propyl]carbodi-imide

Et = Ethyl

Fmoc = Fluorenylmethoxycarbonyl

G = Guanine

Gln = Glutamine

Glu = Glutamic acid

Gly = Glycine

His = Histidine

HOBT = 1-hydroxybenzotriazole

Ile = Isoleucine

IN = Integrase

*i*Bu = Isobutyl

*i*Pr = Isopropyl

*i*PrMgCl = Isopropylmagnesium chloride

LC = Liquid chromatography

Leu = Leucine

Lys = Lysine

MBHA = 4-methylbenzhydrylamine

Me = Methyl

MS = Mass spectrometry

NRTI = Nucleoside reverse transcriptase inhibitors

NNRTI = Non-nucleoside reverse transcriptase inhibitors

Orn = Ornithine

PEG = Polyethylene glycol

Ph = Phenyl

Phe = Phenylalanine

PNA = Peptide nucleic acid

Pro = Proline

RT = Reverse transcriptase

Ser = Serine

Sta = Statine

T = Thymine

TBS = *tert*-butyldimethylsilyl

TEA = Triethanolamine

TBTU = 2-(1*H*-Benzotriazol-1-yl)-1,1,3,3-tetramethylur-onium tetrafluoroborate

*t*Bu = *tert*-butyl

TBZ = 1-aryl-1*H*,3*H*-thiazolo[3,4-a]benzimidazole

TCEP = tris-(2-carboxyethyl)phosphine

TFA = Trifluoroacetic acid

THF = Tetrahydrofuran

Thr = Threonine

TMS = Trimethylsilyl

Tr = Trityl

Trp = Tryptophan

Tyr = Tyrosine

Val = Valine

## REFERENCES


[1] http://www.who.int

[2] Maeda, K.; Nakata, H.; Ogata, H.; Koh, Y.; Miyakawa, T.; Mitsuya, H. *Curr. Opin. Pharmacol.*, **2004**, *4*, 447.

[3] Pierson, T. C.; Doms, R. W.; Poehlmann, S. *Rev. Med. Virol.*, **2004**, *14*, 255.

[4] Markovic, I.; Clouse, K. A. *Curr. HIV Res.*, **2004**, *2*, 223.

[5] Seibert, C.; Sakmar, T. P. *Curr. Pharm. Des.*, **2004**, *10*, 2041.

[6] Shaheen, F.; Collman, R. G. *Curr. Opin. Infect. Dis.*, **2004**, *17*, 7.

[7] Root, M. J.; Steger, H. K. *Curr. Pharm. Des.*, **2004**, *10*, 1805.

[8] Este, J. A. *Curr. Med. Chem.*, **2003**, *10*, 1617.

[9] Locatelli, G. A.; Cancio, R.; Spadari, S.; Maga, G. *Curr. Drug Metab.*, **2004**, *5*, 283.

[10] Milinkovic, A.; Martinez, E. *Expert Rev. Anti Infect. Ther.*, **2004**, *2*, 367.

[11] Anthony, N. J. *Curr. Top. Med. Chem.*, **2004**, *4*, 979.

[12] De Clercq, E. *Chem. Biodivers.*, **2004**, *1*, 44.

[13] Imamichi, T. *Curr. Pharm. Des.*, **2004**, *10*, 4039.

[14] Pereira, C. F.; Paridaen Judith, T. M. L. *Curr. Pharm. Des.*, **2004**, *10*, 4005.

[15] Tarby, C. M. *Curr. Top. Med. Chem.*, **2004**, *4*, 1045.

[16] Andreola, M. L. *Curr. Pharm. Des.*, **2004**, *10*, 3713.

[17] Turlure, F.; Devroe, E.; Silver, P. A.; Engelman, A. *Front. Biosci.*, **2004**, *9*, 3187.

[18] Gupta, S. P.; Nagappa, A. N. *Curr. Med. Chem.*, **2003**, *10*, 1779.

[19] Witvrouw, M.; Van Maele, B.; Vercammen, J.; Hantson, A.; Engelborghs, Y.; De Clercq, E.; Pannecouque, C.; Debyser, Z. *Curr. Drug Metab.*, **2004**, *5*, 291.

[20] Johnson, A. A.; Marchand, C.; Pommier, Y. *Curr. Top. Med. Chem.*, **2004**, *4*, 1059.

[21] Chiu, T. K.; Davies, D. R. *Curr. Top. Med. Chem.*, **2004**, *4*, 965.

[22] Parrill, A. L. *Curr. Med. Chem.*, **2003**, *10*, 1811.

[23] Devadas, K.; Dhawan, S. *Recent Research Developments in Biochemistry*, **2003**, *4*, 447.

[24] Baba, M. *Curr. Top. Med. Chem.*, **2004**, *4*, 871.

[25] Schiavoni, I.; Muratori, C.; Piacentini, V.; Giammarioli, A. M.; Federico, M. *Curr. Drug Targets Immune Endocr. Metabol. Disord.*, **2004**, *4*, 19.

[26] Morita, E.; Sundquist, W. I. *Annu. Rev. Cell Dev. Biol.*, **2004**, *20*, 395.

[27] Bukrinskaya, A. G. *Arch. Virol.*, **2004**, *149*, 1067.

[28] De Michelis, C.; Rocheblave, L.; Priem, G.; Chermann, J. C.; Kraus, J. L. *Bioorg. Med. Chem.*, **2000**, *8*, 1253.

[29] http://www.aidsinfonet.org

[30] Mitsuya, H.; Weinhold, K. J.; Furman, P. A.; St.Clair, M. H.; Lehrman, S. N.; Gallo, R. C.; Bolognesi, D.; Barry, D. W.; Broder, S. *Proc. Natl. Acad. Sci. USA*, **1985**, *82*, 7096.

[31] Herdewijn, P.; Balzarini, J.; De Clercq, E.; Pauwels, R.; Baba, M.; Broder, S.; Vanderhaeghe, H. *J. Med. Chem.*, **1987**, *30*, 1270.

[32] De Clercq, E.; Van Aerschot, A.; Herdewijn, P.; Baba, M.; Pauwels, R.; Balzarini, J. *Nucleosides Nucleotides*, **1989**, *8*, 659.

[33] Mitsuya, H.; Broder, S. *Proc. Natl. Acad. Sci. USA*, **1986**, *83*, 1911.

[34] Chu, C. K.; Schinazi, R. F.; Arnold, B. H.; Cannon, D. L.; Doboszewski, B.; Bhadti, V. B.; Gu, Z. P. *Biochem. Pharmacol.*, **1988**, *37*, 3543.

[35] Lin, T. S.; Schinazi, R. F.; Prusoff, W. H. *Biochem. Pharmacol.*, **1987**, *36*, 2713.

[36] Balzarini, J.; Van Aerschot, A.; Herdewijn, P.; De Clercq, E. *Biochem. Pharmacol.*, **1989**, *38*, 869.

[37] Coates, J. A.; Cammack, N.; Jenkinson, H. J.; Mutton, I. M.; Pearson, B. A.; Storer, R.; Cameron, J. M.; Penn, C. R. *Antimicrob. Agents Chemother.*, **1992**, *36*, 202.

[38] Larder, B. A.; Kemp, S. D.; Harrigan, P. R. *Science*, **1995**, *269*, 696.

[39] Daluge, S. M.; Good, S. S.; Faletto, M. B.; Miller, W. H.; St.Clair, M. H.; Boone, L. R.; Tisdale, M.; Parry, N. R.; Reardon, J. E.; Dornsife, R. E.; Averett, D. R.; Krenitsky, T. A. *Antimicrob. Agents Chemother.*, **1997**, *41*, 1082.

[40] Tisdale, M.; Alnadaf, T.; Cousens, D. *Antimicrob. Agents Chemother.*, **1997**, *41*, 1094.

[41] Faletto, M. B.; Miller, W. H.; Garvey, E. P.; St.Clair, M. H.; Daluge, S. M.; Good, S. S. *Antimicrob. Agents Chemother.*, **1997**, *41*, 1099.

[42] Arimilli, M. N.; Kim, C. U.; Dougherty, J.; Mulato, A.; Oliyai, R.; Shaw, J. P.; Cundy, K. C.; Bischofberger, N. *Antivir. Chem. Chemother.*, **1997**, *8*, 557.

[43] Robbins, B. L.; Srinivas, R., V; Kim, C.; Bischofberger, N.; Fridland, A. *Antimicrob. Agents Chemother.*, **1998**, *42*, 612.

[44] Merluzzi, V. J.; Hargrave, K. D.; Labadia, M.; Grozinger, K.; Skoog, M.; Wu, J. C.; Shih, C. K.; Eckner, K.; Hattox, S.; Adams, J. *Science*, **1990**, *250*, 1411.

[45] De Clercq, E. *Med. Res. Rev.*, **1996**, *16*, 125.

[46] Balzarini, J.; Perez-Perez, M. J.; Velazquez, S.; San Felix, A.; Camarasa, M. J.; De Clercq, E.; Karlsson, A. *Proc. Natl. Acad. Sci. USA*, **1995**, *92*, 5470.

[47] Romero, D. L.; Olmsted, R. A.; Poel, T. J.; Morge, R. A.; Biles, C.; Keiser, B. J.; Kopta, L. A.; Friis, J. M.; Hosley, J. D.; Stefanski, K. J.; Wishka, D. G.; Evans, D. B.; Morris, J.; Stehle, R. G.; Sharma, S. K.; Yagi, Y.; Voorman, R. L.; Adams, W. J.; Tarpley, W. G.; Thomas, R. C. *J. Med. Chem.*, **1996**, *39*, 3769.

[48] Romero, D. L.; Morge, R. A.; Genin, M. J.; Biles, C.; Busso, M.; Resnick, L.; Althaus, I. W.; Reusser, F.; Thomas, R. C.; Tarpley, W. G. *J. Med. Chem.*, **1993**, *36*, 1505.

[49] Young, S. D.; Britcher, S. F.; Tran, L. O.; Payne, L. S.; Lumma, W. C.; Lyle, T. A.; Huff, J. R.; Anderson, P. S.; Olsen, D. B.; Carroll, S. S. *Antimicrob. Agents Chemother.*, **1995**, *39*, 2602.

[50] Roberts, N. A.; Martin, J. A.; Kinchington, D.; Broadhurst, A., V; Craig, J. C.; Duncan, I. B.; Galpin, S. A.; Handa, B. K.; Kay, J.; Krohn, A. *Science*, **1990**, *248*, 358.

[51] Craig, J. C.; Duncan, I. B.; Hockley, D.; Grief, C.; Roberts, N. A.; Mills, J. S. *Antiviral Res.*, **1991**, *16*, 295.

[52] Ohta, Y.; Shinkai, I. *Bioorg. Med. Chem.*, **1997**, *5*, 465.

[53] Kempf, D. J.; Marsh, K. C.; Denissen, J. F.; McDonald, E.; Vasavanonda, S.; Flentge, C. A.; Green, B. E.; Fino, L.; Park, C. H. *Proc. Natl. Acad. Sci. USA*, **1995**, *92*, 2484.

[54] Markowitz, M.; Mo, H.; Kempf, D. J.; Norbeck, D. W.; Bhat, T. N.; Erickson, J. W.; Ho, D. D. *J. Virol.*, **1995**, *69*, 701.

[55] Molla, A.; Korneyeva, M.; Gao, Q.; Vasavanonda, S.; Schipper, P. J.; Mo, H. M.; Markowitz, M.; Chernyavskiy, T.; Niu, P.; Lyons, N.; Hsu, A.; Granneman, G. R.; Ho, D. D.; Boucher, C. A.; Leonard, J. M.; Norbeck, D. W.; Kempf, D. J. *Nat. Med.*, **1996**, *2*, 760.

[56] Vacca, J. P.; Dorsey, B. D.; Schleif, W. A.; Levin, R. B.; McDaniel, S. L.; Darke, P. L.; Zugay, J.; Quintero, J. C.; Blahy, O. M. *Proc. Natl. Acad. Sci. USA*, **1994**, *91*, 4096.

[57] Patick, A. K.; Mo, H.; Markowitz, M.; Appelt, K.; Wu, B.; Musick, L.; Kalish, V.; Kaldor, S.; Reich, S. *Antimicrob. Agents Chemother.*, **1996**, *40*, 292.

[58] Shetty, B. V.; Kosa, M. B.; Khalil, D. A.; Webber, S. *Antimicrob. Agents Chemother.*, **1996**, *40*, 110.

[59] Baba, M.; Okamoto, M.; Makino, M.; Kimura, Y.; Ikeuchi, T.; Sakaguchi, T.; Okamoto, T. *Antimicrob. Agents Chemother.*, **1997**, *41*, 1250.

[60] Clair, M. H. S.; Millard, J.; Rooney, J.; Tisdale, M.; Parry, N.; Sadler, B. M.; Blum, M. R.; Painter, G. *Antiviral Res.*, **1996**, *29*, 53.

[61] Kim, E. E.; Baker, C. T.; Dwyer, M. D.; Murcko, M. A.; Rao, B. G.; Tung, R. D.; Navia, M. A. *J. Am. Chem. Soc.*, **1995**, *117*, 1181.

[62] Sham, H. L.; Kempf, D. J.; Molla, A.; Marsh, K. C.; Kumar, G. N.; Chen, C. M.; Kati, W.; Stewart, K.; Lal, R.; Hsu, A.; Betebenner, D.; Korneyeva, M.; Vasavanonda, S.; McDonald, E.; Saldivar, A.; Wideburg, N.; Chen, X.; Niu, P.; Park, C.; Jayanti, V.; Grabowski, B.; Granneman, G. R.; Sun, E.; Japour, A. J.; Norbeck, D. W. *Antimicrob. Agents Chemother.*, **1998**, *42*, 3218.

[63] Fikkert, V.; Hombrouck, A.; Van Remoortel, B.; De Maeyer, M.; Pannecouque, C.; De Clercq, E.; Debyser, Z.; Witvrouw, M. *AIDS*, **2004**, *18*, 2019.

[64] Kilby, J. M.; Hopkins, S.; Venetta, T. M.; DiMassimo, B.; Cloud, G. A.; Lee, J. Y.; Alldredge, L.; Hunter, E.; Lambert, D.; Bolognesi, D.; Matthews, T.; Johnson, M. R.; Nowak, M. A.; Shaw, G. M.; Saag, M. S. *Nat. Med.*, **1998**, *4*, 1302.

[65] Maclean, D.; Martin, E. J. *J. Comb. Chem.*, **2004**, *6*, 1.

[66] Liu, S.; Jiang, S. *Curr. Pharm. Des.*, **2004**, *10*, 1827.

[67] Kuhn, P.; Wilson, K.; Patch, M. G.; Stevens, R. C. *Curr. Opin. Chem. Biol.*, **2002**, *6*, 704.
[68] Marchand, C.; Neamati, N.; Pommier, Y. *Meth. Enzymol.*, **2001**, *340*, 624.
[69] Pascual, R.; Mateu, M.; Gasteiger, J.; Borrell, J. I.; Teixidó, J. *J. Chem. Inf. Comput. Sci.*, **2003**, *43*, 199.
[70] Eckstein, F. *Angew. Chem. Int. Ed. Eng.*, **1983**, *22*, 423.
[71] Iyer, R. P.; Phillips, L. R.; Egan, W.; Regan, J. B.; Beaucage, S. L. *J. Org. Chem.*, **1990**, *55*, 4693.
[72] Wyatt, J. R.; Vickers, T. A.; Roberson, J. L.; Buckheit, R. W., Jr.; Klimkait, T.; DeBaets, E.; Davis, P. W.; Rayner, B.; Imbach, J. L.; Ecker, D. J. *Proc. Natl. Acad. Sci. USA*, **1994**, *91*, 1356.
[73] Zhou, G.; Ferrer, M.; Chopra, R.; Kapoor, T. M.; Strassmaier, T.; Weissenhorn, W.; Skehel, J. J.; Oprian, D.; Schreiber, S. L.; Harrison, S. C.; Wiley, D. C. *Bioorg. Med. Chem.*, **2000**, *8*, 2219.
[74] Ferrer, M.; Kapoor, T. M.; Strassmaier, T.; Weissenhorn, W.; Skehel, J. J.; Oprian, D.; Schreiber, S. L.; Wiley, D. C.; Harrison, S. C. *Nat. Struct. Biol.*, **1999**, *6*, 953.
[75] Dorn, C. P.; Finke, P. E.; Oates, B.; Budhu, R. J.; Mills, S. G.; MacCoss, M.; Malkowitz, L.; Springer, M. S.; Daugherty, B. L.; Gould, S. L.; DeMartino, J. A.; Siciliano, S. J.; Carella, A.; Carver, G.; Holmes, K.; Danzeisen, R.; Hazuda, D.; Kessler, J.; Lineberger, J.; Miller, M.; Schleif, W. A.; Emini, E. A. *Bioorg. Med. Chem. Lett.*, **2001**, *11*, 259.
[76] Finke, P. E.; Meurer, L. C.; Oates, B.; Mills, S. G.; MacCoss, M.; Malkowitz, L.; Springer, M. S.; Daugherty, B. L.; Gould, S. L.; DeMartino, J. A.; Siciliano, S. J.; Carella, A.; Carver, G.; Holmes, K.; Danzeisen, R.; Hazuda, D.; Kessler, J.; Lineberger, J.; Miller, M.; Schleif, W. A.; Emini, E. A. *Bioorg. Med. Chem. Lett.*, **2001**, *11*, 265.
[77] Hale, J. J.; Budhu, R. J.; Mills, S. G.; MacCoss, M.; Malkowitz, L.; Siciliano, S.; Gould, S. L.; DeMartino, J. A.; Springer, M. S. *Bioorg. Med. Chem. Lett.*, **2001**, *11*, 1437.
[78] Finke, P. E.; Meurer, L. C.; Oates, B.; Shah, S. K.; Loebach, J. L.; Mills, S. G.; MacCoss, M.; Castonguay, L.; Malkowitz, L.; Springer, M. S.; Gould, S. L.; DeMartino, J. A. *Bioorg. Med. Chem. Lett.*, **2001**, *11*, 2469.
[79] Finke, P. E.; Oates, B.; Mills, S. G.; MacCoss, M.; Malkowitz, L.; Springer, M. S.; Gould, S. L.; DeMartino, J. A.; Carella, A.; Carver, G.; Holmes, K.; Danzeisen, R.; Hazuda, D.; Kessler, J.; Lineberger, J.; Miller, M.; Schleif, W. A.; Emini, E. A. *Bioorg. Med. Chem. Lett.*, **2001**, *11*, 2475.
[80] Hale, J. J.; Budhu, R. J.; Holson, E. B.; Finke, P. E.; Oates, B.; Mills, S. G.; MacCoss, M.; Gould, S. L.; DeMartino, J. A.; Springer, M. S.; Siciliano, S.; Malkowitz, L.; Schleif, W. A.; Hazuda, D.; Miller, M.; Kessler, J.; Danzeisen, R.; Holmes, K.; Lineberger, J.; Carella, A.; Carver, G.; Emini, E. *Bioorg. Med. Chem. Lett.*, **2001**, *11*, 2741.
[81] Willoughby, C. A.; Berk, S. C.; Rosauer, K. G.; Degrado, S.; Chapman, K. T.; Gould, S. L.; Springer, M. S.; Malkowitz, L.; Schleif, W. A.; Hazuda, D.; Miller, M.; Kessler, J.; Danzeisen, R.; Holmes, K.; Lineberger, J.; Carella, A.; Carver, G.; Emini, E. A. *Bioorg. Med. Chem. Lett.*, **2001**, *11*, 3137.
[82] Hale, J. J.; Budhu, R. J.; Mills, S. G.; MacCoss, M.; Gould, S. L.; DeMartino, J. A.; Springer, M. S.; Siciliano, S. J.; Malkowitz, L.; Schleif, W. A.; Hazuda, D.; Miller, M.; Kessler, J.; Danzeisen, R.; Holmes, K.; Lineberger, J.; Carella, A.; Carver, G.; Emini, E. A. *Bioorg. Med. Chem. Lett.*, **2002**, *12*, 2997.
[83] Justus, S. E. A.; Lee, H. T.; Pontrello, J. K.; Roth, B. D.; Sexton, K. E.; Wilson, M. W. US Patent US 6506751, 2003. (*Chem. Abstr.* 2003, *138*, 89804)
[84] Boussard, C.; Doyle, V. E.; Mahmood, N.; Klimkait, T.; Pritchard, M.; Gilbert, I. H. *Eur. J. Med. Chem.*, **2002**, *37*, 883.
[85] Chimirri, A.; Grasso, S.; Molica, C.; Monforte, A. M.; Monforte, P.; Zappala, M.; Bruno, G.; Nicolo, F.; Witvrouw, M.; Jonckeere, H.; Balzarini, J.; De Clercq, E. *Antivir. Chem. Chemother.*, **1997**, *8*, 363.
[86] Chimirri, A.; Monforte, A. M.; Monforte, P.; Rao, A.; Zappala, M.; Bruno, G.; Nicolo, F.; Pannecouque, C.; Witvrouw, M.; De Clercq, E. *Antivir. Chem. Chemother.*, **1998**, *9*, 431.
[87] Chimirri, A.; Grasso, S.; Monforte, P.; Rao, A.; Zappala, M.; Monforte, A. M.; Pannecouque, C.; Witvrouw, M.; Balzarini, J.; De Clercq, E. *Antivir. Chem. Chemother.*, **1999**, *10*, 211.
[88] Barreca, M. L.; Balzarini, J.; Chimirri, A.; De Clercq, E.; De Luca, L.; Höltje, H. D.; Höltje, M.; Monforte, A. M.; Monforte, P.; Pannecouque, C.; Rao, A.; Zappalà, M. *J. Med. Chem.*, **2002**, *45*, 5410.
[89] Maurer, K.; Tang, A. H.; Kenyon, G. L.; Leavitt, A. D. *Bioorg. Chem.*, **2000**, *28*, 140.
[90] Skillman, A. G.; Maurer, K. W.; Roe, D. C.; Stauber, M. J.; Eargle, D.; Ewing, T. J. A.; Muscate, A.; Davioud-Charvet, E.; Medaglia, M. V.; Fisher, R. J.; Arnold, E.; Gao, H. Q.; Buckheit, R.; Boyer, P. L.; Hughes, S. H.; Kuntz, I. D.; Kenyon, G. L. *Bioorg. Chem.*, **2002**, *30*, 443.
[91] Oiry, J.; Mialocq, P.; Puy, J.-Y.; Fretier, P.; Dereuddre-Bosquet, N.; Dormont, D.; Imbach, J.-L.; Clayette, P. *J. Med. Chem.*, **2004**, *47*, 1789.
[92] de Frutos, O.; Curran, D. P. *J. Comb. Chem.*, **2000**, *2*, 639.
[93] Curran, D. P.; Parniak, M. A.; Gabarda, A.; Zhang, W.; Luo, Z.; Hiu-tung, C. C. PCT Int. Appl. WO 03074524, 2003. (*Chem. Abstr.* **2003**, *139*, 246140)
[94] Lutzke, R. A. P.; Eppens, N. A.; Weber, P. A.; Houghten, R. A.; Plasterk, R. H. A. *Proc. Natl. Acad. Sci. USA*, **1995**, *92*, 11456.
[95] Srivastava, P.; Schito, M.; Fattah, R. J.; Hara, T.; Hartman, T.; Buckheit, R. W.; Turpin, J. A.; Inman, J. K.; Appella, E. *Bioorg. Med. Chem.*, **2004**, *12*, 6437.
[96] Park, W. K. C.; Auer, M.; Jaksche, H.; Wong, C. H. *J. Am. Chem. Soc.*, **1996**, *118*, 10150.
[97] Zambias, R. A.; Bolton, D. A.; Hogan, J. C.; Furth, P.; Casebier, D.; Tu, C.; Arenas, J. E. PCT Int. Appl. WO 9635953, **1996**. (*Chem. Abstr.* **1996**, *126*, 54853)
[98] Hamy, F.; Felder, E. R.; Heizmann, G.; Lazdins, J.; Aboul-ela, F.; Varani, G.; Karn, J.; Klimkait, T. *Proc. Natl. Acad. Sci. USA*, **1997**, *94*, 3548.
[99] Cabrera, C.; Gutierrez, A.; Barretina, J.; Blanco, J.; Litovchick, A.; Lapidot, A.; Clotet, B.; Este, J. A. *Antiviral Res.*, **2002**, *53*, 1.
[100] An, H.; Haly, B. D.; Cook, P. D. *Bioorg. Med. Chem. Lett.*, **1998**, *8*, 2345.
[101] Hwang, S.; Tamilarasu, N.; Kibler, K.; Cao, H.; Ali, A.; Ping, Y. H.; Jeang, K. T.; Rana, T. M. *J. Biol. Chem.*, **2003**, *278*, 39092.
[102] Owens, R. A.; Gesellchen, P. D.; Houchins, B. J.; DiMarchi, R. D. *Biochem. Biophys. Res. Commun.*, **1991**, *181*, 402.
[103] Dorsey, B. D.; Levin, R. B.; McDaniel, S. L.; Vacca, J. P.; Guare, J. P.; Darke, P. L.; Zugay, J. A.; Emini, E. A.; Schleif, W. A. *J. Med. Chem.*, **1994**, *37*, 3443.
[104] Cheng, Y.; Lu, Z.; Chapman, K. T.; Tata, J. R. *J. Comb. Chem.*, **2000**, *2*, 445.
[105] Rano, T. A.; Cheng, Y.; Huening, T. T.; Zhang, F.; Schleif, W. A.; Gabryelski, L.; Olsen, D. B.; Kuo, L. C.; Lin, J. H.; Xu, X.; Olah, T. V.; McLoughlin, D. A.; King, R.; Chapman, K. T.; Tata, J. R. *Bioorg. Med. Chem. Lett.*, **2000**, *10*, 1527.
[106] Cheng, Y.; Rano, T. A.; Huening, T. T.; Zhang, F.; Lu, Z.; Schleif, W. A.; Gabryelski, L.; Olsen, D. B.; Stahlhut, M.; Kuo, L. C.; Lin, J. H.; Xu, X.; Jin, L.; Olah, T. V.; McLoughlin, D. A.; King, R. C.; Chapman, K. T.; Tata, J. R. *Bioorg. Med. Chem. Lett.*, **2002**, *12*, 529.
[107] Raghavan, S.; Yang, Z.; Mosley, R. T.; Schleif, W. A.; Gabryelski, L.; Olsen, D. B.; Stahlhut, M.; Kuo, L. C.; Emini, E. A.; Chapman, K. T.; Tata, J. R. *Bioorg. Med. Chem. Lett.*, **2002**, *12*, 2855.
[108] Sheha, M. M.; Mahfouz, N. M.; Hassan, H. Y.; Youssef, A. F.; Mimoto, T.; Kiso, Y. *Eur. J. Med. Chem.*, **2000**, *35*, 887.
[109] Papanikos, A.; Meldal, M. *J. Comb. Chem.*, **2004**, *6*, 181.
[110] Kempf, D. J.; Codacovi, L.; Wang, X. C.; Kohlbrenner, W. E.; Wideburg, N. E.; Saldivar, A.; Vasavanonda, S.; Marsh, K. C.; Bryant, P. *J. Med. Chem.*, **1993**, *36*, 320.
[111] Reid, R. C.; Pattenden, L. K.; Tyndall, J. D. A.; Martin, J. L.; Walsh, T.; Fairlie, D. P. *J. Med. Chem.*, **2004**, *47*, 1641.
[112] Leroux, M. L.; Di Giorgio, C.; Patino, N.; Condom, R. *Tetrahedron Lett.*, **2002**, *43*, 1641.

**Received: March 09, 2005** **Revised: April 29, 2005** **Accepted: June 05, 2005**

DOI: 10.1002/cmdc.200800145

# Discovery of Novel Non-Cyclam Polynitrogenated CXCR4 Coreceptor Inhibitors

Sofia Pettersson,[a] Violeta I. Pérez-Nueno,[a] Laia Ros-Blanco,[a] Raimon Puig de La Bellacasa,[a] María Obdulia Rabal,[a] Xavier Batllori,[a] Bonaventura Clotet,[b] Imma Clotet-Codina,[b] Mercedes Armand-Ugón,[b] José Esté,[b] José I. Borrell,[a] and Jordi Teixidó*[a]

*HIV cell fusion and entry have been validated as targets for therapeutic intervention against infection. Bicyclams were the first low-molecular-weight compounds to show specific interaction with CXCR4. The most potent bicyclam was AMD3100, in which the two cyclam moieties are tethered by a 1,4-phenylenebis(methylene) bridge. It was withdrawn from clinical trials owing to its lack of oral bioavailability and cardiotoxicity. We have designed a combinatorial library of non-cyclam polynitrogenated compounds by preserving the main features of AMD3100. At least two nitrogen atoms on each side of the* p*-phenylene moiety, one in the benzylic position and the other(s) in the heterocyclic system were maintained, and the distances between them were similar to the nitrogen atom distances in cyclam. A selection of diverse compounds from this library were prepared, and their in vitro activity was tested in cell cultures against HIV strains. This led to the identification of novel potent CXCR4 coreceptor inhibitors without cytotoxicity at the tested concentrations.*

## Introduction

Studies in human immunodeficiency virus (HIV) biology have provided deep knowledge of the molecular events that are involved in the HIV life cycle, which consist of several steps: viral entry,[1,2] reverse transcription,[3–9] integration,[3,10–16] gene expression,[17,18] gene assembly,[19] budding[20] and maturation.[21] There is a need for the development of new drugs that are capable of suppressing HIV strains that are resistant to the currently used reverse transcriptase inhibitors (RTI) or protease inhibitors (PI), and for new drugs that target different stages in the virus life cycle.

HIV cell fusion and entry have been validated as targets for therapeutic intervention against infection.[2] The virus needs a primary receptor (CD4) and a coreceptor, either the chemokine receptor CXCR4 or CCR5, to fuse with the cell. Thus, they became new therapeutic targets for the treatment or prevention of HIV infection.

There are two approved entry and fusion inhibitors: T-20 (Fuzeon or enfuvirtide, developed by Roche–Trimeris), a linear 36 amino acid synthetic peptide with an acetylated N terminus and a carboxamide C terminus that is composed of naturally occurring L-amino acid residues, and maraviroc (Selzentry),[22] a CCR5 inhibitor. The first nonpeptidic CCR5 antagonist was TAK-779[23] (Figure 1), from Takeda Chemicals, although it could not be developed as an anti-HIV-1 drug because of its variable activity and poor oral bioavailability. Later, SCH-D[24] (vicriviroc, Figure 1), was developed by Schering–Plough; it had improved antiviral potency and better pharmacological properties relative to its predecessor SCH-C,[25] and has continued to phase III clinical trials. GW873140 (aplaviroc),[26] a spiroketopiperazine-based agent from Ono Pharmaceutical/GlaxoSmithKline, exhibited potent antiviral activity but has been discontinued for clinical development as an anti-HIV agent. Another class of anti-HIV agents that targets CCR5 includes PRO 140[27] (Progenics Pharmaceuticals), a humanized monoclonal antibody that is designed to block the ability of HIV to enter and infect cells; this antibody is in phase Ib clinical studies. In addition, CCR5 antagonists and monoclonal antibodies have shown potent synergistic antiviral effects by co-binding the receptor.[28]

Bicyclams were the first low-molecular-weight compounds with a specific interaction with CXCR4.[29–32] The most potent bicyclam was AMD3100 (Figure 1) in which the two cyclam moieties are tethered by a 1,4-phenylenebis(methylene) bridge. It has an $IC_{50}$ of 1–10 ng mL$^{-1}$, which is at least 100 000-fold lower than the cytotoxic concentration. Samples of virus that were recovered from patients whom had been treated with AMD3100 (bicyclam) showed a change in virus phenotype, from X4 to R5; this suggests that AMD3100 blocked selectively those viruses that use CXCR4, although it was not effective in inhibiting CCR5-dependent replication of HIV in vivo. However, AMD3100 has shown poor oral absorption and toxicity, which is related to its high positive charge at physiological

[a] *S. Pettersson, V. I. Pérez-Nueno, L. Ros-Blanco, R. Puig de La Bellacasa, Dr. M. O. Rabal, Dr. X. Batllori, Dr. J. I. Borrell, Dr. J. Teixidó*
*Grup d'Enginyeria Molecular*
*Institut Químic de Sarrià, Universitat Ramon Llull*
*Via Augusta 390, 08017 Barcelona (Spain)*
*Fax: (+34) 93-205-6266*
*E-mail: j.teixido@iqs.url.edu*

[b] *Dr. B. Clotet, Dr. I. Clotet-Codina, Dr. M. Armand-Ugón, Dr. J. Esté*
*Retrovirology Laboratory IrsiCaixa*
*Hospital Universitari Germans Trias i Pujol*
*Universitat Autònoma de Barcelona*
*08916 Badalona (Spain)*

Supporting information for this article is available on the WWW under http://dx.doi.org/10.1002/cmdc.200800145.

  

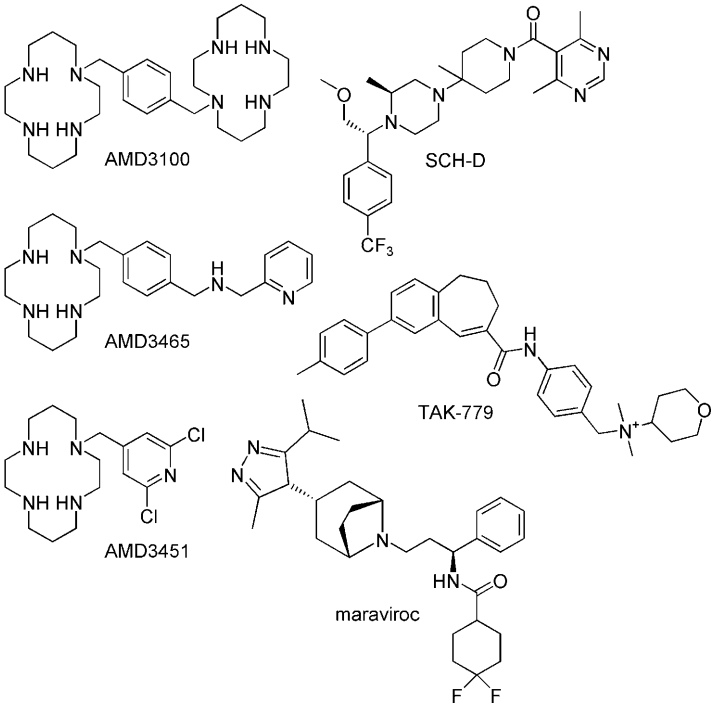


**Figure 1.** Structures of the main CXCR4 and CCR5 antagonist leads; they have aromatic or aliphatic linkers in polynitrogenated systems.

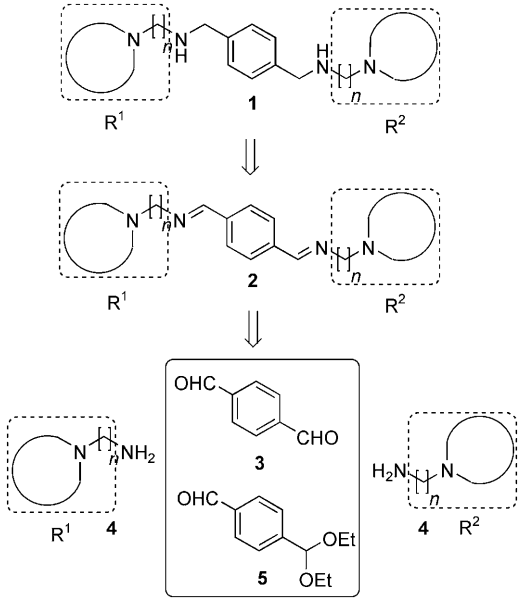


**Figure 2.** Retrosynthetic analysis for target diamines **1** ($n \geq 1$) and dihydrazones **2** ($n = 0$).

pH, therefore new analogous compounds should improve these characteristics.[33]

CXCR4 and CCR5 antagonist leads, such as AMD3100 (bicyclam), SCH-D or TAK-779 contain aromatic or aliphatic linkers in polynitrogenated systems. Among all of the compounds under study, bicyclams in general, and particularly AMD3100, appear to be the most active. *p*-Phenylenic compounds with a single cyclam moiety have also been developed, such as AMD3465 (Figure 1),[33] which is a CXCR4 antagonist, and AMD3451,[34] which shows antagonist activity against both CXCR4 and CCR5 coreceptors in cell culture studies. This led us to consider the possibility of obtaining symmetrical and nonsymmetrical systems that contain a *p*-phenylenic spacer and nitrogenated cyclic subunits in the search for new compounds that are potentially active against HIV-1. Herein we present the results of these studies.

### Library design and compound selection

We designed a combinatorial library[35] by preserving the main features of AMD3100: a) at least two nitrogen atoms on each side of the *p*-phenylene moiety, one in the benzylic position and the other(s) in a heterocyclic system and b) similar distances between these nitrogen atoms as those that are present in cyclam. Such considerations led us to diamines **1** as target compounds (Figure 2). Very recently a similar but less restrictive approach was used by Liotta and colleagues[36] to propose a family of compounds whose general structure, $R^3R^4NCH_2C_6H_4CH_2NR^1R^2$, led to a large scaffold diversity. The most active compound in their library blocks in vitro CXCR4/SDF-1-mediated signaling more effectively than AMD3100, but they found it to be weakly active against HIV propagation in cell culture tests.

A retrosynthetic analysis for target compounds **1** in which $R^1 = R^2$ and $n \geq 1$ led to the symmetrical diimines **2** as precursors, which can be further disconnected to terephthalaldehyde (**3**) and two equivalents of the corresponding amine **4** ($n \geq 1$). When $R^1 = R^2$ and $n = 0$, compounds **2** are in fact symmetrical hydrazones, which can be obtained by condensation of terephthalaldehyde and the corresponding hydrazine **4** ($n = 0$). These dihydrazones were also included in our library.

To obtain nonsymmetrical ($R^1 \neq R^2$) diamines **1** ($n \geq 1$) and dihydrazones **2** ($n = 0$), it was necessary to slightly modify our synthetic approach by using 4-(diethoxymethyl)benzaldehyde (**5**) as the core precursor (Scheme 1). Thus, intermediate hydrazono and aminobenzaldehydes **6** and **7** allowed us to include such nonsymmetrical compounds and nonsymmetrical aminohydrazones **8** as target compounds.

The first selection of nitrogenated building blocks was based on commercial availability; the use of synthetic building blocks is currently under development. A search for available building blocks resulted in 18 commercially available nitrogenated building blocks that consist of a nitrogen-containing heterocyclic system (piperidine, piperazine, morpholine, pyrrolidine, imidazole and triazole), a polymethylene spacer, and a terminal amine group (Figure 3). Consequently, the virtual combinatorial library was built by using three hydrazines **4**{*1–3*} and eight amines **4**{*4–11*} as building blocks for substituents $R^1$ and $R^2$ of diamines **1**, dihydrazones **2** and aminohydrazones **8**, and it was subsequently enumerated with Cerius2.[37]

In an attempt to explore the chemical space that is covered by the library, we initially decided to select a reduced set of 19 compounds by using PRALINS[38] (*Program for Rational Analysis of Libraries in silico*) and by applying a diversity criteria, which decreases the number of compounds to be synthesized and

  

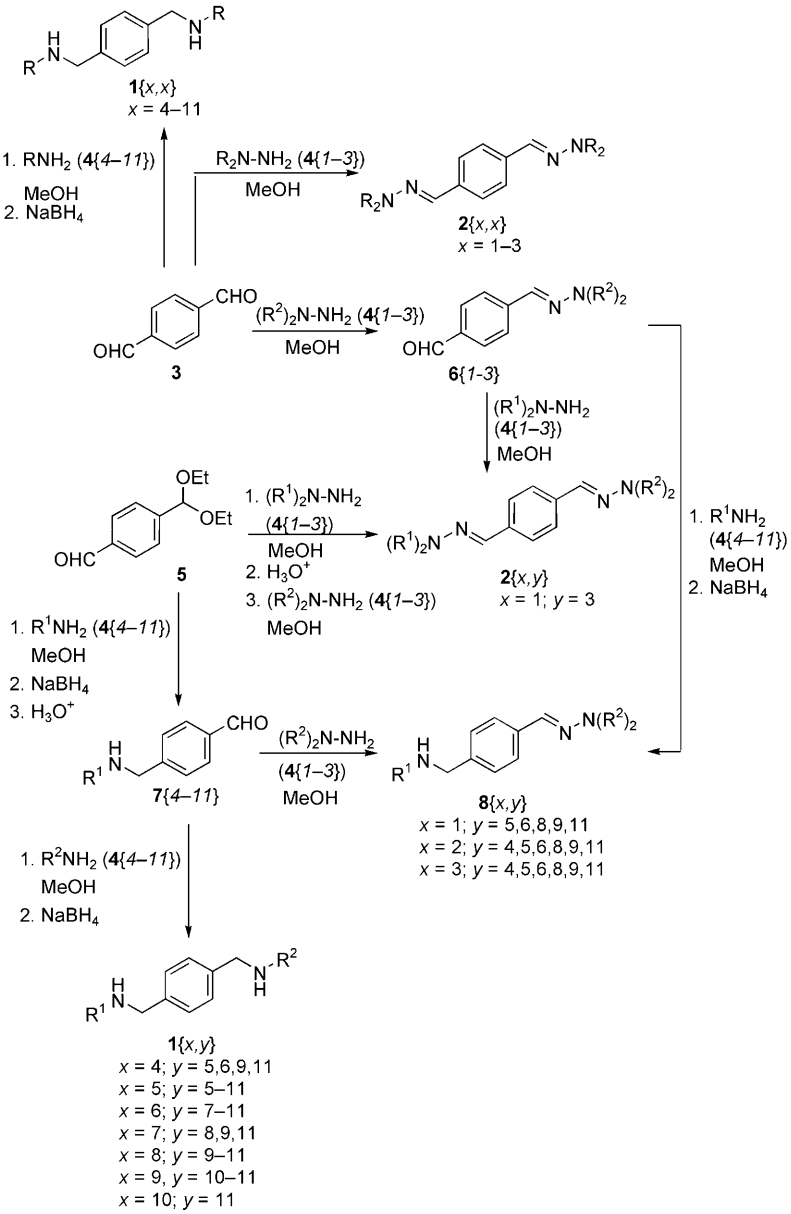


**Scheme 1.** Synthesis of symmetrical and nonsymmetrical diamines **1**, dihydrazones **2**, and aminohydrazones **8**.

strategies that were used to obtain diamines **1**, dihydrazones **2** and aminohydrazones **8** are depicted in Scheme 1. For the synthesis of symmetrical diamines **1** ($R^1 = R^2$), we used a stepwise reductive amination:[41] a) reflux of a mixture of **3** and the corresponding amine **4**{*4–11*} (1:2 molar ratio) in anhydrous methanol by using molecular sieves as a dehydrating agent, and b) subsequent reduction with $NaBH_4$.[35]

Symmetrical dihydrazones **2** ($R^1 = R^2$) were obtained by condensation of **3** with the corresponding hydrazines **4**{*1–3*} in methanol (Scheme 1). Nonsymmetrical ($R^1 \neq R^2$) diamines **1**, dihydrazones **2**, and aminohydrazones **8** needed more complex approaches. Thus, hydrazonobenzaldehydes **6** were synthesized by coupling terephthalaldehyde (**3**) with hydrazines **4**{*1–3*} in a 2:1 molar ratio, followed by chromatographic separation from unreacted **3** and the symmetrical dihydrazone **2** byproduct. The subsequent coupling with a second hydrazine **4**{*1–3*} would afford the nonsymmetrical dihydrazones **2** ($R^1 \neq R^2$) (Scheme 1). This procedure has been used to obtain dihydrazone **2**{*1,3*}.

On the other hand, 4-(diethoxymethyl)benzaldehyde (**5**) was selected as building block to obtain aminobenzaldehydes **7** by reacting equimolar amounts of **5** and the corresponding amine **4**{*4–11*}, followed by reduction of the intermediate iminoacetal and subsequent acetal cleavage with a dilute solution of aqueous hydrochloric acid.[42–44] Treatment of these aminobenzaldehydes **7** with a second amine **4**{*4–11*} in anhydrous MeOH, by using molecular sieves as dehydrating agent, followed by reduction with $NaBH_4$, yielded the nonsymmetrical diamines **1** ($R^1 \neq R^2$) (Scheme 1). Finally, aminohydrazones **8** were accessible either by reductive amination of hydrazonobenzaldehydes **6** with the appropriate amine **4**{*4–11*} or by coupling of the aminobenzaldehydes **7** with the corresponding hydrazine **4**{*1–3*} (Scheme 1).

evaluated without decreasing the chance of hit/lead finding. Thus, a series of molecular 2D (physicochemical, topological and topological based on information theory) and 3D (potential energy, surface, shape and volume) descriptors (computed with MOE[39]) were used for the definition of the chemical space. A subsequent principal component analysis decreased the initial set of descriptors to five components (explaining 90% of the variance) which were used as input for the diversity selection with PRALINS; this resulted in the selection of 19 compounds (Table 1).

### Chemistry

Combinatorial approaches have been widely used in the identification of novel anti-HIV drugs;[40] in our case, the synthetic

## Results and Discussion

The first subset of compounds synthesized and tested (anti-HIV activity and cytotoxicity) included eight compounds: two dihydrazones (**2**{*1,1*} and **2**{*2,2*}) and six diamines (**1**{*3,4*}, **1**{*5,5*}, **1**{*6,6*}, **1**{*6,11*}, **1**{*9,9*} and **1**{*11,11*}) chosen among the 19 compounds result of the diversity selection. Three of them (**1**{*5,5*}, **1**{*9,9*} and **1**{*6,11*}) showed very promising anti-HIV activities, $EC_{50}$ in the range 0.9–18 $\mu g\,mL^{-1}$ (Table 1), so we decided to include structural modifications of them together with the remaining initial 19 candidates.

Thus, the second subset of compounds synthesized and tested was formed by seventeen compounds: one dihydrazone (**2**{*1,3*}), ten diamines (**1**{*6,7*}, **1**{*5,8*}, **1**{*5,10*}, **1**{*5,11*}, **1**{*4,5*}, **1**{*5,6*}, **1**{*5,7*}, **1**{*5,9*}, **1**{*9,10*} and **1**{*9,11*}) and six amino hydrazones (**8**{*3,5*}, **8**{*3,6*}, **8**{*3,8*}, **8**{*3,9*}, **8**{*1,5*} and **8**{*2,5*}). Twelve of these

  

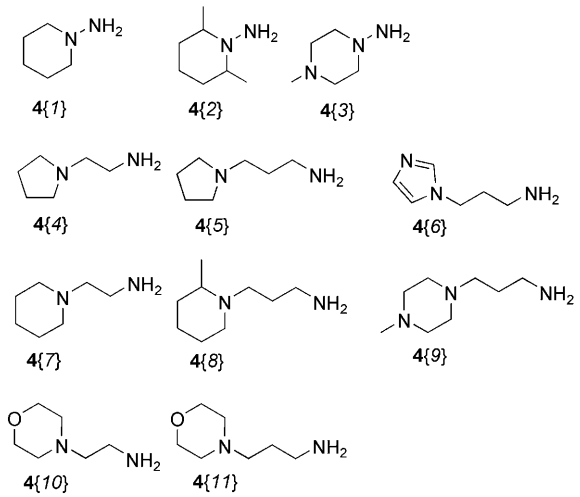


**Figure 3.** Amine building blocks used in the construction of the virtual combinatorial library.

compounds presented $EC_{50}$ in the range 0.2 to 2.7 μg mL$^{-1}$, the most potent being **1**{*5,6*} and **1**{*5,8*} (0.2 μg mL$^{-1}$) (Table 1).

The third and final subset, which included 28 compounds, thus covering the total of 53 compounds synthesized and tested (Table 1), was selected by using computational analysis tools such as quantitative structure–activity relationships (QSAR) techniques and ligand- and structure-based drug design (for CXCR4 and CCR5 modeled HIV-1 entry coreceptors).[45,46] Notable compounds of this subset are **1**{*6,8*} ($EC_{50}$ = 0.03 μg mL$^{-1}$), **1**{*8,9*} ($EC_{50}$ = 0.03 μg mL$^{-1}$), and the most active compound in the library, **1**{*8,8*}, which has an $EC_{50}$ value of 0.008 μg mL$^{-1}$ and a $CC_{50}$ > 25 μg mL$^{-1}$.

Among the different polynitrogenated building blocks, $RNH_2$, amines **4**{*5*} and **4**{*8*} gave the most active compounds. $EC_{50}$ results suggest that higher activity values could be obtained by using a propylenic spacer between the heterocyclic ring and the nitrogen that supports the *p*-phenylenic moiety, and for heterocyclic systems that contain one nitrogen atom.

To evaluate the results, we determined the $EC_{50}$ and $CC_{50}$ of AMD3100 ($EC_{50}$ = 0.001 μg mL$^{-1}$; $CC_{50}$ > 5 μg mL$^{-1}$) and DS (dextran sulfate) ($EC_{50}$ = 0.011 μg mL$^{-1}$; $CC_{50}$ > 125 μg mL$^{-1}$) by following the same methodology as for our compounds. As can be seen, compound **1**{*8,8*} presents nearly the same level of activity as the reference compounds, **1**{*8,8*} ($EC_{50}$ = 0.019 μM) and AMD3100 ($EC_{50}$ = 0.002 μM), and shows no cell toxicity at the tested concentrations of up to 25 μg mL$^{-1}$.

Computational blind docking and ligand binding within the CXCR4 site-directed mutagenesis (SDM)-defined binding pocket[47] were analyzed in detail by using AutoDock[48,49] to study the interactions between **1**{*8,8*} and the CXCR4 coreceptor. To perform these calculations, CXCR4 was first homology modeled with MODELLER[50] and CONGEN[51] by using bovine rhodopsin as a template[52] as described in Pérez-Nueno et al.[53] The compound **1**{*8,8*} structure was built, assigned Gasteiger partial charges,[54] and minimized in MOE with the MMFF94 force field. For the AutoDock blind docking experiment, a 181×181×181 grid with a grid spacing of 0.375 Å was

**Table 1.** $EC_{50}$ and $CC_{50}$ values of diamines **1**, dihydrazones **2**, and aminohydrazones **8**.

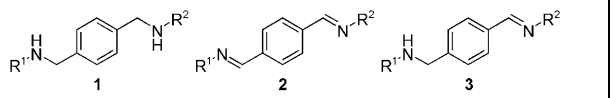


| Subset[a] | Compound | $R^1NH_2$ | $R^2NH_2$ | $EC_{50}$ [μg mL$^{-1}$][b] | $CC_{50}$ [μg mL$^{-1}$][c] |
|---|---|---|---|---|---|
| **1** | **2**{*1,1*} | **4**{*1*} | **4**{*1*} | > 125 | > 125 |
| **2** | **2**{*1,3*} | **4**{*1*} | **4**{*3*} | > 25 | > 25 |
| 2 | **8**{*1,5*} | **4**{*1*} | **4**{*5*} | 2.7 | 10.1 |
| 3 | **8**{*1,6*} | **4**{*1*} | **4**{*6*} | > 25 | > 25 |
| 3 | **8**{*1,8*} | **4**{*1*} | **4**{*8*} | > 4.1 | 4.1 |
| 3 | **8**{*1,9*} | **4**{*1*} | **4**{*9*} | > 9.8 | 9.8 |
| 3 | **8**{*1,11*} | **4**{*1*} | **4**{*11*} | 10.6 | > 25 |
| **1** | **2**{*2,2*} | **4**{*2*} | **4**{*2*} | > 125 | > 125 |
| **3** | **8**{*2,4*} | **4**{*2*} | **4**{*4*} | 14.7 | > 25 |
| 2 | **8**{*2,5*} | **4**{*2*} | **4**{*5*} | 2.0 | 9.8 |
| 3 | **8**{*2,6*} | **4**{*2*} | **4**{*6*} | > 25 | > 25 |
| 3 | **8**{*2,8*} | **4**{*2*} | **4**{*8*} | 0.6 | 14.6 |
| 3 | **8**{*2,9*} | **4**{*2*} | **4**{*9*} | 3.8 | 19.2 |
| 3 | **8**{*2,11*} | **4**{*2*} | **4**{*11*} | 15.7 | > 25 |
| 3 | **2**{*3,3*} | **4**{*3*} | **4**{*3*} | > 125 | > 125 |
| **1** | **8**{*3,4*} | **4**{*3*} | **4**{*4*} | > 84.9 | 84.9 |
| **2** | **8**{*3,5*} | **4**{*3*} | **4**{*5*} | 1.8 | 14.3 |
| **2** | **8**{*3,6*} | **4**{*3*} | **4**{*6*} | 11.2 | > 25 |
| **2** | **8**{*3,8*} | **4**{*3*} | **4**{*8*} | 1.4 | 10.3 |
| **2** | **8**{*3,9*} | **4**{*3*} | **4**{*9*} | 11.7 | > 25 |
| 3 | **8**{*3,11*} | **4**{*3*} | **4**{*11*} | 8.1 | > 25 |
| 3 | **1**{*4,4*} | **4**{*4*} | **4**{*4*} | 10.2 | > 25 |
| 2 | **1**{*4,5*} | **4**{*4*} | **4**{*5*} | 1.7 | > 25 |
| 3 | **1**{*4,6*} | **4**{*4*} | **4**{*6*} | 4.8 | > 25 |
| 3 | **1**{*4,9*} | **4**{*4*} | **4**{*9*} | 8.2 | > 25 |
| 3 | **1**{*4,11*} | **4**{*4*} | **4**{*11*} | > 25 | > 25 |
| **1** | **1**{*5,5*} | **4**{*5*} | **4**{*5*} | 0.9 | 32.4 |
| 2 | **1**{*5,6*} | **4**{*5*} | **4**{*6*} | 0.2 | > 25 |
| 2 | **1**{*5,7*} | **4**{*5*} | **4**{*7*} | 1.7 | > 25 |
| **2** | **1**{*5,8*} | **4**{*5*} | **4**{*8*} | 0.2 | > 25 |
| 2 | **1**{*5,9*} | **4**{*5*} | **4**{*9*} | 0.5 | > 25 |
| **2** | **1**{*5,10*} | **4**{*5*} | **4**{*10*} | 2.4 | > 25 |
| **2** | **1**{*5,11*} | **4**{*5*} | **4**{*11*} | 1.6 | > 25 |
| **1** | **1**{*6,6*} | **4**{*6*} | **4**{*6*} | > 59.5 | 59.5 |
| **2** | **1**{*6,7*} | **4**{*6*} | **4**{*7*} | 2.0 | > 25 |
| 3 | **1**{*6,8*} | **4**{*6*} | **4**{*8*} | 0.03 | > 25 |
| 3 | **1**{*6,9*} | **4**{*6*} | **4**{*9*} | > 25 | > 25 |
| 3 | **1**{*6,10*} | **4**{*6*} | **4**{*10*} | > 25 | > 25 |
| **1** | **1**{*6,11*} | **4**{*6*} | **4**{*11*} | 18.4 | > 125 |
| 3 | **1**{*7,7*} | **4**{*7*} | **4**{*7*} | > 11.7 | 11.7 |
| 3 | **1**{*7,8*} | **4**{*7*} | **4**{*8*} | 0.5 | > 25 |
| 3 | **1**{*7,9*} | **4**{*7*} | **4**{*9*} | 2.5 | > 25 |
| 3 | **1**{*7,11*} | **4**{*7*} | **4**{*11*} | 2.7 | > 25 |
| 3 | **1**{*8,8*} | **4**{*8*} | **4**{*8*} | 0.008 | > 25 |
| 3 | **1**{*8,9*} | **4**{*8*} | **4**{*9*} | 0.03 | > 25 |
| **3** | **1**{*8,10*} | **4**{*8*} | **4**{*10*} | 0.4 | > 25 |
| 3 | **1**{*8,11*} | **4**{*8*} | **4**{*11*} | 0.5 | > 25 |
| **1** | **1**{*9,9*} | **4**{*9*} | **4**{*9*} | 9.5 | > 125 |
| 2 | **1**{*9,10*} | **4**{*9*} | **4**{*10*} | > 25 | > 25 |
| 2 | **1**{*9,11*} | **4**{*9*} | **4**{*11*} | 9.1 | > 25 |
| 3 | **1**{*10,10*} | **4**{*10*} | **4**{*10*} | > 85.7 | 85.7 |
| 3 | **1**{*10,11*} | **4**{*10*} | **4**{*11*} | > 25 | > 25 |
| **1** | **1**{*11,11*} | **4**{*11*} | **4**{*11*} | > 125 | > 125 |

[a] Subsets of synthesized and tested compounds, in bold for the diversity selection with PRALINS. [b] Effective concentration 50 or the concentration required to inhibit HIV-induced cell death by 50% as evaluated with the MTT method in MT-4 cells. [c] Cytotoxic concentration 50 or the concentration required to induce 50% death of non-infected MT-4 cells as evaluated with the MTT method. Reference compounds: AMD3100: $EC_{50}$ = 0.001 μg mL$^{-1}$, $CC_{50}$ = > 5 μg mL$^{-1}$; DS: $EC_{50}$ = 0.011 μg mL$^{-1}$, $CC_{50}$ = > 125 μg mL$^{-1}$.

  

used, and was centered on the SDM-defined ligand-binding site. This grid enclosed the whole protein structure, and the ligand was initially placed far from the protein to include the possibility of finding other binding sites. A smaller (61×61×61) grid was used for the subsequent binding mode analysis calculations. In each case, 100 independent Lamarckian genetic algorithm (LGA) runs were performed and pseudo-Solis and Wets minimization methods were applied by using default parameters. Each docking run was repeated five times. Results from docking analyses were assessed by using the knowledge of the SDM data. They showed two main electrostatic interactions between two positively charged nitrogen atoms in compound **1**{*8,8*} and negatively charged Asp262 and Glu288 residues of the CXCR4 coreceptor (Figure 4). The lowest distances

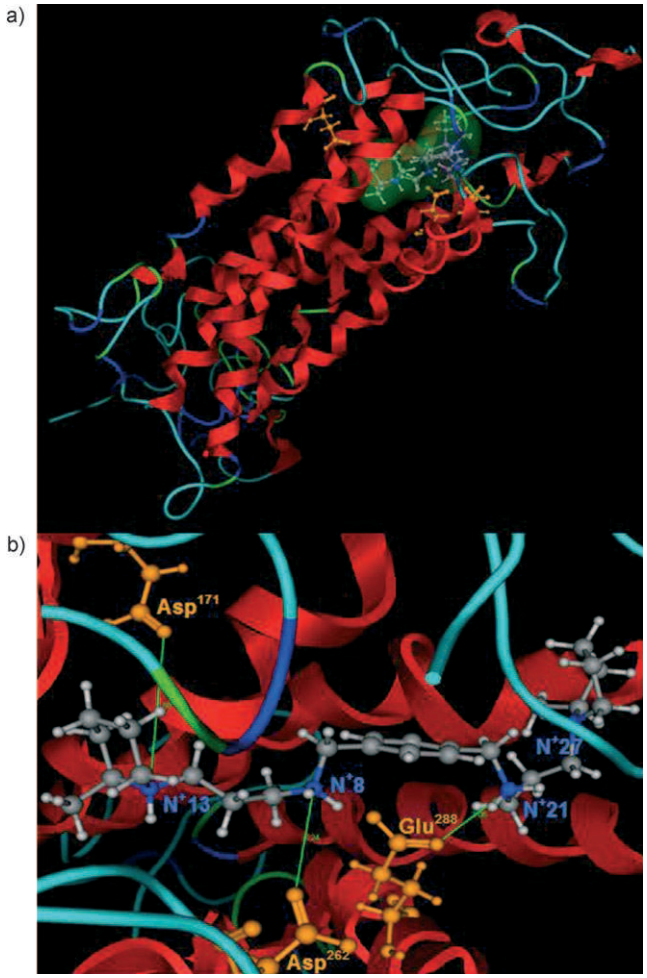


**Figure 4.** Predicted binding conformation between **1**{*8,8*} and CXCR4 from blind docking analysis. a) Compound **1**{*8,8*} docked within the CXCR4 pocket; b) detailed view of the calculated binding conformation.

from the carboxylic oxygen atoms of the three key binding residues Asp171, Asp262, and Glu288, to the four nitrogen atoms (N27, N21, N8, N13) of **1**{*8,8*} are shown in green: 6.88 Å between $N^+13$ and O(sp2) Asp171, 5.24 Å between $N^+8$ and O(sp2) Asp262, and 3.06 Å between $N^+21$ and O(sp2) Glu288.

Our docking results for **1**{*8,8*} agree with those of Gerlach et al.[55] on the mutagenic substitution of 16 CXCR4 amino acids, in which the three acidic residues, Asp171, Asp262, and Glu288, were identified as the main electrostatic interaction points for positively charged AMD3100 bicyclam rings binding. Moreover, the same study was performed with the AMD3100 ligand as is described in Pérez-Nueno et al.[53] Results with this known active ligand, by using only the same docking protocol as mentioned above, also agree with the **1**{*8,8*} docking results. It is worth mentioning that by using molecular dynamics (MD) it is possible to refine the CXCR4 docking poses to obtain ligand conformations that are closer to the key SDM residues.[56–58] For example, applying 200 ps of AMBER MD to our docking poses by using a protocol as described by Orozco and co-workers[59] gives ligand conformations with an average distance of 2 Å closer to the key binding residues. However, in this work we were more interested in the possibility of predicting a binding site and a binding mode of our more active synthesized molecules by using a docking tool only.

Finally, we carried out time-of-drug-addition experiments to identify the time and site of interaction of our anti-HIV compounds. It is known that the time delay before the addition of a drug is an estimate of its mode of action. Consequently, we determined the time of drug addition for the four most active compounds **1**{*8,8*}, **1**{*6,8*}, **1**{*8,9*} and **1**{*8,10*} compared with a CXCR4 antagonist (AMD3100), a reverse transcriptase inhibitor (AZT; azidothymidine), a fusion inhibitor (C34) and an adhesion inhibitor (DS; dextran sulfate) to confirm the initial hypothesis that the designed compounds act as CXCR4 inhibitors. The results that were obtained (Figure 5) clearly show that these compounds share a time/site of interaction that is similar to that of AMD3100 and act as blockers of the CXCR4 coreceptor. Furthermore, compounds **1**{*8,8*}, **1**{*6,8*}, **1**{*8,9*} completely blocked the binding of the 12G5 monoclonal antibody that targets CXCR4 at 25 μg mL$^{-1}$ as measured by flow cytometry analysis in CXCR4+ cells, but failed to block the binding of antibodies that target CD4, CCR5 or CD45 (data not shown); this

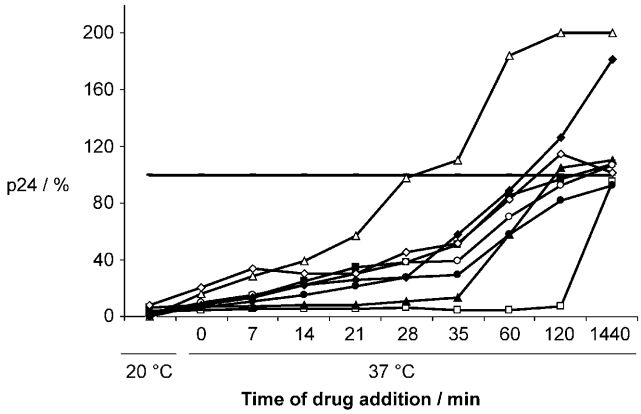


**Figure 5.** Time of drug addition in MT-4 cells of **1**{*8,8*} (◇), **1**{*6,8*} (●), **1**{*8,9*} (○), and **1**{*8,10*} (◆) in comparison with AZT (□), AMD3100 (■), DS (△), and C34 (▲); control: (——). Virus production was measured by p24 antigen determination in the cell supernatant 30 h post-infection, and is expressed as percentage of control values.

  

suggests that this class of compounds is very selective for the CXCR4 receptor.

## Conclusions

We have designed a combinatorial library of non-cyclam AMD3100 analogues that preserves the main features of AMD3100: a) at least two nitrogen atoms on each side of the *p*-phenylene moiety, one in the benzylic position and the other(s) in a heterocyclic system, and b) similar distances between these nitrogen atoms as those present in cyclam. A diversity-oriented selection has allowed the synthesis of diamines **1**, dihydrazones **2** and aminohydrazones **8**; these compounds cover a broad range of activity values and are useful for calculating QSAR models. This approach led to the synthesis of compounds **1**{*6,8*}, **1**{*8,9*} and **1**{*8,8*}, which show anti-HIV activity values below 0.03 μg mL$^{-1}$ but have displayed no cytotoxic effects at the tested concentrations. Studies on the mode of action of these compounds showed that they inhibited the CXCR4 coreceptor, thus validating the initial target compound design. A combinatorial optimization of the anti-HIV activity of this new family of compounds by using noncommercial amines of general structure **4** is currently on the way.

## Experimental Section

### *Chemistry*

IR spectra were recorded in a Nicolet Magna 560 FTIR spectrophotometer. $^1$H and $^{13}$C NMR spectra were recorded in a Varian Gemini 300 spectrometer that was operating at a field strength of 300 and 75.5 MHz, respectively. Chemical shifts were reported in parts per million ($\delta$) and coupling constants ($J$) were in Hz by using, in the case of $^1$H NMR spectroscopy, TMS as an internal standard, and in the case of $^{13}$C NMR spectroscopy the solvent at 77.0 ppm ($CDCl_3$) as an internal reference. Standard and peak multiplicities are designated as follows: s, singlet; d, doublet; t, triplet; q, quartet; quint, quintet; m, multiplet; br, broad signal. MS data (*m/z* (%), EI, 70 eV) were obtained by using a Hewlett–Packard HP5988A spectrometer, and HRMS data were obtained by using a Micromass Autospec instrument. Elemental microanalyses were obtained on a Carlo–Erba CHNS-O/EA 1108 analyzer. Thin-layer chromatography (TLC) was performed on precoated sheets of silica 60 Polygram SIL N-HR/$UV_{254}$ (Macherey–Nagel, art. 804023). Flash chromatography was performed with silica gel 35–70 μm (SDS, art. 2000027).

***N*-(4-((2-(Pyrrolidin-1-yl)ethylamino)methyl)benzyl)-2-(pyrrolidin-1-yl)ethanamine (1{*4,4*})**. Terephthalaldehyde (**3**) (0.61 g, 4.5 mmol), 1-(2-aminoethyl)pyrrolidine **4**{*4*} (1.04 g, 9.0 mmol) and molecular sieves (4 Å) were mixed in anhydrous MeOH (30 mL) and held at reflux under a $N_2$ atmosphere for 24 h. The molecular sieves were filtered, and the intermediate imine in MeOH was cooled to 0 °C and treated with solid $NaBH_4$ (0.34 g, 9.0 mmol). The mixture was stirred at RT overnight. Then $H_2O$ was added and the product was extracted with $CH_2Cl_2$ The organic layers were combined, washed with brine, dried over $MgSO_4$ and the solvent was removed to give **1**{*4,4*} as a yellow oil (1.32 g, 89%). $^1$H NMR (300 MHz, $CDCl_3$, 25 °C, TMS): $\delta$ = 7.27 (s, 4H; Ph), 3.79 (s, 4H; C*H*$_2$Ph), 2.73 (t, $^3J_{H,H}$ = 6.0 Hz, 4H; C*H*$_2$NH), 2.59 (t, $^3J_{H,H}$ = 6.0 Hz, 4H; $CH_2$N), 2.47 (m, 8H; $CH_2$N), 2.20 (br s, 2H; NH), 1.75 ppm (quint, $^{33}J_{H,H}$ = 3.3 Hz, 8H; $CH_2$); $^{13}$C NMR (75.5 MHz, $CDCl_3$, 25 °C): $\delta$ = 138.8 (Cq), 128.0 (CH), 55.9 ($CH_2$), 54.2 ($CH_2$), 53.8 ($CH_2$), 47.8 ($CH_2$), 23.5 ppm ($CH_2$); IR (film): $\tilde{\nu}$ = 3310 (NH), 2962, 2928, 2874, 2794 (CH), 1485, 1444 cm$^{-1}$ (CH); MS (FAB): *m/z* (%): 331.3 (100) $[M+H]^+$, 330.3 (18) $[M]^+$, 329.3 (77) $[M-H]^+$; HRMS calcd for $C_{20}H_{35}N_4$: 331.2862 $[M+H]^+$, found: 331.2867.

***N*-(4-((3-(2-Methylpiperidin-1-yl)propylamino)methyl)benzyl)-3-(2-methylpiperidin-1-yl)propan-1-amine (1{*8,8*})**. The procedure was the same as that stated above for **1**{*4,4*}, but was carried out by using terephthalaldehyde (**3**) (0.43 g, 3.2 mmol), 1-(3-aminopropyl)-2-methyl-piperidine **4**{*8*} (1.04 g, 6.4 mmol) and $NaBH_4$ (0.25 g, 6.4 mmol) to give **1**{*8,8*} as a pale-brown oil (1.33 g, 100%). $^1$H NMR (300 MHz, $CDCl_3$, 25 °C, TMS): $\delta$ = 7.27 (s, 4H; Ph), 3.77 (s, 4H; C*H*$_2$Ph), 2.87 (m, 2H; $CH_{eq}$N), 2.73 (m, 2H; $CH_{eq}$), 2.63 (t, $^3J_{H,H}$ = 6.9 Hz, 4H; C*H*$_2$NH), 2.36 (m, 2H; $CH_{ax}$N), 2.26 (m, 2H; C*H*$CH_3$), 2.14 (br s, 2H; NH), 2.11 (m, 2H; $CH_{ax}$N),1.68 (quint, $^3J_{H,H}$ = 6.9 Hz, 4H; $CH_2$), 1.61 (m, 2H; $CH_{eq}$), 1.58 (m, 2H; $CH_{eq}$), 1.52 (m, 2H; $CH_{eq}$), 1.44 (m, 2H; $CH_{ax}$), 1.28 (m, 4H; $CH_{ax}$), 1.05 ppm (d, $^3J_{H,H}$ = 6.3 Hz, 6H; $CH_3$); $^{13}$C NMR (75.5 MHz, $CDCl_3$, 25 °C): $\delta$ = 138.8 (Cq), 128.0 (CH), 55.9 (CH), 53.7 ($CH_2$), 52.3 ($CH_2$), 52.1 ($CH_2$), 48.3 ($CH_2$), 34.7 ($CH_2$), 26.2 ($CH_2$), 25.7 ($CH_2$), 24.0 ($CH_2$), 19.1 ppm ($CH_3$); IR (film): $\tilde{\nu}$ = 3282 (NH), 2929, 2854, 2793 (CH), 1449, 1372 cm$^{-1}$ (CH); MS (EI): *m/z* (%): 415.4 (0.4) $[M+H]^+$, 112.1 (100) $[C_7H_{14}N]^+$; Anal. ($C_{26}H_{46}N_4$) C, H, N.

**((4-(*N*-(Piperidin-1-yl)imino)methyl)phenyl)-*N*-(piperidin-1-yl)methanamine (2{*1,1*})**. Terephthalaldehyde (**3**) (0.99 g, 7.3 mmol), 1-aminopiperidine **4**{*1*} (1.51 g, 14.7 mmol) and 4 Å molecular sieves were mixed in anhyd MeOH (30 mL) and held at reflux under a $N_2$ atmosphere for 16 h. The molecular sieves were filtered, and the solvent was partially removed. The crude oil was cooled, and the resulting precipitate was filtered and rinsed with cold MeOH to give **2**{*1,1*} as a yellow solid (1.42 g, 65%). $^1$H NMR (300 MHz, $CDCl_3$, 25 °C, TMS): $\delta$ = 7.55 (s, 4H; Ph), 7.53 (s, 2H; CH=N), 3.16 (m, 8H; CHN), 1.79–1.71 (m, 8H; $CH_2$), 1.58–1.50 ppm (m, 4H; $CH_2$); $^{13}$C NMR (75.5 MHz, $CDCl_3$, 25 °C): $\delta$ = 136.0 (Cq), 134.3 (CH), 125.9 (CH), 52.1 ($CH_2$), 25.3 ($CH_2$), 24.2 ppm ($CH_2$); IR (film): $\tilde{\nu}$ = 1576 cm$^{-1}$ (C=N); Anal. ($C_{18}H_{26}N_4$) C, H, N.

**4-((2-(Pyrrolidin-1-yl)ethylamino)methyl)benzaldehyde (7{*4*})**. 4-(Diethoxymethyl)benzaldehyde (**5**) (2.01 g, 9.3 mmol), 1-(2-aminoethyl)pyrrolidine **4**{*4*} (1.09 g, 9.3 mmol) and 4 Å molecular sieves were mixed in anhyd MeOH (30 mL) and held at reflux under a $N_2$ atmosphere for 36 h. The molecular sieves were filtered and the intermediate imine in MeOH was cooled to 0 °C and treated with solid $NaBH_4$ (0.36 g, 9.3 mmol). The mixture was stirred at RT for 5 h. Then $H_2O$ was added, and the product was extracted with $CH_2Cl_2$. The organic extracts were combined, washed with brine, dried over $MgSO_4$, and the solvent was removed to give the corresponding 4-(diethoxymethyl)benzylamine as a yellow oil (2.66 g, 93%). This intermediate aminoacetal (2.64 g, 8.6 mmol) was treated with 2 M HCl (20 mL) at RT for 2 h. The resulting mixture was basified with NaOH and extracted with $CH_2Cl_2$. The $CH_2Cl_2$ extracts were combined, washed with brine, dried over $MgSO_4$, and the solvent was removed to give the product **7**{*4*} as a brownish oil (1.79 g, 89%). $^1$H NMR (300 MHz, $CDCl_3$, 25 °C, TMS): $\delta$ = 10.00 (s, 1H; CHO), 7.84 (d, $^3J_{H,H}$ = 8.1 Hz, 2H; Ph), 7.51 (d, $^3J_{H,H}$ = 8.1 Hz, 2H; Ph), 3.90 (s, 2H; C*H*$_2$Ph), 2.75 (t, $^3J_{H,H}$ = 6.0 Hz, 2H; C*H*$_2$NH), 2.64 (t, $^3J_{H,H}$ = 6.0 Hz, 2H; $CH_2$N), 2.51 (m, 4H; $CH_2$N), 2.01 (br s, 1H; NH), 1.77 ppm (m, 4H; $CH_2$); $^{13}$C NMR (75.5 MHz, $CDCl_3$, 25 °C): $\delta$ = 191.8 (CH), 147.6 (Cq), 135.1 (Cq), 129.7 (CH), 128.4 (CH), 55.8 ($CH_2$), 54.2 ($CH_2$), 53.7 ($CH_2$), 47.8 ($CH_2$), 23.5 ppm ($CH_2$); IR (film): $\tilde{\nu}$ = 3309 (NH), 2961, 2930, 2875, 2799 (CH), 1700 (C=O), 1606 (CC), 1459, 1446 cm$^{-1}$ (CH); MS (EI): *m/z* (%): 233.2 (1) $[M+H]^+$, 232.2 (22) $[M]^+$

  

, 84.1 (100) $[C_5H_{10}N]^+$; HRMS: *m/z* calcd for $C_{14}H_{20}N_2O$: 232.1576 $[M+H]^+$, found: 232.1572.

**4-((3-(1*H*-Imidazol-1-yl)propylamino)methyl)benzaldehyde (7{*6*}).** The procedure was the same as that stated above for **7**{*4*} but by using 4-(diethoxymethyl)benzaldehyde (**5**) (2.01 g, 9.3 mmol), 1-(3-aminopropyl)imidazole **4**{*6*} (1.20 g, 9.3 mmol) and $NaBH_4$ (0.36 g, 9.3 mmol). The intermediate aminoacetal was obtained as a yellow oil (2.68 g, 90%). This acetal (2.68 g, 9.3 mmol) was deprotected to afford **7**{*6*} (1.76 g, 86%) as a yellow oil. $^1$H NMR (300 MHz, $CDCl_3$, 25 °C, TMS): $\delta = 10.00$ (s, 1H; CHO), 7.85 (d, $^3J_{H,H} = 8.1$ Hz, 2H; Ph), 7.48 (d, $^3J_{H,H} = 8.1$ Hz, 2H; Ph), 7.46 (s, 1H; CHN), 7.05 (s, 1H; CHN), 6.90 (s, 1H; CHN), 4.07 (t, $^3J_{H,H} = 6.9$ Hz, 2H; $CH_2N$), 3.85 (s, 2H; $CH_2Ph$), 2.62 (t, $^3J_{H,H} = 6.9$ Hz, 2H; $CH_2NH$), 1.95 (quint, $^3J_{H,H} = 6.9$ Hz, 2H; $CH_2$), 1.75 ppm (br s, 1H; NH); $^{13}$C NMR (75.5 MHz, $CDCl_3$, 25 °C): $\delta = 191.7$ (CH), 147.2 (Cq), 137.0 (CH), 135.3 (Cq), 129.8 (CH), 129.3 (CH), 128.4 (CH), 118.7 (CH), 53.6 ($CH_2$), 45.8 ($CH_2$), 44.6 ($CH_2$), 31.3 ppm ($CH_2$). IR (film): $\tilde{\nu} = 3268$ (NH), 3108, 2936, 2831, 2738 (CH), 1696 (C=O), 1606 (C-C), 1508 $cm^{-1}$ (imidazole); MS (EI): *m/z* (%): 244.1 (17) $[M+H]^+$, 243.1 (65) $[M]^+$, 119.0 (100) $[C_8H_7O]^+$; HRMS: *m/z* calcd for $C_{14}H_{17}N_3O$: 243.1372 $[M]^+$, found: 243.1366.

**4-((3-(2-Methylpiperidin-1-yl)propylamino)methyl)benzaldehyde (7{*8*}).** The procedure was the same as that stated above for **7**{*4*} but by using 4-(diethoxymethyl)benzaldehyde (**5**) (2.01 g, 9.3 mmol), 1-(3-aminopropyl)-2-methylpiperidine **4**{*8*} (1.52 g, 9.3 mmol) and $NaBH_4$ (0.36 g, 9.3 mmol). The intermediate aminoacetal was obtained as a yellow oil (3.18 g, 98%). This acetal (3.18 g, 9.1 mmol) was deprotected to afford **7**{*8*} (2.45 g, 98%) as a yellow oil. $^1$H NMR (300 MHz, $CDCl_3$, 25 °C, TMS): $\delta = 10.00$ (s, 1H; CHO), 7.85 (d, $^3J_{H,H} = 8.1$ Hz, 2H; Ph), 7.50 (d, $^3J_{H,H} = 8.1$ Hz, 2H; Ph), 3.87 (s, 2H; $CH_2NH$), 2.87 (m, 1H; $CH_{eq}N$), 2.77 (m, 1H; $CH_{eq}N$), 2.65 (t, $^3J_{H,H} = 6.8$ Hz, 2H; $CH_2NH$), 2.36 (m, 1H; $CH_{ax}N$), 2.27 (m, 1H; $CHCH_3$), 2.11 (m, 1H; $CH_{ax}N$), 2.00 (br s, 1H; NH), 1.75–1.48 (m, 6H; $CH_2$), 1.29 (m, 2H; $CH_{ax}$), 1.06 ppm (d, $^3J_{H,H} = 6.0$ Hz, 3H; $CH_3$); $^{13}$C NMR (75.5 MHz, $CDCl_3$, 25 °C): $\delta = 191.8$ (CH), 147.7 (Cq), 135.2 (Cq), 129.8 (CH), 128.4 (CH), 56.1 (CH), 53.8 ($CH_2$), 52.3 ($CH_2$), 52.0 ($CH_2$), 48.5 ($CH_2$), 34.6 ($CH_2$), 26.1 ($CH_2$), 25.9 ($CH_2$), 23.9 ($CH_2$), 19.0 ppm ($CH_3$); IR (film): $\tilde{\nu} = 3271$ (NH), 2930, 2852, 2793, 2732 (CH), 1702 (C=O), 1606 (C–C), 1449, 1372 $cm^{-1}$ (CH); MS (EI): *m/z* (%): 275.2 (9) $[M+H]^+$, 274.2 (37) $[M]^+$, 112.1 (100) $[C_7H_{14}N]^+$; HRMS: *m/z* calcd for $C_{17}H_{26}N_2O$: 274.2045 $[M]^+$, found: 274.2046.

**4-((Piperidin-1-ylimino)methyl)benzaldehyde (6{*1*}).** Terephthalaldehyde (**3**) (1.00 g, 7.4 mmol) was dissolved in anhydrous MeOH (30 mL) with 4 Å molecular sieves, followed by the dropwise addition of a solution of 1-aminopiperidine **4**{*1*} (0.38 g, 3.8 mmol) in anhydrous MeOH (5 mL) under a $N_2$ atmosphere. The mixture was held at reflux for 36 h. Upon removal of the solvent, the residue was separated by chromatography on silica gel by eluting with hexane/EtOAc (5:1). The resulting product was once again separated by chromatography on silica gel by eluting with $CH_2Cl_2$ /EtOAc (gradient 25:1 to 1:1) to give **6**{*1*} (0.48 g, 60%) as a yellow oil. $^1$H NMR (300 MHz, $CDCl_3$, 25 °C, TMS): $\delta = 9.96$ (s, 1H; CHO), 7.83 (d, $^3J_{H,H} = 8.4$ Hz, 2H; Ph), 7.71 (d, $^3J_{H,H} = 8.4$ Hz, 2H; Ph), 7.48 (s, 1H; CH=N), 3.25 (t, $^3J_{H,H} = 5.7$ Hz, 4H; $CH_2N$), 1.76 (quint, $^3J_{H,H} = 5.7$ Hz, 4H; $CH_2$), 1.61–1.54 ppm (m, 2H; $CH_2$); $^{13}$C NMR (75.5 MHz, $CDCl_3$, 25 °C): $\delta = 191.6$ (CH), 142.8 (Cq), 135.0 (Cq), 131.0 (CH), 130.0 (CH), 125.8 (CH), 51.7 ($CH_2$), 25.1 ($CH_2$), 24.0 ppm ($CH_2$); IR (film): $\tilde{\nu} =$ 2938, 2854, 2818, 2731 (CH), 1694 (C=O), 1605 (C–C), 1579 (C=N), 1549 (C–C), 1448 $cm^{-1}$ (CH); MS (EI): *m/z* (%): 217.0 (17) $[M+H]^+$, 216.0 (100) $[M]^+$; Anal. ($C_{13}H_{16}N_2O$) C, H, N.

**4-((2,6-Dimethylpiperidin-1-ylimino)methyl)benzaldehyde (6{*2*}).** The procedure was the same as that stated above for **6**{*1*} but terephthalaldehyde (**3**) (3.82 g, 28.2 mmol) and 1-amino-2,6-dimethylpiperidine **4**{*2*} (2.01 g, 14.1 mmol) were used. Upon removal of the solvent, the residue was separated by chromatography on silica gel by eluting with hexane/EtOAc (3:1) to afford **6**{*2*} (2.71 g, 78%) as a yellow oil. $^1$H NMR (300 MHz, $CDCl_3$, 25 °C, TMS): $\delta = 9.95$ (s, 1H; CHO), 7.81 (d, $^3J_{H,H} = 8.3$ Hz, 2H; Ph), 7.69 (d, $^3J_{H,H} = 8.3$ Hz, 2H; Ph), 7.35 (s, 1H; CH=N), 3.92 (m, 2H; $CH$-$CH_3$), 1.87–1.56 (m, 6H; $CH_2$), 1.15 ppm (d, $^3J_{H,H} = 6.6$ Hz, 6H; $CH_3$); $^{13}$C NMR (75.5 MHz, $CDCl_3$, 25 °C): $\delta = 191.5$ (CH), 143.5 (Cq), 134.4 (Cq), 130.0 (CH), 129.5 (CH), 125.3 (CH), 53.1 (CH), 30.8 ($CH_2$), 18.3 ($CH_3$), 15.6 ppm ($CH_2$); IR (film): $\tilde{\nu} = 2967$, 2935, 2869, 2820, 2728 (C–H), 1693 (C=O), 1604 (C–C), 1572 (C=N), 1539 (C–C), 1468, 1372 $cm^{-1}$ (C-H); MS (EI): *m/z* (%): 245.2 (5) $[M+H]^+$, 244.2 (16) $[M]^+$, 229.2 (100) $[C_{14}H_{17}N_2O]^+$, Anal. ($C_{15}H_{20}N_2O$) C, H, N.

***N*-(4-((2,6-Dimethylpiperidin-1-ylimino)methyl)benzyl)-2-(pyrrolidin-1-yl)ethylamine (8{*2,4*}).** 1-(2-Aminoethyl)pyrrolidine **4**{*4*} (0.52 g, 2.1 mmol) and **6**{*2*} (0.52 g, 2.1 mmol) were dissolved in anhyd MeOH (30 mL). 4 Å Molecular sieves were added, and the mixture was held at reflux under a $N_2$ atmosphere for 36 h. The molecular sieves were filtered, and the intermediate imine in MeOH was cooled to 0 °C and treated with solid $NaBH_4$ (0.08 g, 2.1 mmol). The reaction was stirred at RT for 16 h. Then $H_2O$ was added, and the product was extracted with $CH_2Cl_2$. The organic layers were combined, washed with brine, dried over $MgSO_4$, and the solvent was removed to afford **8**{*2,4*} as a yellow oil (0.61 g, 85%). $^1$H NMR (300 MHz, $CDCl_3$, 25 °C, TMS): $\delta = 8.07$ (s, 1H; CH=N), 7.64 (d, 2H, $^3J = 8.1$ Hz; Ph), 7.34 (d, 2H, $^3J = 8.1$ Hz; Ph), 3.83 (s, 2H; $CH_2Ph$), 3.06 (m, 2H; $CHCH_3$), 2.77 (t, $^3J_{H,H} = 6.0$ Hz, 2H; $CH_2NH$), 2.63 (t, $^3J_{H,H} = 6.0$ Hz, 2H; $CH_2N$), 2.50 (m, 4H; $CH_2N$), 2.34 (br s, 1H; NH), 1.77 (m, 8H; $CH_2$), 1.50 (m, 2H; $CH_2$), 1.00 ppm (d, $^3J_{H,H} = 6.3$ Hz, 6H; $CH_3$); IR (film): $\tilde{\nu} = 3311$ (NH), 2962, 2931, 2872, 2794 (CH), 1624 (CC), 1584 (C=N), 1556 (C–C), 1459, 1447, 1369 (CH) $cm^{-1}$; MS (EI): *m/z* (%): 342.3 (0.5) $[M]^+$, 84.0 (100) $[C_5H_{10}N]^+$; HRMS: *m/z* calcd for $C_{21}H_{34}N_4$: 342.2783 $[M]^+$, found: 342.2786.

***N*-(4-((3-(1*H*-Imidazol-1-yl)propylamino)methyl)benzyl)-3-(2-methylpiperidin-1-yl)propan-1-amine (1{*6,8*}).** The procedure was the same as that stated above for **8**{*2,4*}, but 1-(3-aminopropyl)-2-methyl-piperidine **4**{*8*} (0.59 g, 3.6 mmol), **7**{*6*} (0.88 g, 3.6 mmol) and $NaBH_4$ (0.14 g, 3.6 mmol) were used to give **1**{*6,8*} (1.20 g, 86%) as a yellow oil. $^1$H NMR (300 MHz, $CDCl_3$, 25 °C, TMS): $\delta = 7.44$ (s, 1H; CHN), 7.27 (s, 4H; Ph), 7.03 (s, 1H; CHN), 6.89 (s, 1H; CHN), 4.04 (t, $^3J_{H,H} = 6.9$ Hz, 2H; $CH_2N$), 3.77 (s, 2H; $CH_2Ph$), 3.74 (s, 2H; $CH_2$-Ph), 2.87 (m, 1H; $CH_{eq}N$), 2.74 (m, 1H; $CH_{eq}N$), 2.65 (t, $^3J_{H,H} = 6.9$ Hz, 2H; $CH_2NH$), 2.60 (t, $^3J_{H,H} = 6.9$ Hz, 2H; $CH_2NH$), 2.37 (m, 1H; $CH_{ax}N$), 2.27 (m, 1H; $CHCH_3$), 2.12 (m, 1H; $CH_{ax}N$), 2.09 (br s, 2H; NH), 1.92 (quint, $^3J_{H,H} = 6.9$ Hz, 2H; $CH_2$), 1.72–1.53 (m, 6H; $CH_2$), 1.29 (m, 2H; $CH_{ax}$), 1.05 ppm (d, $^3J_{H,H} = 6.3$ Hz, 3H; $CH_3$); $^{13}$C NMR (75.5 MHz, $CDCl_3$, 25 °C): $\delta = 138.9$ (Cq), 138.7 (Cq), 137.1 (CH), 129.2 (CH), 128.2 (CH), 128.0 (CH), 118.7 (CH), 56.0 (CH), 53.7 ($CH_2$), 52.3 ($CH_2$), 52.0 ($CH_2$), 48.3 ($CH_2$), 45.7 ($CH_2$), 44.7 ($CH_2$), 34.6 ($CH_2$), 31.4 ($CH_2$), 26.1 ($CH_2$), 25.7 ($CH_2$), 23.9 ($CH_2$), 19.1 ppm ($CH_3$); IR (film): $\tilde{\nu} = 3277$ (N–H), 3104, 2929, 2853, 2802 (C–H), 1508 (imidazole), 1450, 1373 $cm^{-1}$ (CH); MS (EI): *m/z* (%): 385.3 (2) $[M+2H]^+$, 384.3 (26) $[M+H]^+$, 383.3 (4) $[M]^+$, 112.0 (100) $[C_7H_{14}N]^+$; HRMS: *m/z* calcd for $C_{23}H_{37}N_5$: 383.3049 $[M+H]^+$, found: 383.3048.

***N*-(4-((3-(4-Methylpiperazin-1-yl)propylamino)methyl)benzyl)-3-(2-methylpiperidin-1-yl)propan-1-amine (1{*8,9*}).** The procedure was the same as that stated above for **8**{*2,4*} but 1-(3-aminopropyl)-2-methylpiperidine **4**{*8*} (0.45 g, 2.7 mmol), **7**{*9*} (0.75 g, 2.7 mmol) and $NaBH_4$ (0.10 g, 2.7 mmol) were used to give **1**{*8,9*} (0.45 g, 39%) as a yellow oil. $^1$H NMR (300 MHz, $CDCl_3$, 25 °C, TMS): $\delta = 7.28$ (s, 4H; Ph), 3.77 (s, 4H; $CH_2Ph$), 2.88 (m, 1H; $CH_{eq}N$), 2.75

  

(m, 1H; $CH_{eq}N$), 2.67 (t, $^3J_{H,H}$ = 6.6 Hz, 2H; $CH_2NH$), 2.65 (t, $^3J_{H,H}$ = 6.6 Hz, 2H; $CH_2NH$), 2.43 (brs, 12H; $CH_2N$, $CH_{ax}N$, $CHCH_3$), 2.27 (s, 3H; $CH_3N$), 2.23 (brs, 2H; NH), 2.12 (m, 1H; $CH_{ax}N$), 1.76–1.53 (m, 8H; $CH_2$), 1.32–1.21 (m, 2H; $CH_{ax}N$), 1.05 ppm (d, $^3J_{H,H}$ = 6.3 Hz, 3H; $CH_3$); $^{13}C$ NMR (75.5 MHz, $CDCl_3$, 25 °C): $\delta$ = 138.8 (Cq), 138.6 (Cq), 128.1 (CH), 128.0 (CH), 57.0 ($CH_2$), 56.0 (CH), 55.1 ($CH_2$), 53.7 ($CH_2$), 53.2 ($CH_2$), 52.3 ($CH_2$), 52.0 ($CH_2$), 48.3 ($CH_2$), 48.1 ($CH_2$), 46.0 ($CH_3$), 34.5 ($CH_2$), 26.9 ($CH_2$), 26.0 ($CH_2$), 25.6 ($CH_2$), 23.9 ($CH_2$), 19.0 ppm ($CH_3$); IR (film): $\tilde{\nu}$ = 3280 (N–H), 2931, 2875, 2852, 2793 (C–H), 1458, 1448, 1372 $cm^{-1}$ (C–H); MS (EI): *m/z* (%): 415.4 (0.3) $[M]^+$, 112.2 (100) $[C_7H_{14}N]^+$; HRMS: *m/z* calcd for $C_{25}H_{45}N_5$: 415.3675 $[M]^+$, found: 415.3660.

**((4-(*N*-(4-Methylpiperazin-1-yl)imino)methyl)phenyl)-*N*-(piperidin-1-yl)methanamine (2{*1*,*3*})**. 1-Amino-4-methylpiperazine **4**{*3*} (0.24 g, 2.3 mmol) and **6**{*3*} (0.53 g, 2.3 mmol) were dissolved in anhydrous MeOH (30 mL). Molecular sieves (4 Å) were added and the mixture was held at reflux under a $N_2$ atmosphere for 36 h. The molecular sieves were filtered, and the solvent was removed to afford **2**{*1*,*3*} as a yellow solid (0.69 g, 95%). $^1H$ NMR (300 MHz, $CDCl_3$, 25 °C, TMS): $\delta$ = 7.56 (s, 4H; Ph), 7.53 (s, 1H; $CH_2Ph$), 7.52 (s, 1H; $CH_2$-Ph), 3.22 (t, $^3J_{H,H}$ = 5.1 Hz, 4H; $CH_2N$), 3.17 (t, $^3J_{H,H}$ = 5.6 Hz, 4H; $CH_2N$), 2.62 (t, $^3J_{H,H}$ = 5.1 Hz, 4H; $CH_2N$), 2.36 (s, 3H; $CH_3$), 1.75 (m, 4H; $CH_2$), 1.54 ppm (m, 2H; $CH_2$); $^{13}C$ NMR (75.5 MHz, $CDCl_3$, 25 °C): $\delta$ = 136.4 (Cq), 135.6 (CH), 135.5 (Cq), 134.0 (CH), 126.2 (CH), 126.0 (CH), 54.6 ($CH_2$), 52.1 ($CH_2$), 51.0 ($CH_2$), 46.0 ($CH_3$), 25.3 ($CH_2$), 24.2 ppm ($CH_2$); IR (film): $\tilde{\nu}$ = 2934, 2837, 2798 (C–H), 1577 (C=N), 1452, 1365 $cm^{-1}$ (C–H); MS (EI): *m/z* (%): 315.2 (2) $[M+2H]^+$, 314.2 (22) $[M+H]^+$, 313.2 (100) $[M]^+$; HRMS: *m/z* calcd for $C_{18}H_{27}N_5$: 313.2266 $[M-H]^+$, found: 313.2266.

**4-((2-(Piperidin-1-yl)ethylamino)methyl)benzaldehyde (7{*7*})**. 4-(diethoxymethyl)benzaldehyde (**5**) (0.91 g, 4.2 mmol) and 1-(2-aminoethyl)piperidine **4**{*7*} (0.55 g, 4.2 mmol) were dissolved in anhydrous MeOH (3 mL) in a 5 mL microwave reaction vessel. $Na_2SO_4$ was added and the vessel was sealed. The mixture was heated for 2 h at 100 °C in the microwave. The mixture was filtered and the solvent removed to yield *N*-(4-(diethoxymethyl)benzyliden)-2-(piperidin-1-yl)ethanamine as a reddish oil (1.35 g, 100%). $^1H$ NMR (300 MHz, $CDCl_3$, 25 °C, TMS): $\delta$ = 8.31 (s, 1H; CH=N), 7.71 (d, $^3J_{H,H}$ = 8.1 Hz, 2H; Ph), 7.52 (d, $^3J_{H,H}$ = 8.1 Hz, 2H; Ph), 5.53 (s, 1H; CH), 3.79 (t, $^3J_{H,H}$ = 7.1 Hz, 2H; $CH_2N$), 3.57 (m, 4H; $CH_2CH_3$), 2.68 (t, $^3J_{H,H}$ = 7.1 Hz, 2H; $CH_2N$), 2.51 (brs, 4H; $CH_2N$), 1.61 (m, 4H; $CH_2$), 1.45 (m, 2H; $CH_2$), 1.24 ppm (t, $^3J_{H,H}$ = 7.1 Hz, 6H; $CH_3$). This imine (1.32 g, 4.1 mmol) was dissolved in anhyd MeOH (30 mL), cooled to 0 °C, and treated with solid $NaBH_4$ (0.16 g, 4.1 mmol). The mixture was stirred at RT for 5 h. Then $H_2O$ was added, and the product was extracted with $CH_2Cl_2$. The organic extracts were combined, washed with brine, dried over $MgSO_4$, and the solvent was removed to give *N*-(4-(diethoxymethyl)benzyl)-2-(piperidin-1-yl)-ethanamine as a yellow oil (1.23 g, 92%). $^1H$ NMR (300 MHz, $CDCl_3$, 25 °C, TMS): $\delta$ = 7.42 (d, $^3J_{H,H}$ = 8.1 Hz, 2H; Ph), 7.31 (d, $^3J_{H,H}$ = 8.1 Hz, 2H; Ph), 5.49 (s, 1H; CH), 3.80 (s, 2H; $CH_2Ph$), 3.57 (m, 4H; $CH_2CH_3$), 2.71 (t, $^3J_{H,H}$ = 6.3 Hz, 2H; $CH_2NH$), 2.46 (t, $^3J_{H,H}$ = 6.3 Hz, 2H; $CH_2N$), 2.36 (br, 4H; $CH_2N$), 2.24 (brs, 1H; NH), 1.56 (quint, $^3J_{H,H}$ = 5.7 Hz, 4H; $CH_2$), 1.43 (m, 2H; $CH_2$), 1.23 ppm (t, $^3J_{H,H}$ = 7.1 Hz, 3H, $CH_3$). This aminoacetal (2.64 g, 8.6 mmol) was treated with 2 M HCl (20 mL) at RT for 2 h. The resulting mixture was basified with NaOH and extracted with $CH_2Cl_2$. The $CH_2Cl_2$ extracts were combined, washed with brine, dried over $MgSO_4$, and the solvent was removed to afford aldehyde **7**{*7*} as a brownish oil (0.87 g, 94%). $^1H$ NMR (300 MHz, $CDCl_3$, 25 °C, TMS): $\delta$ = 10.00 (s, 1H; CHO), 7.84 (d, $^3J_{H,H}$ = 8.1 Hz, 2H; Ph), 7.50 (d, $^3J_{H,H}$ = 8.1 Hz, 2H; Ph), 3.89 (s, 2H; $CH_2$-Ph), 2.70 (t, $^3J_{H,H}$ = 6.2 Hz, 2H; $CH_2NH$), 2.47 (t, $^3J_{H,H}$ = 6.2 Hz, 2H; $CH_2N$), 2.36 (br, 4H; $CH_2N$), 2.18 (brs, 1H; NH), 1.57 (quint, $^3J_{H,H}$ = 5.7 Hz, 4H; $CH_2$), 1.43 ppm (m, 2H; $CH_2$).

***N*-(4-((2-(Piperidin-1-yl)ethylamino)methyl)benzyl)-3-(2-methylpiperidin-1-yl)propan-1-amine (1{*7*,*8*})**. 1-(3-aminopropyl)-2-methylpiperidine **4**{*8*} (0.44 g, 2.7 mmol) and **7**{*7*} (0.66 g, 2.7 mmol) were dissolved in anhyd MeOH (3 mL) in a 5 mL microwave vessel, $Na_2SO_4$ was added, and the vessel was sealed. The mixture was heated for 2 h at 100 °C in the microwave. Then it was filtered, diluted with MeOH (10 mL), cooled to 0 °C, and treated with solid $NaBH_4$ (0.10 g, 2.7 mmol). The mixture was stirred at RT for 4 h. Then $H_2O$ was added and the product was extracted with $CH_2Cl_2$. The organic extracts were combined, washed with brine, dried over $MgSO_4$ and the solvent was removed to give **1**{*7*,*8*} as a yellow oil (0.98 g, 95%). $^1H$ NMR (300 MHz, $CDCl_3$, 25 °C, TMS): $\delta$ = 7.27 (s, 4H; Ph), 3.78 (s, 2H; $CH_2$-Ph), 3.77 (s, 2H; $CH_2$-Ph), 2.86 (m, 1H; $CH_{eq}N$), 2.78 (m, 1H; $CH_{eq}N$), 2.69 (t, $^3J_{H,H}$ = 6.3 Hz, 2H; $CH_2NH$), 2.63 (t, $^3J_{H,H}$ = 6.9 Hz, 4H; $CH_2NH$), 2.44 (t, $^3J_{H,H}$ = 6.3 Hz, 2H; $CH_2N$), 2.34 (m, 5H; $CH_{ax}N$, $CH_2N$), 2.25 (m, 1H; $CHCH_3$), 2.11 (m, 1H; $CH_{ax}N$), 2.07 (brs, 2H; NH), 1.68 (quint, $^3J_{H,H}$ = 6.9 Hz, 2H; $CH_2$), 1.55 (m, 8H; $CH_2$), 1.42 (m, 2H; $CH_2$), 1.28 (m, 2H; $CH_{ax}$), 1.05 ppm (d, $^3J_{H,H}$ = 6.3 Hz, 3H; $CH_3$); $^{13}C$ NMR (75.5 MHz, $CDCl_3$, 25 °C): $\delta$ = 139.0 (Cq), 138.8 (Cq), 128.0 (CH), 58.6 ($CH_2$), 55.9 (CH), 54.7 ($CH_2$), 53.7 ($CH_2$), 52.3 ($CH_2$), 52.1 ($CH_2$), 48.3 ($CH_2$), 45.9 ($CH_2$), 34.7 ($CH_2$), 26.2 ($CH_2$), 26.1 ($CH_2$), 25.7 ($CH_2$), 24.5 ($CH_2$), 24.0 ($CH_2$), 19.1 ppm ($CH_3$); IR (film): $\tilde{\nu}$ = 3301 (N–H), 2932, 2852, 2802 (C–H), 1467, 1443, 1373 $cm^{-1}$ (C–H); Anal. ($C_{24}H_{42}N_4$) C, H, N.

### *Biological evaluation*

**Antiviral activity**: HIV-1 strains were titered in MT-4 cells after acute infection, and infectivity was measured by evaluating the cytopathic effect that was induced after 5 day cultures as described.[60] Anti-HIV activity ($EC_{50}$) and cytotoxicity ($CC_{50}$) measurements in MT-4 cells were based on the viability of cells that had been infected or not infected with HIV-1, all were exposed to various concentrations of the test compound. After the MT-4 cells were allowed to proliferate for 5 days, the number of viable cells was quantified by a tetrazolium-based colorimetric method (MTT method) as described.

**Time-of-drug-addition studies**: MT-4 cells were infected with HIV-1 NL4–3 at a multiplicity of infection of 0.5 and incubated for 1 h at 20 °C in the presence or absence of test compounds. Cells were then washed twice in cool PBS and seeded in 96-well plates at a concentration of $2\times10^5$ cells per well (final volume 200 μL) at a temperature of 37 °C. Test compounds, dextran sulfate, AMD3100, C34 or AZT were added at various times post-infection, or the cells were cultured in the absence of drug (control). Test compounds were added at concentrations that completely block HIV replication (roughly 100-fold higher than the determined $EC_{50}$) of each drug in the standard assay performed with MT-4 cells. Virus production was measured by p24 antigen determination in the cell supernatant 30 h post-infection with a commercial p24 antigen ELISA (Innogenetics, Barcelona, Spain).[61]

## *Acknowledgements*

*This work was supported in part by the Fundació Marató de TV3 project 020930 and the Spanish Ministerio de Educación y Ciencia project SAF-2007-6322 (J.I.B. and B.C.) and BFU-200600966 (J.A.E.). I. Clotet-Codina, R. Puig de la Bellacasa, L. Ros-Blanco,*

  

*and V. Pérez-Nueno hold an FI scholarship from Generalitat de Catalunya and S. Pettersson, from IQS.*

**Keywords:** antiviral agents · heterocycles · medicinal chemistry · molecular modeling · reductive amination

[1] J. A. Este, *Curr. Med. Chem.* **2003**, *10*, 1617–1632.
[2] J. A. Este, A. Telenti, *Lancet* **2007**, *370*, 81–88.
[3] N. J. Anthony, *Curr. Top. Med. Chem.* **2004**, *4*, 979–990.
[4] E. De Clercq, *Chem. Biodiversity* **2004**, *1*, 44–64.
[5] T. Imamichi, *Curr. Pharm. Des.* **2004**, *10*, 4039–4053.
[6] G. A. Locatelli, R. Cancio, S. Spadari, G. Maga, *Curr. Drug Metab.* **2004**, *5*, 283–290.
[7] A. Milinkovic, E. Martinez, *Expert Rev. Anti-Infect. Ther.* **2004**, *2*, 367–373.
[8] C. F. Pereira, T. M. L. Paridaen Judith, *Curr. Pharm. Des.* **2004**, *10*, 4005–4037.
[9] C. M. Tarby, *Curr. Top. Med. Chem.* **2004**, *4*, 1045–1057.
[10] M. L. Andreola, *Curr. Pharm. Des.* **2004**, *10*, 3713–3723.
[11] T. K. Chiu, D. R. Davies, *Curr. Top. Med. Chem.* **2004**, *4*, 965–977.
[12] S. P. Gupta, A. N. Nagappa, *Curr. Med. Chem.* **2003**, *10*, 1779–1794.
[13] A. A. Johnson, C. Marchand, Y. Pommier, *Curr. Top. Med. Chem.* **2004**, *4*, 1059–1077.
[14] A. L. Parrill, *Curr. Med. Chem.* **2003**, *10*, 1811–1824.
[15] F. Turlure, E. Devroe, P. A. Silver, A. Engelman, *Front. Biosci.* **2004**, *9*, 3187–3208.
[16] M. Witvrouw, B. Van Maele, J. Vercammen, A. Hantson, Y. Engelborghs, E. De Clercq, C. Pannecouque, Z. Debyser, *Curr. Drug Metab.* **2004**, *5*, 291–304.
[17] M. Baba, *Curr. Top. Med. Chem.* **2004**, *4*, 871–882.
[18] K. Devadas, S. Dhawan, *Recent Res. Dev. Biochem.* **2003**, *4*, 447–466.
[19] I. Schiavoni, C. Muratori, V. Piacentini, A. M. Giammarioli, M. Federico, *Curr. Drug Targets Immune Endocr. Metab. Disord.* **2004**, *4*, 19–27.
[20] E. Morita, W. I. Sundquist, *Annu. Rev. Cell Dev. Biol.* **2004**, *20*, 395–425.
[21] A. G. Bukrinskaya, *Arch. Virol.* **2004**, *149*, 1067–1082.
[22] P. Dorr, M. Westby, S. Dobbs, P. Griffin, B. Irvine, M. Macartney, J. Mori, G. Rickett, C. Smith-Burchnell, C. Napier, R. Webster, D. Armour, D. Price, B. Stammen, A. Wood, M. Perros, *Antimicrob. Agents Chemother.* **2005**, *49*, 4721–4732.
[23] M. Baba, O. Nishimura, N. Kanzaki, M. Okamoto, H. Sawada, Y. Iizawa, M. Shiraishi, Y. Aramaki, K. Okonogi, Y. Ogawa, K. Meguro, M. Fujino, *Proc. Natl. Acad. Sci. USA* **1999**, *96*, 5698–5703.
[24] J. R. Tagat, S. W. McCombie, D. Nazareno, M. A. Labroli, Y. Xiao, R. W. Steensma, J. M. Strizki, B. M. Baroudy, K. Cox, J. Lachowicz, G. Varty, R. Watkins, *J. Med. Chem.* **2004**, *47*, 2405–2408.
[25] J. M. Strizki, S. Xu, N. E. Wagner, L. Wojcik, J. Liu, Y. Hou, M. Endres, A. Palani, S. Shapiro, J. W. Clader, W. J. Greenlee, J. R. Tagat, S. W. McCombie, K. Cox, A. B. Fawzi, C.-C. Chou, C. Pugliese-Sivo, L. Davies, M. E. Moreno, D. D. Ho, A. Trkola, C. A. Stoddart, J. P. Moore, G. R. Reyes, B. M. Baroudy, *Proc. Natl. Acad. Sci. USA* **2001**, *98*, 12718–12723.
[26] K. Maeda, H. Nakata, Y. Koh, T. Miyakawa, H. Ogata, Y. Takaoka, S. Shibayama, K. Sagawa, D. Fukushima, J. Moravek, Y. Koyanagi, H. Mitsuya, *J. Virol.* **2004**, *78*, 8654–8662.
[27] A. Trkola, T. J. Ketas, K. A. Nagashima, L. Zhao, T. Cilliers, L. Morris, J. P. Moore, P. J. Maddon, W. C. Olson, *J. Virol.* **2001**, *75*, 579–588.
[28] C. Ji, J. Zhang, M. Dioszegi, S. Chiu, E. Rao, A. Derosier, N. Cammack, M. Brandt, S. Sankuratri, *Mol. Pharmacol.* **2007**, *72*, 18–28.
[29] K. De Vresse, D. Reymen, P. Griffin, A. Steinkasserer, G. Werner, G. J. Bridger, J. Esté, W. James, G. W. Henson, J. Desmyter, J. Anné, E. De Clercq, *Antiviral Res.* **1996**, *29*, 209–219.
[30] D. Schols, J. A. Esté, G. Henson, E. De Clercq, *Antiviral Res.* **1997**, *35*, 147–156.
[31] E. De Clercq, *Mol. Pharmacol.* **2000**, *57*, 833–839.
[32] J. A. Esté, C. Cabrera, E. De Clercq, S. Struyf, J. Van Damme, G. Bridger, R. T. Skerlj, M. J. Abrams, G. Henson, A. Gutierrez, B. Clotet, D. Schols, *Mol. Pharmacol.* **1999**, *55*, 67–73.
[33] S. Hatse, K. Princen, E. De Clercq, M. M. Rosenkilde, T. W. Schwartz, P. E. Hernandez-Abad, R. T. Skerlj, G. J. Bridger, D. Schols, *Biochem. Pharmacol.* **2005**, *70*, 752–761.
[34] K. Princen, S. Hatse, K. Vermeire, S. Aquaro, E. De Clercq, L.-O. Gerlach, M. Rosenkilde, T. W. Schwartz, R. Skerlj, G. Bridger, D. Schols, *J. Virol.* **2004**, *78*, 12996–13006.
[35] J. Teixidó, J. I. Borrell, S. Nonell, S. Pettersson, L. Ros, R. Puig de La Bellacasa, M. O. Rabal, V. Pérez, J. Esté, I. Clotet-Codina, M. Armand-Ugón, ES Patent ES200602764, **2006** (filing date: October 26, 2006).
[36] W. Zhan, Z. Liang, A. Zhu, S. Kurtkaya, H. Shim, J. P. Snyder, D. C. Liotta, *J. Med. Chem.* **2007**, *50*, 5655–5664.
[37] Cerius2, Version 6.6, Accelrys Inc., San Diego, CA (USA) **2001**.
[38] R. Pascual, J. I. Borrell, J. Teixidó, *Mol. Diversity* **2000**, *6*, 121–133.
[39] MOE, Molecular Operating Environment, Chemical Computing Group Inc., Montréal, QC (Canada) **2006**.
[40] S. Pettersson, I. Clotet-Codina, J. A. Esté, J. I. Borrell, J. Teixidó, *Mini-Rev. Med. Chem.* **2006**, *6*, 91–108.
[41] A. F. Abdel-Magid, K. G. Carson, B. D. Harris, C. A. Maryanoff, R. D. Shah, *J. Org. Chem.* **1996**, *61*, 3849–3862.
[42] T. H. Fife, L. H. Brod, *J. Org. Chem.* **1968**, *33*, 4136–4140.
[43] J. L. Jensen, R. Siegel, *J. Org. Chem.* **1988**, *53*, 6105–6106.
[44] C. Yue, I. Gauthier, J. Royer, H.-P. Husson, *J. Org. Chem.* **1996**, *61*, 4949–4954.
[45] R. Pascual, PhD Thesis, Universitat Ramon Llull (Barcelona, Spain), **2003**.
[46] M. O. Rabal, PhD Thesis, Universitat Ramon Llull (Barcelona, Spain), **2006**.
[47] A. Brelot, N. Heveker, M. Montes, M. Alizon, *J. Biol. Chem.* **2000**, *275*, 23736–23744.
[48] AutoDock 3.0, Department of Molecular Biology, The Scripps Research Institute, MB-5, La Jolla, CA (USA) **1989**.
[49] G. M. Morris, D. S. Goodsell, R. Halliday, R. Huey, W. E. Hart, R. K. Belew, A. J. Olson, *J. Comput. Chem.* **1998**, *19*, 1639–1662.
[50] A. Sali, T. L. Blundell, *J. Mol. Biol.* **1993**, *234*, 779–815.
[51] R. E. Bruccoleri, *Mol. Simul.* **1993**, *10*, 151–174.
[52] C. Seibert, T. P. Sakmar, *Curr. Pharm. Des.* **2004**, *10*, 2041–2062.
[53] V. I. Pérez-Nueno, D. W. Ritchie, M. O. Rabal, R. Pascual, J. I. Borrell, J. Teixidó, *J. Chem. Inf. Model.* **2008**, *48*, 509–533.
[54] J. Gasteiger, M. Marsili, *Tetrahedron* **1980**, *36*, 3219–3228.
[55] L.-O. Gerlach, R. Skerlj, G. Bridger, T. W. Schwartz, *J. Biol. Chem.* **2001**, *276*, 14153–14160.
[56] C. Bissantz, G. Folkers, D. Rognan, *J. Med. Chem.* **2000**, *43*, 4759–4767.
[57] H. Gutiérrez-de-Terán, M. Pastor, N. B. Centeno, J. Aqvist, F. Sanz, *ChemBioChem* **2004**, *5*, 841–849.
[58] X. Huang, J. Shen, M. Cui, L. Shen, X. Luo, K. Ling, G. Pei, H. Jiang, K. Chen, *Biophys. J.* **2003**, *84*, 171–184.
[59] G. C. Shields, C. A. Laguthton, M. Orozco, *J. Am. Chem. Soc.* **1997**, *119*, 7463–7469.
[60] G. Moncunill, M. Armand-Ugón, B. Clotet, J. A. Este, *AIDS* **2008**, *22*, 23–31.
[61] G. Moncunill, M. Armand-Ugón, I. Clotet, E. Pauls, E. Ballana, A. Llano, B. Romagnoli, J. W. Vrijbloed, F. O. Gombert, B. Clotet, S. De Marco, J. A. Este, *Mol. Pharmacol.* **2008**, *73*, 1264–1273.

Received: May 9, 2008
Revised: June 3, 2008
Published online on July 31, 2008

  

# Discovery of Novel HIV Entry Inhibitors for the CXCR4 Receptor by Prospective Virtual Screening

Violeta I. Pérez-Nueno,*,† Sofia Pettersson,† David W. Ritchie,‡ José I. Borrell,† and Jordi Teixidó*,†

Grup d'Enginyeria Molecular, Institut Químic de Sarrià (IQS), Universitat Ramon Llull, Barcelona, Spain, and INRIA Nancy Grant Est, Laboratoire Lorrain de Recherche en Informatique et ses Applications (LORIA), UMR 7503, BP 239, 54506 Vandoeuvre-les-Nancy, France

Received January 31, 2009

The process of HIV entry begins with the binding of the viral envelope glycoprotein gp120 to both the CD4 receptor and one of CXCR4 or CCR5 chemokine coreceptors. There is currently considerable interest in developing novel ligands which can attach to these coreceptors and hence block virus-cell fusion. This article compares the application of structure-based (docking) and ligand-based (QSAR analyses, pharmacophore modeling, and shape matching) virtual screening tools to find new potential HIV entry inhibitors for the CXCR4 receptor. The comparison is based on retrospective virtual screening of a library containing different known CXCR4 inhibitors from the literature, a smaller set of active CXCR4 inhibitors selected from a large combinatorial virtual library and synthesized by us, and some druglike presumed inactive molecules as the reference set. The enrichment factors and diversity of the retrieved molecular scaffolds in the virtual hit lists was determined. Once the different virtual screening approaches had been validated and the best parameters had been selected, prospective virtual screening of our virtual library was applied to identify new anti-HIV compounds using the same protocol as in the retrospective virtual screening analysis. The compounds selected using these computational tools were subsequently synthesized and assayed and showed activity values ranging from 4 to 0.022 $\mu$g/mL.

## INTRODUCTION

According to the World Health Organization, about 33 million people live with Acquired Immune Deficiency Syndrome (AIDS).[1] The entry of human immunodeficiency virus (HIV) into the host cell begins with binding of the viral envelope glycoprotein gp120 to both the CD4 cell surface receptor and one of CXCR4 or CCR5 chemokine coreceptors and leads to fusion of the viral capsid with the cell membrane. Current antiretroviral therapies (ARTs) against AIDS are generally based on reverse transcriptase inhibitors and protease inhibitors. Despite advances in the development of these potent agents which block HIV transcription and assembly, there remain problems regarding drug resistance, latent viral reservoirs, and drug induced toxic effects, which can all compromise effective control of the virus. Hence there is a need to develop new classes of anti-HIV drugs with different modes of action. Several researchers have recognized that knowledge of the mechanism of viral entry into the host cell provides further therapeutic targets against HIV infection.[2,3] To date, at least three subclasses of HIV viral entry/fusion inhibitors have emerged, namely the following: CD4 binding or attachment inhibitors, which target initial recognition and binding of the viral glycoprotein gp120 to the cell-surface CD4 antigen;[4] chemokine coreceptor binding inhibitors, which target binding of virus to the CCR5 or CXCR4 coreceptor;[5] and cell fusion inhibitors, which target the gp41 viral glycoprotein.[6] Therefore, there is considerable interest in developing novel ligands which can modulate these receptors and block virus-cell fusion.[7−11]

To make progress toward this goal, we compiled a data set of CXCR4 antagonists from the literature comprising several AMD3100 derivatives, macrocycles, KRH1636 derivatives, dipicolil amine zinc(II) complexes, cyclic peptides, and tetrahydroquinolin-amine derivatives. Several of the AMD3100 derivatives are novel and have been synthesized in our group.[12] To this set was added some 4700 presumed inactive druglike compounds from the Maybridge Screening Collection[13] which have several 1D properties similar to those of the actives. The active molecules synthesized by us belong to a diverse but restricted set of compounds, selected using our PRALINS[14] program (Program for Rational Analysis of Libraries in Silico) from a large virtual combinatorial library. This library was designed to preserve the main features of AMD3100, i.e. polynitrogenated systems separated by a *p*-phenylene moiety, which is treated as an ideal reference CXCR4 antagonist. The compounds selected by PRALINS showed activities ranging from 20 to 0.008 $\mu$g/mL, and experimental binding assays confirmed that their mode of action was indeed to block the CXCR4 receptor.[12]

In order to find other active compounds without having to synthesize the whole of the combinatorial virtual library, ligand-based and structure-based virtual screening tools were used. For ligand-based virtual screening, QSAR analysis was performed with MOE,[15] and a good quantitative structure−activity relationship function was obtained. 3D pharmaco-

* Corresponding author phone: +34-93-267.20.00; fax: +34-93-2050.62.66; e-mail: j.teixido@iqs.url.es (J.T.); phone: +33 3 83 59 30 00; fax: +33 3 83 27 83 19; e-mail: violetaperezn@iqs.url.edu.
† Universitat Ramon Llull.
‡ INRIA Nancy Grant Est.

10.1021/ci800468q CCC: $40.75 
Published on Web 04/09/2009

phore modeling using MOE and Discovery Studio[16] was applied in order to study the characteristic features of the actives necessary for interaction with the coreceptor. Shape matching using the PARAFIT,[17] ROCS,[18] and HEX[19] programs was also carried out to select molecules from the library with similar shapes to known actives. Because the 3D structure of CXCR4 has not yet been solved, a homology model of the protein built previously[20] using bovine rhodopsin[21] as the template was used for receptor-based analyses using AUTODOCK,[22] GOLD,[23] FRED,[24] and HEX.[25]

In order to validate the different virtual screening approaches and to set the best parameters for each one, a retrospective virtual screening analysis was performed on the compiled active and inactive data sets. Once the best approaches were selected, prospective analysis of the as yet unsynthesized compounds in our combinatorial virtual library was applied to establish a ranked list of new candidate CXCR4 inhibitors. A final virtual hit list was obtained from a consensus ranking of the different virtual screening approaches. Five molecules in the resulting hit list were synthesized and tested and were found to have activity values ranging from 4 to 0.022 $\mu$g/mL. The most active of these are monocyclams, as might be expected of AMD3100 derivatives,[26−28] and these coincided with the compounds in the first ranking positions of our hit list.

## METHODS

**Library Design.** In this study, AMD3100, one of the earliest and still one of the most potent CXCR4 antagonists to be developed, was used as a reference ligand from which a combinatorial library was derived.[12,29] The compounds in this library were designed in such a way as to retain the main physicochemical features of this ligand, i.e. a central *p*-phenylene moiety with at least two nitrogen-containing substituents, one in the benzylic position and the other(s) in a heterocyclic system, and with similar distances between such nitrogens as those observed in cyclam. These considerations led us to design target compounds such as the diamines, **1,** as shown in Figure 1. A retrosynthetic analysis of those cases in which $R_1 = R_2$ and the number, *n*, of methyl linkers led to the selection of symmetrical diimines **2** as precursors, which can be extended with further methyls to give terephthalaldehyde (**3**) and two equivalents of the corresponding amine **4** where $n \geq 1$ (see Figure 2). When $R_1 = R_2$ and $n = 0$, compounds **2** are in fact symmetrical hydrazones which can be obtained by condensation of terephthalaldehyde and the corresponding hydrazine **4** ($n = 0$). These dihydrazones were also included in our library. In order to obtain nonsymmetric ($R_1 \neq R_2$) diamines **1** ($n \geq 1$) and dihydrazones **2** ($n = 0$), it was necessary to modify slightly our synthetic approach by using 4-(diethoxymethyl)benzaldehyde (**5**) as the core precursor. Thus, the intermediate hydrazono and aminobenzaldehydes **6** and **7** allowed such nonsymmetric compounds and other nonsymmetric aminohydrazones **8** to be included as further compounds in the combinatorial library (see Scheme 1). Overall, the virtual library consists of 66 amino/hydrazono-amine/hydrazone compounds (**1**, **2**, and **8**), 11 amino/hydrazono-aldehyde compounds (**6** and **7**), and 11 cyclam-amine/hydrazone compounds (**9** and **10**). Some representative examples of these structures are shown in Figure 3.

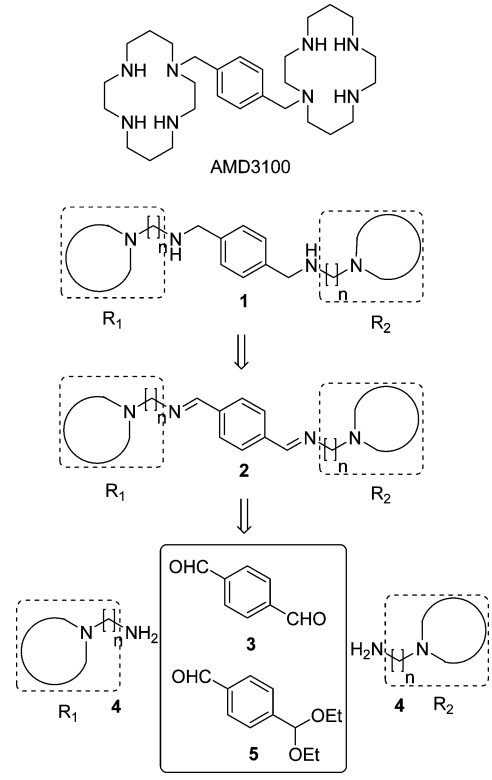


**Figure 1.** The AMD3100 reference antagonist for CXCR4 and schematic illustration of the target library construction. Top: the AMD3100 reference antagonist for CXCR4, with a *p*-phenyl linker and nitrogen-containing heterocyclic systems on each side of the linker. Bottom: a schematic illustration of the construction of the target library which preserves these features.

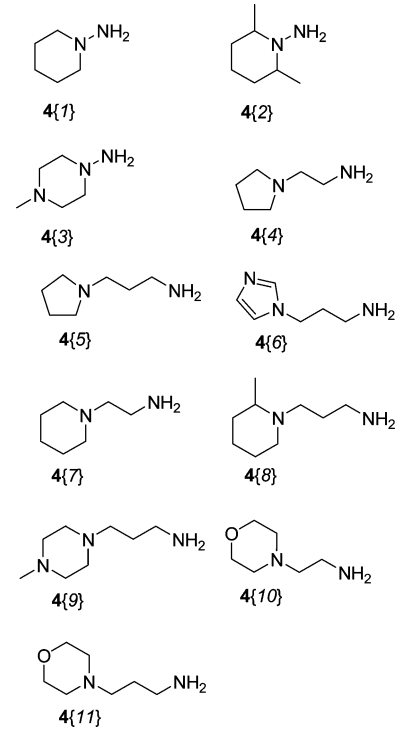


**Figure 2.** Amine and hydrazine building blocks used for the combinatorial virtual library.

**Virtual Screening Data Sets.** For the retrospective virtual screening analysis, a data set of 248 CXCR4 antagonists with activity values lower than 100 $\mu$M against CXCR4 was assembled from the literature. This set was used for receptor-

**Scheme 1.** Synthetic Scheme for the Symmetrical and Nonsymmetrical Diamines **1**, Dihydrazones **2,** and Aminohydrazones **8**

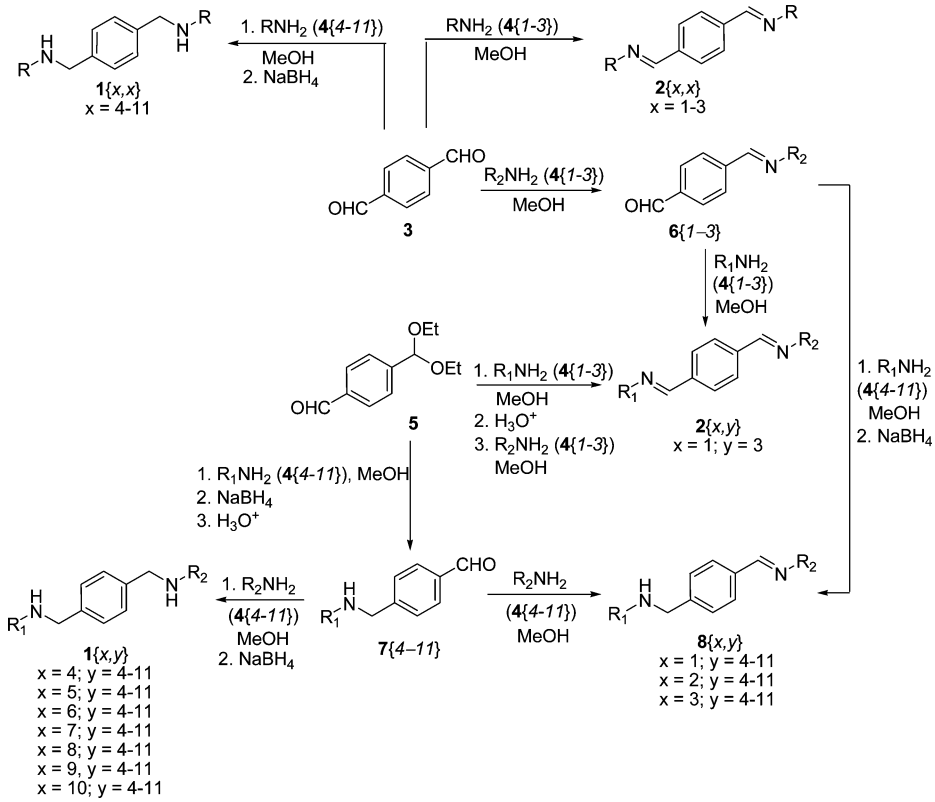


based docking and ligand-based screening analyses. A subset of the 103 most active compounds plus 48 compounds representative of other scaffold classes was then used for pharmacophore modeling. As summarized in Table 1, these compounds mainly belong to seven representative families, i.e., AMD3100 derivatives, macrocycles, KRH1636 derivatives, dipicolil amine zinc(II) complexes, tetrahydroquinolinamine derivatives, cyclic peptides, and also the most active CXCR4 inhibitors from our combinatorial virtual library which had been synthesized by us.[12] Figure 4 shows some representative members of each family. These data sets were augmented with two further sets of druglike presumed inactive compounds from the Maybridge Screening Collection (1462 for pharmacophore modeling and 4696 for the docking and shape matching approaches), selected in such a way that several of their 1D properties were similar to those of the actives (i.e., molecular weight, number of rotatable single bonds, numbers of hydrogen-bond donor and acceptor atoms, number of hydrophobic atoms, and octanol−water partition coefficient), as shown in Table 2.

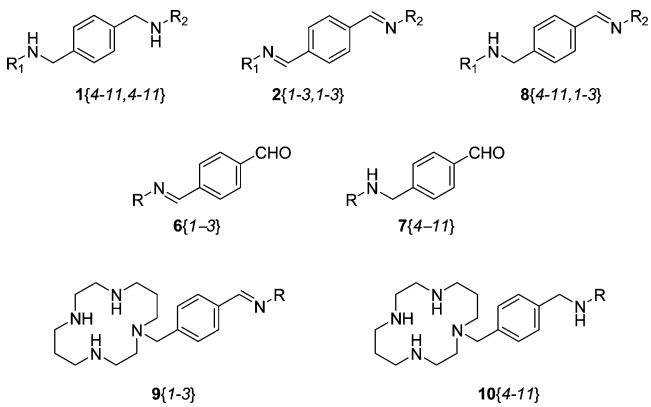


**Figure 3.** Representative examples of compounds in the combinatorial virtual library. Compounds **1** are symmetrical ($R_1 = R_2$) or nonsymmetrical ($R_1 \neq R_2$) diamines, compounds **2** are symmetrical ($R_1 = R_2$) or nonsymmetrical ($R_1 \neq R_2$) dihydrazones, compounds **8** are aminohydrazones, compounds **6** and **7** correspond to hydrazonobenzaldehydes and aminobenzaldehydes, respectively, and compounds **9** and **10** are hydrazone or amino substituted monocyclams.

For the prospective virtual screening analysis, the same presumed inactive compounds as in the retrospective analysis were used, and a subset of 34 hitherto unsynthesized compounds from the amino/hydrazono-amine/hydrazone (compounds **1, 2**, and **8**), hydrazono/amino-aldehyde (compounds **6** and **7**), and cyclam-hydrazone/amine (**9** and **10**) families was selected from the virtual library for synthesis and testing. The 3D structures of all compounds were protonated at physiological pH, assigned Gasteiger partial charges, and geometry-optimized using the MMFF94 force field. All molecules were aligned with the MOE FlexAlign module[46] using as superposition template the AMD3100 conformation obtained previously from a CXCR4 docking study[20] (see Figure 5).

**QSAR Analysis.** QSAR analysis applies statistical methods to describe quantitative relationships between chemical structures and biological activities of a series of analogues. The process can be divided into three general steps: 1) data set selection, 2) data analysis, and 3) model validation. In the present QSAR study, a data set of 39 compounds with known $EC_{50}$ activity values consisting of AMD3100 plus 38 further compounds synthesized by us (structures **1, 2, 6, 7**, and **8**) was used. This data set was divided into a training subset of 30 compounds and an external test set of 9 compounds, as described in Tables 3 and 4. A total of 194 descriptors were calculated with

**Table 1.** Summary of the CXCR4 Inhibitor Families Used in the Current Study

| family | no. of compds | refs |
|---|---|---|
| CXCR4 Inhibitors for Retrospective Docking and Shape Based Virtual Screening | | |
| tetrahydroquinolin-amine derivatives | 123 | 11, 30−34 |
| KRH1636 derivatives | 23 | 11, 35−38 |
| macrocycles | 4 | 39 |
| AMD3100 derivatives | 94 | 11, 26, 27, 39−42 |
| cyclic peptides | 2 | 43 |
| other | 2 | 44 |
| total | 248 | |
| CXCR4 Inhibitors for Retrospective Pharmacophore Model Based Virtual Screening | | |
| KRH1636 derivatives | 13 | 11, 35−38 |
| dipicolil amine zinc(II) complexes | 10 | 45 |
| AMD3100 derivatives and macrocycles | 90 | 11, 26, 27, 39−42 |
| active molecules from the combinatorial virtual library (amino-amine, amino-aldehyde) | 38 | 12 |
| total | 151 | |

MOE, including 2D and 3D descriptors. These descriptors were then pruned using correlation analysis and forward-selection and backward-elimination methods.

Partial Least Squares (PLS) regression was used to build the QSAR models using the above descriptors as independent variables and using the biological activities as the dependent variables. Model outliers were detected using the Grubbs test, as implemented in MOE, by quantifying how far away the experimental biological activities are from the model by calculating the *Z-SCORE* ratio, defined as the difference between the experimental and model $pEC_{50}$ values divided by the RMSE (root mean squared error) of the whole data set. Molecules with *Z-SCOREs* of 2.5 or higher were considered to be possible outliers. The model was then

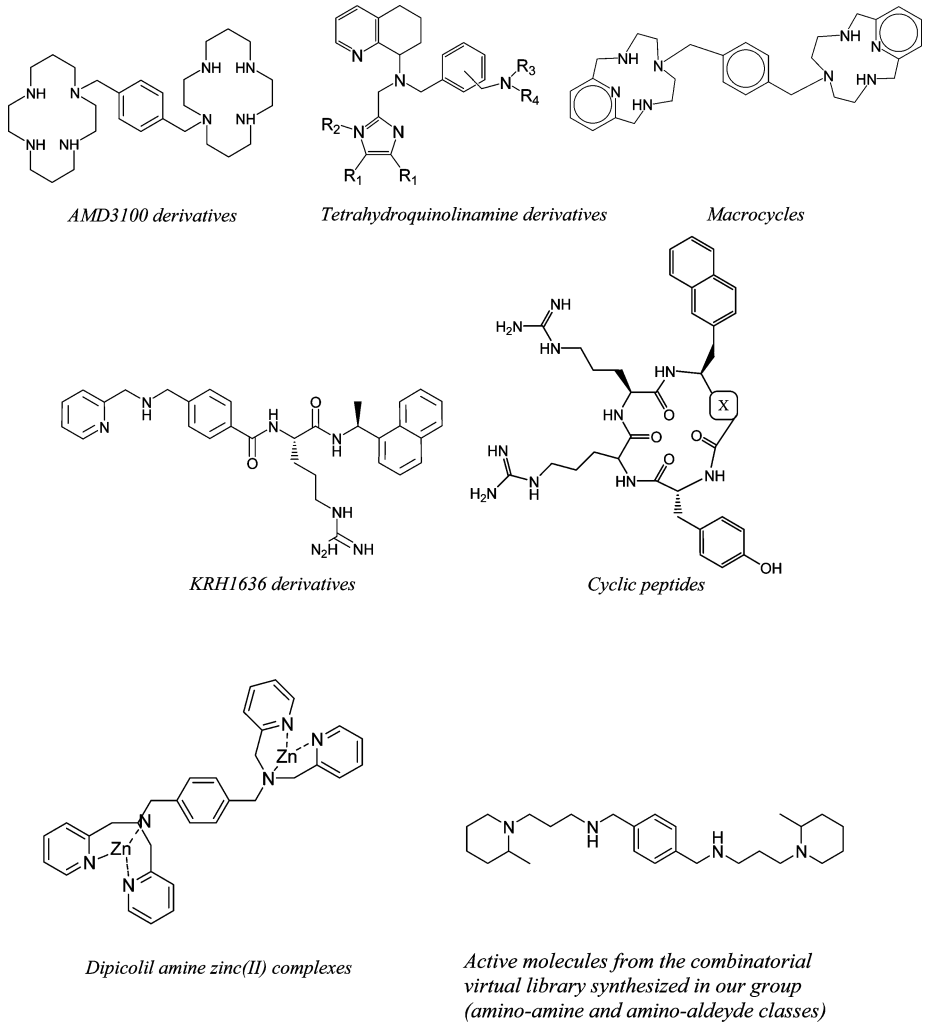


**Figure 4.** Representative structures of seven families of CXCR4 inhibitor.

**Table 2.** Summary of the 1D Physico-Chemical Properties of Active and Inactive Molecules in the Screening Databases Used in Pharmacophore Modelling, Docking, and Shape Matching Approaches[a]

| comparison of data sets used in pharmacophore modeling | MW | b_1rotN | a_acc | a_don | a_hyd | SlogP |
|---|---|---|---|---|---|---|
| 151 CXCR4 actives | 485.2 (104.9) | 6.9 (3.9) | 3.5 (1.5) | 1.5 (1.5) | 26.3 (5.0) | −0.8 (2.5) |
| 1462 inactives | 381.4 (64.9) | 5.1 (2.0) | 4.0 (1.1) | 1.2 (1.1) | 16.6 (2.6) | 2.6 (0.9) |

| comparison of data sets used in docking and shape matching approaches | MW | b_1rotN | a_acc | a_don | a_hyd | SlogP |
|---|---|---|---|---|---|---|
| 248 CXCR4 actives | 507.3(74.4) | 9.2(4.9) | 4.9(1.1) | 1.7(1.3) | 27.6(4.2) | 4.3(3.0) |
| 4696 inactives | 497.4(45.6) | 6.2(2.4) | 3.6(1.6) | 0.9(1.0) | 21.8(4.1) | 5.5(1.9) |

[a] This table shows the average and standard deviation (in parentheses) of the following properties: MW (molecular weight); b_1rotN (number of rotatable single bonds); a_acc (number of hydrogen-bond acceptor atoms); a_don (number of hydrogen-bond donor atoms); a_hyd (number of hydrophopic atoms); S_logP (octanol-water partition coefficient).

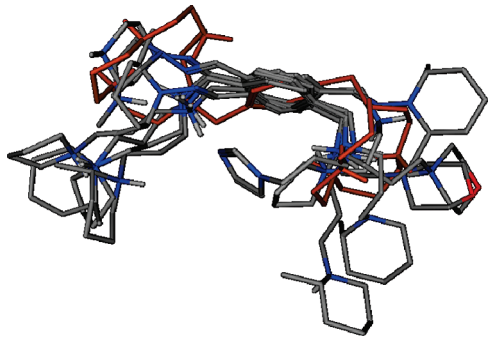

**Figure 5.** The MOE alignments of active database compounds with AMD3100 (shown in brown).

validated using leave-one-out (LOO) cross-validation and validation with an external test set (9 compounds). Several statistical parameters were used to evaluate the performance of the model:

• Correlation coefficient R2, cross-validated R2, and test set validation R2 against an external data set, where $x$ is the experimental pEC50 and $y$ is the model value

$$R = \frac{\sum (x - \bar{x}) \cdot (y - \bar{y})}{\sqrt{\sum (x - \bar{x})^2 \cdot \sum (y - \bar{y})^2}} \quad (1)$$

• Root mean squared error, *RMSE*, for the model, the cross-validation, and the external test set validation, where *PRESS* is the prediction error sum of squares and $n$ the number of compounds

$$RMSE = \sqrt{\frac{PRESS}{n}} \quad (2)$$

*PRESS* is an important cross-validation parameter to measure the accuracy of a model. When *PRESS* is less than *SSY* (sum of the squared deviations for the experimental values from their mean), it indicates that the model is significant and predicts better than chance. Furthermore, a *PRESS*/*SSY* ratio of less than 0.4 indicates that the model is a reasonable QSAR model.[47]

• Cross-validated R2 has widely been used as a criterion of model robustness and predictive ability, with a threshold of 0.5 (0.6 for model R2).[48] Nevertheless, a high cross-validated R2 is considered a necessary condition for a model to have a high predictive power, but it is not a sufficient condition. Therefore, models are often evaluated with external test sets to estimate their true predictive power. For example, Tropsha et al. consider a QSAR model to be predictive if the following conditions are satisfied[49]

$$\frac{R^2 - R_0^2}{R^2} < 0.1 \quad (3)$$

$$0.85 \leq k \leq 1.15 \quad (4)$$

where $R_o$ is the correlation coefficient, and $k$ is the value of the slope for the regression line through the origin (i.e., with the intercept set to 0).

• The Fisher test, or F-test, reflects the ratio of the variance explained by the model and the variance due to the error in the model. High values of the F-test indicate the reliability of the QSAR equation.

**Ligand-Based Pharmacophore Modeling.** Pharmacophore modeling studies were performed using the MOE and Discovery Studio software suites with four families of known actives from the above virtual screening data set, namely the following: AMD3100 derivatives, KRH1636 derivatives, dipicolil amine zinc(II) complexes, and the most active CXCR4 inhibitors from the combinatorial virtual library. 50 conformations and a maximum of 255 conformations of each compound were calculated in MOE (MMFF94 forcefield) and Discovery Studio (Catalyst Confirm algorithm), respectively. The training set consisted of the most active compound from each family of CXCR4 inhibitors. The pharmacophore queries were built on the alignment of these four structures with the FlexAlign module in MOE and using the Common Feature Pharmacophore Generation protocol in Discovery Studio. The pharmacophore scheme of PCH (polarity-charge-hydrophobicity) was applied throughout the MOE study. Chemical features and their tolerance radii were selected between those suggested by MOE to achieve better balance between sensitivity and specificity. Also, in Discovery Studio, hydrogen bond acceptor, hydrogen bond donor, hydrophobic, ionizable positive, and charged positive pharmacophore features were used. The maximum number of omitted features was set to one.

**Ligand-Based Shape Matching Virtual Screening.** Shape based virtual screening was performed using PARAFIT 08 Shape Tanimoto, ROCS 2.2 Combo Score and Shape Tanimoto, and HEX 4.8 Shape Tanimoto scores by superposing each database compound onto the docked AMD3100 query conformation. The PARAFIT and HEX superpositions were calculated using the conformation of each database

**Table 3.** Training Set Used for the QSAR Model Building Calculations[a]

| | Compound | Name | $pEC_{50}$ | predicted $pEC_{50}$ | Residue | | Compound | Name | $pEC_{50}$ | predicted $pEC_{50}$ | Residue |
|---|---|---|---|---|---|---|---|---|---|---|---|
| 1 | 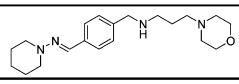 | **8**{*1,11*} | 4.512 | 4.864 | -0.352 | 16 | 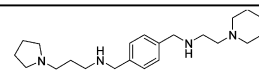 | **1**{*5,7*} | 5.327 | 5.465 | -0.138 |
| 2 | 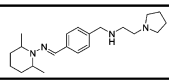 | **8**{*2,4*} | 4.367 | 5.303 | -0.936 | 17 | 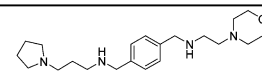 | **1**{*5,10*} | 5.177 | 5.070 | 0.107 |
| 3 | 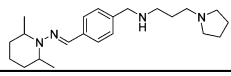 | **8**{*2,5*} | 5.251 | 5.772 | -0.521 | 18 | 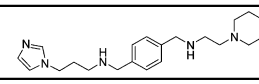 | **1**{*6,7*} | 5.254 | 5.321 | -0.067 |
| 4 | 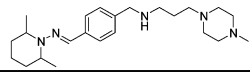 | **8**{*2,9*} | 5.005 | 4.957 | 0.048 | 19 | 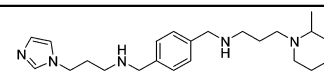 | **1**{*6,8*} | 1.106 | outlier | outlier |
| 5 | 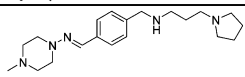 | **8**{*3,5*} | 5.281 | 4.695 | 0.586 | 20 | 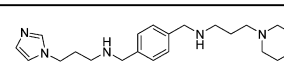 | **1**{*6,11*} | 4.305 | 5.038 | -0.733 |
| 6 | 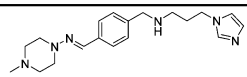 | **8**{*3,6*} | 4.483 | 4.578 | -0.095 | 21 | 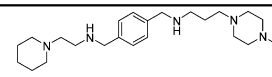 | **1**{*7,9*} | 5.190 | 5.520 | -0.330 |
| 7 | 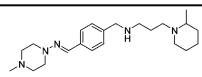 | **8**{*3,8*} | 5.424 | 5.135 | 0.289 | 22 | 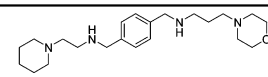 | **1**{*7,11*} | 5.142 | 5.105 | 0.037 |
| 8 | 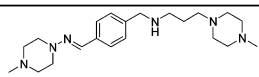 | **8**{*3,9*} | 4.503 | 4.238 | 0.265 | 23 | 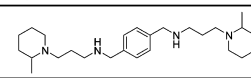 | **1**{*8,8*} | 7.715 | 6.843 | 0.872 |
| 9 | 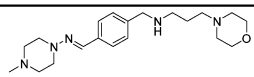 | **8**{*3,11*} | 4.647 | 4.061 | 0.586 | 24 | 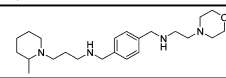 | **1**{*8,10*} | 5.987 | 5.599 | 0.388 |
| 10 | 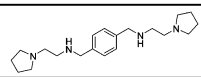 | **1**{*4,4*} | 4.511 | 4.917 | -0.406 | 25 | 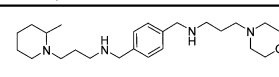 | **1**{*8,11*} | 5.906 | 5.890 | 0.016 |
| 11 | 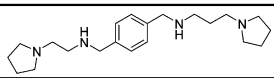 | **1**{*4,5*} | 5.299 | 5.291 | 0.008 | 26 | 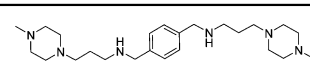 | **1**{*9,9*} | 4.642 | 5.047 | -0.405 |
| 12 | 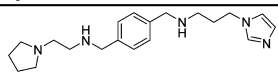 | **1**{*4,6*} | 4.852 | 4.962 | -0.110 | 27 | 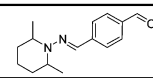 | **6**{*2*} | 4.432 | 4.724 | -0.292 |
| 13 | 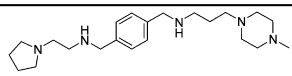 | **1**{*4,9*} | 4.659 | 4.913 | -0.254 | 28 | 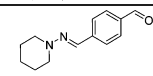 | **6**{*1*} | 4.235 | 4.169 | 0.066 |
| 14 | 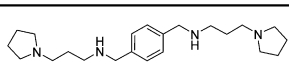 | **1**{*5,5*} | 5.600 | 5.548 | 0.052 | 29 | 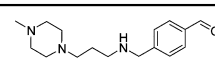 | **7**{*9*} | 4.233 | 3.811 | 0.422 |
| 15 | 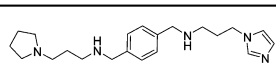 | **1**{*5,6*} | 6.250 | 5.351 | 0.899 | 30 | 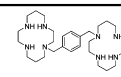 | AMD3100 | 8.688 | 8.688 | 0 |

[a] $pEC_{50}$ (derived from $EC_{50}$ in $\mu$M) refers to the experimental activity values. The two last columns show the predicted and residual $pEC_{50}$values obtained from QSAR model 1. Compound **19** gave a *Z-SCORE* > 2.5 and was therefore considered to be an outlier and was excluded from the training set.

compound that was calculated by MOE FlexAlign. However, as described previously,[20] the ROCS superpositions used ten further conformations of each molecule calculated by OMEGA.[50] Spherical harmonic consensus shape matching[51] was also performed using PARAFIT 08 by superposing each database compound onto a consensus shape query molecule calculated from three known CXCR4 actives from different scaffold families (an AMD derivative, a macrocycle derivative, and a KRH derivative). Database molecules were ranked according to their shape Tanimoto scores with respect to the query shape. The ROCS calculations also used the "color optimization" mode to maximize both the shape and chemical property overlays (e.g., proton donor/acceptor, cationic/anionic, and hydrophobicity/aromaticity).

**Receptor-Based Virtual Screening.** Receptor-based screening against CXCR4 was performed using AUTODOCK 3.0, GOLD 3.0.1, FRED 2.2.1, and HEX 4.8. In AUTODOCK and GOLD, ten independent LGA and GA runs were carried out, respectively, using the same protocol as described.[20] In GOLD, the ligands were constrained to form a hydrogen bond with a carbonyl oxygen of either Glu288, Asp171, or Asp262 which had been identified previously as key binding residues by site-directed mutagenesis (SDM).[44,52−54] The ligand databases were ranked by AUTODOCK Docked Energy, Gold GoldScore and ChemScore, and a consensus score "Rank-by-Rank"[55] of these three scoring functions. In FRED, exhaustive rigid body optimization was carried out starting from the ligand conformations aligned to the docked AMD3100 conformation. PLP, Chemgauss3, Shapegauss, OEChemScore, ScreenScore, ChemScore scoring functions, and a consensus combination of these scores were used to rank the ligand databases. In HEX, docking and ranking was performed using a six-dimensional shape-only superposition correlation search with a translational distance range of 10 Å from the SDM-defined active site center and Hex Docked energy, respectively.

**Analyzing Virtual Screening Hit Lists and Pharmacophores.** Before virtual screening protocols and pharmacophoric models may be used prospectively, it is first

**Table 4.** External Test Set Used for QSAR Model Validation[a]

| | Compound | Name | $pEC_{50}$ | predicted $pEC_{50}$ | Residue |
|---|---|---|---|---|---|
| 1 | 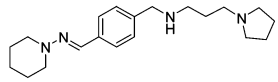 | **8**{*1,5*} | 5.079 | 5.297 | -0.218 |
| 2 | 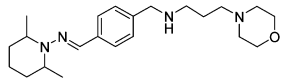 | **8**{*2,11*} | 4.375 | 5.006 | -0.631 |
| 3 | 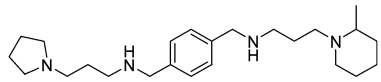 | **1**{*5,8*} | 6.357 | 6.045 | 0.312 |
| 4 | 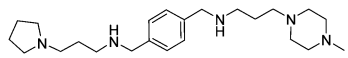 | **1**{*5,9*} | 5.889 | 5.336 | 0.553 |
| 5 | 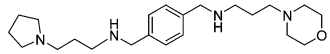 | **1**{*5,11*} | 5.369 | 5.239 | 0.130 |
| 6 | 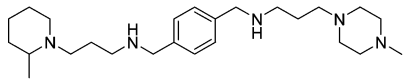 | **1**{*8,9*} | 7.142 | 5.783 | 1.359 |
| 7 | 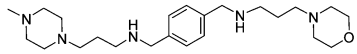 | **1**{*9,11*} | 4.647 | 5.101 | -0.454 |
| 8 | 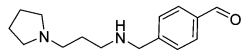 | **7**{*5*} | 4.337 | 4.249 | 0.088 |
| 9 | 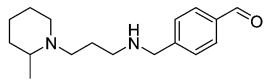 | **7**{*8*} | 5.183 | 4.962 | 0.221 |

[a] The column headings are described in Table 3.

**Table 5.** Correlation Analysis for the Descriptors Used in the QSAR Models

| | $pEC_{50}$ | VAdjEq | Q_VSA_HYD | dipoleY | SlogP_VSA8 | SMR_VSA5 | FASA+ |
|---|---|---|---|---|---|---|---|
| $pEC_{50}$ | 100 | | | | | | |
| VAdjEq | −60 | 100 | | | | | |
| Q_VSA_HYD | 84 | −68 | 100 | | | | |
| dipoleY | 41 | −14 | 20 | 100 | | | |
| SlogP_VSA8 | 56 | −26 | 41 | 42 | 100 | | |
| SMR_VSA5 | 54 | −39 | 37 | 49 | 68 | 100 | |
| FASA+ | 38 | −16 | 59 | −6 | −34 | −12 | 100 |

necessary to validate them by measuring their ability to retrieve actives from a database of compounds with known biological activities. Several formulas have been proposed to score quantitatively the quality of hit lists achieved in this way.[56] For example, for a database of $D$ compounds containing $A$ actives, and where $H_t$ is the number of compounds in a hit list, and $H_a$ is the number of actives in that list, the following terms may be defined:[57]

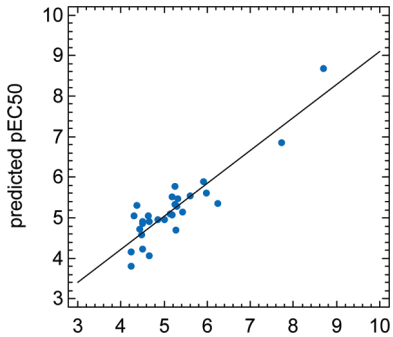


**Figure 6.** Correlation of experimental versus predicted $pEC_{50}$ for QSAR model 1.

Percent yield of actives:

$$Y(\%) = \frac{H_a}{H_t} \times 100 \tag{5}$$

Percent ratio of the actives in the hit list:

$$A(\%) = \frac{H_a}{A} \times 100 \tag{6}$$

Enrichment (enhancement):

$$EF = \frac{H_a/H_t}{A/D} = \frac{H_a \times D}{H_t \times A} \tag{7}$$

Goodness of Hit list:

$$GH = \left(\frac{H_a(3A + H_t)}{4H_tA}\right) \times \left(1 - \frac{H_t \times H_a}{D - A}\right) \tag{8}$$

False Negatives:

$$A - H_a \tag{9}$$

False Positives:

$$H_t - H_a \tag{10}$$

For each scoring method, the resulting hit lists were analyzed using the above terms. Following the pharmacoph-

**Table 6.** Prediction of Activity Values Using QSAR Model 1

| Compound | Name | predicted $EC_{50}$ (μM) |
|---|---|---|
| 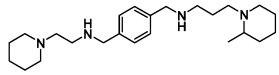 | **1**{*7,8*} | 0.66 |
| 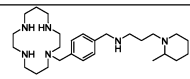 | **10**{*8*} | 0.87 |
| 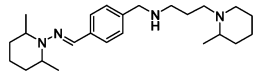 | **8**{*2,8*} | 1.58 |
| 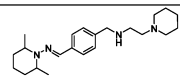 | **8**{*2,7*} | 1.88 |
| 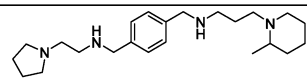 | **1**{*4,8*} | 2.16 |
| 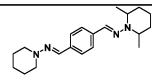 | **2**{*1,2*} | 2.24 |
| 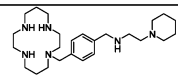 | **10**{*7*} | 2.70 |
| 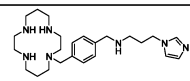 | **10**{*6*} | 2.87 |
| 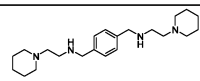 | **1**{*7,7*} | 2.93 |
| 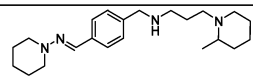 | **8**{*1,8*} | 3.70 |
| 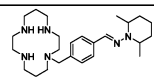 | **9**{*2*} | 3.85 |
| 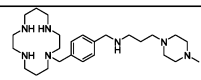 | **10**{*9*} | 4.61 |
| 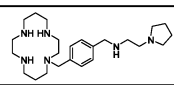 | **10**{*4*} | 4.75 |
| 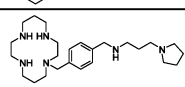 | **10**{*5*} | 5.23 |
| 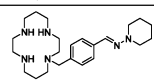 | **9**{*1*} | 5.90 |
| 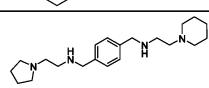 | **1**{*4,7*} | 5.94 |
| 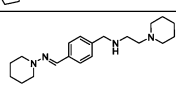 | **8**{*1,7*} | 5.98 |
| 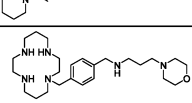 | **10**{*11*} | 7.30 |
| 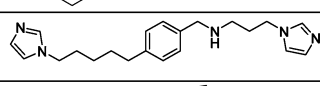 | **1**{*6,6*} | 7.53 |
| 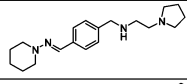 | **8**{*1,4*} | 9.28 |
| 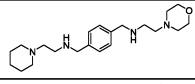 | **1**{*7,10*} | 9.95 |
| 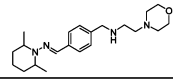 | **8**{*2,10*} | 10.13 |
| 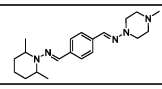 | **2**{*2,3*} | 10.52 |

**Table 6.** Continued

| Compound | Name | predicted $EC_{50}$ (μM) |
|---|---|---|
| 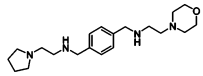 | **1**{*4,10*} | 17.35 |
| 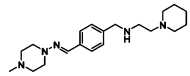 | **8**{*3,7*} | 18.96 |
| 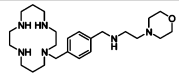 | **10**{*10*} | 19.70 |
| 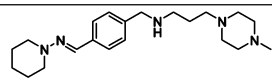 | **8**{*1,9*} | 21.50 |
| 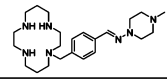 | **9**{*3*} | 24.95 |
| 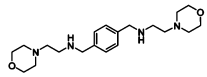 | **1**{*10,10*} | 30.06 |
| 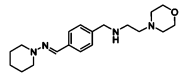 | **8**{*1,10*} | 30.44 |
| 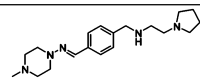 | **8**{*3,4*} | 43.40 |
| 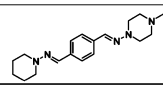 | **2**{*1,3*} | 48.09 |
| 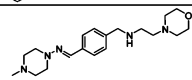 | **8**{*3,10*} | 58.34 |
| 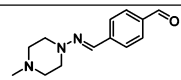 | **6**{*3*} | > 100 |

**Table 7.** Summary of the Results Obtained for the Retrospective Screening Analysis of the Generated Pharmacophore Models[a]

| model | $H_a$ | $H_t$ | false + | false - | *EF* | *Y(%)* | *A(%)* | *GH* |
|---|---|---|---|---|---|---|---|---|
| 1 | 142 | 142 | 0 | 9 | 10.68 | 100 | 94 | 0.99 |
| 2 | 139 | 140 | 1 | 12 | 10.61 | 99 | 92 | 0.97 |
| 3 | 122 | 157 | 35 | 29 | 8.30 | 78 | 81 | 0.77 |
| 4 | 133 | 186 | 53 | 18 | 7.64 | 72 | 88 | 0.73 |
| 5 | 123 | 168 | 45 | 28 | 7.82 | 73 | 81 | 0.73 |
| 6 | 132 | 132 | 0 | 19 | 10.68 | 100 | 87 | 0.97 |
| 7 | 96 | 96 | 0 | 55 | 10.68 | 100 | 64 | 0.91 |
| 8 | 106 | 107 | 1 | 45 | 10.58 | 99 | 70 | 0.92 |
| 9 | 92 | 92 | 0 | 59 | 10.68 | 100 | 61 | 0.90 |

[a] The quantities $H_a$, $H_t$, false +, false -, *EF*, *Y(%)*, *A(%)*, and *GH* are defined in eqs 5−10. Overall, QSAR model 1 can be seen to give the best statistics.

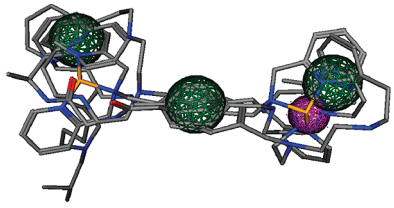

**Figure 7.** Alignment of the compounds in the training set and the pharmacophore model 1. Hydrophobic and aromatic features (HydlAro) are shown in green. Cationic (Cat) features are shown in purple.

ore modeling, shape matching, and docking calculations, all compounds were sorted into ranked lists based upon their rmsd, shape matching scores, and docking energies, respectively. These lists were then used to plot the percentage of known actives found versus the percentage of the ranked database screened and to calculate enrichment factors (EFs) at 1%, 5%, and 10% of the screened database.

## RESULTS

**PLS Analysis and Validation of QSAR Models.** After descriptor pruning had been applied, five descriptors were selected to build the QSAR models, namely the following: VAdjEq, Q_VSA_HYD, dipoleY, SlogP_VSA8, and FASA+. Table 5 shows the correlation analysis for these descriptors. Three QSAR models were calculated as follows:

Model 1 (Figure 6):

$$pEC_{50} = 2.52586 + 0.00940 \cdot (Q\_VSA\_HYD) + 0.00507 (\cdot SlogP\_VSA8) + 0.10611 \cdot (dipoleY)$$

$N = 29$, $R^2 = 0.81$, RMSE = 0.42, $F = 36.45$, $R^2_{LOO} = 0.75$, $RMSE_{LOO} = 0.49$, $R^2_{test} = 0.69$, $RMSE_{test} = 0.57$, $n = 9$, $R_o^2 = 0.77$, $(R^2\text{-}R_o^2)/R^2 = 0.049$, $k = 0.99$, PRESS = 5.20, SSY = 27.93, PRESS/SSY = 0.19

Model 2:

$$pEC_{50} = 2.52568 + 0.00940 \cdot (Q\_VSA\_HYD) + 0.10611 \cdot (dipoleY) + 0.00507 \cdot (SlogP\_VSA8) + 0.00130 \cdot (FASA+)$$

$N = 29$, $R^2 = 0.81$, RMSE = 0.42, $F = 26.24$, $R^2_{LOO} = 0.75$, $RMSE_{LOO} = 0.49$, $R^2_{test} = 0.69$, $RMSE_{test} = 0.57$, $n = 9$, $R_o^2 = 0.77$, $(R^2\text{-}R_o^2)/R^2 = 0.049$, $k = 0.99$, PRESS = 5.20, SSY = 27.93, PRESS/SSY = 0.19

**Table 8.** Pharmacophore-Based Prospective Virtual Screening Results[a]

| compound | model 1 | model 2 | model 3 | model 4 | model 5 |
|---|---|---|---|---|---|
| **2**{*1,2*} | - | - | - | - | - |
| **2**{*1,3*} | 0.9169 | 0.9086 | - | 0.9870 | - |
| **8**{*1,4*} | 0.7352 | 0.5261 | 0.5712 | 0.7153 | 1.4686 |
| **8**{*1,7*} | - | 0.5190 | 0.6307 | 0.7327 | - |
| **8**{*1,8*} | 0.6071 | 0.4723 | 0.6284 | 0.9790 | - |
| **8**{*1,9*} | 0.6714 | 0.3698 | 0.5487 | 0.7998 | - |
| **8**{*1,10*} | - | 0.5110 | 0.6307 | 0.7305 | 1.2161 |
| **2**{*2,3*} | 0.7664 | 0.9129 | - | 0.8400 | - |
| **8**{*2,7*} | - | 0.8506 | 0.6338 | 0.6678 | 1.3628 |
| **8**{*2,8*} | 0.4375 | 0.4742 | 0.6199 | 0.6860 | - |
| **8**{*2,10*} | - | 0.7040 | 0.6339 | 0.6660 | 0.8185 |
| **8**{*3,4*} | 0.4417 | 0.5261 | 0.5711 | 0.6690 | 0.9981 |
| **8**{*3,7*} | 0.5551 | 0.4368 | 0.6306 | 0.6317 | 0.8388 |
| **8**{*3,10*} | 0.5551 | 0.4289 | 0.6306 | 0.6291 | 0.8327 |
| **1**{*4,7*} | 0.7565 | 0.3962 | 0.5227 | 0.4716 | 0.8880 |
| **1**{*4,8*} | 0.4157 | 0.3923 | 0.4166 | 0.4902 | 0.8354 |
| **1**{*4,10*} | 0.7308 | 0.3284 | 0.5119 | 0.5366 | 0.7563 |
| **1**{*6,6*} | 0.6027 | 0.9477 | 0.4127 | - | - |
| **1**{*7,7*} | 0.6990 | 0.5077 | 0.5190 | 0.6907 | 1.0076 |
| **1**{*7,8*} | 0.4157 | 0.3625 | 0.4166 | 0.5070 | 0.8043 |
| **1**{*7,10*} | 0.7308 | 0.3284 | 0.5119 | 0.4728 | 0.7508 |
| **1**{*10,10*} | 1.1377 | 0.4894 | 0.5079 | 0.4643 | 0.7041 |
| **6**{*3*} | - | 0.9007 | - | - | - |
| **9**{*1*} | 0.4288 | 0.4014 | 0.4803 | 0.5879 | 1.1812 |
| **9**{*2*} | 0.3235 | 0.3832 | 0.4742 | 0.5254 | 0.8217 |
| **9**{*3*} | 0.4747 | 0.4012 | 0.4805 | 0.5449 | 0.5568 |
| **10**{*4*} | 0.3409 | 0.4270 | 0.4640 | 0.4845 | 0.6615 |
| **10**{*5*} | 0.3671 | 0.3329 | 0.4250 | 0.4800 | 0.7907 |
| **10**{*6*} | 0.3925 | 0.4079 | 0.4250 | 0.4800 | 1.1394 |
| **10**{*7*} | 0.2826 | 0.3789 | 0.4512 | 0.3739 | 0.5394 |
| **10**{*8*} | 0.3321 | 0.4755 | 0.4248 | 0.3568 | 0.5311 |
| **10**{*9*} | 0.2655 | 0.3462 | 0.4248 | 0.3320 | 0.5408 |
| **10**{*10*} | 0.2809 | 0.3786 | 0.4512 | 0.3727 | 0.5405 |
| **10**{*11*} | 0.3755 | 0.2856 | 0.4248 | 0.3483 | 0.5304 |

[a] This table lists the overall (RMSD) score obtained for each compound using pharmacophore models 1, 2, 3, 4, and 5. Hyphens denote compounds that do not match the pharmacophore model.

Model 3:

$$pEC_{50} = 2.52606 + 0.00940 \cdot (Q\_VSA\_HYD) + 0.00507 \cdot (SlogP\_VSA8) + 0.10611 \cdot (dipoleY) - 0.00040 \cdot (VAdjEq)$$

$N = 29$, $R^2 = 0.81$, RMSE $= 0.42$, $F = 26.24$, $R^2_{LOO} = 0.75$, $RMSE_{LOO} = 0.49$, $R^2_{test} = 0.69$, $RMSE_{test} = 0.57$, $n = 9$, $R_o^2 = 0.77$, $(R^2\text{-}R_o^2)/R^2 = 0.049$, $k = 0.99$, PRESS $= 5.20$, SSY $= 27.93$, PRESS/SSY $= 0.19$

One compound **1**{*6,8*} was deleted from the training set because it gave a *Z-SCORE* > 2.5, which indicated it is an outlier. This was confirmed by recalculating the models without it to obtain better overall statistics. All three resulting models showed $R^2$ values above 0.6 and $R^2$ for the cross-validation and external test set validation above 0.5. In all cases, the *PRESS/SSY* ratio was below 0.4, $(R^2\text{-}R_o^2)/R^2$ was less than 0.1, and $k$ was between the above thresholds. Because the statistical results were broadly similar for all models, model 1 was selected as the most parsimonious because it used only three descriptors, whereas models 2 and 3 required four descriptors. The use of *dipoleY*, an external 3D descriptor, as independent variable in the three models enhanced the importance of a correct alignment of the molecules in order to obtain a reliable predicted activity value. Prediction of activity values for the training set and the external test set using model 1 are shown in Tables 3 and 4. Predictions were made for compounds in the virtual library that had not yet been synthesized (**1, 2**, and **8**) and for monocyclams **9** and **10**. These results are shown in Table 6.

**Pharmacophore Hypothesis Generation and Validation.** Pharmacophore models were generated and retrospective analyses were performed to select models which achieved a good balance between sensitivity and specificity. Several models were proposed (Table 7), five using MOE (Models 1 to 5) and four using Discovery Studio (Models 6 to 9). Model 1 was built using the MOE Pharmacophore Elucidate module. Features in models 2 and 3 were selected from the consensus analysis performed with MOE Pharmacophore Query module. Models 4 and 5 were manually designed based on the description of the interactions of AMD3100 and CXCR4.[44,54,58−62] Finally, models 6 to 9 were built in Discovery Studio using the Hypogen and HipHop algorithms to generate hypotheses and to select the best common pharmacophore features produced. The retrospective analysis of the models showed that pharmacophore model 1 (Figure 7) was highly selective with our data set, giving no false positives and only nine false negatives. This model accurately classified and ranked all the known actives in the data set, except for the KRH1636 analogues which were positioned at the end of the hit list. Visual inspection of the hit lists in the retrospective analysis showed that the ranking of each compound depended on the model and type of compound. More reliable results were obtained using a consensus of the five MOE models in Table 7.

A prospective analysis using the consensus pharmacophore model was then applied to select new compounds for synthesis and testing. These molecules included hitherto unsynthesised compounds from the virtual combinatorial library (i.e., amino/hydrazono-amine/hydrazone compounds **1**, **2,** and **8**, amino/hydrazono-aldehyde compounds **6** and **7** and cyclam-amine/hydrazone compounds **9** and **10**). All of these compounds can be seen to match the pharmacophore model equally well. The screened compounds selected by the consensus of pharmacophore models and their score values are shown in Table 8.

**Docking Enrichments.** In order to analyze the ability of the receptor model structure to discriminate active compounds from decoys, retrospective analysis of docking enrichment curves was performed as described previously.[20] Next, enrichment curves for the virtual combinatorial library compounds were calculated using the same protocol. Figure 8 shows the enrichment curves obtained. Inspection of these results shows that the enrichments obtained with the FRED consensus, Consensus scoring (AUTODOCK Docked Energy, GOLD GoldScore and ChemScore), and ChemScore scoring functions are the best, as was observed in the retrospective analysis. Looking at the first percentages of the ranked hit lists, the compounds selected by these three scoring functions can be seen to belong to **9**, **10**, **1**, **2,** and **8**. The compounds found at the top 10% of the ranked hit list using these three scoring functions as well as AUTODOCK Docked Energy, HEX Docked Energy, and FRED Chemgauss3 are nearly the same. The screened compounds selected by these scoring functions and their score value are shown in Table 9.

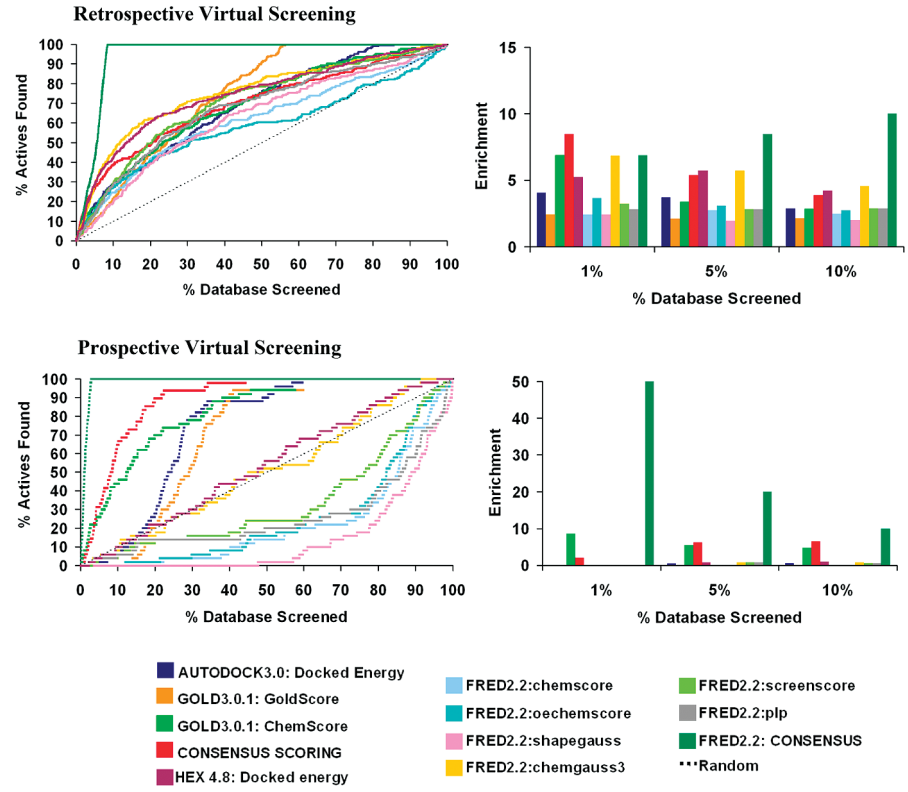


**Figure 8.** CXCR4 docking-based enrichment plots. On the left, enrichment results for several docking protocols for retrospective (top) and prospective (bottom) virtual screening analyses. The dotted black line represents the expected values if actives are selected at random. On the right, enrichment factors for actives found within the top-ranking 1%, 5%, and 10% of the screened inhibitor database (top) and screened virtual combinatorial library (bottom).

**Table 9.** Docking Scores of Hits from the Screened Combinatorial Library[a]

| compound | consensus score | GOLD ChemScore | FRED consensus | AUTODOCK docked energy | HEX docked energy | FRED Chemgauss3 |
|---|---|---|---|---|---|---|
| **10**{*8*} | 512.70 | 27.20 | 446 | −16.27 | −345.80 | −16.97 |
| **10**{*9*} | 455.30 | 25.88 | 408 | −17.69 | −373.90 | −30.96 |
| **10**{*11*} | 1129.30 | 8.07 | 388 | −15.76 | −396.30 | −31.67 |
| **10**{*5*} | 920.30 | 15.29 | 464 | −16.59 | −343.70 | −14.77 |
| **9**{*2*} | 707 | 26.42 | 329 | −14.78 | −409.50 | −29.98 |
| **8**{*2,8*} | 743.70 | 35.55 | 119 | −14.59 | −374.70 | −47.45 |
| **1**{*7,8*} | 738 | 31.29 | 427 | −15.14 | −407.80 | −62.70 |
| **8**{*1,8*} | 904.30 | 25.06 | 212 | −14.69 | −325.70 | −49.30 |
| **1**{*4,10*} | 922.70 | 28.29 | 207 | −14.03 | −421.60 | −46.24 |
| **8**{*2,7*} | 656 | 30.80 | 160 | −14.46 | −421.20 | −57.50 |
| **1**{*4,8*} | 492.70 | 33.11 | 422 | −14.92 | −443.60 | −42.65 |
| **1**{*7,10*} | 738.30 | 26.30 | 341 | −14.10 | −420.50 | −40.59 |
| **1**{*4,7*} | 683 | 28.39 | 185 | −15.90 | −381.3 | −69.14 |

[a] This table shows compounds found within the top 10% of the ranked hit list using Consensus score (AUTODOCK Docked Energy, GOLD GoldScore, and ChemScore), GOLD ChemScore, FRED consensus (PLP, Chemgauss3, Shapegauss, OEChemScore, ScreenScore, ChemScore), AUTODOCK Docked Energy, HEX Docked Energy, and Chemgauss3 scoring functions.

**Shape Matching Enrichments.** Because no crystallographic ligand conformation is available for the current system, the SDM-compatible conformation of AMD3100 found previously from computational docking was used as the database query. In order to study the performance of this query structure and the parameters used in the screening protocol, a retrospective analysis of shape matching enrichment curves was first performed.[20] Next, enrichment curves for the combinatorial virtual library compounds were calculated using the same protocol. Moreover, a consensus query was built from three different scaffold CXCR4 known actives (an AMD derivative, a macrocycle derivative, and a KRH derivative), and a retrospective analysis was performed. Enrichment curves for the virtual combinatorial library compounds were also calculated showing similar results to the basic PARAFIT AMD3100 query shape Tanimoto score. Figure 9 shows that the ROCS Combo Score and PARAFIT Tanimoto Score and Consensus Shape Tanimoto give the best EFs, as in the retrospective analysis. HEX Shape Tanimoto and ROCS Shape Tanimoto also perform well. Overall, the ligand-based shape matching tools perform better than the docking tools used here. However, looking at the first percentages of the ranked hit lists obtained, the compounds selected by these shape matching methods belong to **9**, **10**, **1**, **2,** and **8**, as found with the docking tools. Molecules found at the top 10% hit ranking list are the same

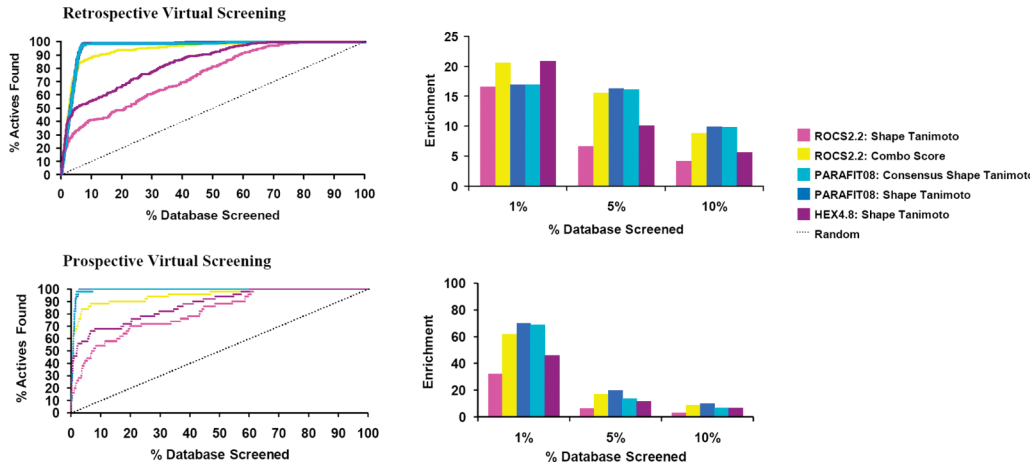


**Figure 9.** CXCR4 shape matching-based enrichments. On the left, enrichment curves obtained for various shape matching protocols on the known inhibitor database (top) and compounds from the virtual combinatorial library (bottom). The dotted line represents the expected enrichment if actives are selected at random. On the right, enrichment values for actives found within the top-ranking 1%, 5%, and 10% of the screened database (top) and screened virtual combinatorial library (bottom).

**Table 10.** Shape Matching Scores for Hits from the Screened Combinatorial Library[a]

| compound | PARAFIT Shape Tanimoto | PARAFIT Consensus Shape | ROCS Shape Tanimoto | ROCS Combo Score | HEX Shape Tanimoto |
|---|---|---|---|---|---|
| **10**{*11*} | 0.9725 | 0.9763 | 0.5970 | 0.9010 | 0.9109 |
| **10**{*8*} | 0.9492 | 0.9506 | 0.5070 | 0.6320 | 0.8479 |
| **10**{*9*} | 0.8996 | 0.9028 | 0.4820 | 0.8160 | 0.8422 |
| **10**{*5*} | 0.9193 | 0.9334 | 0.5280 | 0.8720 | 0.8490 |
| **9**{*2*} | 0.9570 | 0.9507 | 0.6330 | 0.6940 | 0.9145 |
| **8**{*2,8*} | 0.9651 | 0.966 | 0.5170 | 0.6840 | 0.8741 |
| **1**{*7,8*} | 0.9597 | 0.9471 | 0.5420 | 0.7320 | 0.8855 |
| **8**{*1,8*} | 0.9393 | 0.9416 | 0.5730 | 0.6070 | 0.8948 |
| **2**{*1,2*} | 0.9230 | 0.9307 | 0.5200 | 0.5580 | 0.8449 |
| **8**{*2,7*} | 0.9101 | 0.9053 | 0.4950 | 0.5480 | 0.8581 |
| **1**{*7,10*} | 0.9498 | 0.9547 | 0.4460 | 0.6240 | 0.8457 |
| **1**{*4,7*} | 0.9015 | 0.9139 | 0.4950 | 0.8100 | 0.8442 |

[a] This table shows compounds found within the top 10% of the ranked database using PARAFIT Shape Tanimoto and Consensus Shape Tanimoto, ROCS Combo Score and Shape Tanimoto, and HEX Shape Tanimoto scores.

using these different shape matching approaches. The screened compounds selected by these shape-based methods and their score value are shown in Table 10.

**Hit Selection.** A consensus "Rank-by-Vote"[55] of all the first hit ranking lists compounds found was performed, and five compounds were selected to be synthesized: **1**{*7,8*}, **8**{*2,8*}, **8**{*1,8*}, **10**{*11*}, and **10**{*8*}. Both of the cyclam-amine compounds (**10**) were classified in the top of the ranked list in the virtual screenings, but we selected the two best ranked and the three best classified amino/hydrazono-amines. Compound **8**{*1,8*} was toxic at a concentration of 4.1 $\mu$g/mL and showed no activity below this concentration (Table 11). However, compounds **1**{*7,8*} and **8**{*2,8*} showed anti-HIV activity values of 0.6 and 0.4 $\mu$g/mL, respectively, and the cyclam-amine compounds **10**{*11*} and **10**{*8*} showed the best anti-HIV activities of 0.058 $\mu$g/mL and 0.022 $\mu$g/mL, respectively.

**Table 11.** Summary of the Five VS-Selected Hits[a]

| Compound | Name | $EC_{50}$ / µg/ml | $CC_{50}$ / µg/ml |
|---|---|---|---|
| 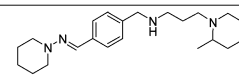 | **8**{*1,8*} | > 4.1 | 4.1 |
| 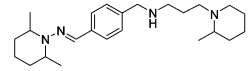 | **8**{*2,8*} | 0.6 | 14.6 |
| 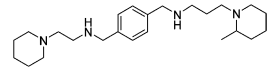 | **1**{*7,8*} | 0.4 | > 25 |
| 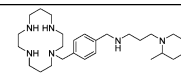 | **10**{*8*} | 0.022 | > 25 |
| 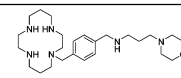 | **10**{*11*} | 0.058 | > 25 |

[a] $EC_{50}$ denotes anti-HIV activity, and $CC_{50}$ is the cytotoxicity value ($\mu$g/ml).

## DISCUSSION

A combination of ligand-based and receptor-based screening tools was used to select molecules from the virtual combinatorial library. The different approaches used generally select similar molecules at the first percentages of the ranked hit lists. Compounds selected by the various ligand-based virtual screening tools are practically the same, whereas those selected by the structure-based docking tools also include some others. All shape-based and pharmacophore ligand-based approaches, and consensus scoring of AUTODOCK and GOLD scoring functions, FRED consensus and Chemgauss3, and the HEX Docked Energy approaches select nearly the same molecules at first percentages of database screened. However, although ligand-based searches

give better results than structure-based docking for both retrospective and prospective virtual screening analyses, the pharmacophore models and also AUTODOCK Docked Energy give the best correlation with experimental data. Of the five compounds selected by the Rank-by-Vote consensus, compound **8**{*1,8*} was toxic below 5 $\mu$g/mL, but **1**{*7,8*} and **8**{*2,8*} showed activity values below 1 $\mu$g/mL, and the remaining two, **10**{*11*} and **10**{*8*}, both of which are monocyclams, showed activity values below 0.06 $\mu$g/mL. Our proposed QSAR model agrees well with the experimental results, especially for the nonmonocyclam compounds, with predicted activities of 0.66, 1.58, 7.30, and 0.87 $\mu$M for **1**{*7,8*}, **8**{*2,8*}, **10**{*11*}, and **10**{*8*}, which differ by only 0.37, 0.02, 7.17, and 0.82 $\mu$M, respectively, from the experimental biological values.

Overall, our screening procedure selects the most active compounds from our combinatorial virtual library (i.e., **1**{*8,8*} 0.008 $\mu$g/mL, **1**{*8,9*} 0.03 $\mu$g/mL, **1**{*5,6*} 0.2 $\mu$g/mL, **1**{*8,10*} 0.4 $\mu$g/mL) in the first ranking positions of the final consensus list. Moreover, the first five unsynthesized compounds which were also predicted to be active were ranked in order of their known activities. Hence our screening procedure can be seen to perform rather well.

## CONCLUSION

A database of CXCR4 inhibitors and similar presumed inactive compounds was compiled from the literature in order to perform retrospective virtual screening. This database was used to compare docking-based and ligand-based (i.e., pharmacophore modeling and shape matching) virtual screening approaches. Additionally, a large virtual combinatorial library of candidate CXCR4 antagonists was designed, and the above screening approaches were used to select five compounds for synthesis and testing. The actives identified in this way had activities in the range 20 to 0.008 $\mu$g/mL. Experimental binding assays of those compounds confirmed that their mode of action was to block the CXCR4 receptor. Activity values were used for the development of ligand-based QSAR models in order to use them to predict activity of hitherto unsynthesised molecules. Prospective virtual screening, using the same protocol as in retrospective screening analysis, was then used to guide the selection of other molecules from the virtual combinatorial library. Molecules found at the first positions of the consensus ranked hit list showed activity values in the range from 4 to 0.022 $\mu$g/mL.

## ACKNOWLEDGMENT

We are grateful to OpenEye Scientific Software Inc. for providing an Academic Licence for ROCS and to Cepos Insilico Ltd. for providing PARASURF and PARAFIT. The authors are grateful to José Esté, Imma Clotet-Codina, and Mercedes Armand-Ugón from Laboratori de Reroviologia IrsiCaixa, Hospital Universitari Germans Trias I Pujol, Universitat Autonoma de Barcelona for carrying out the biological activity tests. S.P. thanks the Institut Químic de Sarrià (IQS) for a predoctoral grant, and V.I.P.N. thanks the Generalitat de Catalunya - DURSI for a grant within the Formació de Personal Investigador (2008FI) program. This work was supported by The TV3 Marathon Foundation (AIDS-2001) promoted by the Catalan Radio and Television Corporation (Corporació Catalana de Ràdio i Televisió, CCRTV) and the Programa Nacional de Biomedicina (Ministerio de Educación y Ciencia, SAF2007-63622-C02-01).

## REFERENCES AND NOTES

(1) UNAIDS. AIDS epidemic update: December 2007. http://www.unaids.org/en/KnowledgeCentre/HIVData/EpiUpdate/EpiUpdArchive/2007/default.asp (accessed Nov 11, 2008).
(2) De Clercq, E. Emerging anti-HIV drugs. *Expert Opin. Emerging Drugs* **2005**, *10*, 241–274.
(3) De Clercq, E. Anti-HIV chemotherapy: current state of the art. *Med. Chem. Res.* **2004**, *13*, 439–478.
(4) Kadow, J.; Wang, H. G.; Lin, P. F. Small-molecule HIV-1 gp120 inhibitors to prevent HIV-1 entry: an emerging opportunity for drug development. *Curr. Opin. Invest. Drugs (Thomson Sci.)* **2006**, *7*, 721–726.
(5) Berger, E. A.; Murphy, P. M.; Farber, J. M. Chemokine receptors as HIV-1 coreceptors: Roles in viral entry, tropism, and disease. *Annu. Rev. Immunol.* **1999**, *17*, 657–700.
(6) Jiang, S.; Lin, K.; Strick, N.; Neurath, A. R. Inhibition of HIV-1 infection by a fusion domain binding peptide from the HIV-1 envelope glycoprotein GP41. *Biochem. Biophys. Res. Commun.* **1993**, *195*, 533–538.
(7) De Clercq, E. New antiviral agents in preclinical or clinical development. *Adv. Antiviral Drug Des.* **2004**, *4*, 1–62.
(8) De Clercq, E. New Anti-HIV Agents and Targets. *Med. Res. Rev.* **2002**, *22*, 531–565.
(9) Bean, P. New Drugs Targets for HIV. *Clin. Infect. Dis.* **2005**, *41*, 96–100.
(10) Markovic, I.; Clouse, K. A. Recent advances in understanding the molecular mechanisms of HIV-1 entry and fusion: revisiting current targets and considering new options for therapeutic intervention. *Curr. HIV Res.* **2004**, *2*, 223–34.
(11) Kazmierski, W. M.; Peckman, J. P.; Duan, M.; Kenakin, T. P.; Jenkinson, S.; Gudmundsson, K. S.; Piscitelli, S. C.; Feldman, P. L. Recent Progress in the Discovery of New CCR5 and CXCR4 Chemokine Receptor Antagonists as Inhibitors of HIV-1 Entry. Part 2. *Curr. Med. Chem. - Anti Infect. Agents* **2005**, *4*, 133–152.
(12) Pettersson, S.; Pérez-Nueno, V. I.; Ros-Blanco, L.; Puig de la Bellacasa, R.; Rabal, O.; Batllori, X.; Clotet, B.; Clotet-Codina, I.; Armand-Ugón, M.; Esté, J.; Borrell, J. I.; Teixidó, J. Discovery of novel non-cyclam polynitrogenated CXCR4 coreceptor inhibitors. *ChemMedChem* **2008**, *3*, 1549–1557.
(13) *Maybridge Bringing life to drug discovery*; Maybridge Databases Autumn 2005; Fisher Scientific International: England, 2005.
(14) Pascual, R.; Borrell, J. I.; Teixido, J. Analysis of selection methodologies for combinatorial library design. *Mol. Diversity* **2003**, *6*, 121–133.
(15) *MOE (Molecular Operating Environment), 2006.08 Release*; Chemical Computing Group, Inc.: Montreal, Canada, 2004.
(16) *Discovery Studio, version 2.0*; Accelrys Software Inc.: San Diego, 2007.
(17) Lin, J.; Clark, T. An analytical, variable resolution, complete description of static molecules and their intermolecular binding properties. *J. Chem. Inf. Model.* **2005**, *45*, 1010–1016.
(18) Grant, A. J.; Pickup, B. T. A fast method of molecular shape comparison: a simple application of a Gaussian description of molecular shape. *J. Comput. Chem.* **1996**, *17*, 1653–1659.
(19) Ritchie, D. W.; Kemp, G. J. L. Fast computation, rotation, and comparison of low resolution spherical harmonic molecular surfaces. *J. Comput. Chem.* **1999**, *20*, 383–395.
(20) Pérez-Nueno, V. I.; Ritchie, D. W.; Rabal, O.; Pascual, R.; Borrell, J. I.; Teixidó, J. Comparison of Ligand-Based and Receptor-Based Virtual Screening of HIV Entry Inhibitors for the CXCR4 and CCR5 Receptors Using 3D Ligand Shape-matching and Ligand-Receptor Docking. *J. Chem. Inf. Model.* **2008**, *48*, 509–533.
(21) Palczewski, K.; Kumasaka, T.; Hori, T.; Behnke, C. A.; Motoshima, H.; Fox, B. A.; Le Trong, I.; Teller, D. C.; Okada, T.; Stenkamp, R. E.; Yamamoto, M.; Miyano, M. Crystal structure of rhodopsin: A G-protein-coupled receptor. *Science* **2000**, *289*, 739–745.
(22) Morris, G. M.; Goodsell, D. S.; Halliday, R. S.; Hart, W.; Belew, R. K.; Olson, A. J. Automated Docking Using a Lamarckian Genetic Algorithm and Empirical Binding Free Energy Function. *J. Comput. Chem.* **1998**, *19*, 1639–1662.
(23) Verdonk, M. L.; Cole, J. C.; Hartshorn, M. J.; Murray, C. W.; Taylor, R. D. Improved Protein-Ligand Docking Using GOLD. *Proteins: Struct., Funct., Genet.* **2003**, *52*, 609–623.
(24) McGann, M. R.; Almond, H. R.; Nicholls, A.; Grant, J. A.; Brown, F. K. Gaussian docking functions. *Biopolymers* **2003**, *68*, 76–90.

(25) Ritchie, D. W.; Kemp, G. J. L. Protein docking using spherical polar Fourier correlations. *Proteins: Struct., Funct., Genet.* **2000**, *39*, 178–194.
(26) Hatse, S.; Princen, K.; De Clercq, E.; Rosenkilde, M. M.; Schwartzb, T. W.; Hernandez-Abad, P. E.; Skerlj, R. T.; Bridger, G. J.; Schols, D. AMD3465, a monomacrocyclic CXCR4 antagonist and potent HIV entry inhibitor. *Biochem. Pharmacol.* **2005**, *70*, 752–761.
(27) Princen, K.; Hatse, S.; Vermeire, K.; Aquaro, S.; De Clercq, E.; Gerlach, L.-O.; Rosenkilde, M.; Schwartz, T. W.; Skerlj, R.; Bridger, G.; Schols, D. Inhibition of Human Immunodeficiency Virus Replication by a Dual CCR5/CXCR4 Antagonist. *J. Virol.* **2004**, *78*, 12996–13006.
(28) Rosenkilde, M. M.; Gerlach, L.-O.; Hatse, S.; Skerlj, R. L.; Schols, D.; Bridger, G.; Schwartz, T. W. Molecular mechanism of action of monocyclam versus bicyclam non-peptide antagonist in the CXCR4 chemokine receptor. *J. Biol. Chem.* **2007**, *282*, 27354–27365.
(29) Teixidó, J.; Borrell, J. I.; Nonell, S.; Pettersson, S.; Ros, L.; Puig de la Bellacasa, R.; Rabal, M. O.; Pérez-Nueno, V. I.; Esté, J.; Clotet-Codina, I.; Armand-Ugón, M. Nuevos sistemas polinitrogenados como agentes anti-VIH. ES Patent ES200602764, 2006 (filing date: October 26, 2006).
(30) Bridger, G.; Skerlj, R.; Kaller, A.; Harwing, C.; Bogucki, D.; Wilson, T. R.; Crawford, J.; McEachern, E. J.; Atsma, B.; Nan, S.; Zhou, Y. World Patent WO 0022600, 2002.
(31) Bridger, G.; Skerlj, R.; Kaller, A.; Harwing, C.; Bogucki, D.; Wilson, T. R.; Crawford, J.; McEachern, E. J.; Atsma, B.; Nan, S.; Zhou, Y. World Patent WO 0022599, 2002.
(32) Bridger, G.; Skerlj, R.; Kaller, A.; Harwing, C.; Bogucki, D.; Wilson, T. R.; Crawford, J.; McEachern, E. J.; Atsma, B.; Nan, S.; Zhou, Y. World Patent WO 00234745, 2002.
(33) Bridger, G.; Skerlj, R.; Kaller, A.; Harwing, C.; Bogucki, D.; Wilson, T. R.; Crawford, J.; McEachern, E. J.; Atsma, B.; Nan, S.; Zhou, Y. World Patent WO 055876, 2003.
(34) Bridger, G.; Skerlj, R.; Kaller, A.; Harwing, C.; Bogucki, D.; Wilson, T. R.; Crawford, J.; McEachern, E. J.; Atsma, B.; Nan, S.; Zhou, Y.; Smith, C. D.; Di Fluir, R. M. U.S. Patent 0019058, 2004.
(35) Ichiyama, K.; Yokohama-Kumakura, S.; Tanaka, Y.; Tanaka, R.; Hirose, K.; Bannai, K.; Edamatsu, T.; Yanaka, M.; Niitani, Y.; Miyako-Kurosaki, N.; Takaku, H.; Koyanagi, Y.; Yamamoto, N. *Proc. Natl. Acad. Sci. U.S.A.* **2003**, *100*, 4185–4190.
(36) Murakami, T.; Yoshida, A.; Tanaka, R.; Mitsuhashi, S.; Hirose, K.; Yanaka, M.; Yamamato, N.; Tanaka, Y. KRH-2731: An Orally Bioavailable CXCR4 Antagonist Is a Potent Inhibitor of HIV-1 Infection. In *2004 Antivirals Pipeline Report*; Camp, R., Ed.;Proceedings of the 11th Conference on Retroviruses and Opportunistic Infections, San Francisco, CA, Feb 8−11, 2004; Treatment Action Group: San Francisco, CA, 2004; Abstract No. 541.
(37) Yamazaki, T.; Saitou, A.; Ono, M.; Yokohama, S.; Bannai, K.; Hiroswe, K.; Yanaka, M. World Patent WO 029218, 2003.
(38) Yamazaki, T.; Kikumoto, S.; Ono, M.; Saitou, A.; Takahashi, H.; Kumakura, S.; Hirose, K. World Patent WO 024697, 2004.
(39) Bridger, G. J.; Skerlj, R. T.; Padmanabhan, S.; Martellucci, S. A.; Henson, G. H.; Struyf, S.; Witvrouw, M.; Schols, D.; De Clercq, E. Synthesis and Structure-Activity Relationships of Phenylenebis(methylene)-Linked Bis-azamacrocycles That Inhibit HIV-1 and HIV-2 Replication by Antagonism of the Chemokine Receptor CXCR4. *J. Med. Chem.* **1999**, *42*, 3971–3981.
(40) De Clercq, E. Inhibition of HIV Infection by Bicyclams, Highly Potent and Specific CXCR4 Antagonists. *Mol. Pharmacol.* **2000**, *57*, 833–839.
(41) Esté, J. A.; Cabrera, C.; De Clercq, E.; Struyf, S.; Damme, J. V.; Bridger, G.; Skerlj, R. T.; Abrams, M. J.; Henson, G.; Gutierrez, A.; Clotet, B.; Schols, D. Activity of Different Bicyclam Derivatives against Human Immunodeficiency Virus Depends on Their Interaction with the CXCR4 Chemokine Receptor. *Mol. Pharmacol.* **1999**, *55*, 67–73.
(42) Egberink, H. F.; De Clercq, E.; Van Vliet, A. L. W.; Balzarini, J.; Bridger, G. J.; Henson, G.; Horzinek, M. C.; Schols, D. Bicyclams, Selective Antagonists of the Human Chemokine Receptor CXCR4, Potently Inhibit Feline Immunodeficiency Virus Replication. *J. Virol.* **1999**, *73*, 6346–6352.
(43) Tamamura, H.; Araki, T.; Ueda, S.; Wang, Z.; Oishi, S.; Esaka, A.; Trent, J. O.; Nakashima, H.; Yamamoto, N.; Peiper, S. C.; Otaka, A.; Fujii, N. Identification of novel low molecular weight CXCR4 antagonists by structural tuning of cyclic tetrapeptide scaffolds. *J. Med. Chem.* **2005**, *48*, 3280–3289.
(44) Gerlach, L.-O.; Skerlj, R. T.; Bridger, G. J.; Schwartz, T. W. Molecular Interaction of Cyclam and Bicyclam Non-peptide Antagonists with the CXCR4 Chemokine Receptor. *J. Biol. Chem.* **2001**, *276*, 14154–14160.
(45) Tamamura, H.; Ojida, A.; Ogawa, T.; Tsutsumi, H.; Masuno, H.; Nakashima, H.; Yamamoto, N.; Hamachi, I.; Fujii, N. Identification of a new class of low molecular weight antagonists against the chemokine receptor CXCR4 having the dipicolylamine-zinc(II) complex structure. *J. Med. Chem.* **2006**, *49*, 3412–3415.
(46) Labute, P. Flexible Alignment of Small Molecules. Chemical Computing Group, Inc.: Montreal, Canada, 2004. (Available on the Internet at http://www.chemcomp.com/journal/malign.htm (accessed June 2, 2008)).
(47) Agrawal, V. K.; Singh, J.; Gupta, M.; Jaliwala, Y. A.; Khadikar, P. V.; Supuran, C. T. QSAR studies on benzopyran potassium channel activators. *Eur. J. Med. Chem.* **2006**, *41*, 360–366.
(48) Golbraikh, A.; Shen, M.; Xiao, Z.; Xiao, Y.-D.; Lee, K.-H.; Tropsha, A. Rational selection of training and test sets for the development of validated QSAR models. *J. Comput.-Aided Mol. Des.* **2003**, *17*, 241–253.
(49) Golbraikh, A.; Tropsha, A. Beware of q2! J. *Mol. Graphics Modell.* **2002**, *20*, 269–276.
(50) *OMEGA, version 2.1.0*; OpenEye Scientific Software Inc.: Santa Fe, NM., 2006.
(51) Pérez-Nueno, V. I.; Ritchie, D. W.; Borrell, J. I.; Teixidó, J. Clustering and classifying diverse HIV entry inhibitors using a novel consensus shape based virtual screening approach: Further evidence for multiple binding sites within the CCR5 extracellular pocket. *J. Chem. Inf. Model.* **2008**, *48*, 2146–2165.
(52) Hatse, S.; Princes, K.; Vermeire, K.; Gerlach, L.-O.; Rosenkilde, M. M.; Schwartz, T. W.; Bridger, G.; De Clercq, E.; Schols, D. Mutations at the CXCR4 interaction sites for AMD3100 influence anti-CXCR4 antibody binding and HIV-1 entry. *FEBS Lett.* **2003**, *546*, 300–306.
(53) Brelot, A.; Heveker, N.; Montes, M.; Alizon, M. Identification of Residues of CXCR4 Critical for Human Immunodeficiency Virus Coreceptor and Chemokine Receptor Activities. *J. Biol. Chem.* **2000**, *275*, 23736–23744.
(54) Hatse, S.; Princen, K.; Gerlach, L.-O.; Bridger, G.; Henson, G.; Clercq, E.; Schwartz, T. W.; Schols, D. Mutation of Asp171 and Asp262 of the chemokine receptor CXCR4 impairs its coreceptor function for human immunodeficiency virus-1 entry and abrogates the antagonistic activity of AMD3100. *Mol. Pharmacol.* **2001**, *60*, 164–173.
(55) Wang, R.; Wang, S. How does consensus scoring work for virtual library screening? An idealized computer experiment. *J. Chem. Inf. Comput. Sci.* **2001**, *41*, 1422–1426.
(56) Güner, O. F.; Henry, D. R. Metric for analyzing hit lists and pharmacophores. Chapter 11. In *Pharmacophore, perception, development and use in drug design*; Güner, O. F., Ed.; International University Line: La Jolla, CA, 2000; pp 195−212.
(57) Gürner, O. F.; Hoffman, R.; Li, H. Techniques and strategies in 3D data mining. In Report by Wendy A. Warr; 217th ASC National Metting and Exposition, Anaheim, California, March 12−25, 1999; Wendy Warr & Associates: London, 1999; pp 50−53.
(58) Hunter, T. M.; McNae, I. W.; Simpson, D. P.; Smith, A. M.; Moggach, S.; White, F.; Walkinshaw, M. D.; Parsons, S.; Sadler, P. J. Configurations of nickel-cyclam antiviral complexes and protein recognition. *Chem.--Eur. J.* **2007**, *13*, 40–50.
(59) Liang, X.; Parkinson, J. A.; Wishäupl, M.; Gould, R. O.; Paisey, S. J.; Park, H.; Hunter, T. M.; Blindauer, C. A.; Parsons, S.; Sadler, P. J. Structure and dynamics of metallomacrocycles: recognition of zinc xylyxl-bicyclam by an HIV coreceptor. *J. Am. Chem. Soc.* **2002**, *124*, 9105–9112.
(60) Hunter, T. M.; McNae, I. W.; Liang, X.; Bella, J.; Parsons, S.; Walkinshaw, M. D.; Sadler, P. J. Protein recognition of macrocycles: Binding of anti-HIV metallocyclams to lysozyme. *Proc. Natl. Acad. Sci. U.S.A.* **2005**, *102*, 2288–2292.
(61) Rosenkilde, M. M.; Gerlach, L.-O.; Jakobsern, J. S.; Skerlj, R. T.; Bridger, G. J.; Schwartz, T. W. Molecular mechanism of AMD3100 antagonism in the CXCR4 receptor. *J. Biol. Chem.* **2004**, *279*, 3033–3041.
(62) Valks, G. C.; McRobbie, G.; Lewis, E. A.; Hubin, T. J.; Hunter, T. M.; Sadler, P. J.; Pannecouque, C.; De Clercq, E.; Archibald, S. J. Configurationally restricted bismacrocyclic CXCR4 receptor antagonists. *J. Med. Chem.* **2006**, *49*, 6162–6165.

CI800468Q